



The University of
Nottingham

UNITED KINGDOM • CHINA • MALAYSIA

Identifying canopy architecture traits to optimize light and increase radiation-use efficiency and grain yield in wheat

By: Marcela Alejandra Moroyoqui Parra

BSc

**Thesis submitted to the University of Nottingham for the degree
of Doctor of Philosophy**

**University of Nottingham
School of Biosciences**

March 2022

Dedication

To Arturo and Sonia

ACKNOWLEDGEMENTS

First, I would like to thank my supervisor John Foulkes for his invaluable guidance, support, patient throughout my PhD. I would also like to acknowledge my co-supervisor Eric H. Murchie and my internal examiner Debbie Sparkes for his guidance.

I would like to express my gratitude to my supervisors Matthew Reynolds and Gemma Molero for all the support, guidance, advices, encouragement and for believing in me.

My deepest appreciation to Reshmi for her encouragement, support and friendship.

I gratefully acknowledge the physiology group at CIMMYT for assist me in the field experiments, especially to Carolina Rivera, Francisco Pinera, Jacinta Gimeno, Araceli Torres, Nayeli Quiche and Jazmine Rowaldez. I would like to thank Angela Pacheco from CIMMYT for providing statistical advice.

Many thanks to my friends from Mexico and Nottingham for supporting during these years me and providing me inspiration during my thesis writing. Also, many thanks to my friends Lucia, Francesca, Itzel, Ferdinando, Carlos and Anelya for their support.

My deepest appreciation goes to my dad and mom for always being there for me, for their love and support throughout my life. I am forever indebted to my parents for giving me the opportunities that have made me who I am.

I would like to acknowledge The National Council of Science and Technology (CONACYT) and the Secretariat of Agriculture and Rural Development (SADER) through the MasAgro initiative (MasAgro) as well as the International Wheat Yield Partnership Program (IWYP) for funding the PhD.

ABSTRACT

Wheat is the most widely grown crop which produces ~766 million tonnes per year (FAOSTAT, 2019) supplying 20% of the calories and protein for the human population (Braun et al., 2010). Staple crops (wheat, maize, rice and soybean) must increase their yield by 2.4% per year to meet the food demand for a growing population (Ray et al., 2013). Climate change has been predicted to increase the global temperature by ~ 2-4°C by the end of the 21st century (IPCC, 2014), with more frequent flooding and drought decreasing the production of grain crops (IPCC, 2014; Asseng et al., 2015). Harvest index (grain dry matter as a proportion of above-ground dry matter; HI) is approaching its theoretical limit (Austin et al., 1980; Foulkes et al., 2011), so other alternatives must be explored to increase biomass and hence grain yield. Radiation-use efficiency (above-ground dry matter per unit radiation interception; RUE) has therefore become an important trait for raising biomass and grain yield potential in plant breeding (Foulkes and Murchie, 2011a). In recent decades, growers in the Northwest of Mexico have adopted a raised-bed planting system (Fahong et al., 2004). This planting system showed advantages compared to the traditional flat-basin planting system such as water savings and reduced weeds and diseases (Fahong et al., 2004). However, effects on grain yield are still inconsistent so further studies are needed to prove grain yield benefits.

The overall objective of this thesis was to quantify genetic variation in canopy architecture traits and associations with light interception, radiation-use efficiency and grain yield in twelve spring wheat CIMMYT cultivars evaluated under two planting systems (raised beds and flat basins). These cultivars were evaluated in three field experiments under irrigated, yield potential conditions in 2017-18, 2018-19 and 2019-20 in the NW of Mexico. In the field experiments, measurements were taken of phenology, light interception, RUE during different phenophases, canopy architecture traits including flag-leaf angle and curvature, leaf size, biomass and dry matter partitioning at key developmental stages and grain yield and yield components. Two more experiments were carried out in the glasshouse at Sutton Bonington, UK in 2018 and 2019 to examine the photosynthetic rate of the 12 cultivars and its relation with radiation-use efficiency and biomass in the field experiments.

Results in the field experiments across the three years showed a planting system (PS) difference in grain yield which was 10.6% higher in beds than flats and a PS \times G interaction. A planting system effect was also shown for grains per m² (GM2), HI, grains per spike (GPS) and above-ground biomass at physiological maturity (BMPM). The higher grain yield obtained in beds was mainly explained by the 7.6 % greater biomass at maturity in beds. Biomass was initially lower in raised beds compared to flat basins at initiation of booting. The higher radiation-use efficiency calculated from initiation of booting to anthesis + 7 days (RUE_InBA7) in raised beds contributed to this PS catching up the biomass accumulation in the flat basins at anthesis + 7 days. A wide genetic variation was found for RUE calculated at five different phenophases from initiation of booting to physiological maturity. However, only RUE from emergence + 40 days to initiation of booting (RUE_E40InB), from initiation of booting to anthesis + 7 days (RUE_InBA7) and from emergence + 40 days to physiological maturity (RUET) showed a PS effect. A PS \times G interaction was found for all the RUE's except for RUE_InBA7. In both, PS positive associations were found among cultivars between RUE_preGF and biomass at GS65 + 7 days and biomass at physiological maturity. In addition, positive correlations were found among cultivars between each of RUE_preGF and RUET and grain yield in beds and flats. Results showed that grain yield responses of cultivars to planting system were mainly explained through effects on final biomass. Biomass responses to planting system were, in turn, associated with responses of RUE to planting system in the pre-anthesis period. Additionally, taller cultivars showed greater biomass increases at physiological maturity in B compared to F than shorter cultivars.

The flag-leaf curvature (FLcv; cm) was measured as the distance from the point of inflexion to the tip of the leaf. Genetic variation was found among the cultivars in flag-leaf angle and flag-leaf curvature at initiation of booting and anthesis+7 days. In flats, a strong negative association was found between flag-leaf angle and RUE during grain filling (RUE_GF), i.e. more upright flag leaves had higher RUE_GF. Additionally, a positive correlation between flag-leaf curvature at initiation of booting and anthesis + 7 days was found with RUE_InBA7 and RUE_GF in flats. In, beds, flag-leaf curvature at booting was positively associated with greater pre-anthesis radiation interception.

The planting system also affected flag-leaf angle at GS65 + 7 days with leaf angle decreasing (more upright leaves) in flat basins compared to raised beds, but cultivars differed

in the extent of the decrease. Plant height measured in the beds was associated with responses PS of grain yield, biomass at physiological maturity and fractional light interception at anthesis + 7 days.

Averaging across the three years, a strong positive correlation among cultivars between grain yield and HI was found in flats whereas no significant correlation was found in beds. A negative correlation was observed between spike partitioning measured at anthesis + 7 days (SPI) and each of stem partitioning index (StemPI) and stem-internode 2 and 3 length. No associations between SPI and peduncle length was found. The genetic variation in GM2 was strongly associated with fruiting efficiency (grains per unit spike dry matter at GS65+7 days; FE) in flats and a trend was found in beds. FE accounted for more genetic variation in GM2 than SPI. The results in the present study confirm that plant breeders should consider the planting system when selecting canopy architecture traits to enhance RUE, biomass and grain yield as well as selecting lines with high FE.

In the glasshouse experiments, genetic variation among the cultivars was found for flag-leaf light-saturated photosynthetic rate (A_{\max}) at anthesis. Encouragingly, a positive correlation was found between A_{\max} at initiation of booting and anthesis measured in the glasshouse and biomass at physiological maturity in raised beds and flat basins measured in the field experiments.

LIST OF CONTENTS

ACKNOWLEDGEMENTS	3
ABSTRACT	4
List of Abbreviations	20
1 INTRODUCTION	23
1.1 Wheat world production	23
1.2 Wheat growth and development	25
1.3 Planting systems	27
1.3.1 Description of raised beds and flat basins systems.....	27
1.3.2 Differences between raised beds and flat basins	28
1.4 Genetic gains of grain yield and associated traits.....	30
1.5 Light interception.....	31
1.5.1 Traits to enhance light interception	33
1.5.1.1 Delayed senescence / stay green	33
1.6 Radiation-use efficiency	34
1.6.1 Traits to enhance radiation-use efficiency.....	34
1.6.1.1 Canopy architecture	34
1.6.1.2 Vertical N distribution in canopy.....	37
1.6.1.3 Leaf photosynthesis and leaf photosynthesis per unit N.....	38
1.6.1.4 Rubisco capacity	39
1.7 Spike fertility and fruiting efficiency.....	40
1.8 Dry-matter partitioning	41
1.9 Source-sink balance	42
1.10 Main objectives and hypotheses	43
1.11 Thesis layout	45
2 CHAPTER 2 . RADIATION-USE EFFICIENCY AND BIOMASS IN WHEAT DIFFERS BETWEEN RAISED BEDS AND FLAT BASINS PLANTING SYSTEM: CONSIDERATIONS FOR CULTIVAR SELECTION.....	47
2.1 Abstract.....	47
2.2 Introduction.....	48
2.3 Materials and methods	51
2.3.1 Experiment site, design and treatments	51
2.3.2 Crop measurements	53
2.3.2.1 Phenology and growth analysis	53

2.3.2.2	Light interception.....	54
2.3.2.3	Radiation-use efficiency	54
2.3.2.4	Normalized Differenced Vegetation Index (NDVI)	55
2.3.3	Statistical analysis	56
2.4	Results.....	57
2.4.1	Grain yield, yield components and developmental stages.....	57
2.4.2	Biomass, radiation interception and NDVI during the season	59
2.4.3	Radiation-use efficiency and correlations with biomass, yield and yield components	65
2.5	Discussion.....	69
2.5.1	Effects of planting systems.....	69
2.5.2	Genetic variation in RUE and association with biomass and grain yield.....	69
2.5.3	Cultivar responses to planting systems.....	70
2.6	Conclusion	72
2.7	Author contribution.....	73
2.8	Funding	73
2.9	Acknowledgements.....	73
2.10	Supplementary information	74
3	CHAPTER 3. EFFECTS OF CANOPY ARCHITECTURE TRAITS ON RADIATION-USE EFFICIENCY (RUE) IN WHEAT CULTIVARS IN RAISED BEDS AND FLAT BASINS PLANTING SYSTEMS.....	80
3.1	Abstract.....	80
3.2	Introduction.....	81
3.3	Materials and methods	85
3.3.1	Experimental site, design and treatments	85
3.3.2	Crop measurements	86
3.3.2.1	Phenology	86
3.3.2.2	Growth analysis at emergence + 40 days, GS41 and GS65 + 7 days.....	86
3.3.2.3	Light interception and radiation-use efficiency	86
3.3.2.4	Canopy architecture	88
3.3.2.5	Flag-leaf relative chlorophyll content.....	89
3.3.2.6	Growth analysis at physiological maturity, grain yield and yield components.....	89
3.3.3	Statistical analysis	89
3.4	Results.....	90
3.4.1	Grain yield, yield components and above-ground biomass.....	90

3.4.2	Canopy architecture traits	91
3.4.3	GAI, k_{par} and RUE	92
3.4.4	Canopy architecture traits and correlations with light interception, RUE, grain yield and yield components	94
3.5	Discussion	101
3.5.1	Associations between canopy architecture traits	101
3.5.2	Canopy architecture and its relations with light interception, grain yield and yield components	102
3.5.3	Canopy architecture and its relation with RUE	104
3.5.4	Genetic basis of canopy architecture	107
3.6	Conclusions	108
3.7	Author contribution	108
3.8	Funding	109
3.9	Acknowledgements	109
3.10	Supplementary information	110
4	Chapter 4. GRAIN PARTITIONING TRAITS TO INCREASE HARVEST INDEX AND GRAIN YIELD IN WHEAT: EVALUATED UNDER TWO PLANTING SYSTEMS	
	114	
4.1	Abstract	114
4.2	Introduction	115
4.3	Materials and methods	119
4.3.1	Experimental site, design and treatment	119
4.3.2	Crop measurements	119
4.3.2.1	Phenology	119
4.3.2.2	Growth analysis at GS41 and GS65 + 7 days	119
4.3.2.3	Radiation-use efficiency	120
4.3.2.4	Canopy architecture	120
4.3.2.5	Growth analysis at physiological maturity, grain yield and yield components	121
4.3.3	Statistical analysis	121
4.4	Results	122
4.4.1	Genetic variation in grain yield, yield components and grain partitioning traits	122
4.4.2	Phenotypic correlations between grain partitioning traits, yield and yield components	125
4.4.3	Radiation-use efficiency and canopy architecture traits	128

4.4.4	Stem-internode partitioning traits and correlations with source and sink traits	128
4.4.5	Spike morphological partitioning and correlations with fruiting efficiency and yield components	134
4.5	Discussion	135
4.5.1	Optimizing internode traits for spike growth	135
4.5.2	FE and its correlation with GM2 and grain yield	138
4.5.3	Associations between grain partitioning traits and source traits	139
4.6	Implications for plant breeders	141
4.7	Author contribution.....	142
4.8	Funding	142
4.9	Acknowledgements.....	143
4.10	Supplementary information	144
5	Chapter 5. GLASSHOUSE EXPERIMENTS: IDENTIFYING FLAG-LEAF PHOTOSYNTHETIC TRAITS TO ENHANCE RUE, BIOMASS, GRAIN YIELD AND N-USE EFFICIENCY IN SPRING WHEAT CULTIVARS	147
5.1	Introduction.....	147
5.2	Materials and methods	150
5.2.1	Plant measurements	151
5.2.1.1	Phenology and growth analysis	151
5.2.1.2	Flag-leaf photosynthesis and stomatal conductance	151
5.2.1.3	Flag-leaf chlorophyll content.....	152
5.2.1.4	Radiation-use efficiency and canopy architecture traits	152
5.2.1.5	Nitrogen-use efficiency (NUE), NUE components, NHI and flag-leaf N content	153
5.2.2	Statistical analysis	153
5.3	Results.....	154
5.3.1	Growing conditions in glasshouse experiments	154
5.3.2	Developmental stages and plant height	154
5.3.3	Harvest measurements in glasshouse experiments	155
5.3.4	Flag-leaf photosynthesis rate and stomatal conductance.....	156
5.3.5	Correlations between grain yield, yield components and physiological traits in glasshouse experiments	157
5.3.6	RUE, NUE, NUE components and flag-leaf N% in field experiments.....	158
5.3.7	Correlations between flag-leaf A_{max} and g_s in the glasshouse experiments and grain yield, yield components, NUE and NUE components and canopy architecture traits in the field experiments.....	160

5.4	Discussion	163
5.4.1	Flag-leaf photosynthesis traits	163
5.4.2	Nitrogen traits and correlation with flag-leaf photosynthetic traits and RUE 164	
5.5	Conclusion	167
6	GENERAL DISCUSSION	168
6.1	Review of hypotheses	168
6.2	Ideal crop ideotype in raised bed and flat basin planting systems.....	170
6.3	Implications for plant breeders	176
6.4	Translating from glasshouse to field experiments	178
7	CONCLUSIONS	179
8	FUTURE WORK.....	180
9	APPENDIX.....	183
10	REFERENCES	192

LIST OF FIGURES

Fig. 1.1 Wheat grain production worldwide from 1990 - 2019 (FAOSTAT, 2019).....	24
Fig. 1.2. Wheat area harvested worldwide from 1990 - 2019 (FAOSTAT, 2019).	24
Fig. 1.3. Diagram of growth stages of a wheat plant. Adapted from Sreenivasulu and Schnurbusch (2012).....	26
Fig. 1.4. Dimensions for A flat basins: same distance between the 8 rows and B raised beds: two or three rows per bed with a wider furrow gap. Adapted from Fischer et al. (2005). Created with Biorender.com.....	28
Fig. 2.1. Dimensions for A flat basins: same distance between the 8 rows and B raised beds: two or three rows per bed with a wider furrow gap. Adapted from (Fischer et al., 2005). Created with Biorender.com.....	53
Fig. 2.2. Environmental conditions in the field experiments (average mean temperature (°C), average minimum temperature (Tmin, °C), average maximum temperature (Tmax, °C), average monthly rainfall (mm) and average monthly radiation (MJ m ⁻²) in the field experiments during (A) 2017-18, (B) 2018-19 and (C) 2019-20.	57
Fig. 2.3. Boxplot of aboveground biomass at (A) emergence + 40 days, (B) initiation of booting, (C) anthesis + 7 days and (D) physiological maturity in raised beds (B) and flat basins (F). Values represent means across 2017-18, 2018-19 and 2019-20. The middle dotted line is the adjusted mean across lines. Statistical significances for genotype (G), planting systems (PS) and the interaction between them (PS × G) are presented below each boxplot.	61
Fig. 2.4. Linear regression between cultivar responses to plant system at (A) biomass at forty days after emergence (BME40; g m ⁻²), (B) biomass at initiation of booting (BMInB, g m ⁻²) and (C) biomass at seven days after anthesis (BMA7; g m ⁻²) with cultivar responses to planting system for biomass at physiological maturity (BMPM; g m ⁻²) evaluated across-years in 2017-18, 2018-19 and 2019-20.....	62
Fig. 2.5. Mean, minimum and maximum values of NDVI across 12 CIMMYT spring wheat genotypes with thermal time on (A) raised beds and (B) flat basins planting systems. Error bars represent the LSD (5%) for each NDVI measurement. Black line represents the vegetative stage cross-year mean 2017-18, 2018-19 and 2019-20 and the blue line the grain-filing stage cross-year mean 2017-18 and 2018-19. Arrows show anthesis date (GS65)...	64
Fig. 2.6. Boxplot of accumulated radiation interception (MJ m ⁻²) for (A) emergence + 40 days to initiation of booting, (B) initiation of booting to anthesis + 7 days, (C) anthesis + 7 days to physiological maturity (D) emergence + 40 days to physiological maturity in raised beds (B) and flat basins (F). Values represent means across 2018-19 and 2019-20. The middle dotted line is the adjusted mean across cultivars. Statistical significances for genotype (G), planting systems (PS) and the interaction between them (PS × G) are presented below each boxplot.	65
Supplementary Fig. 2.1. Above-ground biomass accumulation during the crop cycle for 12 CIMMYT spring wheat genotypes evaluated across-years in 2017-18, 2018-19 and 2019-20 in raised beds (B) and flat basins (F). TT = thermal time post-emergence. *P < 0.05.....	76

Fig. 3.1. Diagram of canopy architecture measurements on the flag leaf in wheat.	88
Fig. 3.2. Boxplots of genetic variation in RUE (g MJ ⁻¹) at a) RUE_E40InB: from 40 days after emergence to initiation of booting, b) RUE_InBA7: from initiation of booting to seven days after anthesis, c) RUE_preGF: pre grain-filling, from forty days after emergence to seven days after emergence, d) RUE_GF: grain-filling, from seven days after emergence to physiological maturity and e) RUET: from forty days after emergence to physiological maturity, for 12 CIMMYT spring wheat cultivars evaluated across-years 2018-19 and 2018-19 in raised beds (B) and flat basins (F). The middle dotted line is the adjusted mean across lines. Statistical significances for genotype (G), planting systems (PS) and the interaction between them (PS × G) are presented below each boxplot.	94
Fig. 3.3. Regression of RUE grain-filling (RUE_GF; g MJ ⁻¹) on flag-leaf angle at seven days after anthesis (FLAA7; °) for 12 CIMMYT spring wheat genotypes across the years for 12 CIMMYT spring wheat genotypes in raised beds (B) and flat basins (F) across the years 2018-19 and 2019-20.....	95
Fig. 3.4. Regression of RUE grain-filling (RUE_GF; g MJ ⁻¹) on a) flag-leaf curvature at seven days after anthesis (FLCA7; cm) and b) flag-leaf curvature at initiation of booting (FLCInB; cm) for 12 CIMMYT spring wheat genotypes across the years for 12 CIMMYT spring wheat genotypes in raised beds (B) and flat basins (F).	95
Fig. 3.5. Regression of plant height at physiological maturity on A flag-leaf angle at initiation of booting (FLAInB; °) and B flag-leaf curvature at initiation of booting (FLcvInB; cm) in raised beds (B) and flat basins (F) for 12 CIMMYT spring wheat cultivars evaluated across the years 2018-19 and 2019-20.	99
Fig. 3.6. Regression of RUE from forty days after emergence to seven days after anthesis (RUE_preGF) (g MJ ⁻¹) on relative chlorophyll content (SPAD) in leaf 3 at seven days after anthesis in raised beds (B) and flat basins (F) for 12 CIMMYT spring wheat cultivars evaluated across the years 2018-19 and 2019-20.	99
Fig. 4.1. Boxplots of genetic variation in A grain yield (YLD, 0 % DM), B thousand-grain weight (TGW), C harvest index (HI), D biomass at physiological maturity (BMPM), E grains per square meter (GM2) and F spikes per square meter (SM2) for 12 CIMMYT spring wheat genotypes evaluated across-years 2017-18 and 2018-19 in raised beds (B) and flat basins (F). The dotted line is the adjusted mean across lines. Statistical significances for genotype (G), planting systems (PS) and the interaction (PS × G) are presented below each boxplot.....	123
Fig. 4.2. Regression of grains per m ⁻² (GM2) on A fruiting efficiency (FE), B spike partitioning index (SPI) and C biomass at seven days after anthesis (BMA7) for 12 CIMMYT spring wheat cultivars across 2017-18 and 2018-19 in raised beds (B) and flat basins (F).	125
Figure 4.3. Linear regressions of each of spike partitioning index (SPI) and stem partitioning index (StemPI) on peduncle length at physiological maturity, stem-internode 2 length at seven days after anthesis and stem-internode 3 length at seven days after anthesis for 12 CIMMYT spring wheat cultivars across 2017-18 and 2018-19 in raised beds (B) and flat basins (F).	126

Fig. 4.4. Diagram showing the genetic variation in PedTSPI: peduncle true-stem partitioning index, Int2TSPI: internode 2 true-stem partitioning index, Int3TSPI: internode 3 true-stem partitioning index, PedLSPI: peduncle leaf-sheath partitioning index, Int2LSPI: internode 2 leaf-sheath partitioning index, Int3LSPI: internode 3 leaf-sheath partitioning index, Int4+PI: internode 4+ partitioning index (TS-LS), PedLSW: peduncle specific weight, Int2SW: internode 2 specific weight, Int 3SW: internode 3 specific weight for 12 CIMMYT spring wheat genotypes across 2017-18 and 2018-19 in A raised beds and B flat basins. Genotype and planting system significance are shown in A raised beds. Diagram created with BioRender.com.	130
Fig. 4.5. Principal component analyses (PCA) for grain number (GM2), harvest index (HI), fruiting efficiency (FE), and traits measure at seven days after anthesis: spike partitioning index (SPI), peduncle, internode 2 and internode 3 length (PedL, Int2L, Int3L, respectively), internode 2 and 3 true-stem partitioning index, light interception (LI%A7) for 12 CIMMYT spring wheat cultivars during 2018-19 in A raised beds and B flat basins.	134
Supplementary Fig. 4.1. Environmental conditions in the field experiments (average mean temperature (°C), average minimum temperature (Tmin, °C), average maximum temperature (Tmax, °C), average monthly rainfall (mm) and average monthly radiation (MJ m ⁻²) in the field experiments during (A) 2017-18, (B) 2018-19 and (C) 2019-20.	144
Figure 5.1. Glasshouse experiment at Sutton Bonington Campus in 2018.	151
Figure 5.2. Measurements with LI-COR 6400 XT Portable Photosynthesis System in glasshouse experiment.	152
Fig. 5.3. Daily mean (average minimum and maximum) temperature (°C) in the glasshouse experiments in a) 2018 and b) 2019. Arrows indicate anthesis date.	154
Appendix Fig. 1. Field arrangement in raised beds (B) in 2017-18. Created with BioRender.com.	183
Appendix Fig. 2. Field arrangement in flat basins (F) in 2017-18. Created with BioRender.com.	184
Appendix Fig. 3. Field arrangement in raised beds (B) in 2018-19. Created with BioRender.com.	185
Appendix Fig. 4. Field arrangement in flat basins (F) in 2018-19. Created with BioRender.com.	186
Appendix Fig. 5. Field arrangement in raised beds (B) in 2019-20. Created with BioRender.com.	187
Appendix Fig. 6. Field arrangement in flat basins (F) in 2019-20. Created with BioRender.com.	188

LIST OF TABLES

Table 2.1. List of twelve CIMMYT elite spring bread wheat cultivars and advanced lines in the experiments in 2017-2018, 2018-19 and 2019-20. *Two lines added in 2018-19 and 2019-20.....	52
Table 2.2. Mean, minimum, maximum, and ANOVA for yield, yield components, biomass at maturity and phenology expressed in days after emergence (DAE) from the combined analysis across 2017-18, 2018-19 and 2019-20 in raised beds (B) and flat basins (F).	58
Table 2.3. Phenotypic correlations for grain yield, HI, yield components, height at physiological maturity, number of shoots at emergence + 40 days and anthesis + 7 days (m ²) and phenology in days after emergence (DAE) among the 12 spring CIMMYT wheat genotypes. Values based on means in 2017-18, 2018-19 and 2019-20 in raised beds (B) and flat basins (F). For abbreviations, see Table 2.2. *P < 0.05, **P < 0.01, ***P < 0.001, †P < 0.10.	60
Table 2.4. Radiation-use efficiency (RUE; g MJ ⁻¹) calculated from forty days after emergence to initiation of booting (RUE_E40InB), from initiation of booting to seven days after emergence (RUE_InBA7), during the grain filling period from seven days after anthesis to physiological maturity (RUE_GF), pre grain-filling from forty days after emergence to seven days after anthesis (RUE_preGF) and from forty days after emergence to physiological maturity (RUET) for 12 CIMMYT spring wheat genotypes. Values represent means across 2018-19 and 2019-20 in raised beds (B) and flat basins (F) planting systems. ***P < 0.001, **P < 0.01, *P < 0.05, <i>italics: P < 0.10</i> , ns: not significant.	66
Table 2.5. Phenotypic correlations between yield, yield components, height, above-ground biomass at different growth stages and shoot number with RUE (g MJ ⁻¹) for 12 spring CIMMYT wheat genotypes. Values based on means from the combined analysis in 2018-19 and 2019-20 in raised beds (B) and flat basins (F).....	68
Supplementary Table 2.1. Sowing date, fertilizer applications and irrigation applications in the planting systems (PS) raised beds (B) and flat basins (F) in the field experiments in 2017-18, 2018-19 and 2019-20. ‡Drip irrigation.	74
Supplementary Table 2.2. ANOVA for grain yield, harvest index, yield components and biomass at physiological maturity for 12 CIMMYT spring wheat genotypes from the combined analysis across 2017-18, 2018-19 and 2019-20 in raised beds (B) and flat basins (F).	75
Supplementary Table 2.3. Mean, minimum, maximum, and ANOVA for fractional light interception at emergence + 40 days (FLI.E40), initiation of booting (FLI.InB) and seven days after anthesis (FLI.A7)	76
Supplementary Table 2.4. Phenotypic correlations between IPARacc for each phenophase and above-ground biomass accumulated at different phenophases and plant height at physiological maturity among 12 spring CIMMYT wheat genotypes. Values based on means from the combined analysis in 2018-19 and 2019-20 in raised beds (B) and flat basins (F). *P < 0.05, **P < 0.01, ***P < 0.001, †P < 0.10.	77

Supplementary Table 2.5. Phenotypic correlations between percentage light interception and above-ground biomass at different growth stages among 12 spring CIMMYT wheat genotypes. Values based on means from the combined analysis in 2018-19 and 2019-20 in raised beds (B) and flat basins (F).....	77
BME40: biomass at emergence + 40 days (g m^{-2}), BMInB: biomass at initiation of booting (g m^{-2}), BMA7: biomass at anthesis + 7 days (g m^{-2}), BMPM: biomass at physiological maturity (g m^{-2}), LI%E40: light interception at emergence + 40 days, LI%InB: light interception at initiation of booting, LI%A7: light interception at anthesis + 7 days. *P < 0.05, **P < 0.01, ***P < 0.001, †P < 0.10.....	77
Supplementary Table 2.6. Phenotypic correlations between yield, yield components, height, above-ground biomass at different growth stages and shoot number with crop growth rate (CGR; $\text{g m}^{-2} \text{ day}^{-1}$) for 12 spring CIMMYT wheat genotypes. Values based on means from the combined analysis in 2018-19 and 2019-20 in raised beds (B) and flat basins (F).....	78
Supplementary Table 2.7. Broad-sense heritability (H^2) for yield, yield components, biomass at maturity, phenology expressed in days after emergence (DAE), number of shoots for 12 CIMMYT spring wheat genotypes from the three combined analysis across 2017-18, 2018-19 and 2019-20 and RUE from the two combined analysis (2018-19 and 2019-20). Plants (m^{-2})‡ (data 2019-20).....	79
Table 3.1. Mean, minimum, maximum, heritability (H^2) and ANOVA for grain yield, yield components and above-ground biomass at different growth stages from the combined analysis across 2018-19 and 2019-20 in raised beds (B) and flat basins (F).....	90
Table 3.2. Flag-leaf angle (FLA), flag-leaf curvature visual score (1-10, FLcv _v) and distance from point of inflexion of the flag-leaf to the tip (FLcv) at initiation of booting (GS41, InB) and seven days after anthesis (GS65, A7) for 12 CIMMYT spring wheat genotypes from the combined analysis across 2018-19 and 2019-20 in raised beds (B) and flat basins (F).....	92
Table 3.3. Green area index (GAI) and light extinction coefficient (k_{par}) at initiation of booting and seven days after anthesis for 12 CIMMYT spring wheat cultivars from the combined analysis across 2018-19 and 2019-20 in raised beds (B) and flat basins (F).....	93
Table 3.4. Phenotypic correlations among 12 CIMMYT spring wheat cultivars evaluated across the years 2018-19 and 2019-20 in raised beds and flat basins between canopy architecture and RUE traits using different methodologies (flag-leaf angle and curvature / visual score).....	97
Table 3.5. Phenotypic correlations between canopy architecture traits at initiation of booting (InB) and seven days after anthesis (A7) and yield and yield components for 12 spring CIMMYT wheat genotypes. Values based on means from the combined analysis in 2018-19 and 2019-20 in raised beds (B) and flat basins (F).....	100
Supplementary table 3.1. Flag-leaf length and width at initiation of booting (GS41) and seven days after anthesis (GS65) and SPAD in the leaf 3 at seven days after anthesis for 12 CIMMYT spring wheat cultivars from the combined analysis across 2018-19 and 2019-20 in raised beds (B) and flat basins (F).....	110
Supplementary Table 3.2. Phenotypic correlations among 12 CIMMYT spring wheat cultivars of RUE_InBA7, K_{PAR} and SPAD at initiation of booting and seven days after	

anthesis for 12 CIMMYT spring wheat genotypes evaluated across the years 2019 and 2020 in raised beds and flat basins. 111

Supplementary table 3.3. Phenotypic correlations among 12 CIMMYT spring wheat cultivars evaluated across the years 2018-19 and 2019-20 in raised beds and flat basins (*italics*) between canopy architecture and accumulated radiation interception: accumulated radiation interception from initiation of booting to seven days after anthesis (IPARaccInBA7; MJ M⁻²), accumulated radiation interception from seven days after anthesis to physiological maturity (IPARaccA7PM; MJ m⁻²), total accumulated radiation interception from forty days after emergence to physiological maturity (IPARaccE40PM; MJ m⁻²), flag-leaf angle at initiation of booting (FLAInB; °), flag-leaf curvature at initiation of booting (FLcvInB; cm), flag-leaf length at initiation of booting (LLInB; cm) and flag-leaf width at initiation of booting (LWInB; cm), flag-leaf angle at seven days after anthesis (FLAA7; °), flag-leaf curvature at seven days after anthesis (FLcvA7; cm), flag-leaf length at seven days after anthesis (LLA7; cm), flag-leaf width at anthesis at seven days after anthesis (LWA7; cm), light extinction coefficient at initiation of booting (k_{par}InB) and light extinction coefficient at seven days after anthesis (k_{par}A7). *P < 0.05, **P < 0.01, ***P < 0.001, † < 0.10. 112

Supplementary table 3.4. Phenotypic correlations between canopy architecture traits and biomass through the season among 12 CIMMYT spring wheat cultivars evaluated across the years 2018-19 and 2019-20 in raised beds and flat basins (*italics*)..... 113

Table 4.1. Spike partitioning index (SPI), stem partitioning index (StemPI), lamina partitioning index (LamPI), spike dry matter at seven days after anthesis (DMspkA7), fruiting efficiency (FE), plant height at physiological maturity and biomass at seven days after anthesis (BMA7) for 12 CIMMYT spring wheat genotypes. Values represent means across 2017-18 and 2018-19 in raised beds (B) and flat basins (F) planting systems. *P < 0.05, **P < 0.01, ***P < 0.001, *italics: P < 0.10*, ns: not significant. 124

Table 4.2. Phenotypic correlations among 12 CIMMYT spring wheat genotypes evaluated across 2017-18 and 2018-19 in raised beds and flat basins (*italics*) between grain partitioning traits and yield, yield components and biomass..... 127

Table 4.3. Peduncle (PedL), internode 2 (Int2L) and internode 3 (Int3L) length at GS65 + 7 days for 12 CIMMYT spring wheat genotypes. Values represent means across 2017-18 and 2018-19 in raised bed (B) and flat basin (F) planting systems. *P < 0.05, **P < 0.01, ***P < 0.001, *italics: P < 0.10*, ns: not significant..... 129

Table 4.4. Phenotypic correlations among 12 CIMMYT spring wheat genotypes across 2017-18 and 2018- 19 in raised beds (B) and flat basins (F) between internode traits and sink strength traits. 131

Table 4.5. Phenotypic correlations among 12 CIMMYT spring wheat cultivars evaluated across the years 2017- 18 and 2018-19 in raised beds (B) and flat basins (F) between internode traits and source strength traits. 133

Table 4.6. Mean, minimum, maximum, and ANOVA for spike partitioning indices (PI) at seven days after anthesis for 12 CIMMYT spring wheat genotypes in raised beds (B) and flat basins (F) planting systems evaluated in 2018-19 and phenotypic correlations with yield, yield components and physiological traits measured at seven days after anthesis..... 135

Supplementary Table 4.1. List of twelve CIMMYT elite spring bread wheat cultivars and advanced lines in the experiments in 2017-2018, 2018-19 and 2019-20.	144
Supplementary Table 4.2. Genetic variation for 12 CIMMYT spring wheat cultivars for yield, yield components and biomass at maturity from the three years combined analysis (2017-18, 2018-19 and 2019-20) in raised beds (B) and flat basins (F).	145
Supplementary Table 4.3. Min, Max and average and ANOVA significance levels for RUE during pre grain-filling (RUE_preGF; g MJ ⁻¹), flag leaf angle (FLAA7; °), flag-leaf curvature (FLCA7; cm), flag-leaf length (LLA7; cm) and flag-leaf width (LWA7; cm) for 12 CIMMYT spring wheat cultivars. Values represent one-year data (2018 – 19) in raised beds (B) and flat basins (F) planting systems. *P < 0.05, **P < 0.01, ***P < 0.001, <i>italics</i> : P < 0.10, ns: not significant.	146
Supplementary Table 4.4. Min, Max and average and ANOVA significance levels for plants per m ⁻² , spikes per square meter, internode 2 and 3 specific weight (g cm ⁻¹) for 12 CIMMYT spring wheat cultivars. Values represent means across 2018-19 and 2019-20 in raised beds (B) and flat basins (F) planting systems.	146
Table 5.1. List of eight CIMMYT elite spring bread wheat cultivars and advanced lines used in the glasshouse experiments.	150
Table 5.2. Ranges for phenology expressed in days after emergence (DAE) and thermal time after emergence (TT) (base temp. 0°C) and plant height for 8 CIMMYT spring wheat genotypes. Values represent means across 2018 and 2019	155
Table 5.3. Grain yield, yield components and above-ground biomass at maturity from the combined analysis; values represent means across 2018 and 2019.....	156
Table 5.4. Flag-leaf photosynthesis and stomatal conductance (gs; mol m ⁻² s ⁻¹) for eight spring wheat CIMMYT cultivars. Values represent means across 2018 and 2019 across 2018 and 2019.	157
Table 5.5. Phenotypic correlations between grain yield, yield components and physiological traits for eight spring wheat CIMMYT cultivars in glasshouse experiments. Values based on means across 2018 and 2019.	159
Table 5.6. N-use efficiency (NUE), NUE components and flag-leaf and grain N% for eight spring wheat CIMMYT cultivars across 2017-18 and 2018-19 in beds (B) and flat basins (F) in the field experiments at CIMMYT, Sonora, Mexico.	160
Table 5.7. Phenotypic correlations among eight spring wheat cultivars between nitrogen-related traits and radiation-use efficiencies measured in raised beds (B) and flat basins (F) (<i>italics</i>) the field experiment in 2018-19.	161
Table 5.8. Phenotypic correlations among 8 spring wheat cultivars between flag-leaf photosynthesis rate (A _{max}) and stomatal conductance (g _s) in glasshouse experiments (mean 2018 and 2019) and nitrogen-related traits (mean 2017 – 18 and 2018- 19), radiation-use efficiencies and flag-leaf relative chlorophyll content (mean 2018-19 and 2019- 20), grain yield and yield components (mean 2017-18 and 2018-19) in the field experiments in raised beds and flat basins.....	162
Table 6.1. Traits that contribute to the ideal crop ideotype in raised beds (B) in the twelve spring CIMMYT wheat cultivars.	174

Table 6.2. Traits that contribute to the ideal crop ideotype in flat basins (F) in the twelve spring CIMMYT wheat cultivars.	175
Appendix Table 1. Growing conditions for three years (2017-18, 2018-19 and 2019-20) field experiments in the planting systems (PS) raised beds (B) and flat basins (F). ‡Drip irrigation in flat basins in 2019-20.	189
Appendix Table 2. Fungicide and insecticide applications for glasshouse experiments in 2018 and 2019.	191

LIST OF ABBREVIATIONS

%	Percentage
°C	Degree centigrade
AGDM	Above-ground biomass
A_{\max}	Light-saturated net CO ₂ assimilation rate
ANOVA	Analysis of variance
B	Raised beds
BLUE	Best linear unbiased estimator
BMA7	Biomass at seven days after anthesis
BME40	Biomass at forty days after emergence
BMInB	Biomass at initiation of booting
BMPM	Biomass at physiological maturity
CIMMYT	International Maize and Wheat Improvement Center
CHOS _{st}	Water soluble carbohydrate
cm	Centimetre
CV	Coefficient of variation
DTA	Days after anthesis
DTH	Days after heading
DTInB	Days after initiation of booting
DTPM	Days after physiological maturity
ESWYT	Elite Selection Wheat Yield Trial
F	Flat basins
FAOT	Food and Agriculture Organization of the United Nations
FE	Fruiting efficiency
FLcv	Flag-leaf curvature
FLcvs	Flag-leaf curvature visual score
FW	Fresh weight
g	Grams

gs	Stomatal conductance
G	Genotype
GAI	Green Area Index
g m^{-2}	Grams per square metre
g MJ^{-1}	Grams per megajoule
GM2	Grains per square metre
GPS	Grains per spike
GS41	Initiation of booting
GS65	Anthesis
GS65 + 7 days	Seven days after anthesis
GWPS	Grain weight per spike
H^2	Broad sense heritability
HI	Harvest index
Int2L	Internode 2 length
Int3L	Internode 3 length
K_{par}	Light extinction coefficient
LAI	Leaf Area Index
LamPI	Lamina partitioning index
LI%	Light interception
LL	Leaf length
LSD	Least Significant Difference
LW	Leaf width
M	Metre
m^{-2}	Square metre
Max	Maximum
Mean	Average
Min	Minimum
MJ	Megajoule
N	Nitrogen
NDVI	Normalized Difference Vegetation Index

NHI	Nitrogen harvest index
NUE	Nitrogen Use Efficiency
NU _{TE}	Nitrogen Utilization Efficiency
NU _{PE}	Nitrogen Uptake Efficiency
NW	Northwest
p value	Probability
PAR	Photosynthetically Active Radiation
PCA	Principal Component Analysis
PI	Partitioning index
PS	Planting system
PS × G	Planting system by genotype interaction
QTL	Quantitative Trait Loci
r	Coefficient of correlation
R ²	Coefficient of determination
Rht	Semi-dwarfing genes
RUE	Radiation-Use efficiency
RUE_E40InB	RUE from forty days after emergence to initiation of booting
RUE_InBA7	RUE from initiation of booting to seven days after anthesis
RUE_GF	RUE grain-filling
RUE_preGF	RUE pre grain-filling
RUET	RUE total
SM2	Spikes per square meter
SPI	Spike partitioning index
StemPI	Stem partitioning index
TGW	Thousand grain weight
UK	United Kingdom
Y	Year

1 INTRODUCTION

1.1 Wheat world production

At present, there is a global land surface of ~13.4 billion of hectares of which 1.5 billion hectares are used for food production (FAOSTAT, 2018). Wheat is the most widely grown crop with ~216 million hectares of land (**Fig. 1.1**) planted annually producing ~766 million tonnes of grain (**Fig. 1.2**) (FAOSTAT, 2019) and is one of the most important crops globally supplying 20% of the calories and protein in the diet of the human population (Braun et al., 2010). The United Nations has predicted a global population of 9.3 billion will be reached by 2050 (Nations, 2011). Therefore, food supply will need to be doubled by that date to meet the demand and improved crop genetics to develop new cultivars is one of the targets to solve this challenge (Genetics, 2009). The basis of the diet of the global population is the three major staple crops: wheat, maize, rice and soybean with yield improvements of 0.9%, 1.6% and 1.0% and 1.3% per year, respectively, which are far from the 2.5% per year necessary to meet the food demand (Ray et al., 2013). One in seven people worldwide suffer of micronutrient malnourishment as they do not get the enough proteins in their daily diet (Godfray et al., 2010). Another concern that agriculture is facing is climate change with increased frequency of extreme temperatures as well as droughts and floods (Abberton et al., 2016). High temperature has been associated with low yields and faster propagation of weeds and different diseases (Nelson et al., 2009). Climate change has been predicted to increase global temperature by ~ 4°C by the end of the 21th century and threatens to decrease production of grain crops grown in tropical areas (IPCC, 2014). In addition, climate change has negative effects on photosynthetic efficiency (Maliba et al., 2019). Other negative effects of higher temperatures are shorter developmental phases, spike and pollen sterility and a decrease in grain number and grain weight (Zacharias et al., 2014). Therefore, to satisfy the global demand, plant breeders should develop genotypes with an improved radiation-use efficiency, water-use efficiency and tolerance to abiotic stress (Tshikunde et al., 2019). Additionally, the world has experience an increased urbanization that has some negative implications such as land-cover changed over the years (Patra et al., 2018).

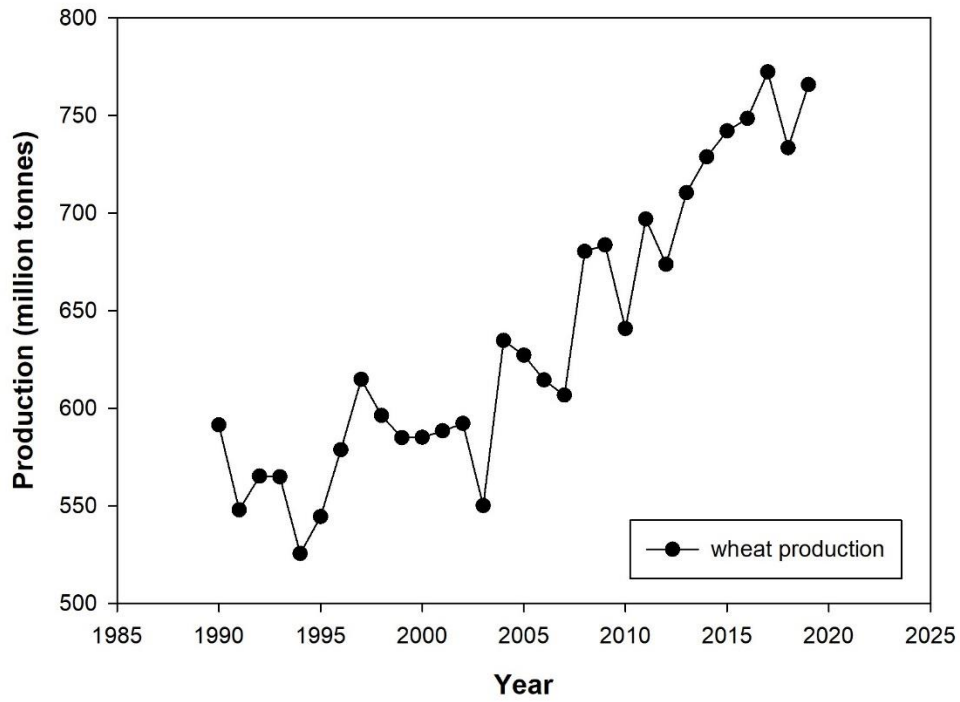


Fig. 1.1 Wheat grain production worldwide from 1990 - 2019 (FAOSTAT, 2019).

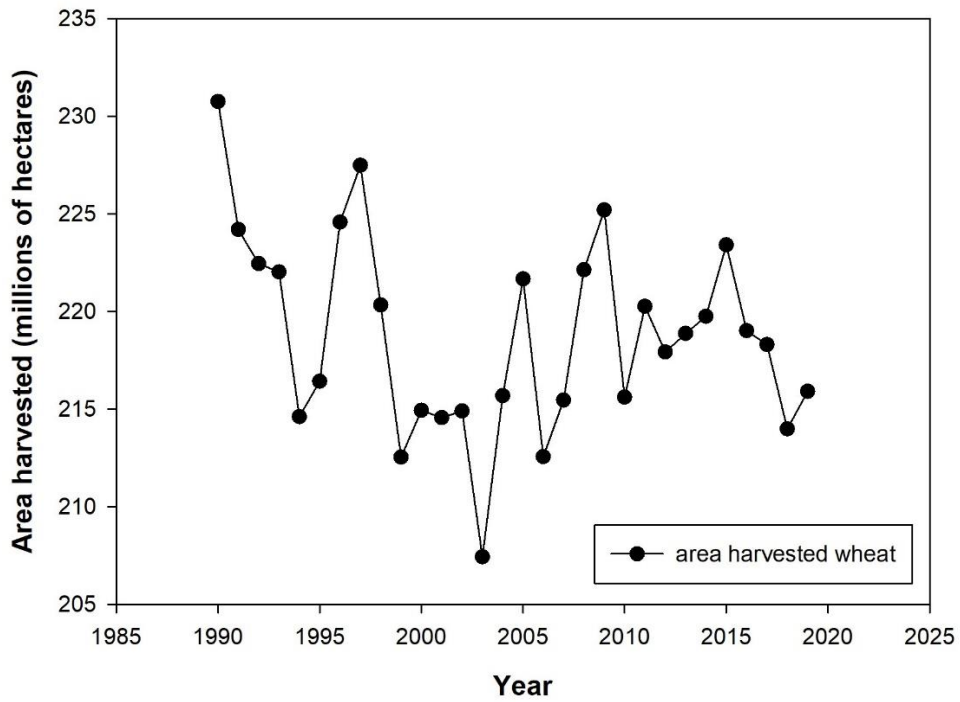


Fig. 1.2. Wheat area harvested worldwide from 1990 - 2019 (FAOSTAT, 2019).

Wheat is one of the first crops to be domesticated (Charmet, 2011). Approximately 95% of wheat corresponds to hexaploid bread wheat (*Triticum aestivum* L.) and the 5% remaining is mostly tetraploid durum wheat (*T. turgidum*) (Salamini et al., 2002; Shewry, 2009). Bread wheat was first domesticated ~ 8000 to 10, 000 years ago in the Fertile Crescent in Northern Iran (Dubcovsky and Dvorak, 2007; Preece et al., 2017). First, there was a hybridization between *T. Urartu* (genome A) and *Aegilops speltoides* (genome B) giving rise to a tetraploid wheat “emmer wheat” (*T. turgidum*) (genome AABB) (Huang et al., 2002). The other hybridization took place between emmer wheat and *Ae. tauschii* (genome D) which gave rise to the hexaploid *T. aestivum* (Salamini et al., 2002; Charmet, 2011; King et al., 2018).

During the Green Revolution in the 1960s and 1970s, there was a huge impact of higher yielding varieties in wheat and rice due to the introduction of the semi-dwarfing genes (*Rht-D1b* and *Rht-B1b*) with the combination of wheat breeding and a better agronomic management (Hedden, 2003). These shorter varieties showed an increased spike partitioning at anthesis and grain number per m², lodging resistance and greater harvest index and grain yield (Hedden, 2003; Slafer et al., 2007). The enhance lodging resistance allowed the application of higher amounts of N fertilizer inputs (Shah et al., 2019).

1.2 Wheat growth and development

Development is considered as the progression of the plant through the life cycle which is independent of growth (Hyles et al., 2020). There are different scales to describe the stages of wheat development such as Zadoks (Zadoks et al., 1974), Haun (Haun, 1973) and Feekes (Feekes, 1941) with the Zadoks scale the most accepted nowadays which applies to any small grain cereal and its stages are easy to identify in the field (Simmons et al., 1985). The Zadoks scale has 10 main stages with 10 sub-stages (Zadoks et al., 1974): germination (GS0 - 09), seedling growth (GS10 -19), tillering (GS20 - 29), stem elongation (GS30 - 39), booting (GS40 - 49), heading (GS50-59), flowering or anthesis (GS60 - 69), grain milk development (GS70 - 79), grain dough development (GS80 - 89) and ripening (GS90 - 99) (**Fig. 1.3**). Factors such as temperature, latitude, day length and moisture have an impact on the duration of developmental phases in wheat crops (Slafer and Rawson, 1994). Canopy expansion starts at crop emergence until spike emergence (SylvesterBradley et al., 2008). Tillering is an important trait for grain yield in wheat since it determines the canopy size and the photosynthetic area as well as the number of fertile shoots (Xie et al., 2016b). Tiller

mortality ceases and tiller number becomes stable just before flowering when the number of spikes is defined (Slafer, 2009). During floral initiation, all spikelets are initiated on the apex and the double ridge stage occurs when half of the spikelets have been initiated (Ochagavía et al., 2018). Grain number and potential grain size are determined during the period from emergence of the penultimate leaf until early grain-filling (Dreccer et al., 2018). The period of “rapid spike growth” (from the initiation of booting to late anthesis) and stem growth overlap and this is when the floret mortality occurs due to the competition for assimilates between the spikes and stems hence affecting grain number per spike (Kirby, 1988; Siddique et al., 1989b; Slafer and Rawson, 1994). The duration of the reproductive phases is affected by changes in response day length and temperature regulated by photoperiod and vernalization sensitivity genes, respectively (González et al., 2002). Canopy senescence occurs when leaf and stem N is transferred to the grain which can be delayed if N and water uptake continue post-anthesis (SylvesterBradley et al., 2008).

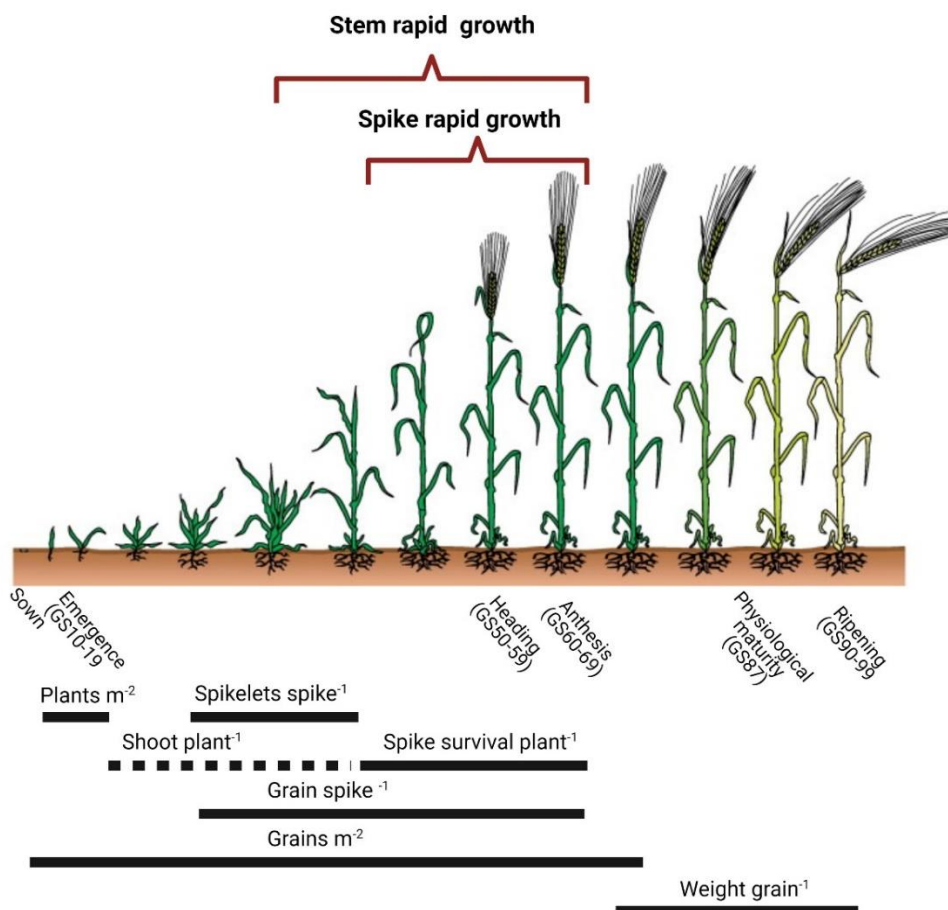


Fig. 1.3. Diagram of growth stages of a wheat plant. Adapted from Sreenivasulu and Schnurbusch (2012).

1.3 Planting systems

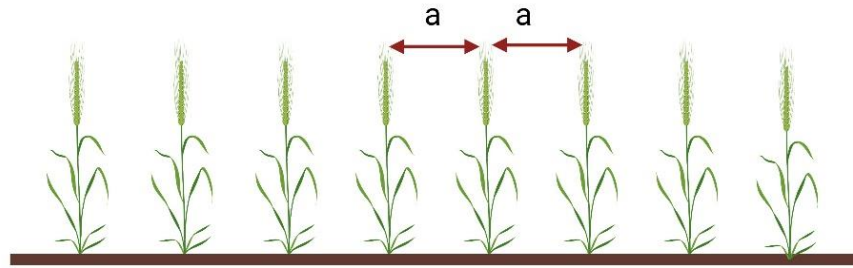
1.3.1 Description of raised beds and flat basins systems

Having the most suitable planting system for the crops is crucial if plant breeders and farmers want to ensure a good establishment and a proper growth of their plants (Iqbal et al., 2021). Wheat crops have been traditionally grown on plains in flat basins systems, especially in irrigated environments (Sayre and Moreno Ramos, 1997) using a flooded irrigation (Fischer et al., 2005). However, researchers and farmers from the Yaqui, Valley in Sonora, Mexico during the 1970s have adopted a raised-bed planting system with irrigation water confined to furrow gaps between the beds, with noticeably better field management and yield increases (Fischer et al., 2005; Tripathi et al., 2005; Majeed et al., 2015).

The traditionally flat planting system consists of plants drilled in rows with the same distance between them using a flood irrigation (Fischer et al., 2005) (**Fig. 1.4**). The raised-bed planting system consists of 2 or 3 rows normally drilled on the top of each bed with a furrow gap between the beds, usually ~ 70 - 90 cm wide (Sayre and Moreno Ramos, 1997). Typically beds are about 25 - 30 cm high with about 50 -70 cm between furrow gaps (Ram et al., 2005). The raised beds are made by moving the soil from the furrow gaps with machinery to the desired location of the bed having as a result a level surface for the plant rows (Ram et al., 2005). These furrow gaps serve as a “channel” for the water which moves upwards towards the top of the bed by evaporation and capillarity and then downwards in the soil of the bed by gravity (Ram et al., 2005).

Some researchers and farmers were concerned by the potential waste of resources in raised beds due to the unplanted area of the furrow gaps (Fischer et al., 2005). However, over the years, farmers and research investigations confirmed that advantages such as lower crop production cost, better yield and greater soil properties were found in raised beds (Fischer et al., 2005). Choosing raised beds for crop production facilitates mechanical cultivation and also because of the rows' orientation and the furrow gaps it facilitates hand weeding, a low cost option for farmers (Majeed et al., 2015). In the next section, the advantages and disadvantages of the two planting systems are further described.

A FLAT BASINS



B RAISED BEDS

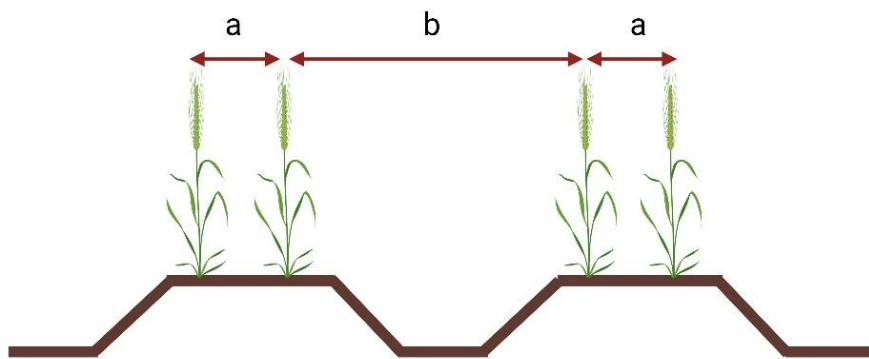


Fig. 1.4. Dimensions for **A** flat basins: same distance between the 8 rows and **B** raised beds: two or three rows per bed with a wider furrow gap. Adapted from Fischer et al. (2005). Created with Biorender.com.

1.3.2 Differences between raised beds and flat basins

Researchers and farmers have found that the implementation of raised beds has several benefits. In raised beds, the seed rates have been reduced from 200 kg ha⁻¹ or more to ~ 80 - 150 kg ha⁻¹ with greater grain yield (Sayre et al., 2005). As mentioned in the previous section, furrow gaps play an important role in the irrigation in raised beds. Having furrow gaps helps to reduce soil compaction (Quanqi et al., 2012) and allows a better water availability for the plants (Wightman et al., 2005) as well as a greater trafficability under irrigation (Tullberg, 2001; Tullberg et al., 2001). Increased transpiration in raised beds caused greater growth and leaf area index compared to the conventional planting system (Li et al., 2008). In environments with low rainfall during the year, the beds system allows a better moisture conservation whereas in areas with heavy rains it can be very effective for drainage (Sayre and Moreno Ramos, 1997).

Additionally, it has been demonstrated in a study of spring wheat in China that the greater ventilation in the raised beds reduces humidity within the canopy which is very useful to avoid diseases and weeds (Fahong et al., 2004; Kiliç, 2010). Water savings in raised beds were found by (Wang et al., 2009) in a spring wheat experiment in China, with 30% water saving in beds compared to flats; similarly Kumar et al. (2010), in a study of spring wheat in India, found 40% water savings and hence an improvement in water productivity and grain yield in raised beds compared to flat basins. In addition, Zaman et al. (2017b) in Bangladesh, showed 14.3% water savings in raised beds compared to flat basins with 15.7% higher grain yield. In rice, the total water use was higher in the flat basins by 42% with an increase of 16% in grain yield, and number of panicles and grains per panicles (Bhuyan et al., 2012). The study of Thind et al. (2010) in India agreed with these studies with a water saving of 49% in wheat crops using raised beds due to the furrow gaps than flat basins.

Lodging resistance has been found to be greater in raised beds compared to flat basins (Kiliç, 2010). For example, thicker basal internodes with higher dry matter but shorter basal internode length in raised beds resulted in greater lodging resistance in wheat this planting system compared to flat basins (Fahong et al., 2004). In addition, less lodging resistance is more usual in flats because in this system less light penetrates to the basal internodes in the canopy which are the most important for lodging resistance (Freeman et al., 2007).

In terms of fertilizer, raised beds tend to have greater fertilizer nitrogen-use efficiency (NUE) rather than flat basins. For example, Fahong et al. (2004) found 10% greater NUE in raised beds than flat basins as well as Limon-Ortega et al. (2000) with 13.2% NUE higher in beds. In addition, Majeed et al. (2015) found higher NUE (25%) and nitrogen uptake efficiency (15%) in wheat crops under raised beds compared to the conventional flat system.

Higher grain yield in raised beds compared to flat basins is mainly reported in various studies comparing systems in different environments and cultivars. Zhang et al. (2007) found in a field experiment using winter wheat that grain yield was 5.2% higher in beds than flats. In Pakistan, grain yield in wheat crops was 13% higher in beds than the conventional planting method as well as 30% higher in maize crops (Hassan et al., 2005). Other studies in wheat have also shown better grain yield in raised beds compared to flat basins such as Meleha et al. (2020) in Egypt, Bakker et al. (2007) in Australia, Mollah et al. (2009) in Bangladesh, Ahmad et al. (2010) in Pakistan, Kong et al. (2010) in China and Jat et al. (2011) in India. However, Fischer et al. (2005) suggested that raised beds might be less

beneficial for short, erect and early and low tillering genotypes since they may not compensate as well for resources in the furrow gaps as taller and high tillering genotypes. Tanveer et al. (2003) and López-Castañeda et al. (2014) found greater grain yield in flat basins than raised beds in wheat crops. The combined advantages of raised beds presented above provide better profitability to farmers. For example, a study carried out in Pakistan showed 29% higher economic profits by choosing raised beds rather than the conventional flat system (Majeed et al., 2015).

The total global wheat area planted using raised beds has not been quantified in the literature. However, from personal communication at CIMMYT, CENEB between Prof Matthew Reynolds (Head of Wheat Physiology) and Ivan Ortiz-Monasterio (Principal Scientist), it has been estimated that around 10% of the irrigated fields globally are planted using raised beds. Future studies are needed to estimate more exactly the percentage of the total global wheat area planted in raised beds vs flat basins.

1.4 Genetic gains of grain yield and associated traits

Evans (1993) defined Yield Potential (YP) as the yield of a cultivar when grown in an adapted environment where stress, lodging, diseases and weed are successfully controlled. During the Green Revolution in the 1960's and 1970's, yield potential in wheat cultivars was raised with the introduction of semi-dwarf genes that achieved a reduction in stature and lodging, allowing increases in N fertilizer inputs, greater spike growth and a markedly increased grain number per unit area (Reynolds, 1996). Increases in grain yield in wheat crops have been reported due to higher grain number and harvest index associated with increased spike partitioning and fruiting efficiency (Foulkes et al., 2011). Quantitatively grain yield (GY) can be explained by the equation (1.1) (Reynolds et al., 2009):

$$GY = LI \times RUE \times HI \quad (1.1)$$

Where LI is radiation interception; RUE is radiation-use efficiency (ratio of above-ground dry matter produced per unit radiation intercepted); and HI is harvest index (partitioning of above-ground dry matter to grain yield).

Evaluating genetic gains in grain yield and the traits associated with those increases is crucial for plant breeders in order to develop new strategies to improve yield further (Beche et al., 2014). A study in NW Mexico in CIMMYT spring wheat cultivars released from 1950 to 1982 showed grain yield increases by $59 \text{ kg ha}^{-1}\text{yr}^{-1}$ (Waddington et al., 1986). In the UK, for 13 winter wheat cultivars (years of release from 1908 - 1986) reported an association between grain yield progress and harvest index (Austin et al., 1989) and a genetic gain of 38 kg ha^{-1} per year. Another study in NW Mexico showed genetic gains in grain yield in spring wheat cultivars (years of release from 1962 - 1988) due to higher flag-leaf photosynthetic rate, stomatal conductance, canopy temperature depression and radiation-use efficiency in the pre-anthesis period (Fischer et al., 1998). Other investigations have also found a positive relation between genetic variation in leaf photosynthetic rates and grain yield in winter wheat (Jiang et al., 2003) and spring wheat (Gutiérrez-Rodríguez et al., 2000). In the UK, eight winter cultivars released from 1972 - 1995 showed a grain yield progress of $0.12 \text{ mg ha}^{-1}\text{yr}^{-1}$ which was positively associated with HI and above-ground biomass (AGDM) (Shearman et al., 2005). Another study in China examined 13 milestone wheat cultivars and two advanced lines released from 1969 to 2006 showing yield progress of $62 \text{ kg ha}^{-1} \text{ yr}^{-1}$ associated with increased grains m^{-2} , biomass and HI and reduced plant height (Xiao et al., 2012). In addition, a more recent study showed genetic gains in grain yield in spring wheat cultivars (1940 - 2009) of $29.9 \text{ kg ha}^{-1}\text{yr}^{-1}$ associated with HI, biomass and grains m^{-2} as well as photosynthetic rates before and after anthesis (Beche et al., 2014). A study in 12 CIMMYT spring wheat semi-dwarf cultivars released from 1966 to 2009, found a genetic grain yield of $30 \text{ kg ha}^{-1} \text{ yr}^{-1}$ which was associated with biomass at harvest and grain weight (Aisawi et al., 2015). Since there is a theoretical limit of 0.65 to increase HI (Austin et al., 1980) which is being approached in some regions and countries, the most feasible way to increase grain yield in the future may be due to improvements in radiation-use efficiency (Gutiérrez-Rodríguez et al., 2000; Molero et al., 2019). In addition, it has been demonstrated in spring wheat that grain yield is mainly sink limited under optimum conditions during grain filling (Acreche et al., 2009) (see **Chapter 1.6** for more information in source-sink limitations).

1.5 Light interception

Canopies must intercept as much radiation as they can in the 400 - 700 nm bandwidth which is preferentially absorbed by chlorophyll, resulting in transmitted light that is depleted in red and blue and enriched in far-red wavelengths (Murchie and Reynolds, 2012). The

photosynthetically active radiation denotes the portion of solar radiation that can be used by plants (400 - 700 nm as mentioned above) (Burgess, 2017; García-Rodríguez et al., 2020). The light interception depends mainly on canopy structure (Zhang et al., 2016; Tao et al., 2018). In fact, light is considered as the most heterogeneous environmental factor that influences canopy growth and survival (Burgess, 2017). Light interception takes place mainly on the leaves; however, other plant organs can absorb amounts of radiations such as stems, petioles, leaf-sheaths and other reproductive organs (Murchie and Reynolds, 2012). Several factors influence light interception among the crop canopies such as leaf orientation and shape, arrangements, geographic location and changes in spectral distribution of PPFD (photosynthetic photon flux density) (Nobel et al., 1993). The light interception by the canopy leaf layers decreases from the top to the bottom of the canopy whereas the photosynthetic efficiency in leaves increases from the bottom to the top of the canopy due to light saturation of photosynthesis in upper leaves (Niinemets, 2007). An optimal light utilization occurs when the incident radiation is uniformly distributed among the leaf layers (Burgess, 2017). Some leaf/canopy traits such as leaf area index (LAI) and specific leaf weight (SLW; leaf dry matter per unit area) are crucial for the ability that leaves have to capture light and photosynthesize (Yang et al., 2017). Furthermore, plant growth depends on the ability to intercept PAR and convert it into biomass (Hikosaka, 2005). The solar radiation that is intercepted depends on the 3-dimensional arrangements of leaves for a given leaf area index (Murchie and Reynolds, 2012). In addition, the term photoacclimation refers to the process where the plants change their structure and composition over some periods of time that can be days or weeks in response to the light environment eg., light intensity (Townsend et al., 2018). Photoacclimation has the ability to convert the radiation intercepted into biomass and yield but also decreased the absorbed solar energy (Townsend et al., 2018). Another important factor is the light extinction coefficient (k) that depends on the canopy structure, species type and sowing pattern (Soleymani, 2016) so that radiation interception is calculated by the equation (1.2) (Murchie and Reynolds, 2012):

$$I = I_0 \exp(-kL) \quad (1.2)$$

Where I refers to radiation at a specific point in the canopy, I_0 refers to incident radiance at the top of the canopy, L refers to leaf area index, and k is the light extinction coefficient for a given waveband.

1.5.1 Traits to enhance light interception

1.5.1.1 Delayed senescence / stay green

Increasing total photosynthesis can be achieved by maintaining green leaf area for a longer period of time, especially after anthesis (Richards, 2000). Senescence is the last process of the entire plant in monocarpic crops that involves degradation of chlorophyll and nutrient remobilization processes (Distelfeld et al., 2014; Chibane et al., 2021). In other words, senescence is a process that leads to the death of a cell, an organ or the whole plant (Lim et al., 2003). During this period, physiological, biochemical, metabolic and transcriptomic changes take place in the plant (Zhang and Zhou, 2013; Sultana et al., 2021). Normally, senescence can be monitored according to the leaf changes in greenness and chlorophyll content during grain filling which can be scored at leaf level or canopy level (Pask et al., 2012a; Shrestha et al., 2012). Xie et al. (2016a) demonstrated in a study of a bread wheat \times spelt mapping population with delayed senescence leaves were able to maintain high photosynthetic rate longer and to produce more assimilates in order to maximize grain yield. The remobilization of nutrients to the grain is influenced by abiotic factors such as drought and high temperatures but also by biotic factors such as pathogens (Joshi et al., 2007; Distelfeld et al., 2014). The term “stay green” refers to the capacity that a genotype has to conserve for a longer period of time their foliar greenness compared to a standard genotype during the grain-filling period (Thomas and Smart, 1993; Sultana et al., 2021). Functionally “Stay green” genotypes have been reported to have greater grain yield production acquiring and assimilating more carbon and nutrients than other genotypes (Luche et al., 2015; Rebetzke et al., 2016b). In modern wheat, light interception is close to 100% canopy closure at around onset of stem extension to the onset of flag leaf senescence at around mid-grain filling (under favourable conditions); therefore increases in light interception could be achieved if green canopy could be prolonged during grain filling (Reynolds et al., 2005). Measurements of genetic variation flag-leaf greenness in winter wheat have been assessed using the Minolta SPAD meter under fully irrigated and unirrigated conditions with a positive association with grain yield (Verma et al., 2004). Recently remote sensing methods to measure senescence at the canopy level use spectral reflectance techniques, e.g. the normalized difference vegetative index (NDVI) using the NTech Greenseeker (Lopes and Reynolds, 2012; Gaju et al., 2016). Bogard et al. (2011) showed in a field study on a winter wheat Toisonder \times CF9107 doubled-haploid population that delayed leaf senescence was associated with increased grain yield but decreased protein

concentration. Additionally, a glasshouse study in durum wheat mutant lines demonstrated increases in grain weight and yield due to a delayed senescence (Spano et al., 2003).

1.6 Radiation-use efficiency

Radiation-use efficiency is an important trait for raising biomass and grain yield (Murchie and Reynolds, 2012). Any genetic increase in RUE could increase above-ground biomass and hence grain yield if HI is maintained at current levels (Molero et al., 2019). RUE refers to the increment of above-ground dry-matter divided by the increment intercepted PAR for the phenophase calculated (Monteith, 1977). It requires measurements of daily radiation interception over the relevant period of time is calculated RUE by positioning instruments above and below the canopy and sequential measurements of biomass (Murchie and Reynolds, 2012). RUE is reduced by some abiotic stress factors such as low water availability (Jamieson et al., 1995), temperature (Goyné et al., 1993; Chaudhary et al., 2016) and nutrients (Ahmad et al., 2012; Zhu et al., 2016). In winter wheat cultivars (released from 1972 - 1995), associations between RUE pre-anthesis and grain yield were found (Shearman et al., 2005). A recent study in a spring wheat high biomass association panel in NW Mexico showed a genetic variation in RUE from initiation of booting to anthesis + 7 days from 1.37 to 3.21 g MJ⁻¹ and during grain-filling period ranged from 0.96 to 2.96 g MJ⁻¹ (Molero et al., 2019).

1.6.1 Traits to enhance radiation-use efficiency

1.6.1.1 Canopy architecture

Canopy architecture is considered as the arrangement of each plant organ among a canopy (Barthélémy and Caraglio, 2007) which can vary within and between species (Burgess, 2017). Modification of canopy architecture traits in bread and durum wheat to increase photosynthetic capacity has been a target in the last decades in breeding programs at the International Maize and Wheat Improvement Center (CIMMYT) (Reynolds et al., 2012a). Canopy architecture influences the light intercepted by the canopy as well as the radiation-use efficiency; increasing RUE during the period between onset of stem elongation and anthesis is especially important for the determination of grain number and yield (Richards et al., 2019). Modifications in canopy architecture have led to improvements in yield (Long et al., 2006; Zhu et al., 2010; Richards et al., 2019). Improvements in canopy structure (more vertical leaf angle at the top of the canopy) avoid light saturation of photosynthesis in the upper leaves in the canopy leading to a more efficient canopy photosynthetic rate and crop productivity (Zhu et al., 2010). Plants with erect leaves are

expected to increase leaf photosynthetic rates in the lower leaves and above-ground biomass when the leaf area index (LAI) is above 3 (Richards et al., 2019). Valladares and Niinemets (2007) and Burgess (2017) explained that the most efficient canopy architecture is where all the leaves in the plant are well illuminated and light is distributed uniformly across leaf layers. A “smart canopy” has been proposed in which leaves at the top of the canopy are upright and the leaves at the bottom of the canopy are more horizontal to maximize the light interception whilst minimizing light saturation and so enhance grain yield (Mantilla-Perez et al., 2020). Studies in rice demonstrated the advantages of erectophile cultivars of leaf photosynthetic rates, crop growth and grain yield (Sinclair and Sheehy, 1999; Sakamoto et al., 2006). In maize a study using two isogenic lines demonstrated that the line with upright leaves produced 40% more grains compared with the line with horizontal leaves due to a better light interception and leaf photosynthetic rate (Pendleton et al., 1968). Similarly, improvements in biomass have been reported in wheat due to the effect of upright leaf angle since it led to a greater photosynthetic capacity especially during the vegetative growth (Parry et al., 2011). Additionally, erect leaves may allow a large leaf area index necessary for provision of nitrogen during grain filling whilst enabling light penetration so that the leaves contribute to net carbon gain (Sinclair and Sheehy, 1999). Recent studies in spring wheat in Australia using a CSIRO 4-way MAGIC population have evaluated how genetic variation in leaf angle determined grain yield using a visual score (Richards et al., 2019) in which erect canopies had a greater grain yield (13%) than canopies with lax leaves due to higher biomass (11%). The latter study measured canopy architecture using a visual score that allows identifying the most erect plants in large trials (Richards et al., 2019). In this method, a score of 10 was given when 100% of the leaves at the top of the canopy were floppy, a score of 6 when 60% of the plants were erect and a score of 1 when 100% of the leaves were erect etc. However, studying canopy architecture of individual leaves under field experiments can be challenging due to overlapping leaves and environmental conditions such as wind (Mantilla-Perez et al., 2020). In some species such as rice, maize (see references above) and in winter wheat in UK (Shearman et al., 2005), canopy architecture may already have been optimized by plant breeding with breeders selecting for more upright leaves optimized. However, these canopy architecture traits may not be fully optimized in spring wheat, especially in bread wheat cultivars at CIMMYT.

1.6.1.1.1 Leaf angle and curvature

Leaf angle is the inclination between the leaf blade midrib and the stem which is considered as the most important canopy architecture trait (Mantilla-Perez and Salas Fernandez, 2017) for its influence on light interception, photosynthesis and canopy density (Wit, 1965; Mantilla-Perez and Salas Fernandez, 2017). Modelling analysis has demonstrated that a more erect leaf angle from the top to the bottom of the plant increased carbon uptake up to 40% compared to horizontal leaves (Long et al., 2006). Canopies with erectophile leaves have a correspondingly low light extinction coefficient (k) than those with planophile leaves (Burgess, 2017). A study in maize lines in glasshouse conditions demonstrated that plants with erect leaves had higher light interception capacity compared to the ones with lax leaves (Cabrera-Bosquet et al., 2016). To date, there are no studies in wheat that have evaluated flag-leaf angle and curvature separately. However, in a study in rice, flag leaf angle was measured as the angle between the leaf blade and the stem, whereas the term “curvature radius” was calculated based on the horizontal distance between leaf tip and stem and the distance between leaf tip and ground surface (Song et al., 2013). Some studies in rice and barley have reported that the hormone brassinosteroids (BRs) are key regulators for leaf angle (Saisho et al., 2004; Sakamoto et al., 2006; Mantilla-Perez and Salas Fernandez, 2017). A QTL analysis in durum wheat was reported by Isidro et al. (2012) in a glasshouse experiment in which genomic regions were identified on chromosomes 2A, 3A, 3B, 5B and 7A controlling the angle of the flag-leaf and penultimate leaf explaining 8.9 - 37.2% of the variation. Using the same cultivars but under field conditions, QTLs were identified on chromosome 7A controlling the flag-leaf and on chromosomes 2B and 4B for the penultimate leaf (Isidro et al., 2012). Other QTLs were identified in winter wheat (Yang et al., 2016) and spring wheat (Richards et al., 2019).

1.6.1.1.2 Leaf size and area and clumping

In hot and arid environments with high light intensities, canopies tend to have smaller leaves (Bonan, 2002; Burgess, 2017). However, leaves in shaded environments are larger in order to capture more light (Parkhurst D.F. and OL., 1972). Leaf area index (LAI) is defined as the leaf lamina area per unit ground surface area (Chen and Black, 1992). Remote sensing is a feasible method to estimate LAI in large trials non-destructively (Tan et al., 2018; Tan et al., 2020). The radiation penetration deeper and deeper in the canopy depends on the 3-dimensional arrangements of leaves for a given LAI and this would depend on canopy architecture traits such as leaf size, clumping, leaf thickness and angle (Murchie and

Reynolds, 2012). Some studies in wheat have demonstrated erectophile canopies have greater LAI and grain yields (Choudhury, 2000; Parry et al., 2011). Foliage clumping refers to the way in which leaves are spatially organized in a canopy (Chen and Black, 1992). Leaves are normally distributed and grouped in some sub-canopy structures, for example, foliage clumps in shrubs, and rows in crops and tree crowns, branches, and shoots in forests (Chen and Black, 1992). Leaf clumping is a variable that influences the transmission of the direct and diffused light among the canopy (Burgess, 2017). Other variables such as shape and size can also alter the transmission of diffused light among the plant and hence alterations in photosynthesis under low and high light conditions can be found (Valladares and Niinemets, 2007).

1.6.1.2 Vertical N distribution in canopy

The optimization of nitrogen distribution is considered as one of the most important variables for carbon gain and a key target for crop productivity (Hikosaka, 2014). The “optimization theory” (Hirose and Werger, 1987) suggested that vertical lamina N distribution in the canopy may be optimized to maximize the photosynthesis rate in the whole plant. This theory proposes that lamina N distribution is related to the light gradient, in which leaf lamina N mass per unit leaf area (SLN) follows an exponential function of the leaf lamina with a downward cumulative N, showing an extinction coefficient for N (KN) equal to that for light (KL) (Equation 1.3):

$$nL = K(Nt - nbLAI_t)e^{-KLAI_c} + nb \cdot 1 - e^{-KLAI_t} \quad (1.3)$$

Where nL = the nitrogen content per area; K = light extinction coefficient; Nt = total amount of leaf canopy nitrogen; nb =leaf nitrogen per area (not involved in photosynthetic process); LAI_c is the leaf area index (LAI) from the top of the canopy and LAI_t the total leaf area index (LAI).

Canopy photosynthesis is maximized when nitrogen is distributed, therefore the N gain is equal among the leaves in the canopy (Field, 1983). Additionally, it has been demonstrated that an optimal nitrogen distribution is steeper under direct and diffuse light rather than only under diffuse light (Hikosaka, 2014). Moreau et al. (2012) explained in a study in spring wheat in a field experiment that N extinction coefficient with respect to light (b) varied with N supply and cultivar, and a relationship was observed between b and the size of the canopy. In addition, it was shown that under low N inputs, the optimum distribution of leaf N in

relation to the light distribution was steeper compared with high N inputs. A glasshouse experiment in the Netherlands using spring wheat demonstrated a relation between leaf photosynthetic rate at saturating irradiance (A_{\max}) and N content per unit area of leaves and explained that vertical N distribution could change during the crop growth (Dreccer et al., 2000). The later study also showed that vertical distribution of leaf N changed according to the gradient of absorbed irradiance and was related to N availability, in which at high N the leaf N vertical distribution tended to be more uniform because of less light intensity fluctuations, and at low N the leaf vertical N distribution was steeper. Other factors such as leaf age also affects the distribution of N in the canopy (Dreccer et al., 2000; Ye et al., 2018).

1.6.1.3 Leaf photosynthesis and leaf photosynthesis per unit N

In the last decades, increasing photosynthesis is a key target to achieve increases in grain yield and consider a key crop improvement trait for plant breeders (Mann, 1999; Long et al., 2006). Irradiance, duration, quality and timing of light are important to have greater photosynthesis and for a good growth and development in crops (Geiger, 1994). In China, a field study in spring wheat was carried out and showed an increase in the photosynthetic capacity rate per unit leaf area with year of release (Jiang et al., 2003). Light-saturated photosynthetic rate (A_{\max}) at the leaf level differs depending of the environmental conditions and metabolic processes during the crop cycle (Horton, 2000). The photosynthetic photon flux density (PPFD) at leaf level and canopy level are crucial for CO₂ assimilation and photosynthesis (Duncan, 1971). The rate of photosynthesis increases until it is saturated (A_{\max}) when the photon flux density increase (Murchie and Niyogi, 2010). Genetic gains in grain yield in spring wheat cultivars were associated with A_{\max} and stomatal conductance in NW Mexico (Fischer et al., 1998; Reynolds et al., 2000a) while other studies have not found a significant association (Sadras et al., 2012; Driever et al., 2014). The photosynthetic process starts with the absorption of light by chlorophyll within the thylakoid membrane of chloroplasts (Murchie and Niyogi, 2010). Once the chlorophyll is in an excited state, an excitation energy is transferred to the PSII and PSI reaction and the photosynthetic electron transport is initiated (Murchie and Niyogi, 2010). The efficiency of the photosystem II (PSII) can be estimated by the ratio of variable chlorophyll fluorescence to maximal fluorescence (F_v/F_m) (Murchie and Niyogi, 2010). Light saturation of the flag leaf occurs during some periods of the day where photoinhibition takes place (Murchie et al., 1999) related to strong solar energy causing damage to the PSII (Demmig-Adams and Adams Iii, 2003).

Photoprotection is a process that controls the absorption and dissipation of light energy especially when the chlorophyll is absorbing more energy than can be used in photosynthesis (Murchie and Niyogi, 2010). This process is not only for photodamage to the photosynthetic apparatus and also include some photoprotective mechanisms (Chow, 1994).

Studies in spring wheat demonstrated that ~30% of the incident radiation is intercepted by the spikes (Sanchez-Bragado et al., 2014). Therefore, improvements on RUE can be achieved by considering genotypic variation of spike photosynthesis (Molero and Reynolds, 2020). Additionally, spikes play an important role as a source during grain filling period under yield potential conditions but also under drought environment (Araus et al., 1993a; Tambussi et al., 2005; Maydup et al., 2010). However, there are only a few studies that evaluate spike photosynthesis (Maydup et al., 2010; Sanchez-Bragado et al., 2014; Sanchez-Bragado et al., 2016; Molero and Reynolds, 2020).

1.6.1.4 Rubisco capacity

Rubisco is the most abundant enzyme in plants and catalyse the assimilation of CO₂ (Reynolds et al., 2009; Perdomo et al., 2021). Although this enzyme plays an important biochemical role, it is also consider slower than other enzymes in central metabolism (Bar-Even et al., 2011). Rubisco has been studied for genetic engineering in order to improve photosynthesis (Parry et al., 2007). It has been demonstrated in studies in Arabidopsis that Rubisco is affected by some environmental factors such as CO₂ and growth temperature (Cavanagh and Kubien, 2014). Rubisco accounts for up to 50% of leaf soluble protein and 25% of leaf N (Reynolds et al., 2009; Parry et al., 2013). Since rubisco catalysis is slow it requires large amounts of it to provide higher photosynthetic rates (Lin et al., 2014). Parry et al. (2011) reviewed approaches to enhance above-ground biomass in C3 crops such as wheat, maize and rice through the optimization of the rubisco properties. Other recent reviews were carried out by (Murchie and Reynolds, 2012; Schuler et al., 2016; Sharwood et al., 2016).

One strategy to increase the amount of Rubisco in the chloroplast especially in high temperatures environment in which the internal CO₂ concentrations are low (Parry et al., 2011). However, this may not be a feasible strategy since it requires a higher nitrogen concentration (Parry et al., 2011). Strategies to enhance RUE due to changes in the efficiency of Rubisco are possible with the introduction of traits to reduce photorespiration from C4 species into C3 species such as wheat and rice (Reynolds et al., 2012b). Photorespiration is a metabolic process in which the 2-phosphoglycolate (2PG) is converted

into 3-phosphoglycerate (3PGA) with a O₂ uptake and a CO₂ release (Hagemann et al., 2016). Higher specificity of Rubisco for CO₂ and higher catalytic rate of Rubisco are some avenues to increase RUE (Reynolds et al., 2000b). The introduction of an effective single-cell CO₂ concentrating mechanism (CCM) has been proposed to improve the performance of Rubisco in C3 crops (Whitney et al., 2010; Price et al., 2012; Zarzycki et al., 2013). For example, C4 species and cyanobacterias have a CCM that utilize form of Rubisco faster than C3 crops, in which Rubisco has lower CO₂ affinity (Whitney et al., 2010). However, research in rice has not found significant positive effects on photosynthesis by incorporating CMM (Taniguchi et al., 2008).

1.7 Spike fertility and fruiting efficiency

Grain number (m⁻²) is a key trait determining grain yield that is established during the rapid-spike growth period when assimilate allocation to the spike determines floret survival affecting final grain number (Fischer, 2008; Zhang et al., 2019). Grain number can be calculated according to equation (1.4) (Fischer, 2008):

$$GN = SEP \times CGR \times SPI \times FE \quad (1.4)$$

Where GN = grains per m², SEP = duration of stem elongation phase (days); CGR = crop growth rate (g m⁻² d); SPI = above-ground biomass partitioning to spike; FE = fruiting efficiency (grains g⁻¹).

Grain number is affected by variation in radiation, temperature and the duration of the rapid spike growth period (Fischer, 2008). A study carried out in Argentina and NW Mexico in spring wheat cultivars showed that genetic variation in photosynthetic active radiation (PAR) intercepted during the spike growth period was positively associated with grain number per m² (Abbate et al., 1997). Several investigations under field conditions showed that the genetic variation in grain number was linked to the spike dry matter at anthesis and related to a competition for assimilates between spikes and stems (Fischer and Stockman, 1986; Miralles and Slafer, 2007). Foulkes et al. (2011) explained that one feasible way to improve grain number and HI could be distributing assimilates among the plant organs at anthesis in order to favour spike growth, whilst maintaining post-anthesis photosynthetic capacity. Several studies in wheat cultivars demonstrated that increasing spike partitioning index (SPI) increased grain number by increasing spike DM at anthesis (Slafer et al., 1990;

Gaju et al., 2009). Alternatively genetic improvement in grain number has been reported due to higher fruiting efficiency (Dreccer et al., 2009; Bustos et al., 2013; Aisawi et al., 2015). Fruiting efficiency is defined as the number of grains produced per unit of spike dry weight at anthesis (Slafer et al., 2015). Genetic variation in FE in the range 41.5 – 141 has been found in spring wheat (García et al., 2014; Aisawi et al., 2015; Rivera-Amado et al., 2019; Sierra-Gonzalez et al., 2021). Ghiglione et al. (2008) proposed two pathways to enhance fruiting efficiency: i) increase assimilates within the spike for the florets during the spike growth before anthesis period and ii) a reduced demand of assimilates by the florets so proximal florets would leave more assimilates available for the distal florets. In addition, it has been demonstrated that increasing FE may decrease grain weight (Gaju et al., 2009; Ferrante et al., 2012). However, other studies have not found any relation between these two traits (González et al., 2014).

1.8 Dry-matter partitioning

Dry-matter partitioning can be described as the end result of coordinated processes that affects the dry matter distributed among the organs of a plant (Marcelis, 1996). A feasible strategy to boost harvest index might be by enhancing the partitioning to spike growth at the expense of dry-matter of stem and other organs such as glumes, paleas, lemmas, rachis, palea, etc. (Foulkes et al., 2011). The introduction of *Rht-B1b* and *Rht-D1b* alleles in wheat crops allowed increases in grain yield by increasing dry matter allocation to the spikes and the number of grains per spike and lodging resistance with a slightly decrease in biomass (Gale and Youssefian., 1985; Hoogendoorn et al., 1990) and increasing dry-matter to the spikes (Brooking and Kirby, 1981). In addition, it has been found that these alleles are associated with an increased in the photosynthetic capacity (Morgan et al., 1990). Semi-dwarf cultivars tend to have a leaf size reduction but a compensation with increased photosynthesis rate per unit leaf area; therefore, biomass is only slightly reduced than taller cultivars (Flintham et al., 1997). Other studies have shown that reductions in leaf area affect the photosynthetic capacity and therefore affect biomass (Reynolds et al., 2009; Foulkes et al., 2011). An increase in spike dry matter at anthesis in *Rht* semi-dwarf isolines was associated with a greater grain number (Miralles and Slafer, 1995). During stem elongation there is an overlap of stem and spike growth so reduced stem partitioning is likely increases spike partitioning (Brooking and Kirby, 1981). Therefore, Richards (1996) suggested that a reduced stem dry matter might be achieved by reducing the peduncle length without reducing the total canopy height. Stem internodes include the peduncle, penultimate and

lower internodes (Ehdaie et al., 2006). Dry-matter partitioning during stem elongation (GS31 - 65) among the organs of the plant will determine the source-sink orientation during grain filling (Kumakov et al., 2001).

Some studies have shown genetic variation of dry-matter partitioning at anthesis. Genetic variation in spring wheat cultivars has in spike partitioning index has been reported in Mexico by Reynolds et al. (2001) with ranges from 0.19 to 0.21 and Gaju (2007) from 0.22 to 0.27. In addition, a study carried out in Australia in spring wheat reported genetic variation in SPI from 0.16 to 0.29 (Siddique et al., 1989b). A field study carried out in winter wheat in UK by Shearman et al. (2005) reported SPI ranges from 0.12 - 0.21. Genetic variation in leaf lamina partitioning at anthesis in 8 winter wheat in UK wheat cultivars by Shearman (2001) ranged from 0.19 to 0.21. Aisawi et al. (2015) showed genetic variation for true-stem and leaf sheath partitioning index in 12 historic spring wheat cultivars during anthesis + 7 days (0.52 - 0.57). More recent studies in spring wheat in Mexico reported values for SPI of 0.21 to 0.26, stem partitioning index (StemPI) of 0.32 to 0.41 and leaf lamina partitioning index (LamPI) of 0.18 to 0.23 (Rivera-Amado et al., 2019). The latter study also demonstrated ranges of peduncle length of 7.1 to 14.5 cm, internode 2 length from 7.0 to 10.9 cm and internode 3 length from 6.3 to 8.0 cm; the peduncle represented 11.8% of above-ground dry-matter whereas internode 2 and 3 represented 25.5% and 19.1% respectively. In addition Sierra-Gonzalez et al. (2021) in her study in spring wheat in Mexico showed ranges for SPI from 0.21 to 0.23, StemPI from 0.46 to 0.57 and LamPI from 0.17 to 0.26.

The dry-matter remobilization from source to sink organs during grain-filling influence the grain yield (Merah and Monneveux, 2015). Additionally, it has been explained that dry-matter for the grain is obtained by the carbon fixed pre-anthesis and carbon accumulated post-anthesis (Chen et al., 2014). In a study in bread and durum spring wheat, it has been demonstrated that 60% of the dry-matter accumulation of the grain is accounted by the water soluble carbohydrates (Ehdaie et al., 2006). In addition, it has been reported a strong association between stem WSC and HI in a study in spring and winter wheat in Australia (Zhang et al., 2012).

1.9 Source-sink balance

The interaction between the source and the sink traits are important for plant breeding programs to enhance yield in wheat (Lichthardt et al., 2020). The sink capacity refers to the

total number of grains per unit area and their potential size (Zhang et al., 2010; Lichthardt et al., 2020) and is considered as the material importer and consumer (Foyer and Paul, 2001). In contrast, source refers to an organ that produces and exports assimilates to the sink (Marcelis, 1996). Sink strength refers to the capacity of the organs to store assimilates (Asseng et al., 2016). Some factors influence the source limitations during grain-filling such as leaf area that increase the light intercepted among the canopy and the photosynthetic capacity (Lichthardt et al., 2020). Source - sink limitation is affected by some environmental factors like temperature, light, humidity, CO₂ concentrations and soil quality (density, pH, nutrients, etc.) (Chang et al., 2017). Source-sink balance plays an important role in determining yield which becomes apparent from the double ridge stage to the end of the grain-filling (Lichthardt et al., 2020). It has been reported in a study in spring wheat that grain growth is co-limited during the grain-filling period (Acreche and Slafer, 2009). Other studies in spring wheat cultivars containing 7DL.7Ag translocation found increases in RUE post-anthesis by increasing sink strength due greater light interception during booting (GS40 - 49) (Reynolds et al., 2005). Source-sink manipulation treatments such as shading, defoliation and de-graining have demonstrated that grain growth is mostly sink-limited during grain filling period under favourable conditions (Borrás et al., 2004). Some investigations in wheat have reported that grain yield is co-limited rather than source limited in modern cultivars, i.e. more sink limited during early to mid-grain filling but source limited during later grain filling (Savin and Slafer, 1991; Slafer and Savin, 1994). In addition, a study in winter wheat using a shading treatment also reported that yield was co-limited by source and sink (Beed et al., 2007). However, a study in bread wheat cultivars found that defoliation after anthesis did not show any negative effects on grain yield or grain weight (Ahmadi et al., 2009).

1.10 Main objectives and hypotheses

Main objectives:

- Evaluate the genetic variation of canopy architecture traits such as flag-leaf angle, flag-leaf curvature and flag-leaf size (length and width) for spring wheat at NW Mexico.

- Quantify the physiological basis of genetic variation in radiation-use efficiency (RUE) at different periods of the season, including investigate associations between canopy architecture traits and RUE and above-ground biomass in spring wheat cultivars.
- Understand the physiological basis of the planting system - genotype (PS × G) interaction for the canopy architecture traits, above-ground biomass and grain yield in relation to effects on radiation interception and radiation-use efficiency, for raised beds versus flat basin planting systems.
- Evaluate the genetic variation of the stem internode and spike partitioning traits in the two planting systems in the two planting systems. Identify key partitioning traits to improve grain yield, harvest index, grain number and fruiting efficiency.
- Understand the physiological basis of the PS × G interaction for the grain partitioning traits.
- Identify possible trade-offs between source traits and stem-internode lengths, spike partitioning index and other grain partitioning traits.
- Understand the relation between flag-leaf A_{max} measured in the glasshouse and RUE measured in the field experiments.

Hypotheses:

1. There are differences in grain yield, yield components and biomass through the season between planting systems.
2. There are differences in RUE calculated at different phenophases between beds and flats and a PS × G interaction.
3. Genotypes with more prostrate flag-leaves increase light interception pre-anthesis (by capturing light in the gaps between the beds) in the raised beds but not in the flat basins.
4. Genotypes with more erect flag-leaves allow a better vertical distribution of light among the canopy leaf layers and increase RUE in both planting systems, but relatively more in the flat basins than raised beds.
5. Flag-leaf curvature affects the genetic variation of RUE and LI% in raised beds and flat basins.
6. Raised beds have higher spike partitioning index than flat basins associated with reduced above-ground biomass accumulation during early stem extension but similar

biomass accumulation during later stem extension than flat basins with relatively more assimilates to be partitioned into the spike.

7. Spike partitioning index is negatively related to the stem-internode lengths 2 and 3 but there is no association with the peduncle in both PS.
8. A reduction in stem-internode 2 and 3 lengths allows a greater spike dry-matter per unit area at GS65 + 7 days in both PS.
9. Genetic variation in flag-leaf A_{max} measured in the glasshouse is associated with RUE measured in the field.

1.11 Thesis layout

This PhD thesis includes a general introduction (literature review), one chapter providing an overview of the of the material and methods for the project experiments, three chapters with the findings obtained in three field experiments carried out at CIMMYT, CENEB NW Mexico, one chapter with the findings obtained in two glasshouse experiments carried out at Sutton Bonington Campus, University of Nottingham and a general discussion. The chapters 3 - 6 were written in an article format to be submitted to journals.

Chapter 1. Introduction/literature review. It includes a summary of the main concepts and previous investigations related to this project. In addition, the overall objective, specific objectives and hypotheses are included in this section.

Chapter 2. Radiation-use efficiency and biomass in wheat differs between raised beds and flat basins planting system: considerations for cultivar selection. It reports the results obtained from the cycles 2017-2018, 2018-2019 and 2019-20 using twelve spring wheat CIMMYT cultivars in the field experiments carried out at NW Mexico.

Chapter 3. Canopy architecture traits determine radiation-use efficiency (RUE) in wheat cultivars in raised beds and flat basins planting systems. It reports the results obtained from the cycles 2018-2019 and 2019-20 using twelve spring wheat CIMMYT cultivars in the field experiments carried out at NW Mexico.

Chapter 4. Grain partitioning traits to increase harvest index and grain yield in wheat: evaluated under two planting systems. It reports the results obtained from the cycles 2017-2018 and 2018-19 using twelve spring wheat CIMMYT cultivars in the field experiments carried out at NW Mexico.

Chapter 5. Glasshouse experiments: Identifying flag-leaf photosynthetic traits to enhance RUE, biomass, grain yield and N-use efficiency in spring wheat cultivars. It reports the results obtained in 2018 and 2019 using eight spring wheat CIMMYT cultivars in the glasshouse experiments carried out at Sutton Bonington.

Chapter 6. General discussion. It includes an overview of the analysis and results included in the chapters 3 - 6 and their interpretation. Additionally, suggestions for future work are included in this chapter.

Chapter 7. Conclusion. It includes the overall conclusions of the results included in the chapters 3 - 6.

Chapter 8. Future work. It suggests future research to support and reinforce the results obtain in this thesis.

2 CHAPTER 2 . RADIATION-USE EFFICIENCY AND BIOMASS IN WHEAT DIFFERS BETWEEN RAISED BEDS AND FLAT BASINS PLANTING SYSTEM: CONSIDERATIONS FOR CULTIVAR SELECTION

Paper submitted to Field Crops Research 14 March 2022

Marcela A. Moroyoqui-Parra¹, Gemma Molero^{2,4}, Matthew P. Reynolds², Oorbessy Gaju³, Erik H. Murchie¹, M. John Foulkes^{1*}

¹Division of Plant and Crop Science, School of Biosciences, University of Nottingham, Sutton Bonington Campus, Leicestershire LE12 5RD, United Kingdom.

²Global Wheat Program, International Maize and Wheat Improvement Center (CIMMYT), carretera Mexico-Veracruz Km 45, El Batan, Texcoco, Mexico, CP 56237.

³Lincoln Institute for Agri-Food and Technology, University of Lincoln, Riseholme Park, Lincoln, Lincolnshire, LN2 2LG, United Kingdom.

⁴KWS Momont Recherche, 7 rue de Martinval, 59246 Mons-en-Pevele, France.

*** Corresponding author:**

John Foulkes

John.Foulkes@nottingham.ac.uk (M.J. Foulkes).

Keywords: Radiation-use efficiency, spring wheat, planting systems, radiation interception.

2.1 Abstract

As harvest index (HI) is approaching its theoretical upper limit, avenues for increasing biomass must be identified for future grain yield improvements. Radiation-use efficiency (RUE) has become an important trait for raising biomass and grain yield potential in plant breeding. Selection of lines in a breeding program is usually done in one planting system which may not always match the system used by farmers. However, the effect of planting system on genetic variation in RUE has scarcely been investigated. Twelve spring CIMMYT wheat cultivars were evaluated under irrigated conditions in three years (2017-18, 2018-19 and 2019-20) at CIMMYT in NW Mexico using raised-bed (B) and flat-basin (F) planting systems (PS). Grain yield (10.6%), above-ground biomass at physiological maturity (BMPM) (7.6%) and RUE measured from initiation of booting to seven days after anthesis (RUE_InBA7) (9.7%) were higher in beds than flats. Biomass at emergence + 40 days in flats was 21.5% higher than in beds but this advantage disappeared at anthesis. Genetic

variation in RUE before the grain filling period (RUE_preGF) was associated with biomass at anthesis + 7 days and grain yield in beds and flats. Moreover, there was a PS × cultivar interaction for RUE_preGF ($P < 0.05$). Our results showed that grain yield responses of cultivars to planting system differed and were mainly explained through effects on final biomass. Biomass responses to planting system were, in turn, associated with responses of RUE to planting system in the pre-anthesis period. It is concluded that plant breeders should consider the planting system when selecting lines for high RUE and biomass since useful lines may be missed by just evaluating germplasm in one or other of the beds and flats planting systems.

2.2 Introduction

Wheat is the most widely grown crop with ~750 million tonnes produced every year (FAOSTAT, 2018) and contributes 20% of the calories of the global human diet (Braun et al., 2010). Wheat yields will need to be doubled by 2050 for food security (Ray et al., 2013). In recent decades in irrigated wheat production in NW Mexico, growers have adopted a raised-bed planting system (**Fig. 2.1**) converting from the traditional flat-basin planting system (Fahong et al., 2004). The raised-bed planting system consists of defined rows planted on the top of the beds with flood irrigation supplied in furrows between the beds and has been associated with grain yield improvements (Fahong et al., 2004). In addition, management advantages of raised beds compared with flat basins are: reduced irrigation water requirements by 20 - 40%, reduced weeds/diseases associated with the wider row spacings facilitating weed control and conferring reduced disease pressure, improved N fertilizer-use efficiency, reduced lodging and improved plant establishment (Sayre et al., 2008). However, results of investigations on raised beds versus flat basins are inconsistent in terms of grain yield effects and there is a need for further studies. Better grain yield in raised beds than flat basins was reported in wheat by 4 - 17 % (Fahong et al., 2004; Wang et al., 2009; Ahmad et al., 2010; Kong et al., 2010; Jat et al., 2011; Noorka and Tabasum, 2013; Majeed et al., 2015). However, Tanveer et al. (2003) and López-Castañeda et al. (2014) found greater grain yield in flat basins than raised beds. Some studies have reported a trend for taller cultivars in raised beds to perform relatively better than in flat basins, potentially associated with earlier canopy closure in the gap between the beds leading to higher radiation interception pre-anthesis (Fischer et al., 2005) and/or to effects on radiation-use efficiency. Therefore, the better-performing cultivars in flat basins may not be better-

performing in raised beds. Yield potential (YP) can be expressed by the simple equation (3.1) (Reynolds et al., 2005):

$$YP = LI \times RUE \times HI \quad (2.1)$$

Where LI is intercepted radiation, RUE is radiation-use efficiency (ratio of above-ground biomass to radiation intercepted (Monteith and Moss, 1977) and HI is harvest index (ratio of grain biomass to above-ground biomass).

During the Green Revolution, many studies observed that grain yield increased due to a greater HI without improvements in above-ground biomass (Austin et al., 1980; Gifford et al., 1984; Sayre et al., 1997; Reynolds et al., 1999). Since then, HI has shown slower genetic progress and in some countries is approaching its theoretical maximum of ca. 0.65 (Austin, 1980; Foulkes et al., 2011). In the UK, genetic gains in grain yield from 1980 to 1995 were associated with above-ground biomass, in turn, associated with RUE (Shearman et al., 2005). Other studies (Reynolds et al., 1999; Donmez et al., 2001; Aisawi et al., 2015) also demonstrated genetic progress in above-ground biomass in wheat in the last decades. Wheat canopies in favourable conditions typically achieve > 95% light interception from canopy closure at around onset of stem extension to the second half of the grain gilling period when flag-leaf senescence begins (Reynolds et al., 2005). Therefore, to raise biomass RUE must be improved in future breeding since light interception is close to approaching its upper limit (Foulkes and Murchie, 2011b).

In wheat crops, RUE is typically in the region of 2.8 g MJ⁻¹ of PAR (Photosynthetically Active Radiation, 400 - 700 nm) (Yunusa et al., 1993; Molero et al., 2019) and 1.4 g MJ⁻¹ of solar radiation (Sinclair and Muchow, 1999). Several recent investigations have demonstrated that RUE has been associated with genetic progress in biomass improvement in bread wheat (Shearman et al., 2005; Molero et al., 2019). Lower RUE in older cultivars may be partly associated with sink limitation of grain growth. For example, a study in bread wheat found lower RUE in old genotypes compared to modern genotypes due to lower grain number and sink limitation (Acreche et al., 2009). There is some evidence that elite landraces and synthetic-derived lines express greater RUE and above-ground biomass compared to elite check lines (Molero et al., 2019). Reynolds and Pfeiffer (2000) proposed that optimized source-sink balance might be one feasible approach to enhance RUE. Indeed, crosses between high source lines and lines favouring sink variables such as HI and thousand

grain weight (TGW) in wheat have achieved gains in RUE in the progeny (Reynolds et al., 2017). Alternatively, optimized canopy architecture may confer more effective light distribution among the canopy leaf layers resulting in improvements in RUE (Murchie E. and Reynolds M., 2012). A study in spring wheat in Australia showed greater RUE in erectophile lines (2.40 g MJ^{-1}) compared to the planophile lines (1.52 g MJ^{-1}) (Yunusa et al., 1993). More recent research in wheat in Australia showed that more erect canopies had greater biomass and grain yield (Richards et al., 2019). However, to date there are no studies investigating the effects of raised beds and flat basins planting systems on RUE and whether genotype rankings for RUE change with planting system affecting the relative performance of biomass and grain yield in the two planting systems.

In the present study 12 CIMMYT elite spring wheat cultivars were grown in the raised-bed and flat-basin planting systems in three years in NW Mexico under irrigated conditions. The aims of this study are to: i) to quantify variation in intercepted radiation and RUE and associations with above-ground biomass and grain yield in the two planting systems and ii) understand the physiological basis of the planting system \times genotype interaction (PS \times G interaction) for grain yield and biomass in relation to PS \times G effects on intercepted radiation and RUE.

2.3 Materials and methods

2.3.1 Experiment site, design and treatments

Three field experiments were performed at CIMMYT CENEB (Campo Experimental Norman E. Borlaug) research station in the Yaqui Valley near Ciudad Obregon, Sonora (27°395 N, 109°926 W, 38 masl) under irrigated conditions in 2017-18, 2018-19 and 2019-20. The soil type was a sandy clay, mixed montmorillonitic typic calciorthid, low in organic matter, and slightly alkaline (pH 7.7) (Sayre et al., 1997). In each year, for each of two planting systems (raised beds and flat basins) a randomised block design was implemented with three replicates testing per cultivar. The two planting systems were sown in adjacent areas in the field, with a 5 m gap between the border plots of the planting systems. Ten genotypes were selected based on contrasting RUE, biomass and canopy architecture from the HiBAP I (High Biomass Association Panel) from previous CIMMYT data sets (**Table 2.1** (Molero et al., 2019) and were grown in all three seasons. Two more erectophile cultivars were added in the experiments in 2018-19 and 2019-20 to increase canopy architecture variation, selected from the ESWYT (Elite Selection Wheat Yield Trial series) in the CIMMYT wheat breeding program. The genotype names are abbreviated in tables and figures but the full names are given in **Table 2.1** together with information on canopy architecture. From the twelve genotypes, three were elite CIMMYT cultivars (BACANORA T88, CHEWINK #1 and BORLAUG100) and the others were elite advanced lines as indicated in **Table 2.1**. For concision, the 12 genotypes will be referred to as cultivars hereafter.

The raised beds (B) planting system consisted of two beds per plot, whereas the flat basins (F) had one flat area per plot. In the raised beds planting system the two beds per plot were each 0.8 m wide and 4 m long (= 6.4 m² per plot) with two rows per bed (0.24 m between rows) and 0.56 m between the inner rows of the two adjacent beds (**Fig. 2.1**). For flat basins in 2017-18 and 2018-19 there were eight rows per basin (2.5 m wide and 5 m long = 12.5 m² per plot) with 0.20 m between rows. In 2019-20, there were six rows per basin (2.5 m wide and 5 m long = 12.5 m² per plot) with 0.24 m between rows. The sowing dates were 30 November 2017, 30 November 2018 and 21 December 2019 in beds and 1 December 2017, 1 December 2018 and 17 December 2019 in flats. The emergence dates were 7 December 2017, 7 December 2018 and 31 December 2019 in beds and 9 December 2017, 9 December 2018 and 26 December 2020 in flats. The seed rate was 102 kg ha⁻¹ in beds for the three years and 107 kg ha⁻¹ in 2017-18 and 2018-19 and 106 kg ha⁻¹ in 2019-20

in flats. In 2017-18 both planting systems were fertilized with 50 kg N ha⁻¹ (urea) during land preparation followed by 50 kg P ha⁻¹ at sowing. A second and third N application (200 and 50 kg N ha⁻¹, respectively, as urea) was applied at the first and second irrigation. In 2017-18 and 2018-19, the irrigation was applied every 3 - 4 weeks during the cycle as flood irrigation in both planting systems. In 2019-20, raised beds were irrigated as for the first two years and the flat basins were irrigated using drip irrigation every 3 - 4 weeks. Herbicides, fungicides and pesticides were applied as necessary in order to minimize the effects of weeds, diseases and pests. Plot management information for the two planting systems is summarized in **Supplementary Table 2.1**. In all experiments there was no evidence for hypoxia in the plants at any stage during the life cycle in any of the plots.

Table 2.1. List of twelve CIMMYT elite spring bread wheat cultivars and advanced lines in the experiments in 2017-2018, 2018-19 and 2019-20. *Two lines added in 2018-19 and 2019-20.

	Year of release	Genotype	Architecture
1	1988	BACANORA T88	erectophile
2		C80.1/3*QT4118//KAUZ/RAYON/3/2*TRCH/7/CMH79A.955/4/	planophile
3	2008	CHEWINK #1	planophile
4		SOKOLL//PUB94.15.1.12/WBLL1	planophile
5		NELOKI	erectophile
6		W15.92/4/PASTOR//HXL7573/2*BAU/3/WBLL1	planophile
7		KUKRI	planophile
8		KUTZ	planophile
9		SOKOLL	planophile
10	2014	BORLAUG100 F2014	planophile
11*		ITP40/AKURI//FRNCLN*2/TECUE #1	erectophile
12*		CHIPAK*2//SUP152/KENYA SUNBIRD	erectophile

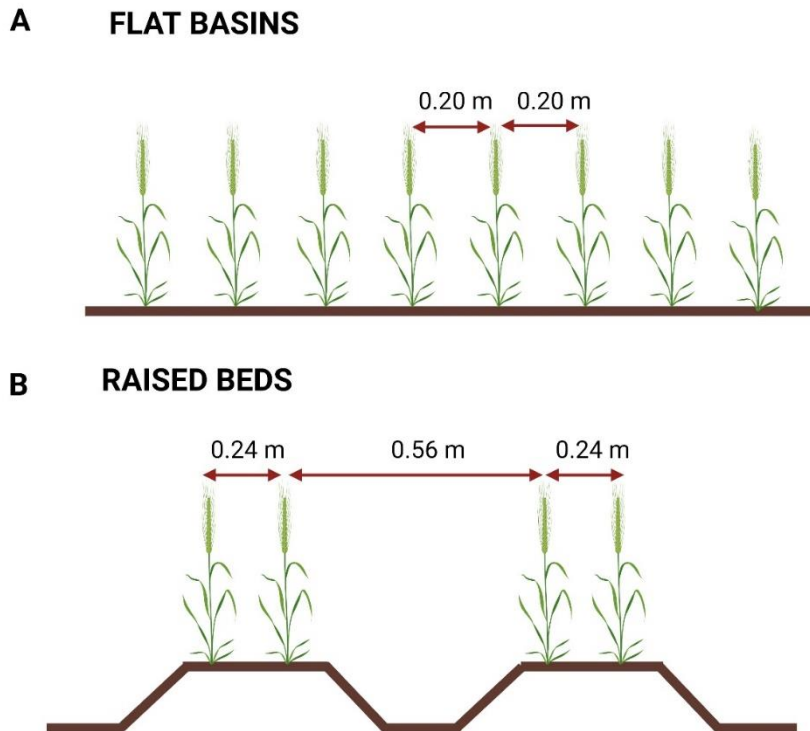


Fig. 2.1. Dimensions for **A** flat basins: same distance between the 8 rows and **B** raised beds: two or three rows per bed with a wider furrow gap. Adapted from (Fischer et al., 2005). Created with Biorender.com.

2.3.2 Crop measurements

2.3.2.1 Phenology and growth analysis

Dates of reaching initiation of booting (GS41), heading (GS55), anthesis (GS65) and physiological maturity (GS87) were recorded (Zadoks et al., 1974) as when 50% of the shoots in the plot reached the stage (Pask et al., 2012b). Biomass samples were taken by cutting shoots at ground level at 40 days after emergence, GS41 and GS65 + 7 days in a 0.8 m² area (0.50 m x 1.6 m) in beds and a 0.9 m² area (0.50 m x 1.8 m) in flats, except for 40 days after emergence (0.40 m²: 0.25 m x 1.6 m in beds; 0.45 m²: 0.25 m x 1.8 m in flats). The biomass sampling was taken leaving 25 cm (40 days after emergence) or 50 cm (GS41 and GS65 + 7 days) from the end of the plot to reduce border effects. At emergence + 40 days, GS41 and GS65 + 7 days a subsample of the sampled material was taken on a fresh weight basis of 50 shoots and weighed after drying at 70°C for 48 h. For biomass at physiological maturity, 50 fertile shoots, e.g., those with a spike, (2017-18 and 2018-19) or 30 fertile shoots (2019-20) were sampled randomly by cutting at ground level to estimate harvest index (ratio of grain dry matter to above-ground dry matter) and grain yield

components as described by (Pask et al., 2012b). Crop growth rate (CGR) for the relevant phenophases was calculated as the above-ground biomass increment per day. After physiological maturity, grain yield was measured in each plot by machine harvesting an average plot area of 3.2 and 4.0 m² per plot in beds and flats, respectively, and values were further adjusted to moisture percentage measured in each plot. In each plot, 50 cm at each end of the plot was discarded in order to remove the border effect. For thousand grain weight, a subsample of *ca.* 20 g was taken and the dry weight recorded after drying at 70°C for 48 h and the grains counted using the digital image system Seed Counter (SeedCount SC5000).

2.3.2.2 Light interception

Fractional interception of photosynthetically active radiation (PAR, 400 – 700 nm) (FI) was measured using a 1 m linear ceptometer (AccuPAR LP-80, Decagon Devices, Pullman, WA, USA) at emergence + 40 days, GS41 and GS65 + 7 days in 2018-19 and 2019-20. The measurements were taken above the crop (incident radiation), inverting the ceptometer 10 cm above the canopy (reflected radiation) and below the canopy at ground level (transmitted radiation) during sunny days from 11 am to 1 pm when the sun was near its zenith and when wind speed was low. The ceptometer was positioned across the plant rows diagonally at approximately a 45° angle. In the raised beds, a small section of the gap between the beds within a plot was included in the measurement so that measurements were representative of the whole plot. A single reading per bed was taken in beds and two readings per plot in flats.

Fractional PAR interception was calculated as follows (3.2):

$$FI = \frac{(PAR_i - PAR_r - PAR_t)}{(PAR_i - PAR_r)} \quad (3.2)$$

Where PAR_i is the incident photosynthetically active radiation, PAR_r is the reflected PAR and PAR_t is the transmitted PAR at the soil surface.

2.3.2.3 Radiation-use efficiency

Radiation-use efficiency (RUE) was calculated in each plot as the increment in the above-ground dry matter divided by the increment in intercepted PAR for the phase (Monteith and Moss, 1977) in 2018-19 and 2019-20. PAR interception for the phenophases up to GS65 + 7 days (IPAR_{accE40} - InB; IPAR_{accInB} - A7; IPAR_{accE40} - A7) was

calculated from the cumulative incident PAR for the days of the phase and then multiplying by the average FI from the start to the end of the phase. For PAR interception for the phase from GS65 + 7 days to physiological maturity (IPARaccA7 - PM) the FI at GS65 + 7 days was applied to the incident PAR for each day during the phase and the daily increments of PAR interception accumulated for the phase; a correction factor of 0.5 was applied to the FI during the last 25% of the grain filling period to account for the interception by senesced canopy (Reynolds et al., 2000b). PAR interception from emergence + 40 days to physiological maturity was calculated as the sum of IPARaccE40 - A7 and IPARaccA7 - PM. RUE was measured over the different phases: RUE_E40InB (from 40 days after emergence (close to canopy closure) to initiation of booting), RUE_InBA7 (from initiation of booting to seven days after anthesis), RUE_preGF (RUE pre-grain-filing from 40 days after emergence to seven days after anthesis) and RUE_GF (RUE grain-filling from seven days after anthesis to physiological maturity) and RUET (from emergence + 40 days to physiological maturity). RUE was therefore calculated using the equations (2.3 – 2.7):

$$\text{RUE}_{\text{E40InB}} = \frac{\text{BMinB} - \text{BME40}}{\text{IPARaccE40} - \text{InB}} \quad (2.3)$$

$$\text{RUE}_{\text{InBA7}} = \frac{\text{BMA7} - \text{BMinB}}{\text{IPARaccInB} - \text{A7}} \quad (2.4)$$

$$\text{RUE}_{\text{preGF}} = \frac{\text{BMA7} - \text{BME40}}{\text{IPARaccE40} - \text{A7}} \quad (2.5)$$

$$\text{RUE}_{\text{GF}} = \frac{\text{BMPM} - \text{BMA7}}{\text{IPARaccA7} - \text{PM}} \quad (2.6)$$

$$\text{RUET} = \frac{\text{BMPM} - \text{BME40}}{\text{IPARaccE40} - \text{PM}} \quad (2.7)$$

Where BM = above-ground dry-matter, IPARacc = accumulated intercepted PAR, E40 = emergence + 40 days, InB = initiation of booting (GS41), A7 = anthesis (GS65) + 7 days and PM = physiological maturity.

2.3.2.4 Normalized Differenced Vegetation Index (NDVI)

Normalized Difference Vegetation Index was measured in raised beds and flats from canopy closure (close to onset of stem extension) to late grain filling using a Green Seeker (Trimble, USA) approximately every two weeks (Pask et al., 2012b). The NDVI measurements provided additional information on green canopy area and senescence profiles to help interpret treatment effects on radiation interception. The NDVI meter sensor

was held 60 - 120 cm above the crop. NDVI was calculated from measurements of reflectance in the red (680 nm) and near infrared (NIR, 800 nm) regions of the spectrum using equation (2.8):

$$\text{NDVI} = \frac{(\text{R800}-\text{R680})}{(\text{R800}+\text{R680})} \quad (2.8)$$

Where R680 and R800 are the reflectance at 680 and 800 nm, respectively.

2.3.3 Statistical analysis

Adjusted means for grain yield, yield components and physiological traits were calculated using a general linear model (GLM) ANOVA procedure from META R 6.04 (Alvarado et al., 2020). Replications, years and planting systems were considered as random effects, and genotypes as a fixed effect. A covariate for anthesis date was used as a fixed effect and was included when significant. Phenotypic correlations between traits were Pearson's correlation coefficient calculated using either the three-year genotype means or the two-year genotype means. Linear regression analysis was applied to two-year or three-year genotype means for selected traits. Broad sense heritability (H^2) was calculated using across the three or two years, using equation (2.9):

$$H^2 = \frac{\sigma_g^2}{\sigma_g^2 + \frac{\sigma_{gy}^2}{y} + \frac{\sigma_{gs}^2}{s} + \frac{(\sigma_{gy})^2(s)}{ys} + \frac{\sigma_e^2}{rys}} \quad (2.9)$$

Where σ^2 = error variance, σ_g^2 = genotypic variance, σ_{gy}^2 = G × Y variance, σ_{gs}^2 = PS variance, s = number of PS, y= number of years, σ_e^2 = residual variance, r = number of replicates.

2.4 Results

Meteorological data including mean monthly temperature, relative humidity, rainfall and solar radiation were collected from a weather station within 1 km of the field experiments. The environmental conditions in the field experiments for the three crop cycles are shown in **Fig. 2.2**. Mean temperature from December to April was similar in 2018-19 (18.0°C) and 2019-20 (17.7°C), but in 2017-18 was *ca.* 1°C warmer (19.1 °C). Low rainfall (< 10 mm per month) was observed during each of the three crop cycles. Average radiation from December to April was higher during 2017-18 than in 2018-19 and 2019-20.

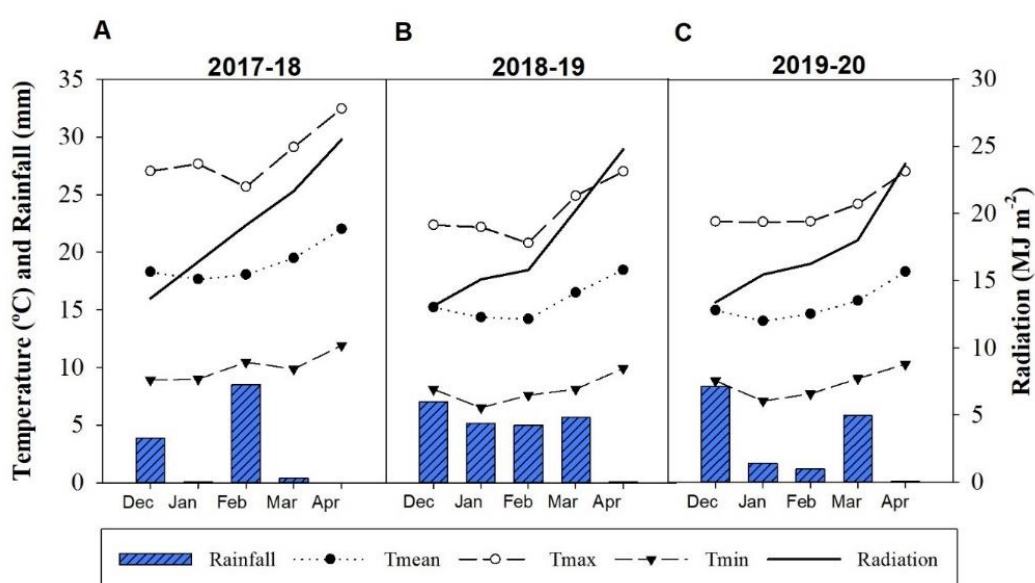


Fig. 2.2. Environmental conditions in the field experiments (average mean temperature (°C), average minimum temperature (Tmin, °C), average maximum temperature (Tmax, °C), average monthly rainfall (mm) and average monthly radiation (MJ m⁻²) in the field experiments during (A) 2017-18, (B) 2018-19 and (C) 2019-20.

2.4.1 Grain yield, yield components and developmental stages

Plant establishment (plant counts in an area of 0.40 m² in beds and 0.45 m² in flats 28 days after emergence) was only measured in 2019-20 when a non-significant difference (153 - 176 plants m⁻²) was observed between the two planting systems (**Table 2.2**). Plant height differed among cultivars from 90.1 - 121.3 cm in beds and 88.3 - 119.4 cm in flats ($P < 0.001$) with a planting system (PS) × genotype (G) interaction ($P < 0.05$); but plant height did not differ between planting systems. The date of initiation of booting, heading and anthesis occurred one day later in beds than flats, and for physiological maturity 3 days later

in beds than flats. Averaging across the three years, grain yield (YLD) varied amongst the cultivars from 539 - 741 g m⁻² in beds and 525 - 693 g m⁻² in flats ($P < 0.001$; **Table 2.2**).

Table 2.2. Mean, minimum, maximum, and ANOVA for yield, yield components, biomass at maturity and phenology expressed in days after emergence (DAE) from the combined analysis across 2017-18, 2018-19 and 2019-20 in raised beds (B) and flat basins (F).

Trait	Mean		Min		Max		<i>p-value</i>			
	B	F	B	F	B	F	G	Y	PS	PS×G
YLD (g m ⁻²)	666	602	539	525	741	693	<0.001	<0.05	<0.001	<0.05
TGW (g)	45.2	44.8	35.2	35.2	51.2	51.6	<0.001	<0.001	0.097	ns
HI	0.47	0.46	0.43	0.42	0.50	0.50	<0.001	<0.001	<0.05	ns
GM2 (m ⁻²)	14883	13581	11584	10611	18067	16785	<0.001	<0.01	<0.001	0.184
SM2 (m ⁻²)	299	289	255	227	379	353	<0.001	<0.001	<0.01	0.068
GPS	50.5	47.8	40.4	40.8	55.9	54.2	<0.001	<0.001	<0.001	<0.001
BMPM (g m ⁻²)	1420	1320	1192	1204	1512	1444	<0.001	<0.01	<0.001	<0.05
HeightPM (cm)	105.7	105.7	90.1	88.3	121.3	119.4	<0.001	<0.001	ns	<0.05
ShootsE40 (m ⁻²)	704	577	619	465	812	678	<0.001	<0.001	<0.001	<0.01
ShootsA7 (m ⁻²)	451	483	396	395	496	483	<0.001	<0.001	<0.001	<0.05
DTInB (DAE)	61	60	57	57	65	63	<0.001	<0.001	<0.001	<0.01
DTH (DAE)	71	70	68	68	76	75	<0.001	<0.001	<0.001	<0.01
DTA (DAE)	77	76	72	72	81	80	<0.001	<0.001	<0.001	0.084
DTPM (DAE)	117	114	113	110	121	118	<0.001	<0.001	<0.001	ns
Plants (m ⁻²)‡	156	173	139	152	180	201	<0.001	-	0.074	ns

YLD: grain yield, TGW: thousand grain weight, HI: harvest index, GM2: grain number per square meter, SM2: spikes per square meter, GPS: grains per spike, BMPM: biomass at physiological maturity, HeightPM: plant height at physiological maturity, ShootsE40: fertile shoots at emergence + 40 days, ShootsA7: fertile shoots at seven days to anthesis, DTInB (DAE, days after emergence): days to initiation of booting (GS41), DTH (DAE): days to heading (GS55), DTA (DAE): days to anthesis (GS65), DTPM (DAE): days to physiological maturity (GS87), Plants: number of plants per square meter. ‡Only one year data (2019-20). * $P < 0.05$, ** $P < 0.01$, *** $P < 0.001$, *italics*: $P < 0.10$, ns: not significant. G: genotype, Y: year, PS: planting system.

On average, yield in beds was 10.6% higher than in flats ($P < 0.001$). A significant PS × G interaction was observed for yield ($P < 0.05$) with the increase in beds compared to flats ranging from 0 to 120 g m⁻² among the cultivars. There was a larger grain yield increase in beds compared to flats for taller than shorter cultivars (**Supplementary Table 2.2**). Harvest index (HI) also showed a significant effect of PS but there was no significant PS × G interaction. Biomass at physiological maturity (BMPM) overall was 7.6% greater in beds (1420 g m⁻²) than in flats (1320 g m⁻²) ($P < 0.001$). Cultivars ranged from 1192-1512 g m⁻² in beds and 1204 - 1444 in flats ($P < 0.001$) and there was a significant PS × G interaction. Genetic variation was found for spikes per m² (SM2), grains per spike (GPS), grains per m² (GM2) and thousand-grain weight (TGW) ($P < 0.001$) with a significant planting system

effect for all these traits ($P < 0.01$, $P < 0.001$, $P < 0.001$ and $P = 0.097$, respectively). However, only GPS ($P < 0.001$) and SM2 ($P = 0.068$) showed a $PS \times G$ interaction.

Correlation coefficients among cultivars between grain yield and yield components are presented in **Table 2.3**. Grain yield was strongly positively associated with BMPM in beds ($r = 0.77$, $P < 0.01$) and flats ($r = 0.78$, $P < 0.01$). A positive association was also found between grain yield and HI in flats ($r = 0.70$, $P < 0.01$), but there was no correlation in beds. No associations between BMPM and HI were observed in this study. Results showed that shorter plants had higher HI (B: $r = -0.53$, $P = 0.08$ and F: $r = -0.62$, $P < 0.05$). A strong positive correlation was found between grain yield and GPS in beds ($r = 0.80$, $P < 0.01$) and flats ($r = 0.61$, $P < 0.05$). There was a trade-off between GM2 and TGW in both planting systems (B: $r = -0.74$, $P < 0.01$, F: $r = -0.79$, $P < 0.01$). Additionally, there was a positive correlation between anthesis date and BMPM in beds ($r = 0.58$, $P < 0.05$) and flats ($r = 0.59$, $P < 0.05$).

2.4.2 Biomass, radiation interception and NDVI during the season

Averaging across the three years, biomass evaluated at the different growth stages during the season showed genetic variation ($P < 0.001$) (**Fig. 2.3**). Biomass at 40 days after emergence (BME40) ranged among the 12 cultivars ($P < 0.001$) from 171 - 218 g m⁻² in beds and 192 - 290 g m⁻² in flats (**Fig. 2.3A**); and was overall 21.5% higher in flats than in beds ($P < 0.001$). Biomass at initiation of booting (BMInB) was 10.7% higher in flats than beds ($P < 0.001$) with genetic ranges from 376 to 635 g m⁻² in beds and 489 to 642 g m⁻² in flats (**Fig. 2.3B**). However, biomass at anthesis + 7 days (BMA7) did not differ between planting systems ($P = 0.63$) with cultivars ranging from 771 to 1124 g m⁻² in beds and 858 to 1143 g m⁻² in flats ($P < 0.001$; **Fig. 2.3C**). At physiological maturity, biomass was 7.6% higher in beds than flats ($P < 0.001$), ranging from 1204 to 1444 g m⁻² in beds and 1192 to 1512 g m⁻² in flats ($P < 0.001$) among cultivars (**Fig. 2.3D**). The biomass at each stage showed a statistically significant $PS \times G$ interaction. At initiation of booting the genotypes SOKOLL//PUB94 and SOKOLL were mainly responsible for the biomass $PS \times G$ interaction with the highest and lowest increases in flats compared to beds, respectively. Whereas at seven days after anthesis the cultivar KUKRI showed the highest increase of biomass in flats compared to beds and KUTZ the smallest. The cultivar SOKOLL showed the greatest biomass increase in beds compared to flats at physiological maturity where beds overall had 226 g m⁻² more biomass than flats and the cultivar NELOKI showed the smallest increase.

Table 2.3. Phenotypic correlations for grain yield, HI, yield components, height at physiological maturity, number of shoots at emergence + 40 days and anthesis + 7 days (m²) and phenology in days after emergence (DAE) among the 12 spring CIMMYT wheat genotypes. Values based on means in 2017-18, 2018-19 and 2019-20 in raised beds (B) and flat basins (F). For abbreviations, see **Table 2.2.** *P < 0.05, **P < 0.01, ***P < 0.001, †P < 0.10.

	RAISED BEDS (B)													
	1	2	3	4	5	6	7	9	10	11	12	13	14	15
1.YLD	-													
2.TGW	0.42	-												
3.HI	0.49	-0.35	-											
4.GM2	0.30	-0.74**	0.76**	-										
5.BMPM	0.77**	0.70*	-0.17	-0.18	-									
6.SM2	-0.52†	-0.87***	0.18	0.50	-0.71*	-								
7.GPS	0.80**	0.08	0.60*	0.54†	0.48	-0.45	-							
8.HeightPM	0.34	0.80**	-0.53†	-0.61*	0.75**	-0.81**	0.17	-						
9.ShootsE40	-0.42	-0.64*	0.31	0.39	-0.65*	0.56†	-0.18	-0.58*	-					
10.ShootsA7	0.12	-0.47	0.45	0.59*	-0.11	0.51†	0.05	-0.55†	0.66*	-				
11.DTIInB	0.46	0.25	-0.09	0.08	0.56*	-0.51†	0.56†	0.67*	-0.15	-0.17	-			
12.DTH	0.47	0.21	-0.08	0.10	0.57†	-0.44	0.55†	0.54*	-0.33	-0.32	0.93***	-		
13.DTA	0.51†	0.16	-0.03	0.17	0.58*	-0.40	0.62*	0.61*	-0.34	-0.26	0.87***	0.96***	-	
14.DTPM	0.31	0.03	-0.03	0.15	0.31	-0.22	0.46	0.42	-0.34	-0.40	0.64*	0.81**	0.83***	-
	FLAT BASINS (F)													
1.YLD	-													
2.TGW	0.08	-												
3.HI	0.70*	-0.30	-											
4.GM2	0.54†	-0.79**	0.71*	-										
5.BMPM	0.78**	0.38	0.10	0.12	-									
6.SM2	-0.01	-0.84***	0.43	0.69*	-0.37	-								
7.GPS	0.61*	-0.01	0.26	0.39	0.59*	-0.38	-							
8.HeightPM	-0.08	0.81**	-0.62*	-0.76**	0.44	-0.87***	0.16	-						
9.ShootsE40	0.03	-0.21	0.33	0.19	-0.29	0.25	-0.13	-0.35	-					
10.ShootsA7	0.21	-0.80**	0.50†	0.80**	-0.17	0.85***	-0.07	-0.79**	0.53†	-				
11.DTIInB	0.24	0.25	-0.16	-0.09	0.44	-0.63*	0.71**	0.61*	-0.06	-0.31	-			
12.DTH	0.05	0.37	-0.36	-0.03	0.37	-0.50†	0.67*	0.53†	-0.21	-0.25	0.89***	-		
13.DTA	0.25	0.07	-0.28	0.04	0.59*	-0.47	0.70*	0.56†	-0.31	-0.24	0.87***	0.95***	-	
14.DTPM	0.16	-0.03	-0.31	0.08	0.49	-0.35	0.66*	0.40	-0.19	-0.20	0.67*	0.78**	0.81***	-

Cultivar SOKOLL was intermediate in the range for plant height amongst the cultivars with a planophile canopy architecture, whereas cultivar NELOKI was the shortest of the 12 cultivars with an erectophile canopy architecture (**Table 2.1 and Supplementary Table 3.2**).

Cultivars showed different temporal patterns of biomass accumulation in the beds and flats during the crop cycle (**Supplementary Fig. 2.1**). The biomass responses to planting system (difference between beds and flats) for the 12 cultivars at physiological maturity were positively associated with the biomass responses at anthesis + 7 days ($R^2 = 0.41$, $P < 0.05$) and those at initiation of booting ($R^2 = 0.27$, $P = 0.10$) (**Fig. 2.4**). There was a larger biomass increase in beds compared to flats for taller compared to shorter cultivars at physiological maturity.

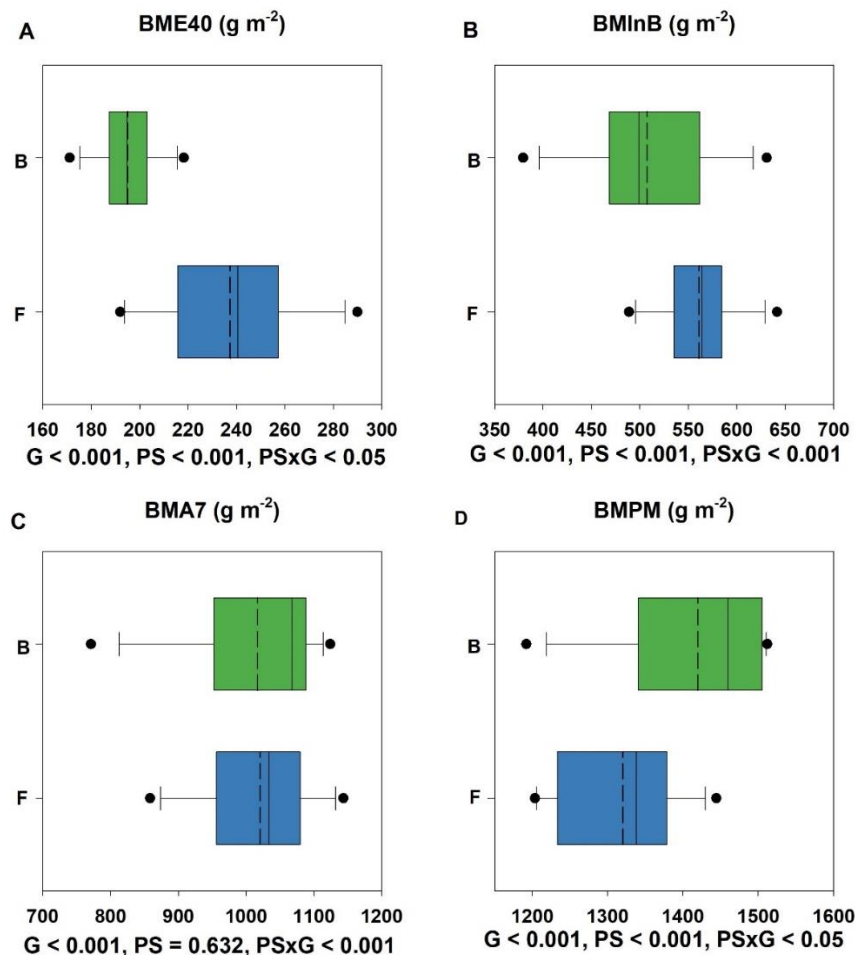


Fig. 2.3. Boxplot of aboveground biomass at (A) emergence + 40 days, (B) initiation of booting, (C) anthesis + 7 days and (D) physiological maturity in raised beds (B) and flat basins (F). Values represent means across 2017-18, 2018-19 and 2019-20. The middle dotted line is the adjusted mean across lines. Statistical significances for genotype (G), planting systems (PS) and the interaction between them (PS × G) are presented below each boxplot.

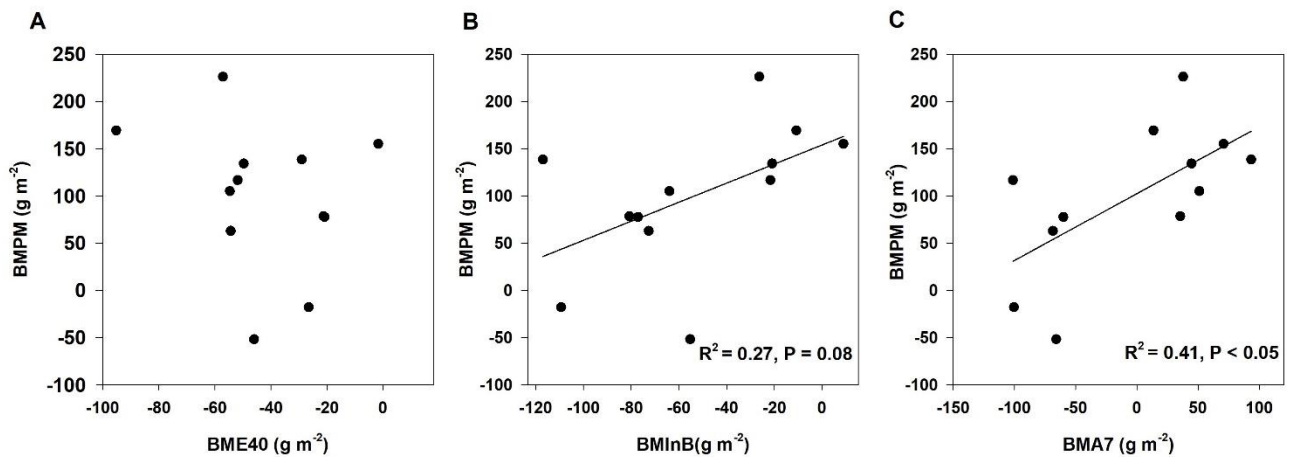


Fig. 2.4. Linear regression between cultivar responses to plant system at (A) biomass at forty days after emergence (BME40; g m⁻²), (B) biomass at initiation of booting (BMInB, g m⁻²) and (C) biomass at seven days after anthesis (BMA7; g m⁻²) with cultivar responses to planting system for biomass at physiological maturity (BMPM; g m⁻²) evaluated across-years in 2017-18, 2018-19 and 2019-20.

NDVI during the season in beds and flats is shown in **Fig. 2.5**. At emergence + 40 days and initiation of booting, both planting systems had similar NDVI values. However, canopy NDVI started to decrease earlier in the flats (at around spike emergence) than in the beds (no decrease from peak until after anthesis).

Radiation interception and radiation-use efficiency were only measured in 2018-19 and 2019-20. Averaging across the two years, fractional radiation interception showed genetic variation at GS41 and GS65 + 7 days ($P < 0.001$ and $P < 0.05$, respectively) with a small planting system effect at both stages ($P < 0.001$ and $P < 0.01$, respectively) (**Supplementary Table 2.3**); FI was marginally higher in flats than beds at both stages (0.99 versus 0.98 at GS41 and 0.98 versus 0.97 at GS65 + 7 days). FI at GS65 + 7 days showed a PS × G interaction ($P < 0.001$) with a marginal interaction also at GS41 ($P = 0.064$). The genetic variation in accumulated intercepted PAR for sequential phenophases during the crop cycle in both planting systems is shown in **Fig. 2.6**. In beds accumulated intercepted radiation (IPARacc) in the pre-anthesis phenophases and in the grain filling phase was slightly greater than in flats. For beds, IPARacc ranged among cultivars from emergence + 40 days to initiation of booting from 128 - 180 MJ m⁻² (**Fig. 2.6A**), from initiation of booting to anthesis + 7 days from 161 - 184 MJ m⁻² (**Fig. 2.6B**), from anthesis + 7 days to physiological maturity from 279 - 351 MJ m⁻² (**Fig. 2.6C**) and from emergence + 40 days to physiological maturity from 582 - 687 MJ m⁻² (**Fig. 2.6D**). In flats, the respective ranges were 128 - 165 MJ m⁻² (**Fig. 2.6A**) 146 - 190 MJ m⁻² (**Fig. 2.6B**), 272 - 327 MJ m⁻² (**Fig.**

2.6C) and 555 - 649 MJ m⁻², respectively (**Fig. 2.6D**). Genetic variation was found for each phase ($P < 0.001$) and a significant planting system effect ($P < 0.01$, $P < 0.01$, $P < 0.01$ and $P < 0.001$, respectively). The small increases in beds compared to flats for accumulated intercepted radiation in the pre-anthesis phase and in the grain filling phase were associated with the slightly extended duration of the phenological phases in the beds compared to the flats. A significant PS \times G interaction was found for each phenophase ($P = 0.052$, $P < 0.01$, $P < 0.01$ and $P < 0.05$, respectively).

Stronger correlations between genetic variation in IPARacc and biomass accumulated were found in beds than flats (**Supplementary Table 2.4**). In beds, a strong positive association was found between IPARacc from emergence + 40 days to booting and biomass accumulated during this phenophase ($r = 0.91$, $P < 0.001$); and similarly for the phenophase from emergence+40 days to physiological maturity ($r = 0.72$, $P < 0.01$). There was no association in flats for these phenophases. However, IPARacc from booting to GS65 + 7 days was positively associated among cultivars with biomass accumulated during this phenophase ($r = 0.64$, $P < 0.05$) in flats.

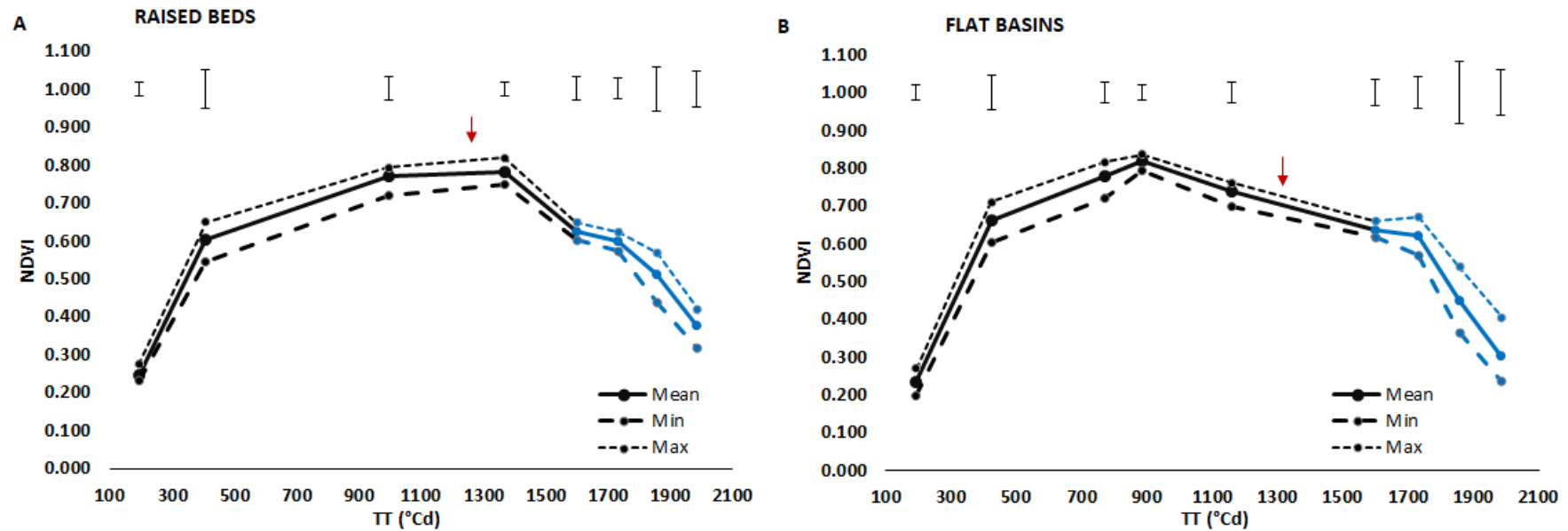


Fig. 2.5. Mean, minimum and maximum values of NDVI across 12 CIMMYT spring wheat genotypes with thermal time on (A) raised beds and (B) flat basins planting systems. Error bars represent the LSD (5%) for each NDVI measurement. Black line represents the vegetative stage cross-year mean 2017-18, 2018-19 and 2019-20 and the blue line the grain-filing stage cross-year mean 2017-18 and 2018-19. Arrows show anthesis date (GS65).

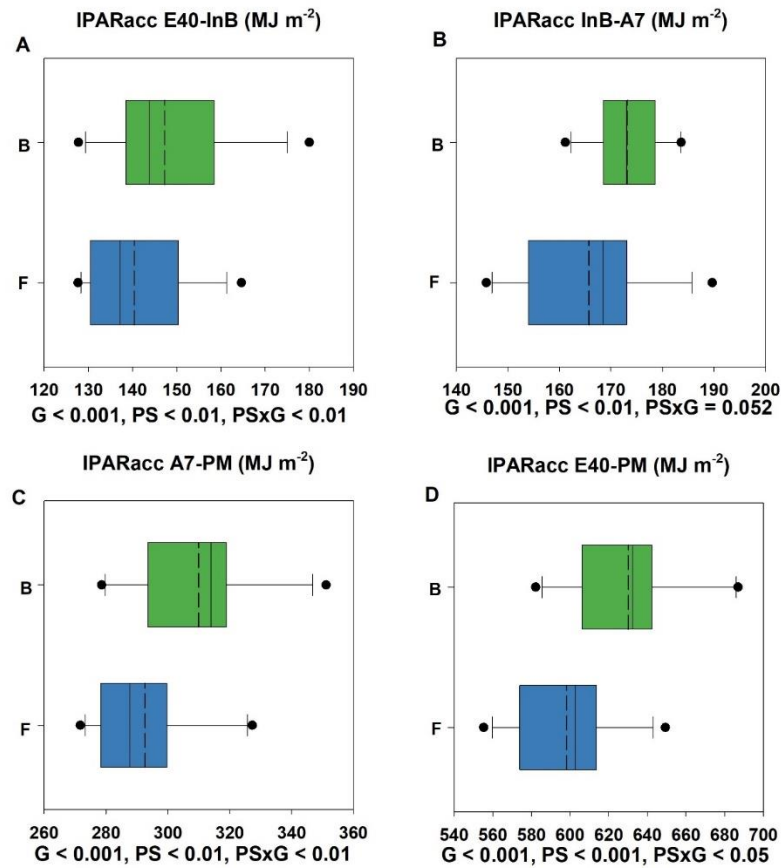


Fig. 2.6. Boxplot of accumulated radiation interception (MJ m⁻²) for (A) emergence + 40 days to initiation of booting, (B) initiation of booting to anthesis + 7 days, (C) anthesis + 7 days to physiological maturity (D) emergence + 40 days to physiological maturity in raised beds (B) and flat basins (F). Values represent means across 2018-19 and 2019-20. The middle dotted line is the adjusted mean across cultivars. Statistical significances for genotype (G), planting systems (PS) and the interaction between them (PS × G) are presented below each boxplot.

2.4.3 Radiation-use efficiency and correlations with biomass, yield and yield components

For the combined analysis in 2018-19 and 2019-20, there was significant genetic variation in RUE for each of the several phenophases for which RUE was estimated in beds and flats (**Table 2.4**). RUE_E40InB ranged from 1.63 - 2.67 g MJ⁻¹ in beds and 2.20 - 3.20 MJ⁻¹ in flats (P < 0.001), and was higher in flats than beds (P < 0.05) with a PS × G interaction (P < 0.001). The genotypes mainly responsible for the interaction were NELOKI (highest increase in flats) and ITP40 (lowest increase in flats). For RUE_InBA7, cultivars ranged from 2.47 - 3.59 g MJ⁻¹ in beds and 2.32 - 3.27 g MJ⁻¹ in flats; and RUE_InBA7 was

higher in beds than flats ($P < 0.05$), but no $PS \times G$ interaction was found. RUE_preGF varied among cultivars from 1.81 - 2.81 g MJ⁻¹ in beds and 2.12 - 2.80 g MJ⁻¹ in flats ($P < 0.001$), but did not show a significant effect of planting system. However, there was a $PS \times G$ interaction ($P < 0.01$) for which the cultivars BORLAUG100 and KUKRI were mainly responsible with the highest and lowest increase in beds compared to flats, respectively. RUE_GF ranged from 1.10- 1.93 g MJ⁻¹ in beds and 0.67 - 1.95 g MJ⁻¹ in flats ($P < 0.001$), but no significant difference between beds and flats was found. BORLAUG100 and KUKRI had the highest and lowest increases in beds compared to flats, respectively ($P < 0.001$). RUET ranged among cultivars in beds from 1.30 to 1.98 g MJ⁻¹ and in flats from 1.41 to 1.85 g MJ⁻¹ ($P < 0.001$) with higher values in beds than flats ($P < 0.05$). For RUET, the cultivar SOKOLL had the greatest increase in beds compared to flats among the cultivars while NELOKI had the smallest increase ($P < 0.05$).

Table 2.4. Radiation-use efficiency (RUE; g MJ⁻¹) calculated from forty days after emergence to initiation of booting (RUE_E40InB), from initiation of booting to seven days after emergence (RUE_InBA7), during the grain filling period from seven days after anthesis to physiological maturity (RUE_GF), pre grain-filling from forty days after emergence to seven days after anthesis (RUE_preGF) and from forty days after emergence to physiological maturity (RUET) for 12 CIMMYT spring wheat genotypes. Values represent means across 2018-19 and 2019-20 in raised beds (B) and flat basins (F) planting systems. *** $P < 0.001$, ** $P < 0.01$, * $P < 0.05$, *italics: $P < 0.10$* , ns: not significant.

Genotype (G)	RUE_E40InB		RUE_InBA7		RUE_GF		RUE_preGF		RUET	
	(g MJ ⁻¹)									
	B	F	B	F	B	F	B	F	B	F
BACANORA T88	2.03	2.63	3.05	2.76	1.44	1.70	2.20	2.59	1.62	1.61
C80.1/3*QT4118	2.56	2.42	2.78	2.33	1.29	1.17	2.40	2.16	1.71	1.52
CHEWINK#1	2.20	2.44	2.67	2.88	1.93	1.34	2.24	2.46	1.87	1.66
SOKOLL//PUB94	2.40	3.20	3.38	2.47	1.50	1.95	2.58	2.45	1.82	1.85
NELOKI	1.63	2.31	2.64	2.34	1.10	1.19	1.81	2.12	1.30	1.41
W15.92/4/PASTOR	1.99	2.37	3.04	2.32	1.48	1.41	2.23	2.16	1.64	1.56
KUKRI	2.41	2.35	2.47	3.06	1.53	0.67	2.31	2.72	1.78	1.63
KUTZ	2.67	2.77	2.84	2.67	1.32	0.81	2.57	2.45	1.71	1.46
SOKOLL	2.54	2.65	3.51	3.05	1.60	0.72	2.79	2.80	1.98	1.67
BORLAUG100	2.00	2.57	3.59	3.10	1.11	1.51	2.81	2.56	1.91	1.73
ITP40/AKURI	2.52	2.20	3.53	3.17	1.43	1.30	2.64	2.47	1.73	1.61
CHIPAK*2//	2.35	2.42	3.28	3.27	1.13	0.96	2.51	2.76	1.73	1.78
Mean	2.27	2.53	3.06	2.79	1.41	1.23	2.42	2.48	1.73	1.62
LSD (G) (5%)	0.524		0.847		0.740		0.378		0.244	
G (p value)	***		**		**		***		***	
PS (p value)	*		*		0.145		ns		*	
Y (p value)	0.163		0.115		ns		*		ns	
PS × G (p value)	***		0.163		**		**		*	

Genetic variation in grain yield was positively correlated with RUE_preGF in beds ($r = 0.75$, $P < 0.01$) and flats ($r = 0.70$, $P < 0.05$) (**Table 2.5**). In addition, YLD was positively correlated with RUET in beds ($r = 0.73$, $P < 0.01$) and flats ($r = 0.67$, $P < 0.05$). Grain yield was positively correlated with RUE_InBA7, but only in flats ($r = 0.87$, $P < 0.001$). A positive correlation was also observed between RUE_InBA7 and BMA7 in beds ($r = 0.63$, $P < 0.05$) and flats ($r = 0.82$, $P < 0.001$). A strong association between RUE_preGF and BMA7 was found in beds ($r = 0.96$, $P < 0.001$) and flats ($r = 0.88$, $P < 0.001$). In addition, a correlation was found between RUE_preGF and BMPM ($r = 0.80$, $P < 0.01$) in beds. RUET was positively related with BMPM in beds ($r = 0.83$, $P < 0.001$) and flats ($r = 0.77$, $P < 0.01$). With regard to other traits, in beds, a strong correlation was found between RUE_InBA7 and HI ($r = 0.65$, $P < 0.05$) and GM2 ($r = 0.62$, $P < 0.05$) as well as between RUE_preGF and HI ($r = 0.50$, $P = 0.10$) and GM2 ($r = 0.58$, $P < 0.05$).

Table 2.5. Phenotypic correlations between yield, yield components, height, above-ground biomass at different growth stages and shoot number with RUE (g MJ^{-1}) for 12 spring CIMMYT wheat genotypes. Values based on means from the combined analysis in 2018-19 and 2019-20 in raised beds (B) and flat basins (F).

	RAISED BEDS (B)					FLAT BASINS (F)				
	RUE_E40InB	RUE_InBA7	RUE_GF	RUE_preGF	RUET	RUE_E40InB	RUE_InBA7	RUE_GF	RUE_preGF	RUET
YLD	0.68*	0.37	0.21	0.75**	0.73**	-0.03	0.87**	-0.03	0.70*	0.67*
TGW	0.44	0.21	0.24	0.50†	0.54†	0.27	-0.16	0.15	-0.20	0.31
HI	-0.19	0.02	-0.28	0.00	-0.06	-0.31	0.65*	-0.03	0.50†	0.18
GM2	0.01	0.08	-0.08	0.03	-0.02	-0.20	0.62*	-0.08	0.58*	0.18
HeightPM	0.63*	-0.01	0.25	0.41	0.48	0.16	-0.22	-0.13	-0.24	0.06
BME40	-0.28	0.28	-0.52†	0.09	-0.14	-0.22	0.15	-0.61*	0.05	-0.23
BMinB	0.89***	-0.18	0.12	0.43	0.39	0.67*	-0.10	-0.22	0.21	0.20
BMA7	0.72**	0.63*	-0.07	0.96***	0.77**	0.01	0.82***	-0.61*	0.88***	0.39
BMPM	0.86***	0.37	0.42	0.80**	0.83***	0.24	0.59*	0.05	0.50†	0.77**
ShootsE40	-0.43	-0.18	-0.39	-0.45	-0.53†	-0.14	0.31	-0.60*	0.39	0.39
ShootsA7	-0.14	0.59*	-0.35	0.31	0.09	-0.22	0.53†	-0.30	0.61*	0.62*

YLD: grain yield (g m^{-2}), TGW: thousand grain weight (g), HI: harvest index, GM2: grain number per square meter (m^{-2}), HeightPM: plant height at physiological maturity (cm), BME40: biomass at emergence + 40 days (g m^{-2}), BMinB: biomass at initiation of booting (g m^{-2}), BMA7: biomass at anthesis + 7 days (g m^{-2}), BMPM: biomass at physiological maturity (g m^{-2}), ShootsE40: fertile shoots at emergence + 40 days (m^{-2}), ShootsA7: fertile shoots at seven days to anthesis (m^{-2}), RUE_E40InB: RUE calculated from forty days after emergence to initiation of booting (g MJ^{-1}), RUE_InBA7: RUE calculated from initiation of booting to seven days after emergence (g MJ^{-1}), RUE_GF: RUE calculated during the grain filling period from seven days after anthesis to physiological maturity (g MJ^{-1}), RUE_preGF: RUE pre grain-filling from forty days after emergence to seven days after anthesis (g MJ^{-1}), RUET: RUET total, from forty days after emergence to physiological maturity (g MJ^{-1}). * $P < 0.05$, ** $P < 0.01$, *** $P < 0.001$, † $P < 0.10$.

2.5 Discussion

2.5.1 Effects of planting systems

The irrigated wheat production in NW Mexico has adopted over the last decades a raised-bed planting system which has increased the efficiency of use of irrigation water and fertilizer N and provided other management benefits over flat basins (Fahong et al., 2004; Sayre et al., 2005). There are other agronomic reasons for farmers choosing raised beds, including lower seed rate, easier access by machinery for weeding and improved lodging control (Sayre et al., 2005). Similar findings to the present results of higher grain yield in beds than flats (10.6%) were previously reported in several investigations (Fahong et al., 2004; Hassan et al., 2005; Ram et al., 2005; Sayre et al., 2005; Kakar et al., 2015; Majeed et al., 2015). Nevertheless, Tanveer et al. (2003) and López-Castañeda et al. (2014) found greater grain yield in flats than beds. We identified several physiological reasons for the higher grain yield in beds than flats in our experiments. RUE from initiation of booting to seven days after anthesis was greater in beds by 9.7% as well as season-long RUE by 6.8% contributing to greater above-ground biomass at physiological maturity in beds than flats. The higher grain yield in beds was also partly related to an extended grain filling duration by 2 days in beds compared with flats which contributed to higher post-anthesis radiation interception in beds. Higher post-anthesis radiation interception and biomass accumulation in beds than flats was additionally associated with a delayed onset of NDVI senescence in beds compared to flats.

Higher RUE from booting to anthesis + 7 days allowed the beds to catch up the flats in biomass at anthesis + 7 days. It can be speculated that the higher RUE from booting to anthesis + 7 days may have been associated with effects of planting system on canopy architecture with the wider row spacing and/or presence of the gap between the beds in the beds plots resulting in changes in canopy architecture favourable for RUE, e.g., a more upright leaf angle contributing to higher RUE (Fischer et al., 2019). There was no evidence that the higher biomass in beds than flats was associated with hypoxia in the flat plots; in all years there were no visible symptoms of hypoxia in any of the plots in either the raised beds or flat basins throughout the life cycle.

2.5.2 Genetic variation in RUE and association with biomass and grain yield

Radiation-use efficiency showed genetic variation in the different periods during the cycle with broadly similar ranges to previous field studies. For example, a study in winter

wheat found genetic variation of RUE based on PAR in the range 2.33 - 2.63 g MJ⁻¹ (Shearman et al., 2005) and a study in bread wheat in Spain reported values based on solar radiation from 0.45 - 0.77 g MJ⁻¹ from seedling to stem elongation and from 0.85 - 1.54 g MJ⁻¹ from anthesis to maturity (Acreche et al., 2009). Genetic variation in RUE_{preGF} showed an association with biomass at GS65 + 7 days and at physiological maturity in both planting systems. Crop growth depends on the way the canopy intercepts radiation among the leaf layers which is related to the LAI (leaf area index) and the canopy architecture. For example, erectophile genotypes caused improved penetration of the light among the canopy leaf layers as well as RUE during the stem-elongation phase, the crucial period when grain number is determined (Fischer, 1985). Our results showed genetic variation in RUE_{preGF} was positively correlated with grain yield in beds and flats. Previous studies by Tao et al. (2018) and Molero et al. (2019) in wheat also demonstrated correlations between pre-anthesis RUE and grain yield among genotypes. In our study the correlation was stronger in flats than beds. Furthermore, there was an indication based on at least the most contrasting cultivars for RUE that erectophile canopies were favouring higher RUE compared planophile canopies in the flats, but differences in canopy architecture appeared to be having less effect in the beds. Our results suggested that erect leaves may have been a relatively more important criteria for genotype performance in flats than beds; and indicated that improving RUE before anthesis is an important target for spring wheat plant breeders to enhance biomass and yield.

We found a strong positive association among cultivars between plant height and biomass at physiological maturity in beds ($r = 0.75$, $P < 0.01$), but no association in flats. The findings under beds are similar to those of Sierra-Gonzalez et al. (2021) in the CIMMYT spring wheat high biomass association panel (HiBAP) and Aisawi et al. (2015) in a set of historic CIMMYT spring wheat cultivars releases from 1965 to 2009 in raised beds. The effect for taller cultivars to accumulate more biomass in beds may have related to their enhanced ability to capture light in the gaps between the beds in the raised beds plots. As expected in both PS reduced plant height increased grains m⁻² and HI but decreased TGW (Acreche and Slafer, 2006; Bustos et al., 2013; Quintero et al., 2018; Jobson et al., 2019).

2.5.3 Cultivar responses to planting systems

A significant PS × G interaction was found for grain yield; for example, the genotype C80.1/3*QT4118 had 18.2% higher grain yield in beds than flats whereas the genotype

ITP40 showed the same grain yield in both planting systems. The grain yield responses to planting system were mainly driven by the above-ground biomass responses at physiological maturity rather than HI. Regarding yield components, grain yield responses to PS were determined by grains m⁻² responses rather than TGW responses. Taller cultivars intercepted relatively more radiation in the beds than the flats before anthesis, consistent with the taller cultivars showing relatively greater increases in YLD and BMPM in beds compared to flats. Above-ground biomass at each stage showed a PS × G interaction. However, differences in radiation interception were not the only ones explaining differences in genotype responses to PS for biomass.

The cultivar responses to planting system for biomass at seven days after anthesis were associated with responses for RUE_InBA7 but more strongly with responses for RUE_preGF. Additionally, responses of cultivars to PS for biomass at physiological maturity were associated with responses to PS for RUE_T. It can be speculated that canopy architecture traits, such as leaf angle and leaf size, and/or leaf chlorophyll content were involved in the cultivar responses for RUE_preGF to the planting systems. Indeed, at the extremes of the RUE range differences in erectophile versus planophile appeared to be associated with responses of RUE to PS. Thus, three of the four genotypes which showed the largest increase in RUE_preGF in flats compared to beds (BACANORA T88, CHIPAK#2// and CHEWINK #1) were erectophile genotypes. Upright leaves tend to permit a more optimal distribution of light among the leaf layers of the canopy reducing light saturation of photosynthesis in leaves at the top of the canopy, so a higher PAR can be received by the light-limited lower leaves hence increasing RUE (Long et al., 2006). Our results suggest that this advantage for upright leaves in terms of increasing RUE was operating more in the flats than the beds. Improved RUE could also be associated with reduced leaf chlorophyll content to allow more light to be transmitted to the lower leaf layers (Slattery et al. (2017). Further research should be conducted to test these potential effects canopy architecture traits and leaf chlorophyll content on RUE in the two planting systems.

The present study found that the CIMMYT cultivars overall performed better in raised beds than flat basins in NW Mexico with higher values of grain yield, BMPM and RUE. In addition, the relative performance of the cultivars differed between the two planting systems. For example, the genotype C80.1/3*QT4118 (tall, planophile) increased grain yield in beds compared to flats by 18.2%, whereas the cultivar NELOKI (short, erectophile) increased only by 2.7%. The apparent association with traits provides some hints on the physiological

bases for plant breeding in the two planting systems. RUE calculations are based on destructive methods that require biomass sampling and light interception measurement at sequential stages, which is not feasible in breeding trials with large numbers of genotypes (Sinclair and Muchow, 1999). Therefore, there is a requirement for rapid, non-destructive phenotyping techniques such as remote sensing technologies to evaluate RUE, e.g. hyperspectral reflectance techniques, for deployment in plant breeding programs (Furbank et al., 2019; Reynolds et al., 2020; Robles-Zazueta et al., 2021). Since plant breeders normally evaluate lines in one planting system this can be different from the one that farmers use for their wheat crops; so phenotyping selection may not be efficient in these cases as some good lines may be missed because they may perform well in one planting system but not in another planting system. Our results therefore indicate that when evaluating germplasm for RUE, biomass and grain yield plant breeders should take into account the planting system.

2.6 Conclusion

Genetic variation in grain yield showed a strong positive association with RUE_{preGF} in both planting systems. Results indicated that raised beds were beneficial for wheat production in the NW Mexico compared to the flat basins. The traits BMPM, HI and GM2 showed greater values in raised beds than flat basins. In addition, genetic variation in RUE_{preGF} showed a positive effect on biomass at GS65 + 7 days in both planting systems and at physiological maturity. The results showed that the grain yield responses to planting system were mainly explained by BMPM, in turn, associated with differential responses of cultivars to PS for both PAR interception and RUE. Therefore plant breeders should focus on improving the RUE before anthesis in order to enhance grain yield and final biomass in wheat. Moreover, evaluation of genotypes for RUE as well as other traits such as biomass, should take into account an evaluation at different planting systems to capture likely G × Management effects in different environments.

2.7 Author contribution

MMP, JF, MR and GM contributed to the conceptualization. MMP, JF, MR and GM contributed to the methodology. MMP contributed to the data analysis. MMP performed the experiments. MAMP, JF, GM and OG contributed to the investigation. MMP and JF contributed to the writing of the original manuscript. MMP, JF, GM, MR, OG and EM contributed to the writing, editing and revising the manuscript. JF and MR contributed to the funding acquisition and project administration. All the authors approved the final version of this manuscript.

2.8 Funding

This work was supported by The National Council of Science and Technology (CONACYT) (CVU 839945), the Sustainable Modernization of Traditional Agriculture (MasAgro) initiative from the Secretariat of Agriculture and Rural Development (SADER) and the International Wheat Yield Partnership Program (IWYP).

2.9 Acknowledgements

We thank to the physiology team at CIMMYT for their technical support. We also acknowledge Richard Richards for his invaluable support in the genotype selection and Angela Pacheco for her advice in the statistical analysis.

2.10 Supplementary information

Supplementary Table 2.1. Sowing date, fertilizer applications and irrigation applications in the planting systems (PS) raised beds (B) and flat basins (F) in the field experiments in 2017-18, 218-19 and 2019-20. ‡Drip irrigation.

Crop Cycle	PS	Sowing	N application (urea)	P application	Irrigations
			kg ha ⁻¹	kg ha ⁻¹	n
2017-2018	B	30/11/2017	50-200-50	50	4
	F	01/12/2017	50-200-50	50	5
2018-2019	B	30/11/2018	50-200	50	6
	F	01/12/2018	50-200	50	6
2019-2020	B	21/12/2019	50-200	50	6
	F	17/12/2019	50-200	50	9‡

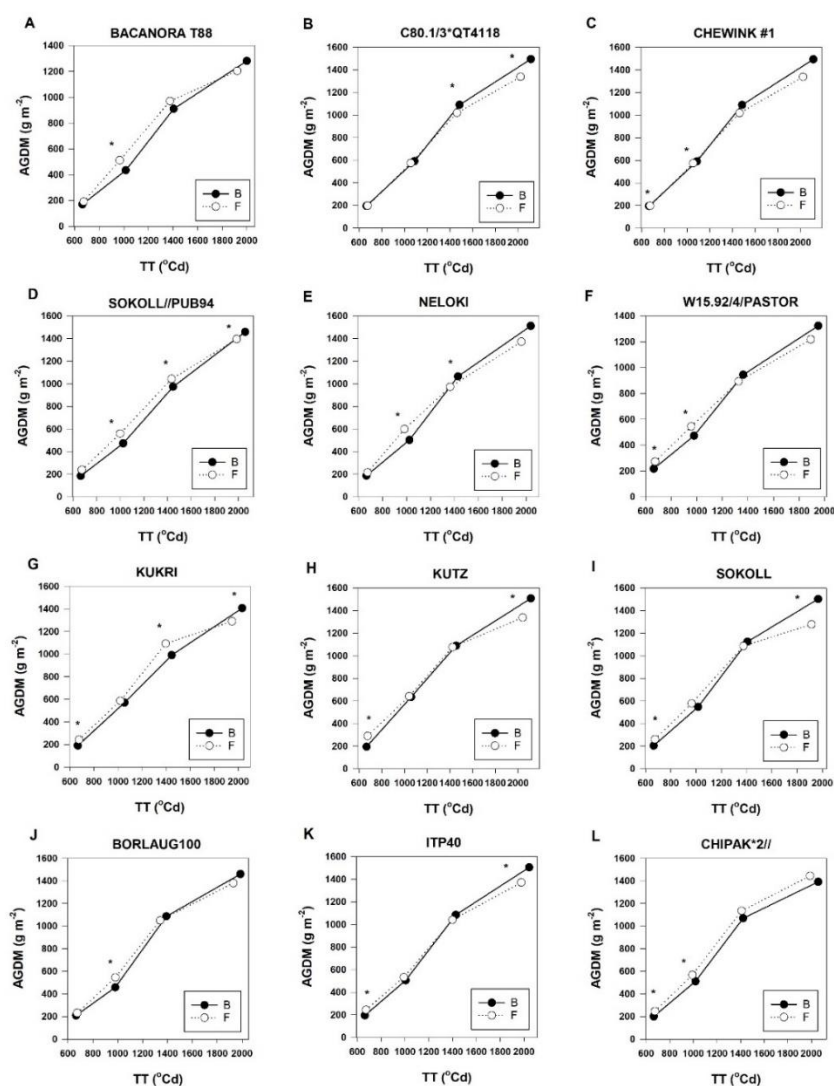
Supplementary Table 2.2. ANOVA for grain yield, harvest index, yield components and biomass at physiological maturity for 12 CIMMYT spring wheat genotypes from the combined analysis across 2017-18, 2018-19 and 2019-20 in raised beds (B) and flat basins (F).

Genotype (G)	YLD		TGW		HI		GM2		BMPM		HeightPM		DTA	
	g m ⁻²		g				m ⁻²		g m ⁻²		cm			
	B	F	B	F	B	F	B	F	B	F	B	F	B	F
BACANORA T88	634	591	35.18	35.20	0.50	0.49	18067	16785	1281	1204	90.1	88.3	75	75
C80.1/3*QT4118	668	565	47.85	46.82	0.44	0.42	13958	12092	1494	1338	121.3	119.4	81	80
CHEWINK#1	683	610	46.61	45.70	0.47	0.44	14654	13377	1459	1396	109.0	110.0	79	78
SOKOLL//PUB94	680	592	51.21	50.44	0.44	0.43	13284	11730	1512	1373	111.3	112.8	77	76
NELOKI	539	525	36.64	37.32	0.45	0.44	14800	14109	1192	1210	93.7	95.4	74	74
W15.92/4/PASTOR	593	547	51.20	51.57	0.45	0.45	11584	10611	1324	1219	107.9	108.1	72	72
KUKRI	695	607	44.07	44.63	0.49	0.47	15792	13637	1407	1290	106.1	106.8	78	76
KUTZ	696	605	47.54	46.66	0.46	0.45	14654	12995	1508	1338	111.1	110.7	79	78
SOKOLL	638	561	44.91	44.30	0.43	0.44	14251	12662	1503	1277	108.2	106.2	76	75
BORLAUG100	730	682	47.78	47.71	0.50	0.50	15300	14301	1460	1381	102.3	102.5	75	75
ITP40/AKURI	741	646	46.16	45.63	0.49	0.48	16029	14158	1505	1371	104.6	107.5	78	77
CHIPAK*2//	693	693	42.89	41.99	0.50	0.48	16227	16511	1393	1444	102.6	100.3	78	77
Mean	666	602	45.17	44.83	0.47	0.46	14883	13581	1420	1320	105.7	105.7	77	76
H ²	0.90		0.95		0.94		0.97		0.86		0.82		0.45	
LSD (G) (5%)	68.239		2.227		0.035		1659.615		165.653		3.916		1.622	
CV%	6.79		3.05		4.73		7.37		7.55		2.28		1.32	
G (p-value)	***		***		***		***		***		***		***	
PS (p-value)	***		0.097		*		***		***		ns		***	
Y (p-value)	*		***		***		*		**		***		***	
PS×G (p-value)	*		ns		ns		0.184		*		*		0.084	

YLD: grain yield, TGW: thousand grain weight, HI: harvest index, GM2: grain number per square meter, BMPM: biomass at physiological maturity, HeightPM: plant height at physiological maturity, DTA: days to anthesis. *P < 0.05, **P < 0.01, ***P < 0.001, *italics*: P < 0.10, ns: not significant.

Supplementary Table 2.3. Mean, minimum, maximum, and ANOVA for fractional light interception at emergence + 40 days (FLI.E40), initiation of booting (FLI.InB) and seven days after anthesis (FLI.A7) for 12 CIMMYT spring wheat genotypes from the combined analysis across 2018-19 and 2019-20 in raised beds (B) and flat basins (F). *P < 0.05, **P < 0.01, ***P < 0.001, italics: P < 0.10, ns: not significant.

Trait	<i>p</i> -value									
	Mean		Min		Max		G	Y	PS	PS×G
	B	F	B	F	B	F				
FLI.E40	0.88	0.90	0.87	0.89	0.90	0.93	ns	**	0.122	ns
FLI.InB	0.98	0.99	0.96	0.98	0.98	0.99	***	***	***	<i>0.064</i>
FLI.A7	0.97	0.98	0.94	0.97	0.98	0.99	*	**	**	***



Supplementary Fig. 2.1. Above-ground biomass accumulation during the crop cycle for 12 CIMMYT spring wheat genotypes evaluated across-years in 2017-18, 2018-19 and 2019-20 in raised beds (B) and flat basins (F). TT = thermal time post-emergence. *P < 0.05.

Supplementary Table 2.4. Phenotypic correlations between IPARacc for each phenophase and above-ground biomass accumulated at different phenophases and plant height at physiological maturity among 12 spring CIMMYT wheat genotypes. Values based on means from the combined analysis in 2018-19 and 2019-20 in raised beds (B) and flat basins (F). *P < 0.05, **P < 0.01, ***P < 0.001, †P < 0.10.

	RAISED BEDS (B)				FLAT BASINS (F)			
	IPARacc_ E40-InB	IPARacc_ InB-A7	IPARacc _A7-PM	IPARacc_ _E40-PM	IPARacc_E4 0-InB	IPARacc_ InB-A7	IPARacc _A7- PM	IPARAac c_E40- PM
HeightPM	0.68*	-0.11	0.34	0.51†	0.50†	0.34	-0.04	0.35
BMaccE40_In B	0.91***	-0.24	0.55†	0.72**	0.44	0.20	0.12	0.38
BMaccInB_A7	-0.44	0.46	-0.34	-0.33	0.28	0.64*	-0.36	0.16
BMaccA7_PM	0.25	0.28	0.12	0.25	-0.24	-0.29	0.17	-0.12

HeightPM: plant height at physiological maturity (cm), BMaccE40_InB: biomass accumulated from emergence + 40 days to initiation of booting (g m^{-2}), BMaccInB_A7: biomass accumulated from initiation of booting to anthesis + 7 days (g m^{-2}), BMaccA7_PM: biomass accumulated from anthesis + 7 days to physiological maturity (g m^{-2}), IPARacc_E40-InB: IPAR accumulated from emergence + 40 days to initiation of booting, IPARacc_InB-A7: IPAR accumulated from initiation of booting to anthesis + 7 days, IPARacc_A7-PM: IPAR accumulated from anthesis + 7 days to physiological maturity, IPARacc_E40-PM: IPAR accumulated from emergence + 40 days to physiological maturity.

Supplementary Table 2.5. Phenotypic correlations between percentage light interception and above-ground biomass at different growth stages among 12 spring CIMMYT wheat genotypes. Values based on means from the combined analysis in 2018-19 and 2019-20 in raised beds (B) and flat basins (F).

	RAISED BEDS (B)			FLAT BASINS (F)		
	LI%E40	LI%InB	LI%A7	LI%E40	LI%InB	LI%A7
BME40	-0.07	-0.32	-0.19	-0.20	0.56†	-0.02
BMinB	0.59*	0.71*	0.50†	0.39	0.48	0.07
BMA7	0.73**	0.72**	0.71**	0.27	0.45	-0.21
BMPM	0.70*	0.82**	0.84***	0.14	0.31	-0.01

BME40: biomass at emergence + 40 days (g m^{-2}), BMinB: biomass at initiation of booting (g m^{-2}), BMA7: biomass at anthesis + 7 days (g m^{-2}), BMPM: biomass at physiological maturity (g m^{-2}), LI%E40: light interception at emergence + 40 days, LI%InB: light interception at initiation of booting, LI%A7: light interception at anthesis + 7 days. *P < 0.05, **P < 0.01, ***P < 0.001, †P < 0.10.

Supplementary Table 2.6. Phenotypic correlations between yield, yield components, height, above-ground biomass at different growth stages and shoot number with crop growth rate (CGR; g m⁻² day⁻¹) for 12 spring CIMMYT wheat genotypes. Values based on means from the combined analysis in 2018-19 and 2019-20 in raised beds (B) and flat basins (F).

	RAISED BEDS (B)					FLAT BASINS (F)				
	CGR_E40InB	CGR_InBA7	CGR_GF	CGR_preGF	CGRT	CGR_E40InB	CGR_InBA7	CGR_GF	CGR_preGF	CGRT
YLD	0.55†	0.53†	0.45	0.75**	0.70	-0.11	0.81***	-0.30	0.76**	0.57†
TGW	0.27	0.34	0.39	0.49	0.57†	0.21	-0.10	0.66*	-0.21	0.33
HI	-0.13	0.18	-0.29	0.02	-0.23	-0.47	0.57†	-0.49	0.51†	-0.04
GM2	0.12	0.08	-0.08	0.04	-0.06	-0.22	0.55†	-0.71*	0.61*	0.06
HeightPM	0.48	0.48	0.40	0.39	0.56†	0.32	-0.10	0.49	-0.17	0.37
BME40	-0.41	0.30	-0.28	0.09	-0.22	-0.22	0.02	-0.10	-0.10	-0.35
BMinB	0.91***	-0.11	0.18	0.42	0.47	0.78**	-0.03	0.03	0.16	0.17
BMA7	0.55†	0.72**	0.37	0.95***	0.77**	0.18	0.81***	-0.61*	0.86***	0.30
BMPM	0.69*	0.44	0.69*	0.79**	0.91***	0.26	0.57†	0.07	0.55†	0.81***
ShootsE40	-0.27	-0.25	-0.63*	-0.42	-0.61*	-0.18	0.14	-0.61*	0.21	-0.62*
ShootsA7	-0.12	0.51†	-0.14	0.34	0.00	-0.23	0.46	-0.65*	0.50†	-0.27

YLD: grain yield (g m⁻²), TGW: thousand grain weight (g), HI: harvest index, GM2: grain number per square meter (m⁻²), HeightPM: plant height at physiological maturity (cm), BME40: biomass at emergence + 40 days (g m⁻²), BMinB: biomass at initiation of booting (g m⁻²), BMA7: biomass at anthesis + 7 days (g m⁻²), BMPM: biomass at physiological maturity (g m⁻²), ShootsE40: fertile shoots at emergence + 40 days (m⁻²), ShootsA7: fertile shoots at seven days to anthesis (m⁻²), CGR_E40InB: crop growth rate from emergence + 40 days to initiation of booting (g m⁻² day⁻¹), CGR_InBA7: crop growth rate from initiation of booting to anthesis + 7 days (g m⁻² day⁻¹), CGR_GF: crop growth rate at grain filling (g m⁻² day⁻¹), CGR_preGF: crop growth rate at pre grain filling, from emergence + 40 days to anthesis + 7 days (g m⁻² day⁻¹), CGRT: crop growth rate total, from emergence + 40 days to physiological maturity (g m⁻² day⁻¹). *P < 0.05, **P < 0.01, ***P < 0.001, †P < 0.10.

Supplementary Table 2.7. Broad-sense heritability (H^2) for yield, yield components, biomass at maturity, phenology expressed in days after emergence (DAE), number of shoots for 12 CIMMYT spring wheat genotypes from the three combined analysis across 2017-18, 2018-19 and 2019-20 and RUE from the two combined analysis (2018-19 and 2019-20). Plants (m^{-2})‡ (data 2019-20).

Trait	H^2
YLD ($g\ m^{-2}$)	0.90
TGW (g)	0.95
HI	0.94
GM2 (m^{-2})	0.97
SM2 (m^{-2})	0.87
GPS	0.73
BMPM ($g\ m^{-2}$)	0.86
HeightPM (cm)	0.82
ShootsE40 (m^{-2})	0.17
ShootsA7 (m^{-2})	0.63
DTInB (DAE)	0.75
DTH (DAE)	0.46
DTA (DAE)	0.45
DTPM (DAE)	0.28
Plants (m^{-2})‡	0.86
RUE_E40InB	0.42
RUE_InBA7	0.71
RUE_GF	0.09
RUE_preGF	0.82
RUET	0.84

YLD: grain yield, TGW: thousand grain weight, HI: harvest index, GM2: grain number per square meter, SM2: spikes per square meter, GPS: grains per spike, BMPM: biomass at physiological maturity, HeightPM: plant height at physiological maturity, ShootsE40: fertile shoots at emergence + 40 days, ShootsA7: fertile shoots at seven days to anthesis, DTInB (DAE, days after emergence): days to initiation of booting (GS41), DTH (DAE): days to heading (GS55), DTA (DAE): days to anthesis (GS65), DTPM (DAE): days to physiological maturity (GS87), Plants: number of plants per square meter, RUE_E40InB: RUE calculated from forty days after emergence to initiation of booting, RUE_InBA7: RUE calculated from initiation of booting to seven days after emergence, RUE_GF: RUE calculated during the grain filling period from seven days after anthesis to physiological maturity, RUE_preGF: RUE pre grain-filling from forty days after emergence to seven days after anthesis, RUET: RUET total, from forty days after emergence to physiological maturity (RUET).

3 CHAPTER 3. EFFECTS OF CANOPY ARCHITECTURE TRAITS ON RADIATION-USE EFFICIENCY (RUE) IN WHEAT CULTIVARS IN RAISED BEDS AND FLAT BASINS PLANTING SYSTEMS.

Paper to be submitted to Field Crops Research

Marcela A. Moroyoqui-Parra¹, Gemma Molero^{2,4}, Matthew P. Reynolds², Oorbessy Gaju³, Erik H. Murchie¹, M. John Foulkes^{1*}

¹Division of Plant and Crop Science, School of Biosciences, University of Nottingham, Sutton Bonington Campus, Leicestershire LE12 5RD, United Kingdom.

²Global Wheat Program, International Maize and Wheat Improvement Center (CIMMYT), carretera Mexico-Veracruz Km 45, El Batan, Texcoco, Mexico, CP 56237.

³Lincoln Institute for Agri-Food and Technology, University of Lincoln, Riseholme Park, Lincoln, Lincolnshire, LN2 2LG, United Kingdom.

⁴KWS Momont Recherche, 7 rue de Martinval, 59246 Mons-en-Pevele, France.

*** Correspondence:**

John Foulkes

John.Foulkes@nottingham.ac.uk (M.J. Foulkes).

Keywords: canopy architecture, radiation-use efficiency, biomass, flag-leaf angle, flag-leaf curvature, leaf size, spring wheat.

3.1 Abstract

Wheat breeders will need to increase radiation-use efficiency (RUE) to raise biomass and grain yield in the future. Canopy architecture influences RUE by affecting the distribution of light among the canopy leaf layers. Erect canopies allow more PAR to be intercepted by leaves lower in the canopy and may increase RUE by reducing light-saturation of photosynthesis in the upper leaves. Canopy architecture traits were evaluated for twelve spring wheat CIMMYT genotypes contrasting for canopy architecture under two planting systems (PS), raised beds (B) and flat basins (F), in NW Mexico in two years under irrigated, optimal conditions. The objectives were: i) to determine whether canopy architecture traits influence radiation interception, RUE, biomass and grain yield of genotypes and ii) examine the interaction between cultivars and planting system. Planting system differences were found between raised beds and flat basins. Flag-leaf angle (FLA) at initiation of booting

(GS41) was decreased by 7° (more upright flag leaf) but seven days after anthesis (GS65 + 7 days) was increased by 14° in B compared to F. In addition, flag-leaf curvature (FLcv) at GS41 (as described by the distance from the point of inflexion of the leaf to the tip) was increased by 6.2 cm in B compared to F. RUE from emergence + 40 days to GS41 (RUE_E40InB) was decreased by 11.5% but from emergence + 40 days to grain filling (RUE_T) was increased 6.2% in B compared to F. More upright flag-leaf angle and a higher leaf curvature at GS65 + 7 days among cultivars were associated with higher RUE during the grain-filling period (RUE_GF) in flat basins. Less upright flag-leaf angle at GS41 also increased light interception from emergence + 40 days to GS41 in raised beds ($r = 0.69$, $P < 0.05$). The planting system affected flag-leaf angle at GS65 + 7 days with leaf angle decreasing (more upright leaves) in flat basins compared to raised beds, but cultivars differed in the extent of the decrease. In addition, cultivars which showed relatively more upright leaves in flat basins showed relatively greater enhancement in season-long RUE as well RUE pre-grain filling RUE in flat basins compared to raised beds. These results suggest that plant breeders should take into account the planting system when selecting canopy architecture traits to enhance RUE, biomass and yield.

3.2 Introduction

Since harvest index (grain dry matter as a proportion of above-ground dry matter) in wheat is approaching its theoretical limit of ca. 0.65 (Austin, 1980; Foulkes et al., 2011) in some environments, it is evident that plant breeders will need to increase radiation-use efficiency (above ground DM per unit radiation intercepted; RUE) to enhance biomass and continue to raise grain yield (Murchie et al., 2009; Foulkes et al., 2011; Parry et al., 2011). In modern wheat cultivars, grain growth is mainly sink limited during grain-filling under favourable conditions (Fischer, 1985; Calderini et al., 2001; Fischer, 2008); whereas biomass growth is source limited during the rapid spike growth period from booting to anthesis when assimilate supply to the spike determines floret survival and grains m^{-2} (Fischer, 1985). Therefore, it is crucial to increase RUE from booting to anthesis to enhance grains m^{-2} (Miralles and Slafer, 2007). Most modern wheat genotypes achieve close to full radiation interception during stem elongation and the first half of grain filling, although radiation may not be distributed among the canopy layers optimally for efficient conversion of intercepted radiation into biomass (Gifford et al., 1984). Therefore, there is scope for increases in radiation-use efficiency due to the alteration of the canopy architecture (Reynolds et al., 2000b; Murchie et al., 2009).

Optimum canopy structure determined by leaf angle, size, shape, density, thickness and area and their distributions and arrangements is essential for optimal light distribution to the lower canopy (Burgess, 2017). Leaf angle can be measured as the angle between the leaf blade midrib and the stem (Mantilla-Perez and Salas Fernandez, 2017) and smaller leaf angle (more upright leaves) has been related with a greater canopy photosynthetic efficiency (Isidro et al., 2012). Duncan (1971) reported a more upright leaf position permitted increased photosynthetic capacity through reduced light saturation of photosynthesis of upper leaves and increased RUE. Thus, upright leaves reduce light saturation of photosynthesis at the top of the canopy and permit greater photosynthetically active radiation (PAR) penetration so more PAR can be intercepted by the lower leaves (Hirose, 2004; Long et al., 2006). Typically lower leaf layers (below flag-leaf) in the canopy are not exposed to high radiation during early hours of the day and late afternoon, but only around midday, when they may be exposed to over $500 \mu\text{mol m}^{-2} \text{s}^{-1}$ for photosynthesis (Horton, 2000), depending on the architectural properties. Excessive radiation intercepted by the upper leaf layers causes photooxidative damage to the photosynthesis apparatus (PSII reaction center) (Parry et al., 2011) but this can be reduced by more erect leaves which reduce light saturation of photosynthesis and increase RUE (Murchie et al., 1999). The advantages of upright leaves in rice genotypes were also described by Murchie et al. (1999) and Peng et al. (2008): less light stress at midday, maximization of PAR interception and a superior carbon assimilation in the canopy.

The concept of an ideal plant architecture in a cereal crop with an erect leaf angle at the top of the canopy, less upright leaves in the middle of the canopy and more planophiles leaves in the lower canopy has been proposed (Duncan, 1971; Ku et al., 2010; Zhu et al., 2010; Ort et al., 2015; Mantilla-Perez et al., 2020). The heterogeneity of light is also reflected in the appearance of sunflecks and shade-flecks inside a canopy, which, in turn, is influenced by the canopy architecture and air movement within a canopy (Percy, 1990). For instance, Murchie et al. (2009) described the importance of changes of leaf posture, size and density in altering architecture and improving the dynamics of light saturation. Effects of more upright leaf angle to increase leaf photosynthetic efficiency, above-ground biomass and net carbon accumulation were shown in a study of spring and winter wheat cultivars in the United States and England by Choudhury (2000). In a study in maize, erectophile lines showed 41% greater grain yield compared with planophiles ones (Pendleton et al., 1968). In a recent study in spring wheat cultivars in Australia erect-leaved canopies yielded 13% more

than canopies with lax leaves (Richards et al., 2019) associated with greater biomass rather than HI. An evaluation of two winter wheat genotypes in the UK with contrasting canopy architecture found that the erect genotypes showed greater photosynthesis during booting (Austin et al., 1976) and maintained higher leaf area index (LAI) during grain filling due to slower senescence rate at the bottom of the canopy and had higher grain yield (Austin et al., 1976; Innes and Blackwell, 2009). Many other studies reported advantages of erectophile lines compared to planophile lines, e.g. in maize (Duncan, 1971; Ku et al., 2010; Cabrera-Bosquet et al., 2016), rice (Murchie et al., 1999; Horton, 2000; Peng et al., 2008) and wheat (Innes and Blackwell, 2009; Reynolds et al., 2012a; Yang et al., 2016; Townsend et al., 2018). Relatively few studies to date have, however, presented detailed results showing the quantitative relationship between genetic variation in canopy architecture traits, light interception and RUE amongst genotypes.

Genetic variation in flag-leaf angle in wheat measured as the angle from the stem (just below the spike) to the flag-leaf midrib was reported from 54.1 to 76.0° at around anthesis in different locations in China (Liu et al., 2018). During the milky ripe stage, Yang et al. (2016) reported flag-leaf values from 46.7 to 50.2° in winter wheat cultivars. The light extinction coefficient (k) describes the efficiency of the light interception by the canopy and is partly determined by the angle and orientation of the leaves whereby erectophile canopies have lower k compared with the canopies with lax leaves (Saeki, 1960; Murchie and Reynolds, 2012; Zhang et al., 2014; Tao et al., 2018). For wheat, genetic variation in k calculated from the photosynthetically active radiation (PAR) is reported to range from 0.37 to 0.82 (Yunusa et al., 1993; O'Connell et al., 2004). Canopy architecture improvement is also related to optimized leaf curvature (Reynolds et al., 2012a). Ledent (1978) observed that leaf curvature was determined by leaf strength, which depends on rigidity and leaf size (leaf length and width), and reported that cultivars with higher yield tended to have less curved leaves. Many winter wheat modern cultivars have already upright leaves (e.g. (Shearman et al., 2005)), but most CIMMYT spring wheat cultivars still have more floppy leaves. Therefore, it is important to examine effects of leaf-angle and leaf-curvature in CIMMYT spring wheat cultivars.

Wheat is predominantly planted on the flat-basin planting system worldwide (Fahong et al., 2004). However, over the past 20 years in Northwest Mexico a raised-bed planting system has been implemented which consists of rows planted on the top of beds (Fahong et al., 2004). Advantages of raised beds over flat basins include reduction of irrigation water

requirements, improvement of nitrogen fertilizer efficiency, plant establishment, and reduction of lodging, weeds and diseases (Sayre and Moreno Ramos, 1997; Fahong et al., 2004; Hassan et al., 2005; Kukal et al., 2005; Ram et al., 2005; Sayre et al., 2008; Limon-Ortega, 2011; Noorka and Tabasum, 2013; Majeed et al., 2015). Higher grain yields were found in raised beds than flats for 12 CIMMYT spring wheat cultivars in the present study (see **Chapter 3**). To date, few studies in wheat have quantified effects of canopy architecture traits on light interception, RUE and biomass accumulation comparing raised beds and flat basin planting systems. In addition, as far as we know, there are no studies reporting genetic variation of flag-leaf curvature using a quantitative method in wheat. Previously we reported on genetic variation in RUE and associations with biomass in twelve CIMMYT spring wheat cultivars in field experiments in two irrigated planting systems in NW Mexico. Therefore, in this study we investigate quantitatively the effects of contrasting canopy architecture on radiation interception, RUE and biomass in this set of contrasting cultivars in the two planting systems.

The aims of the present research are: (i) to determine whether canopy architecture traits influence light interception, RUE and biomass and grain yield in spring wheat genotypes and (ii) to examine the interaction between genotypes with contrasting canopy architecture and two planting systems, raised beds and flat basins.

3.3 Materials and methods

3.3.1 Experimental site, design and treatments

Two field experiments were carried out at CIMMYT CENEB in the Yaqui Valley in Ciudad Obregon, Sonora, Mexico (27°39'5" N, 109°9'26" W, 38 masl) in 2018-19 and 2019-20 under high-yield potential conditions. The soil type was a sandy clay, mixed montmorillonitic typic caliciorthid, low in organic matter, and slightly alkaline (pH 7.7) (Sayre et al., 1997). There were two planting systems: raised beds and flat basins with twelve spring wheat genotypes and three replicates. Each planting system (PS) in an experiment was sown in a rectangular matrix of 36 plots with border plots. The two planting systems were sown in adjacent areas in the field, with a 5 m gap between the border plots of the planting systems. Twelve spring wheat genotypes were chosen based on contrasting RUE and biomass in previous field experiments of which ten were selected from the HiBAP I (High Biomass Association Panel I) (Molero et al., 2019) and two from the ESWYT (Elite Selection Wheat Yield Trial series) in the CIMMYT wheat breeding program (see **Table 2.1** in **Chapter 2.3.1**). From the twelve genotypes, three were elite CIMMYT cultivars and the others were elite advanced lines. The raised beds (B) consisted of two beds per plot (0.8 m wide and 4 m long = 6.4 m² per plot) with two rows per bed (0.24 m between rows) and 0.56 m between the two beds. For flat basins (F) there were eight rows per basin (2.5 m wide and 5 m long = 12.5 m² per plot) with 0.20 m between rows in 2018-19. In 2019-20, there were six rows per basin with 0.24 m between rows. The sowing dates were 30 November 2018 and 21 December 2019 in raised beds and 1 December 2018 and 17 December 2019 in flat basins. Plant emergence date (50% plot) was 7 December 2018 and 31 December 2019 in raised beds and 9 December 2018 and 26 December 2020 in flat basins. The seed rate was 102 kg ha⁻¹ in raised beds for both years and 107 kg ha⁻¹ and 106 kg ha⁻¹ in 2018-19 and 2019-20, respectively, in flat basins. In 2018-19 and 2019-20, both planting systems were fertilized with 50 kg N ha⁻¹ (as urea) during land preparation followed by 50 kg P ha⁻¹ at sowing. The second N application was added at the time of first irrigation (200 kg N ha⁻¹). In 2018-19, the irrigation was applied every 3 – 4 weeks during the cycle as flood irrigation. In 2019-20, raised beds were irrigated as the first year and the flat basins were irrigated using drip irrigation every 3 – 4 weeks. Appropriate applications of herbicides, fungicides and pesticides were applied to minimize the effects of weeds, diseases and pests (see **Appendix Table 1** for details). No plant growth regulators were applied.

Solar radiation, temperature and rainfall were measured in both years from emergence to physiological maturity. The meteorological data were obtained from a station located within 0.5 km of the experiments in the Yaqui Valley.

3.3.2 Crop measurements

3.3.2.1 Phenology

The phenology was measured according to Zadoks et al. (1974) at initiation of booting (GS41), heading (GS55), anthesis (GS65) and physiological maturity (GS87) when 50% of the shoots in the plot reached the stage (Pask et al., 2012b).

3.3.2.2 Growth analysis at emergence + 40 days, GS41 and GS65 + 7 days.

Biomass samples were taken at three stages (emergence + 40 days, E40; initiation of booting, InB; and anthesis + 7 days, A7) by cutting shoots at ground level at least 0.5 m from the end of the plot to avoid border effects. At forty days after emergence plant material was harvested in 0.40 m² area (0.25 m x 1.6 m) in raised beds and 0.45 m² (0.25 m x 1.8 m) in flat basins. At initiation of booting (GS41) and seven days after anthesis (GS65 + 7 days) the sample was taken in a 0.80 m² area (0.50 m x 1.6 m) in raised beds and a 0.90 m² area (0.50 m x 1.8 m) in flat basins. The fresh weight of the sample was recorded. A subsample of 50 shoots (fertile shoots at seven days after anthesis) was collected at each stage and fresh and dry weight was recorded after drying at 70°C for 48 h. In order to calculate green area index (GAI; green area per unit ground area), 12 randomly selected shoots were taken from the fresh sample at initiation of booting and seven days after anthesis (fertile shoots, those with a spike, at GS65 + 7 days). The green area of the leaf lamina and the projected area of the spike and stem was measured separately using a leaf area meter (LI 3100C, Licor Biosciences, Lincoln, NE, USA) and applying the equation (3.1):

$$\text{GAI} = (\text{Green area of leaf lamina, spike and stem per shoot}) \times \text{fertile shoots m}^{-2} \quad (3.1)$$

3.3.2.3 Light interception and radiation-use efficiency

Fractional interception of photosynthetically active radiation (PAR, 400 - 700 nm) (FI) was measured using a 1 m linear ceptometer (AccuPAR LP-80, Decagon Devices, Pullman, WA, USA) at emergence + 40 days, GS41 and GS65 + 7 days in 2018-19 and 2019-20. The measurements were taken above the canopy (incident radiation) inverting the ceptometer 10

cm above the canopy (reflected radiation) and below the canopy at ground level (transmitted radiation) during sunny days from 11 am to 1 pm when the sun was near its zenith and when wind speed was low. The ceptometer was positioned across the plant rows diagonally at approximately at 45° angle. In the raised beds, a small section of the gap between the beds within a plot was included while measuring with the ceptometer. A reading per bed was taken in raised beds and two readings per plot in flat basins. Fractional PAR interception (FI) was calculated using the equation (3.2):

$$FI = \frac{(PAR_i - PAR_r) - (PAR_t)}{(PAR_i - PAR_r)} \quad (3.2)$$

Where PAR_i is the incident photosynthetically active radiation (PAR, 400 – 700 nm), PAR_r is the reflected PAR and PAR_t is the transmitted PAR at the soil surface.

The light extinction coefficient (k_{par}) was calculated as described by (Monsi, 1953) using the equation (3.3):

$$k_{par} = \ln \left(\frac{I}{I_0} \right) / L \quad (3.3)$$

Where I_0 is the incident PAR, I the amount of PAR transmitted and L is GAI.

Radiation-use efficiency (RUE) was calculated in each plot as the increment in the above-ground dry matter divided by the increment in intercepted PAR (IPARacc) for the phase (Monteith and Moss, 1977) in 2018-19 and 2019-20. PAR interception for the phenophases up to GS65 + 7 days (IPARaccE40 - InB; IPARaccInB - A7; IPARaccE40 - A7) was calculated from the cumulative incident PAR for the days of the phase and then multiplying by the average FI from the start to the end of the phase. For PAR interception for the phase from GS65 + 7 days to physiological maturity (IPARaccA7 - PM) the FI at GS65 + 7 days was applied to the incident PAR for each day during the phase and the daily increments of PAR interception accumulated; a correction factor of 0.5 was applied to the FI during the last 25% of the grain filling period to account for the interception by senesced canopy (Reynolds et al., 2000b). PAR interception from emergence + 40 days to physiological maturity was calculated as the sum of IPARaccE40 - A7 and IPARaccA7 - PM. RUE was measured over the different phases: RUE_E40InB (from 40 days after emergence (close to canopy closure) to initiation of booting), RUE_InBA7 (from initiation of booting to seven days after anthesis), RUE_preGF (RUE pre-grain-filing from 40 days after emergence to seven days after anthesis) and RUE_GF (RUE grain-filling from seven

days after anthesis to physiological maturity) and RUET (from emergence + 40 days to physiological maturity). RUE was therefore calculated using the equations 2.3 - 2.7 in **Chapter 2.3.2.3**.

3.3.2.4 Canopy architecture

Canopy architecture was scored for each plot at initiation of booting and seven days after anthesis. A visual score (FLvsc) of overall canopy architecture was made for each plot using the scale of Richards et al. (2019). A score of 1 was given to plots where all leaves were visually erect, a score of 6 was given when about 60% of the leaves in the upper canopy of each plot were planophile and a score of 10 was given to plots where all visible leaves in the upper canopy appeared planophile. More detailed canopy architecture measurements were taken on six fertile shoots per plot (**Fig. 3.1**). The flag-leaf angle (FLA; °) was measured from the vertical stem to the middle part of the flag-leaf using a protractor. The flag-leaf curvature (FLcv; cm) was measured as the distance from the point of inflexion to the tip of the leaf. Total length and total width (at the widest point) of the flag leaf were measured using a ruler. To maximize precision of these measurements, measurements were not taken under windy conditions (Mantilla-Perez et al., 2020). Plant height was measured from the ground to the tip of the spike (awns were not considered) shortly before physiological maturity at six random locations within the plot.

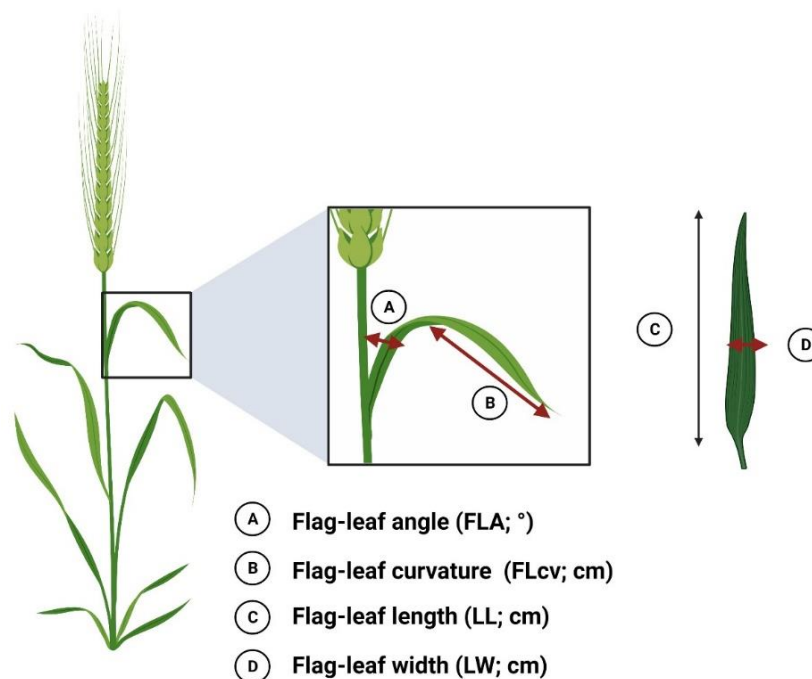


Fig. 3.1. Diagram of canopy architecture measurements on the flag leaf in wheat.

3.3.2.5 Flag-leaf relative chlorophyll content

Relative chlorophyll content of the flag leaf was measured using a hand-held SPAD meter (SPAD 502 Minolta, Japan) in the middle of the leaf 3 at seven days after anthesis taking six readings per plot.

3.3.2.6 Growth analysis at physiological maturity, grain yield and yield components

For biomass at physiological maturity, 50 fertile shoots (2017-18 and 2018-19) or 30 fertile shoots (2019-20) (those with a spike) were sampled randomly by cutting at ground level to estimate harvest index (ratio of grain dry matter to above-ground dry matter) and grain yield components as described in **Chapter 2.3.2**. After physiological maturity, grain yield was measured in each plot by machine harvesting in an average plot area of 3.2 and 4.0 m² per plot in raised beds and flat basins, respectively, and values further adjusted to moisture percentage measured in each plot. In each plot, 50 cm at the end of the plot was discarded in order to remove the border effect. After harvesting, a subsample of grain was taken and dried at 70°C to calculate thousand-grain weight using the digital image system Seed Counter (SeedCountSC5000 Image Analyzer).

3.3.3 Statistical analysis

Adjusted means for grain yield, yield components and physiological traits were calculated using a general linear model (GLM) ANOVA procedure from META R 6.04 (Alvarado et al., 2020). Replications, years and planting systems were considered as random effects, and genotypes as fixed effects. A covariate for anthesis date was used as a fixed effect and was included when significant. Phenotypic correlations between traits were Pearson's correlation coefficient calculated using either the three-year genotype means or the two-year genotype means. Linear regression analysis was applied to the three-year or two-year genotype means for selected traits. Broad sense heritability (H²) was calculated using across the three or two years, using equation (3.4):

$$H^2 = \frac{\sigma_g^2}{\sigma_g^2 + \frac{\sigma_{gy}^2}{y} + \frac{\sigma_{gs}^2}{s} + \frac{(\sigma_{gy})^2(s)}{ys} + \frac{\sigma_e^2}{rys}} \quad (3.4)$$

Where σ^2 = error variance, σ_g^2 = genotypic variance, σ_{gy}^2 = G × Y variance, σ_{gs}^2 = PS variance, s = number of PS, y = number of years, σ_e^2 = residual variance, r = number of replicates.

3.4 Results

3.4.1 Grain yield, yield components and above-ground biomass

Averaging across 2018-19 and 2019-20, genetic ranges of grain yield, HI, yield components and above-ground biomass in each PS are presented in **Table 3.1**. Genetic variation was shown in all the traits. Grain yield varied from 536 to 752 g m⁻² in raised beds and 535 to 701 g m⁻² in flat basins; and was on average 10.8% higher in beds than flats (P < 0.001). In addition, a PS × G interaction was observed for grain yield (P < 0.01) with the increase in raised beds ranging from 1 to 132 g m⁻². Grains per m² (GM2) and spikes per m² were higher in beds than flats (P < 0.001 and P < 0.05, respectively), but no difference was found in thousand-grain weight (TGW) and harvest index (HI). Above-ground biomass was higher in flat basins than raised beds at forty days after emergence (P < 0.05) with genetic ranges from 167 to 237 g m⁻² and 171 to 224 g m⁻², respectively. However, above-ground biomass at physiological maturity was higher in raised beds than flat basins (P < 0.01) ranging from 1182 to 1576 g m⁻² in raised beds and 1192 to 1459 m⁻² in flat basins. A trend was found for lower above-ground biomass at initiation of booting (P = 0.064) in beds than flats, but higher biomass in beds than flats at seven days after anthesis (P = 0.064). There was a PS x G interaction for biomass at forty days after emergence (P < 0.01), initiation of booting (P < 0.001), seven days after anthesis (P < 0.001) and physiological maturity (P < 0.05).

Table 3.1. Mean, minimum, maximum, heritability (H²) and ANOVA for grain yield, yield components and above-ground biomass at different growth stages from the combined analysis across 2018-19 and 2019-20 in raised beds (B) and flat basins (F).

Trait	Mean		Min		Max		<i>p-value</i>				
							H ²	Y	G	PS	PS×G
	B	F	B	F	B	F					
YLD (g m ⁻²)	677	611	536	535	752	701	0.75	ns	***	***	**
TGW (g)	45.68	45.41	35.27	35.52	51.47	51.94	0.99	***	***	ns	ns
HI	0.46	0.46	0.42	0.42	0.50	0.50	0.92	***	***	ns	ns
GM2 (m ⁻²)	14974	13605	11990	10815	18402	16896	0.92	*	***	***	0.157
SM2 (m ⁻²)	286	276	242	206	334	327	0.94	***	***	*	0.165
BME40 (g m ⁻²)	193	206	171	167	224	237	0.00	***	***	*	**
BMI _n B (g m ⁻²)	541	565	410	505	683	639	0.93	***	***	<i>0.064</i>	***
BMA7 (g m ⁻²)	1062	1032	842	867	1187	1151	0.91	ns	***	<i>0.064</i>	***
BMPM (g m ⁻²)	1457	1335	1182	1192	1576	1459	0.87	*	***	**	*
HeightPM (cm)	107.6	105.8	92.0	89.3	124.7	120.3	0.95	***	***	0.148	<i>0.059</i>

Yield: grain yield, TGW: thousand-grain weight, HI: harvest index, GM2: grain number per square meter, SM2: spikes per square meter, BME40: biomass at forty days after emergence, BMI_nB: biomass at initiation of booting, BMA7: biomass at seven days after anthesis, BMPM: biomass at physiological maturity, HeightPM: height at physiological maturity *P < 0.05, **P < 0.01, ***P < 0.001, *italics*: P < 0.10, ns: not significant.

3.4.2 Canopy architecture traits

High values of heritability for canopy architecture traits were observed from 0.81 to 0.99 (**Table 3.2**). Flag-leaf angle was higher (i.e. less upright leaf) in raised beds than flat basins at initiation of booting ($P < 0.001$). However, at seven days after anthesis, flag-leaf angle was higher in raised beds than flat basins ($P < 0.05$). At initiation of booting, FLA varied among cultivars from 3° (BACANORA T88) to 9° (KUTZ) in raised beds and 4° (BACANORA T88) to 26° (KUTZ) in flat basins ($P < 0.001$). At seven days after anthesis, FLA varied from 35° (BACANORA T88) to 103° (KUTZ) in raised beds and 28° to 96° (KUTZ and C80.1/3*QT4118) in flat basins ($P < 0.001$). Flag-leaf curvature (FLCv) ranged among cultivars from 16.4 to 21.8 cm in raised beds and 6.0 to 17.4 cm (increased length from point of inflection to leaf tip representing more curved leaf) in flat basins at initiation of booting ($P < 0.001$). At seven days after anthesis, FLCv varied from 8.6 to 23.2 cm in raised beds and 5.8 to 18.2 cm in flat basins ($P < 0.001$). A planting system effect was observed on FLCv at initiation of booting ($P < 0.01$) with higher values in raised beds. In contrast, no planting system effect on the visual score of flag-leaf curvature was found. Flag-leaf curvature visual score showed genetic variation at GS41 ($P < 0.001$) and GS65 + 7 days ($P < 0.001$). An association between visually assessed flag-leaf curvature and FLCv score measured with a ruler was only found in beds at GS41 ($R^2 = 0.51$, $P < 0.01$) (**Supplementary Table 3.1**). Flag-leaf length was higher in flat basins than raised beds at initiation of booting ($P < 0.001$) but higher in raised beds at seven days after anthesis ($P < 0.001$) (**Supplementary Table 3.1**). A PS \times G interaction was found for flag-leaf angle at GS41 and GS65 + 7 days as well as FLCv at GS41. The increase in flag-leaf angle in beds compared to flats ranged among cultivars from 1 to 18° at GS41 and the decrease in flag-leaf angle in beds compared to flats at GS65 + 7 days ranged from 0 to 29°. For FLCv at GS41 the increase in beds compared to flats ranged from 2.64 to 12.19 cm.

Table 3.2. Flag-leaf angle (FLA), flag-leaf curvature visual score (1-10, FLCvs) and distance from point of inflexion of the flag-leaf to the tip (FLcv) at initiation of booting (GS41, InB) and seven days after anthesis (GS65, A7) for 12 CIMMYT spring wheat genotypes from the combined analysis across 2018-19 and 2019-20 in raised beds (B) and flat basins (F).

Gen	Initiation of booting						Anthesis + 7 days					
	FLAInB		FLcvInB		FLcvInB		FLAA7		FLcvA7		FLcvA7	
	(°)		(cm)				(°)		(cm)			
	B	F	B	F	B	F	B	F	B	F	B	F
BACANORA T88	3	4	22.08	13.86	1	2	35	28	23.64	17.79	3	2
C80.1/3*QT4118	7	20	17.53	12.18	8	6	97	96	17.11	11.33	7	7
CHEWINK#1	7	14	20.97	15.21	9	8	66	61	20.83	15.40	9	8
SOKOLL//PUB94	7	25	17.65	7.91	8	8	53	53	19.51	16.13	7	7
NELOKI	3	6	21.13	16.34	3	3	46	45	20.03	18.52	5	4
W15.92/4/PASTOR	7	12	16.71	7.06	8	7	76	73	18.22	13.37	7	7
KUKRI	8	11	16.38	15.75	8	8	86	98	16.71	6.76	7	7
KUTZ	9	26	18.22	6.03	8	8	103	96	8.59	5.82	7	6
SOKOLL	7	10	17.79	15.15	8	7	67	82	16.59	6.39	7	7
BORLAUG100	8	14	20.18	15.07	9	9	97	68	18.88	12.67	8	8
ITP40/AKURI	4	6	22.33	15.79	2	2	46	49	21.93	17.70	5	2
CHIPAK*2//	6	8	20.78	17.41	5	5	87	63	20.30	8.83	5	5
Mean	6	13	19.31	13.15	6	6	72	68	18.52	12.56	6	6
H ²	0.47		0.53		0.98		0.97		0.80		0.97	
LSD (G) (5%)	2.129		4.026		1.610		10.140		3.829		1.088	
CV%	13.53		15.29		16.11		8.98		15.18		10.97	
G (p value)	***		***		***		***		***		***	
PS (p value)	***		**		0.165		*		0.144		0.080	
Y (p value)	0.110		***		ns		*		***		ns	
PSxG (p value)	***		0.116		ns		***		ns		***	

FLAInB: flag-leaf angle at initiation of booting (°), FLcvInB: point of inflexion of the flag leaf to the tip (cm), FLCvsInB: flag-leaf curvature score at initiation of booting, FLAA7: flag-leaf angle seven days after anthesis (°), FLcvA7: flag-leaf curvature at seven days after anthesis (cm), FLCvsA7score: point of inflexion of the flag leaf to the tip at seven days after anthesis. *P < 0.05, **P < 0.01, ***P < 0.001, *italics*: P < 0.10, ns: not significant.

3.4.3 GAI, k_{par} and RUE

Green Area Index at GS41 ranged among cultivars from 6.59 to 10.10 in raised beds and 7.35 to 11.25 in flat basins and was overall higher in flat basins (P < 0.01; **Table 3.3**). GAI at GS65 + 7 days did not differ between planting systems ranging from 5.71 to 8.18 in raised beds and 6.82 to 8.44 in flat basins (P < 0.001). Light extinction coefficient (k_{par}) at initiation of booting varied from 0.42 to 0.61 in raised beds and 0.42 to 0.57 in flat basins (P < 0.001) with no difference between planting systems. At GS65 + 7 days, k_{par} varied from 0.71 to 0.82 in raised beds and 0.54 to 0.67 in flat basins (P = 0.120) and was overall higher in raised beds (P < 0.001). There was a trend for a negative correlation between genetic

variation in k_{par} and flag-leaf angle at initiation of booting ($P = 0.10$) in raised beds (**Supplementary Table 3.2**).

Table 3.3. Green area index (GAI) and light extinction coefficient (k_{par}) at initiation of booting and seven days after anthesis for 12 CIMMYT spring wheat cultivars from the combined analysis across 2018-19 and 2019-20 in raised beds (B) and flat basins (F).

Genotype	GAI.InB		k_{par} .InB		GAI.A7		k_{par} .A7	
	B	F	B	F	B	F	B	F
BACANORA T88	6.59	8.45	0.61	0.49	6.29	6.82	0.77	0.64
C80.1/3*QT4118	9.53	8.40	0.45	0.50	8.18	7.02	0.71	0.57
CHEWINK#1	8.82	9.56	0.45	0.50	7.77	8.44	0.75	0.50
SOKOLL//PUB94	8.04	8.92	0.53	0.51	7.72	7.08	0.78	0.67
NELOKI	6.71	7.35	0.53	0.57	5.71	6.83	0.82	0.65
W15.92/4/PASTOR	8.36	7.70	0.44	0.57	6.53	6.74	0.79	0.66
KUKRI	8.52	10.64	0.49	0.45	7.36	7.86	0.74	0.61
KUTZ	10.10	11.25	0.42	0.42	7.62	7.18	0.72	0.60
SOKOLL	7.78	8.66	0.53	0.56	7.70	8.13	0.74	0.54
BORLAUG100	7.62	9.09	0.51	0.44	7.89	7.61	0.75	0.59
ITP40/AKURI	8.16	8.65	0.48	0.50	7.23	6.96	0.79	0.63
CHIPAK*2//	9.42	9.41	0.42	0.47	7.30	7.91	0.74	0.54
Mean	8.30	9.01	0.49	0.50	7.27	7.38	0.76	0.60
H ²	0.58		0.36		0.11		0.00	
LSD (G) (5%)	2.062		0.118		1.414		0.163	
CV%	14.67		14.77		11.86		14.73	
G (<i>p-value</i>)	***		***		***		<i>0.120</i>	
PS (<i>p-value</i>)	**		ns		ns		***	
Y (<i>p-value</i>)	***		ns		**		***	
PS×G (<i>p-value</i>)	0.115		<i>0.080</i>		0.121		***	

GAI.InB: green area index at initiation of booting, k_{par} .InB: light extinction coefficient at initiation of booting, GAI.A7: green area index at seven days after anthesis, k_{par} .A7: light extinction coefficient at seven days after anthesis. * $P < 0.05$, ** $P < 0.01$, *** $P < 0.001$, *italics*: $P < 0.10$, ns: not significant

RUE showed genetic variation from forty days after emergence to initiation of booting (RUE_E40InB) ($P < 0.001$), initiation of booting to seven days after anthesis (RUE_InBA7) ($P < 0.01$), forty days after emergence to seven days after anthesis (RUE_preGF; pre-grain filling period) ($P < 0.001$), seven days after anthesis to physiological maturity (RUE_GF; grain filling) ($P < 0.01$) and forty days after emergence to physiological maturity (RUET, total) ($P < 0.001$) (**Fig. 3.2**). RUE_E40InB ($P < 0.05$) was higher in flat basins than raised beds. In contrast, RUET ($P < 0.05$) and RUE_InBA7 ($P < 0.05$) were higher in raised beds. All RUEs showed a PS × G interaction ($P < 0.05$), except for RUE_InBA7.

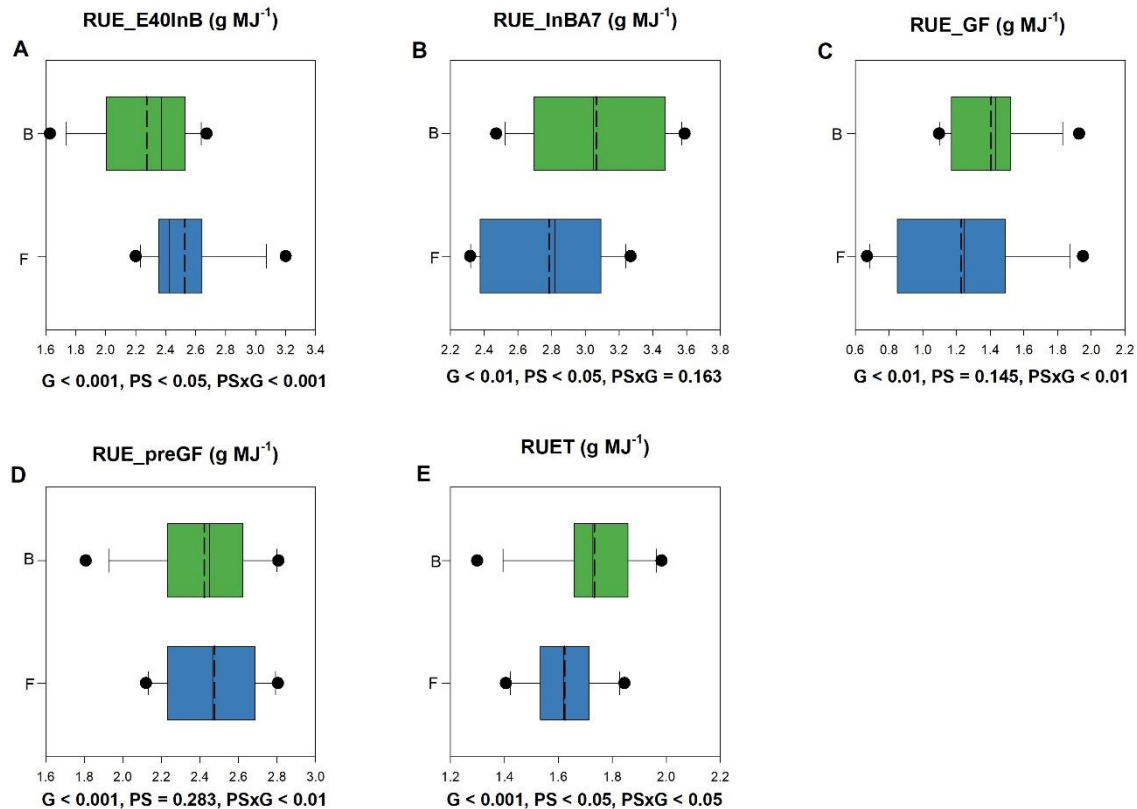


Fig. 3.2. Boxplots of genetic variation in RUE (g MJ⁻¹) at a) RUE_E40InB: from 40 days after emergence to initiation of booting, b) RUE_InBA7: from initiation of booting to seven days after anthesis, c) RUE_preGF: pre grain-filling, from forty days after emergence to seven days after emergence, d) RUE_GF: grain-filling, from seven days after emergence to physiological maturity and e) RUET: from forty days after emergence to physiological maturity, for 12 CIMMYT spring wheat cultivars evaluated across-years 2018-19 and 2018-19 in raised beds (B) and flat basins (F). The middle dotted line is the adjusted mean across lines. Statistical significances for genotype (G), planting systems (PS) and the interaction between them (PS × G) are presented below each boxplot.

3.4.4 Canopy architecture traits and correlations with light interception, RUE, grain yield and yield components

Fig. 3.3 shows the associations between flag-leaf angle at GS65 + 7 days and RUE_GF averaged across years. A significant association was found only in 2018-19 (**Fig. 3.3**) in flat basins ($R^2 = -0.47$, $P < 0.05$) in which canopies with more upright flag-leaf angle at GS65 + 7 days had higher RUE during the grain-filling period. Regressions between FLCv and RUE are shown for GS41 and GS65 + 7 days in **Fig. 3.4**. A strong positive association was found for flat basins between FLCv at initiation of booting and RUE_GF ($R^2 = 0.38$, $P < 0.05$) and an even stronger association was found between FLCv at GS65 + 7 days and RUE_GF in flat basins ($R^2 = 0.65$, $P < 0.01$). Canopies which had a higher distance between the point of inflexion and the tip of the leaf had higher RUE during grain-filling.

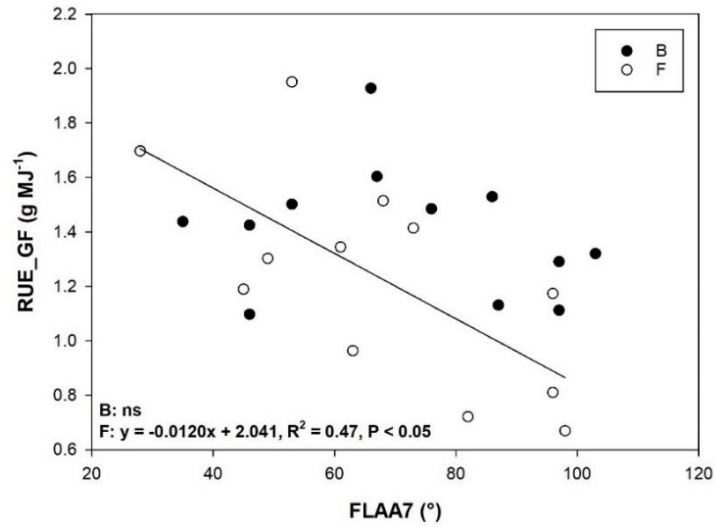


Fig. 3.3. Regression of RUE grain-filling (RUE_GF; g MJ⁻¹) on flag-leaf angle at seven days after anthesis (FLAA7; °) for 12 CIMMYT spring wheat genotypes across the years for 12 CIMMYT spring wheat genotypes in raised beds (B) and flat basins (F) across the years 2018-19 and 2019-20.

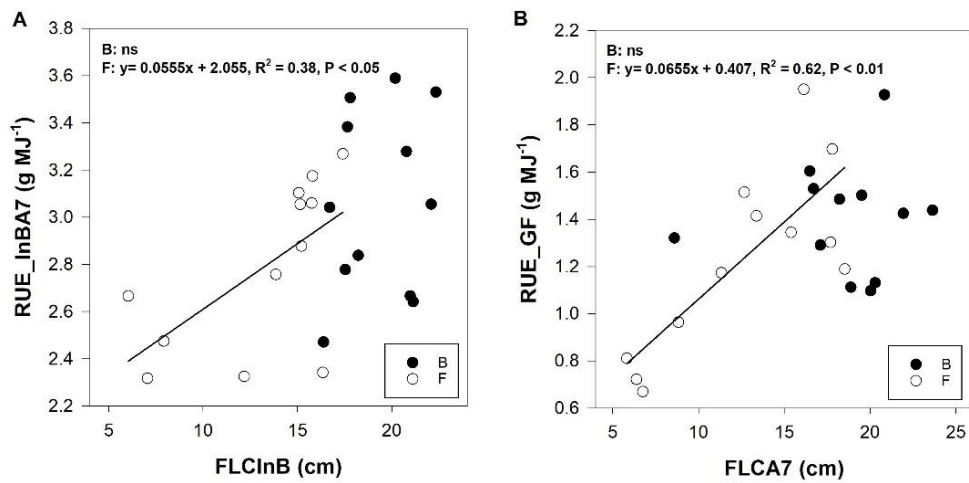


Fig. 3.4. Regression of RUE grain-filling (RUE_GF; g MJ⁻¹) on a) flag-leaf curvature at seven days after anthesis (FLCA7; cm) and b) flag-leaf curvature at initiation of booting (FLCInB; cm) for 12 CIMMYT spring wheat genotypes across the years for 12 CIMMYT spring wheat genotypes in raised beds (B) and flat basins (F).

Stronger correlations with RUE were found for the quantitative estimates of canopy architecture traits rather than the visual score of overall canopy architecture (FLcvs) in the present study (**Table 3.4**). Additionally, stronger correlations between canopy architecture traits and RUE were generally found in flat basins than raised beds. With regard to light interception, in raised beds a strong positive correlation was found between fractional PAR interception at GS41 (FIInB) ($r = 0.67$, $P < 0.05$) and FLA at initiation of booting. A weak correlation was found with FIInB at GS41 using the visual score at initiation of booting in raised beds (0.52 , $P = 0.08$). Flag-leaf angle at GS41 and RUET were positively correlated in beds ($r = 0.64$, $P < 0.05$) and the overall visual score (FLcvs) was also correlated with RUET in beds ($r = 0.65$, $P < 0.05$). In flat basins, a positive correlation with FI at GS65 + 7 days was found only using the visual score ($r = 0.63$, $P < 0.05$). A strong negative association was observed between FLA and FLcv at GS41 ($r = -0.72$ in beds, $P < 0.01$ and $r = -0.74$ in flats, $P < 0.01$) and at GS65 + 7 days ($r = -0.71$ in B, $P < 0.05$ and $r = -0.85$, $P < 0.001$) (**Supplementary table 3.4**). Negative correlations between flag-leaf width at initiation of booting and RUE_InBA7 ($r = -0.65$, $P < 0.05$) and RUE_preGF ($r = -0.75$, $P < 0.01$) were found in the flat basins (**Supplementary Table 3.4**).

Table 3.4. Phenotypic correlations among 12 CIMMYT spring wheat cultivars evaluated across the years 2018-19 and 2019-20 in raised beds and flat basins between canopy architecture and RUE traits using different methodologies (flag-leaf angle and curvature / visual score).

	RAISED BEDS (B)						FLAT BASINS (F)					
	Quantitative method			Visual score			Quantitative method			Visual score		
	FLAInB	FLCvInB	FLAA7	FLCvA7	FLvscInB	FLvscA7	FLAInB	FLCvInB	FLAA7	FLCvA7	FLvscInB	FLvscA7
RUE_InBA7	-0.05	0.23	-0.13	0.23	-0.04	-0.08	-0.38	0.62*	-0.01	-0.31	-0.03	-0.09
RUE_GF	0.19	-0.17	-0.24	0.08	0.30	0.36	0.08	-0.25	-0.68*	0.78**	-0.11	-0.13
RUE_preGF	0.51†	-0.15	0.38	-0.27	0.42	0.34	-0.21	0.40	0.06	-0.49	0.12	-0.00
RUET	0.64*	-0.27	0.35	-0.16	0.65*	0.59*	0.08	0.15	-0.18	-0.02	0.34	0.25
FIIInB	0.67*	-0.45	0.45	-0.39	0.52†	0.34	0.35	-0.23	0.43	-0.53†	0.63*	0.57†
FIA7	0.58*	-0.25	0.34	-0.17	0.52†	0.48	-0.08	-0.11	-0.25	0.28	-0.17	-0.20

RUE_InBA7: from initiation of booting to seven days after anthesis (g MJ⁻¹), RUE_GF: grain-filling, from seven days after emergence to physiological maturity (g MJ⁻¹), RUE_preGF: pre grain-filling, from forty days after emergence to seven days after emergence (g MJ⁻¹), RUET: from forty days after emergence to physiological maturity (g MJ⁻¹), FIIInB: fractional PAR interception at GS41, FIA7: fractional PAR interception at GS65 + 7 days, FLAInB: Flag-leaf angle at GS41 (°), FLCvInB: flag-leaf curvature at GS41 (cm), FLAA7: Flag-leaf angle at GS65 + 7 days (°), FLCvA7: flag-leaf curvature at GS65 + 7 days (cm), FLvscInB: visual score at GS41, FLvscA7: visual score at GS65 + 7 days. *P < 0.05, **P < 0.01, ***P < 0.001, † < 0.10.

Flag-leaf angle and flag leaf curvature (FLcv) at GS41 were strongly correlated with plant height at physiological maturity (**Fig. 3.5**). Less upright flag-leaf angle was associated with taller plants in raised beds ($R^2 = 0.49$, $P < 0.05$) and flat basins ($R^2 = 0.53$, $P < 0.01$); whereas the FLcv and plant height were only associated in raised beds ($R^2 = -0.41$, $P < 0.05$), with increased curvature associated with decreased plant height. In addition, a strong positive association was found between flag-leaf relative chlorophyll content in the leaf 3 (SPAD) at GS65 + 7 days and RUE_preGF in raised beds ($R^2 = 0.54$, $P < 0.01$) and flat basins ($R^2 = 0.43$, $P < 0.05$) (**Fig. 3.6**).

The phenotypic correlations between canopy architecture traits and grain yield, biomass and yield components in raised beds and flat basins are shown in **Table 3.5**. Stronger correlations were generally found with canopy architecture traits at initiation of booting than at GS65 + 7 days. A negative correlation was observed between flag-leaf angle at GS41 and harvest index ($r = -0.60$, $P < 0.05$) and grains per m^2 ($r = -0.64$, $P < 0.05$) in the flat basins. In both planting systems, there was a positive correlation between FLcv at GS41 and grains per m^2 ($r = 0.65$, $P < 0.05$ and $r = 0.66$, $P < 0.05$). In addition, canopies with a higher flag-leaf angle at GS41 had greater thousand-grain weight in raised beds ($r = 0.75$, $P < 0.01$) and flat basins ($r = 0.65$, $P < 0.05$). A positive association between flag-leaf angle at GS41 and biomass at physiological maturity was found but only in raised beds ($r = 0.60$, $P < 0.05$). There was a negative correlation between flag-leaf angle at GS41 and spikes per m^2 in both planting systems ($r = -0.59$ in B, $P < 0.05$ and $r = -0.80$ in F, $P < 0.01$) and a trend for a negative correlation between flag-leaf angle at GS65+ 7 days and spikes per m^2 in flats ($r = -0.58$, $P < 0.10$). FLcv at GS41 showed a positive correlation with spikes per m^2 only in flat basins ($r = 0.66$, $P < 0.05$).

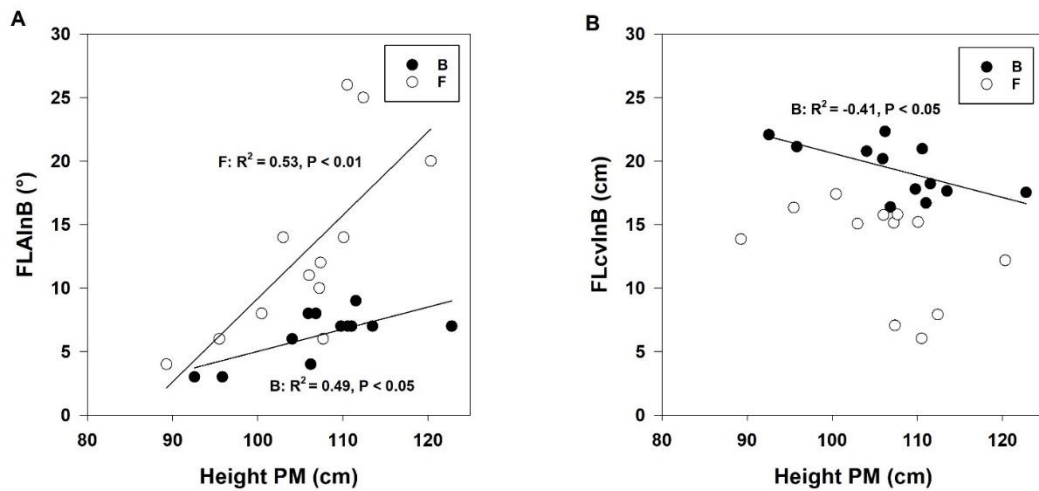


Fig. 3.5. Regression of plant height at physiological maturity on **A** flag-leaf angle at initiation of booting (FLAInB; °) and **B** flag-leaf curvature at initiation of booting (FLCvInB; cm) in raised beds (B) and flat basins (F) for 12 CIMMYT spring wheat cultivars evaluated across the years 2018-19 and 2019-20.

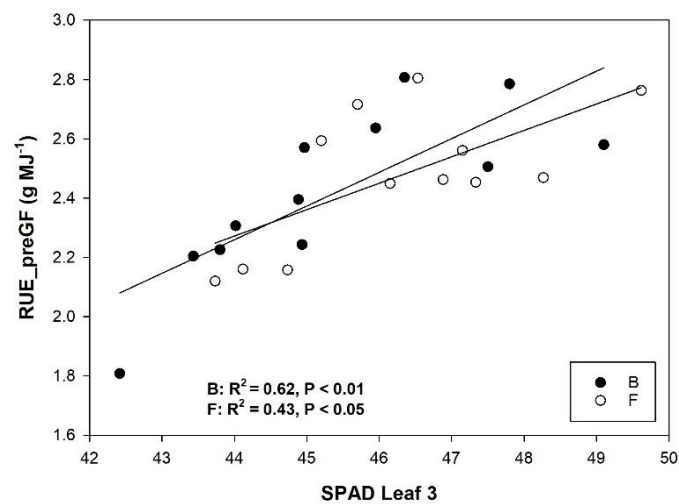


Fig. 3.6. Regression of RUE from forty days after emergence to seven days after anthesis (RUE_preGF) (g MJ^{-1}) on relative chlorophyll content (SPAD) in leaf 3 at seven days after anthesis in raised beds (B) and flat basins (F) for 12 CIMMYT spring wheat cultivars evaluated across the years 2018-19 and 2019-20.

Table 3.5. Phenotypic correlations between canopy architecture traits at initiation of booting (InB) and seven days after anthesis (A7) and yield and yield components for 12 spring CIMMYT wheat genotypes. Values based on means from the combined analysis in 2018-19 and 2019-20 in raised beds (B) and flat basins (F).

	Raised beds (B)				Flat basins (F)			
	FLAInB	FLCvInB	FLAA7	FLCvA7	FLAInB	FLCvInB	FLAA7	FLCvA7
YLD	0.45	0.07	0.36	-0.10	-0.16	0.41	-0.07	-0.19
TGW	0.75**	-0.55†	0.53†	-0.37	0.65*	-0.56†	0.46	-0.20
HI	-0.17	0.51†	0.04	0.32	-0.60*	0.45	-0.30	0.01
GM2	-0.48	0.65*	-0.33	0.38	-0.64*	0.66*	-0.46	0.08
SM2	-0.59*	0.38	-0.46	0.20	-0.80**	0.66*	-0.58†	0.20
ShootsInB	-0.25	0.19	-0.04	0.03	-0.34	0.39	-0.15	-0.28
ShootsA7	-0.37	0.37	-0.30	0.32	-0.74**	0.64*	-0.37	-0.06
BMPM	0.60*	-0.27	0.36	-0.34	0.30	0.14	0.10	-0.21

YLD: grain yield (g m⁻²), TGW: thousand grain-weight (g), HI: harvest index, GM2: grain number per m⁻², SM2: spikes per m⁻², ShootsInB: number of shoots at initiation of booting, ShootsA7: number of shoots at anthesis + 7 days, BMPM: biomass at physiological maturity (g m⁻²), FLAInB: Flag-leaf angle at GS41 (°), FLCvInB: flag-leaf curvature at GS41 (cm), FLAA7: Flag-leaf angle at GS65 + 7 days (°), FLCvA7: flag-leaf curvature at GS65 + 7 days (cm). *P < 0.05, **P < 0.01, ***P < 0.001, † < 0.10.

3.5 Discussion

3.5.1 Associations between canopy architecture traits

The flag leaf is the main component of the canopy responsible for assimilate production (Liu et al., 2009; Biswal and Kohli, 2013). An optimized canopy architecture among the canopy leaf layers can increase the efficiency of light capture and conversion resulting in improvements in biomass (Green, 1987) and yield potential (Murchie and Reynolds, 2012). In this study, canopy architecture traits for the flag leaf were related to light interception, radiation-use efficiency, biomass and grain yield for the 12 spring wheat CIMMYT genotypes. The cultivar responses to planting system for biomass at physiological maturity among these spring wheat genotypes were partly explained by the responses for RUE_InBA7 and RUE_preGF; in addition, taller cultivars showed greater biomass increases in B compared to F than shorter cultivars.

Plants have the ability to regulate the distribution of light that is intercepted among the canopy leaf layers by changing the leaf angle (Burgess, 2017). Visual score of the overall plot has been used to assess canopy architecture over the last decades (Yunusa et al., 1993; Richards et al., 2019). The present study in addition to a canopy visual score also applied more quantitative methodologies focused specifically on flag-leaf angle and curvature to examine the physiological basis of canopy architecture effects. These measurements represented less subjective information on the flag-leaf position. At initiation of booting, the two alternative measurements of flag-leaf curvature and canopy architecture visual score were positively associated among cultivars ($R^2 = 0.51$, $P < 0.01$). This study included genotypes with contrasting upright and floppy leaves but differences in the intermediate genotypes were too small to assess reliably with the visual score. This could explain the relatively weak association between the genetic variation in flag-leaf curvature (distance from the point of inflexion to the tip of the leaf) and the canopy architecture visual score. High heritability was found for all the canopy architecture traits at GS41 and GS65 + 7 days. However, heritability was lower for post-anthesis RUE. This could be due to the increased complexity and number of processes affecting RUE during grain filling such as source-sink balance and upregulation of RUE according to grain sink strength. There was a correlation between flag-leaf angle and flag-leaf curvature with cultivars with lower leaf angle (more upright leaves) tending to have a longer distance from the recurved point of inflexion of the leaf to the tip. This correlation was observed in both planting systems, at GS41 and GS65 + 7 days. Therefore, these results indicate these two traits were not independent and could be

mechanistically linked in the genotypes. Notwithstanding this, the genotypes CHEWINK #1 and BORLAUG100 generally showed a different behaviour to the other cultivars combining a high flag-leaf angle with a high FLcv. It can be speculated that if the inflection point to tip length is short, it may cause an increase of the flag-leaf angle due to the greater weight of the non-recurved part of the leaf lamina. Additionally, a greater specific leaf weight (leaf dry weight per unit area) may cause the leaf lamina to be recurved at a shorter distance from the ligule. No associations between flag-leaf curvature and total leaf length at GS41 or GS65 + 7 days were found for either planting system. A study in winter wheat cultivars in China reported that leaf angle tended to increase when the leaf was larger since the weight of the leaf increased (Liu et al., 2018) which agrees with the present findings. Present results demonstrated that flag-leaf angle and curvature differed between planting systems. Higher flag-leaf curvature was observed in beds at both stages; whereas flag-leaf angle was higher in flats at GS41 but higher in beds at GS65 + 7 days. In addition, present results showed changes through time with FL angle increasing from initiation of booting to seven days after anthesis.

3.5.2 Canopy architecture and its relations with light interception, grain yield and yield components

Cultivar responses of light interception at GS41 and GS65 + 7 days to planting system were not related to the responses of flag-leaf angle and curvature at these stages. In addition, no correlations between the responses of light extinction coefficient (k_{par}) and flag-leaf angle or curvature were found. The correlations between flag-leaf size and angle at initiation of booting in raised beds (**Supplementary Table 3.4**) indicated cultivars with less upright leaves tended to be larger and wider than those with upright leaves. Similar results were found in spring wheat lines in Australia (Richards et al., 2019).

In the present study, there was a positive correlation among cultivars between flag-leaf angle and biomass at initiation of booting (**Supplementary Table 3.4**) in both planting systems. In addition, canopies with less upright flag-leaf angle at GS41 had greater biomass at physiological maturity in raised beds which may have been partly related to their increased fractional light interception pre-anthesis. In flat basins, a positive correlation was also found between flag-leaf angle and biomass at initiation of booting but no correlation was found with biomass at harvest. Results showed cultivars with more recurved leaves at GS41 were better at capturing light (from GS41 to GS65 + 7 days) in raised beds translating to a greater

biomass at harvest. The reason for the improved light capture in raised beds may be that more recurved leaves were better adapted to capture light in the relatively larger gaps between the beds found in raised-bed plots. The planting system difference in light interception for the cultivars could also be partly explained by the greater row spacing in raised beds which may favour lax-leaved genotypes since they can intercept more light per unit leaf area (Fischer et al., 2019).

A negative correlation was found between genetic variation in k_{par} and flag-leaf angle in flat basins as well as a trend in raised beds, which contradicts findings of previous investigations in which genotypes with more upright leaves had lower k_{par} (Murchie and Reynolds, 2012; Zhang et al., 2014). No associations between k_{par} and biomass were found. It can be speculated that the higher k_{par} values observed in the canopies with upright leaves may have been partly because genotypes with high flag-leaf angle did not have high leaf angle in lower leaf layers resulting in the high k_{par} values in the erect genotypes. It is also possible that k_{par} measurements might have been affected by genetic variation in the relative distribution of LAI in the different canopy layers. Therefore, future work should investigate the effects of the leaf size distributions and clustering in the lower canopy leaf layers on light interception.

Averaging over the two years, grain yield was greater in raised beds than flat basins by 10.8% ($P < 0.001$). There were no significant correlations between genetic variation in flag-leaf angle or curvature with grain yield. However, strong and positive associations were found between flag-leaf angle at GS41 and biomass at physiological maturity in beds. Therefore, flag-leaf angle and curvature may be explaining biomass increases through effect on FI in beds as discussed above. There was a positive association between flag-leaf curvature at GS41 and GM2 in both basins and beds. It is possible that autocorrelations with plant height may explain the association, since flag-leaf curvature at GS41 was negatively associated with plant height. The period from flag-leaf emergence to anthesis, particularly during booting to anthesis, is the most critical period determining grain number and grain yield as assimilate supply to the spike determines floret survival (Fischer, 2007). The present study showed that flag-leaf curvature at initiation of booting was greater in raised beds than flat basins with positive association among genotypes with the radiation interception from GS41 to GS65 + 7 days in beds. Positive associations between TGW and flag-leaf angle were also found as reported by Liu et al. (2018) which may be indirectly explained by the positive association between flag-leaf angle and grains per m^2 . Present results also showed

genotypes with more upright flag leaves had a greater number of grains but a lower TGW in basins. Other investigations have reported on the established trade-off between GM2 and TGW in wheat (Acreche and Slafer, 2006; Bustos et al., 2013; García et al., 2013; Quintero et al., 2018).

3.5.3 Canopy architecture and its relation with RUE

In this study higher RUE_{preGF} among cultivars only translated into higher biomass at physiological maturity in raised beds although there was a similar trend for flat basins. In addition, higher RUE_T was associated with higher BMPM in beds and flats (see **Chapter 2**). Positive associations between genetic variation in flag-leaf angle at GS41 and biomass at physiological maturity was found in raised beds but not in flat basins. As described above this may have been partly associated with more horizontal leaves intercepting more light in the gaps between the beds in the raised beds planting system. A field study in Tasmania found higher biomass for more horizontal leaves in advanced wheat lines in raised beds canopies (Merry et al., 2017). However, another study in flat basins (Choudhury (2000) and those summarized in the review by Parry et al. (2011) stated that wheat canopies with more upright leaves have a greater biomass production. Positive associations between flag-leaf angle and plant height were shown in this study, which could also partly explain the association between flag-leaf angle and biomass. In addition the association with biomass could be partly explained by the positive association between flag-leaf angle at GS41 and season-long RUE in raised beds. This could also possibly relate to an indirect association with plant height, in that increased plant height was associated with both increased flag-leaf angle at GS41 and biomass at physiological maturity in raised beds. More upright flag leaves in beds than flats improve RUE responses. RUE_{preGF} was higher than RUE_{GF} in both planting systems, which can be partly explained by the dynamic changes of the leaf position during the season. Other reasons may be due to decreased photosynthetic rates in older leaves and also by brighter days later in the cycle associated with increased frequency of light saturation in the flag leaves.

Present results showed that taller genotypes had higher biomass in both planting system, consistent with previous studies (Bush and Evans, 1988; Aisawi et al., 2015; Rivera-Amado et al., 2019). The present study also showed that taller genotypes tended to have larger and wider leaves in both planting systems compared to shorter genotypes. A field study in winter wheat in the UK demonstrated that smaller flag leaves were related to greater grain yield in more recently introduced cultivars being associated with increased leaf

specific weight and RUE pre-anthesis (Shearman et al., 2005). Mathan et al. (2016) concluded that leaf size was an important trait to consider to boost grain yield and explained that improvements in leaf area should be a major target for plant breeders. Present results indicated that at initiation of booting in raised beds canopies with longer and wider flag leaves tended to have greater flag-leaf angle. However, genetic variation in leaf size did not show a relation with RUE, biomass and grain yield at any stage in either planting system.

There was a strong negative association between genetic variation in flag-leaf angle at GS65 + 7 days and RUE_GF in flat basins with more upright leaves leading to higher RUE which agrees with Reynolds et al. (2000b) and Murchie et al. (2009). In addition, there was a strong positive association between flag-leaf curvature at GS65 + 7 days and RUE_GF in flats, respectively. Previous work has shown that irradiance incident on the top of the canopy saturates the flag-leaf less in erectophile wheat canopies compared to planophiles ones (Araus et al., 1993b; Hirose, 2004). Hence, more light reaches the leaves at the bottom of the canopy and a greater photosynthesis rate can be achieved in lower leaves as well as RUE and biomass (Burgess et al., 2017; Richards et al., 2019). Since HI is approaching its theoretical limit of ca. 0.65 in some countries and regions (Austin, 1980; Foulkes et al., 2011), leaf angle as a determinant of RUE may offer scope for yield improvements in biomass. Therefore, present results in basins indicate breeders should focus more on leaf angle to avoid light saturation of leaves, hence increase RUE and grain yield in plant breeding programs where this trait is not already optimized in spring cultivars. In the study in beds, the case for more upright leaves was not clearly demonstrated: cultivars with more horizontal leaves appeared to have higher fractional light interception in the pre-anthesis phase, biomass at maturity and RUET. In addition, cultivar responses of flag-leaf angle at GS41 to PS showed a trend for a negative association with the responses of RUE_preGF to PS, i.e. cultivars which had relatively more upright flag leaves in B compared to F had high relatively higher RUE in B compared to F. Similarly, responses of flag-leaf angle at GS65 + 7 days to PS showed a trend for a negative association with the responses of RUE_GF to PS.

The positive association between flag-leaf curvature at GS65 + 7 days and RUE_GF in flat basins could imply that more recurved flag-leaves allow more light to reach the lower leaf layers and hence higher RUE. However, no correlation was found between the light intercepted at the bottom of the canopy and flag-leaf curvature for either planting system (data not shown). Turning to consider flag-leaf width, narrower flag-leaves (which

were more upright in most of the genotypes in this study) had a greater RUE_InBA7 and RUE_preGF in flat basins. However, no association between narrower flag-leaves and increased SPAD at seven days after anthesis was found for either planting system (data not shown).

Canopies that have erect leaves early during the season when GAI is small do not use the solar energy efficiently (Monteith, 1969; Richards and Lukacs, 2002). However, Liu et al. (2009) observed that the genotypes which increased flag-leaf angle from anthesis to late grain-filling had a higher canopy photosynthesis than the genotypes maintaining erect leaves during grain filling. In the present study a change in flag-leaf angle was apparent where genotypes increased flag-leaf angle from GS41 to GS65 + 7 days. Some genotypes increased FLA more than others, for example, the genotypes C80.1/3*QT4188, KUTZ and BORLAUG100 in raised beds and C80.1/3*QT4188, KUKRI and SOKOLL in flat basins. Conversely, BACANORA T88, NELOKI and ITP40 increased less than other genotypes in both planting systems. However, there were no associations between the relative changes of flag-leaf angle from GS41 to GS65 + 7 days and either RUE, biomass or grain yield for either planting system. Flag-leaf chlorophyll content differed amongst genotypes but there was no planting system effect (data not shown), in contrast with a previous study where leaf SPAD was higher in raised beds than flat basins associated with higher N uptake (Fahong et al., 2004). Interestingly, in both planting systems, chlorophyll content in leaf 3 (flag leaf = leaf 1) was positively associated among cultivars with RUE_preGF. The vertical distribution of N in leaf layers may not be optimized in modern cultivars with insufficient N in lower layers to maximize RUE. Muurinen and Peltonen-Sainio (2006) concluded that RUE in wheat may be maintained longer during grain filling if the leaf N level remains above a critical value, with prolonged maintenance of RUE associated with delayed N translocation from the leaves to the grains. An investigation on winter wheat cultivars in the UK and New Zealand concluded that a critical level of specific leaf lamina N (SLN) of 2 g N m⁻² was needed to maximize RUE (Pask et al., 2012c). However, in the present study, when the association between genetic variation in leaf SPAD at mid grain-filling and RUE_GF was analyzed, there was not a significant association (data not shown). Further work is required on the relation between leaf nitrogen traits and RUE to understand the critical value of leaf N at which RUE is maximized in raised beds and flat basins.

3.5.4 Genetic basis of canopy architecture

From the 12 CIMMYT genotypes studied only BACANORA T88, CHEWINK #1 and BORLAUG100 F2014 are cultivars that have been released in 1988, 2008 and 2014, respectively. The others are advanced lines. BACANORA T88 had the most erect flag leaves of the released cultivars in the experiment and the other two genotypes were more planophile. Plant breeders have selected wheat canopies with smaller flag leaves and more upright leaves in recent years in some countries, e.g. in winter wheat in the UK (Shearman et al., 2005). However, present results suggested there has not been a systematic change of canopy architecture traits with the year of release in spring bread wheat CIMMYT genotypes, at least not from planophile to erectophile canopies. However, the present results showed how the genotypes with upright leaves allowed a higher RUE during grain filling in flat basins, which is the most common wheat planting system globally. Additionally, results suggested that more horizontal leaves in raised beds may be beneficial for increasing biomass associated with increased light interception. Future work will require more genetic studies to understand better the genes regulating the canopy architecture traits. Present results showed that cultivars which have a combination of a smaller FLA with a greater distance between the point of inflexion of the leaf to the tip could be beneficial to increase RUE in flat basins. No associations between leaf length and RUE were found in B and F. It has been reported that the plant hormone brassinosteroid has an influence on plant height as well as flag-leaf angle in rice (Sakamoto et al., 2006) and barley (Dockter et al., 2014) and genes regulating the brassinosteroid synthesis pathway could potentially be deployed in wheat breeding to modify canopy architecture. Present results indicated that future selection of cultivars with less upright but more recurved leaves may be more beneficial for raising light interception and RUE and biomass in raised beds but more upright leaves in flat basins. There is a need for further studies on how the canopy architecture traits affect RUE in different planting systems and mega-environments but examining cultivars with a reduced range of plant height in order to confirm the present findings.

3.6 Conclusions

Present results showed that more upright flag-leaf angle at GS65 + 7 days was associated with higher post-anthesis RUE but only in flat basins. Genotypes with higher flag leaf curvature at GS41 showed greater RUE_InBA7 in flats as well as at GS65 + 7 days with RUE_GF. This study indicated that less upright flag leaves were better adapted to intercept radiation and associated with higher biomass in raised beds but there was no effect on light interception in flat basins. Stronger correlations between canopy architecture traits and RUE were found in flat basins than raised beds, the former planting system being more common worldwide. Plant breeders have selected wheat canopies with smaller flag leaf and more upright leaves in the recent years in some countries, e.g. in the UK (Shearman et al., 2005). However, modern spring bread wheat CIMMYT cultivars may still require optimization in canopy architecture traits. Present results demonstrated that flag-leaf angle and curvature were very important in explaining the PS \times G interaction for RUE_preGF and RUE_GF. Moreover, the optimum expression of canopy architecture to enhance RUE and biomass differed in the raised beds and flat basins so different selection strategies will be required in the two planting systems. Since there were significant effects of plant height on RUE in the present study, there is still a need for further studies to quantify how canopy architecture traits in wheat affects RUE in the two planting systems but using genotypes with a smaller variation of plant height to confirm the presently reported associations.

3.7 Author contribution

MMP, JF, MR and GM contributed to the conceptualization. MMP, JF, MR and GM contributed to the methodology. MMP contributed to the data analysis. MMP performed the experiments. MAMP, JF, GM and OG contributed to the investigation. MMP and JF contributed to the writing of the original manuscript. MMP, JF, GM, MR, OG and EM contributed to the writing, editing and revising the manuscript. JF and MR contributed to the funding acquisition and project administration. All the authors approved the final version of this manuscript.

3.8 Funding

This work was supported by The National Council of Science and Technology (CONACYT) (CVU 839945), the Sustainable Modernization of Traditional Agriculture (MasAgro) initiative from the Secretariat of Agriculture and Rural Development (SADER) and the International Wheat Yield Partnership Program (IWYP).

3.9 Acknowledgements

We thank to the physiology team at CIMMYT for their technical support. We also acknowledge Richard Richards for his invaluable support in the genotype selection and Angela Pacheco for her advice in the statistical analysis.

3.10 Supplementary information

Supplementary table 3.1. Flag-leaf length and width at initiation of booting (GS41) and seven days after anthesis (GS65) and SPAD in the leaf 3 at seven days after anthesis for 12 CIMMYT spring wheat cultivars from the combined analysis across 2018-19 and 2019-20 in raised beds (B) and flat basins (F).

Genotype	Initiation of booting				Anthesis + 7 days					
	LLInB (cm)		LWInB (cm)		LLA7 (cm)		LWA7 (cm)		SPAD Leaf3	
	B	F	B	F	B	F	B	F	B	F
BACANORA T88	24.9	22.0	1.8	1.8	25.9	22.0	1.7	1.7	43.43	45.20
C80.1/3*QT4118	32.5	34.8	2.1	2.0	34.6	31.9	2.0	2.0	44.88	44.73
CHEWINK#1	35.8	28.4	2.2	1.9	34.8	29.0	2.0	2.0	44.93	46.88
SOKOLL//PUB94	28.9	24.3	1.9	1.9	31.2	25.2	1.8	1.8	49.10	46.15
NELOKI	24.9	24.2	1.8	2.0	28.7	23.0	1.8	1.9	42.42	43.73
W15.92/4/PASTOR	27.2	23.7	2.0	2.0	27.9	22.6	1.9	1.9	43.80	44.12
KUKRI	27.8	25.5	1.9	1.8	28.9	23.1	1.8	1.7	44.02	45.70
KUTZ	26.8	24.9	1.9	1.9	27.3	25.0	1.9	2.0	44.97	47.33
SOKOLL	28.6	24.4	1.8	1.8	30.3	24.6	1.7	1.8	47.80	46.53
BOURLAG100	32.9	26.5	2.1	2.0	32.3	27.6	1.9	2.0	46.35	47.15
ITP40/AKURI	23.9	21.6	1.8	1.8	24.8	22.0	1.7	1.8	45.95	48.27
CHIPAK*2//	25.7	23.0	1.9	1.9	26.3	21.2	1.9	1.8	47.50	49.62
Mean	23.9	25.3	1.9	1.9	29.4	24.8	1.8	1.9	45.43	49.62
H ²	0.79		0.78		0.65		0.68		0.77	
LSD (G) (5%)	3.69		0.15		3.75		0.16		3.24	
CV%	8.48		4.79		8.53		5.41		4.35	
G (p value)	***		***		***		***		***	
PS (p value)	***		0.128		***		0.150		*	
Y (p value)	*		***		*		ns		ns	
PS×G (p value)	***		***		ns		0.065		*	

LLInB: flag-leaf length at initiation of booting (cm), LW: flag-leaf width at initiation of booting (cm), LLA7: flag-leaf length at seven days after anthesis (cm), LWA7: flag-leaf width at seven days after anthesis (cm), SPAD.leaf3: SPAD in the leaf 3 *P < 0.05, **P < 0.01, ***P < 0.001, *italics*: P < 0.10, ns: not significant.

Supplementary Table 3.2. Phenotypic correlations among 12 CIMMYT spring wheat cultivars of RUE_InBA7, K_{PAR} and SPAD at initiation of booting and seven days after anthesis for 12 CIMMYT spring wheat genotypes evaluated across the years 2019 and 2020 in raised beds and flat basins.

Trait	Raised beds (B)		Flat basins (F)	
	k_{parInB}	k_{parA7}	k_{parInB}	k_{parA7}
RUE_InBA7	0.15	-0.07	-0.30	-0.50†
FLAInB	-0.50†	-0.68*	-0.47	0.00
FLcvInB	0.28	-0.36	0.07	-0.44
SPAD.InB	-0.07	-0.37	0.30	0.23
FLAA7	-0.70*	-0.75**	-0.73**	-0.34
FLcA7	0.51	0.55†	0.76**	0.45
SPAD.A7	-0.27	-0.28	-0.53†	-0.67*

RUE from initiation of booting (RUE_InBA7; $g\ m^{-2}$), light extinction coefficient at initiation of booting (k_{parInB}), SPAD at initiation of booting (SPAD.InB), light extinction coefficient at seven days after anthesis (k_{parA7}), SPAD at seven days after anthesis (SPAD.A7), flag- leaf angle at initiation of booting (FLAInB; °), flag-leaf curvature at initiation of booting (FLcvInB; cm), flag-leaf angle at seven days after anthesis (FLAA7; °), flag-leaf curvature at seven days after anthesis (FLcA7; cm). * $P < 0.05$, ** $P < 0.01$, *** $P < 0.001$, † $P < 0.10$.

Supplementary table 3.3. Phenotypic correlations among 12 CIMMYT spring wheat cultivars evaluated across the years 2018-19 and 2019-20 in raised beds and flat basins (*italics*) between canopy architecture and accumulated radiation interception: accumulated radiation interception from initiation of booting to seven days after anthesis (IPARaccInBA7; MJ M⁻²), accumulated radiation interception from seven days after anthesis to physiological maturity (IPARaccA7PM; MJ m⁻²), total accumulated radiation interception from forty days after emergence to physiological maturity (IPARaccE40PM; MJ m⁻²), flag-leaf angle at initiation of booting (FLAInB; °), flag-leaf curvature at initiation of booting (FLcvInB; cm), flag-leaf length at initiation of booting (LLInB; cm) and flag-leaf width at initiation of booting (LWInB; cm), flag-leaf angle at seven days after anthesis (FLAA7; °), flag-leaf curvature at seven days after anthesis (FLcvA7; cm), flag-leaf length at seven days after anthesis (LLA7; cm), flag-leaf width at anthesis at seven days after anthesis (LWA7; cm), light extinction coefficient at initiation of booting (k_{par}InB) and light extinction coefficient at seven days after anthesis (k_{par}A7). *P < 0.05, **P < 0.01, ***P < 0.001, † < 0.10.

Trait	IPARaccInBA7	IPARaccA7PM	IPARaccE40PM	FLAInB	FLcvInB	LLInB	LWInB	k _{par} InB	FLAA7	FLcvA7	LLA7	LWA7	k _{par} A7
IPARaccInBA7	.	-0.25	0.54†	0.07	0.29	0.36	-0.33	-0.36	0.18	-0.17	0.38	0.01	-0.69*
IPARaccA7PM	0.21	.	0.62*	0.28	-0.23	-0.16	0.18	-0.18	0.00	0.02	-0.18	0.35	0.32
IPARaccE40PM	0.20	0.95***	.	0.38	-0.05	0.32	-0.02	-0.51†	0.36	-0.28	0.23	0.33	-0.26
FLAInB	-0.37	0.16	0.30	.	-0.74**	0.46	0.34	-0.33	0.52†	-0.33	0.56†	0.41	0.00
FLcvInB	0.71**	0.05	-0.05	-0.79**	.	-0.06	-0.28	-0.02	-0.27	0.12	-0.13	-0.16	-0.43
LLInB	0.25	0.06	0.21	0.56†	-0.22	.	0.62*	-0.13	0.55†	-0.19	0.93***	0.64*	-0.44
LWInB	0.16	0.29	0.38	0.56†	-0.22	0.87***	.	0.24	0.26	0.09	0.58*	0.83***	-0.05
k _{par} InB	0.14	-0.53†	-0.54†	-0.50†	0.28	-0.25	-0.58*	.	-0.29	0.38	-0.17	-0.10	0.26
FLAA7	-0.37	0.38	0.45	0.81**	-0.53†	0.43	0.57†	-0.70*	.	-0.85***	0.42	0.37	-0.34
FLcvA7	0.48	0.48	-0.45	-0.72**	0.62*	-0.08	-0.13	0.51†	-0.71**	.	-0.08	-0.05	0.44
LLA7	0.19	0.09	0.23	0.47	-0.30	0.94***	0.77**	-0.13	0.32	-0.08	.	0.67*	-0.46
LWA7	0.03	0.43	0.48	0.53†	-0.21	0.74**	0.95***	-0.72**	0.69*	-0.27	0.65*	.	-0.30
k _{par} A7	0.22	-0.36	-0.57†	-0.68*	0.36	-0.44	-0.39	0.45	-0.75**	0.55†	-0.33	-0.47	.

Supplementary table 3.4. Phenotypic correlations between canopy architecture traits and biomass through the season among 12 CIMMYT spring wheat cultivars evaluated across the years 2018-19 and 2019-20 in raised beds and flat basins (*italics*).

Trait	FLAInB	FLcvInB	LLInB	LWInB	FLAA7	FLcvA7	LLA7	LWA7	FLvscInB	FLvscA7	BMIInB	BMA7	BMPM
FLAInB	.	-0.74**	0.47	0.35	0.53†	-0.34	0.56†	0.42	0.70*	0.62*	0.81***	-0.01	0.30
FLcvInB	-0.71**	.	-0.06	-0.28	-0.27	0.12	-0.13	-0.16	-0.39	-0.30	-0.63*	0.35	0.14
LLInB	0.56†	-0.22	.	0.62*	0.54†	-0.19	0.93***	0.64*	0.42	0.54†	0.17	-0.04	0.03
LWInB	0.56†	-0.22	0.87***	.	0.26	0.09	0.58*	0.83***	0.39	0.51†	-0.13	-0.60*	-0.25
FLAA7	0.83***	-0.53†	0.43	0.57†	.	-0.85***	0.41	0.37	0.63*	0.65*	0.59*	0.42	0.10
FLcvA7	-0.73**	0.62*	-0.08	-0.13	-0.71*	.	-0.08	-0.05	-0.54†	-0.47	-0.63*	-0.71**	-0.21
LLA7	0.44	-0.30	0.94***	0.75**	0.32	-0.08	.	0.67*	0.51†	0.60*	0.17	-0.05	0.15
LWA7	0.55†	-0.21	0.74**	0.95***	0.69*	-0.27	0.65*	.	0.38	0.47	-0.06	-0.27	0.03
FLvscInB	0.93***	-0.70*	0.74**	0.66*	0.71**	0.57†	0.67*	0.60*	.	0.97***	0.54†	0.22	0.43
FLvscA7	0.81***	-0.50	0.83***	0.79**	0.61*	0.42	0.75**	0.70*	0.92***	.	0.40	0.13	0.34
BMIInB	0.66*	-0.55†	0.17	0.22	0.67*	-0.74**	0.13	0.32	0.46	0.38	.	0.38	0.34
BMA7	0.58*	-0.20	0.29	0.19	0.55†	-0.35	0.18	0.14	0.47	0.41	0.59*	.	0.56†
BMPM	0.60*	-0.27	0.44	0.30	0.36	-0.34	0.35	0.20	0.54†	0.54†	0.68*	0.84***	.

Flag-leaf angle at initiation of booting (FLAInB; °), flag-leaf curvature at initiation of booting (FLcvInB; cm), flag-leaf length at initiation of booting (LLInB; cm) and flag-leaf width at initiation of booting (LWInB; cm), flag-leaf angle at seven days after anthesis (FLAA7; °), flag-leaf curvature at seven days after anthesis (FLcvA7; cm), flag-leaf length at seven days after anthesis (LLA7; cm), flag-leaf width at anthesis at seven days after anthesis (LWA7; cm), visual score at initiation of booting (FLvscInB), visual score at seven days after anthesis (FLvscA7), biomass at initiation of booting (InB; g m⁻²), biomass at seven days after anthesis (BMA7; g m⁻²) and biomass at physiological maturity (BMPM; g m⁻²). *P < 0.05, **P < 0.01, ***P < 0.001, † < 0.10.

4 CHAPTER 4. GRAIN PARTITIONING TRAITS TO INCREASE HARVEST INDEX AND GRAIN YIELD IN WHEAT: EVALUATED UNDER TWO PLANTING SYSTEMS

Paper to be submitted to Field Crops Research

Marcela A. Moroyoqui-Parra¹, Gemma Molero^{2,4}, Matthew P. Reynolds², Oorbessy Gaju³, Erik H. Murchie¹, M. John Foulkes^{1*}

¹Division of Plant and Crop Science, School of Biosciences, University of Nottingham, Sutton Bonington Campus, Leicestershire LE12 5RD, United Kingdom.

²Global Wheat Program, International Maize and Wheat Improvement Center (CIMMYT), carretera Mexico-Veracruz Km 45, El Batan, Texcoco, Mexico, CP 56237.

³Lincoln Institute for Agri-Food and Technology, University of Lincoln, Riseholme Park, Lincoln, Lincolnshire, LN2 2LG, United Kingdom.

⁴KWS Momont Recherche, 7 rue de Martinval, 59246 Mons-en-Pevele, France.

*** Corresponding author:**

John Foulkes

John.Foulkes@nottingham.ac.uk (M.J. Foulkes).

Keywords: planting systems, spring wheat, harvest index, dry-matter partitioning, fruiting efficiency

4.1 Abstract

Different strategies have been proposed to increase harvest index. One of them is to alter dry-matter partitioning to favour spike growth at anthesis. A field experiment examining twelve spring wheat CIMMYT cultivars was carried out under yield potential conditions in raised beds and flat basins planting systems in two seasons (2017-18 and 2018-19) in the NW of Mexico. The aims of this study were: i) identify grain partitioning traits to increase grains per m², harvest index and grain yield in twelve spring wheat cultivars in two planting systems (raised beds and flat basins) and ii) quantify any trade-offs between grain sink traits and source traits affecting photosynthetic capacity and biomass production in the two planting systems. Grain yield, yield components and fruiting efficiency (grain per unit spike dry matter at anthesis (FE; GS65 + 7 days) were measured in both planting systems.

In addition, dry-matter partitioning traits were assessed at anthesis + 7 days, as well as internode lengths measurements and dry-matter within the spike (glume, palea, lemma, rachis, and awn). HI did not showed significant genetic variation across the years 2017-18 and 2018-19 and was positively correlated with grain yield in flats whereas in beds there was a marginal correlation. Results showed negative associations between spike partitioning index (spike dry matter / above ground dry matter at GS65 + 7 days; SPI) and stem-internode length 2 and 3 in beds and flats indicating a competition for assimilates between these organs; whereas peduncle length did not associate with SPI and seemed to not compete for assimilates with the spike during anthesis. SPI did not, however, correlate with grains per m² (GM2) and HI likely partly due to confounding effects of plant height on above-ground biomass among the 12 cultivars. In both planting systems, it was shown that FE was the most important component determining genetic variation in GM2 and is a promising trait to increase grain sink strength and yield.

4.2 Introduction

To feed an estimated population of ~9 billion, it will be necessary at least to double the agricultural production by 2050 (Ray et al., 2013; FAOSTAT, 2018). Additionally, there is limited land available for expansion of the cropping area for wheat production (Albajes et al., 2013). Therefore, it is crucial to increase yield potential (Reynolds et al., 2012a). Over the last two decades, rates of increase in grain yield production in wheat crops have been reported to be less than the rate required to meet the demand for grain (Calderini and Slafer, 1998; Brisson et al., 2010; Ray et al., 2012). Genetic gains in yield potential are continuing but at a slower rate than in previous decades, at ca. 0.5 - 1% per year under favourable conditions (Aisawi et al., 2015; Crespo-Herrera et al., 2017). Furthermore, production of wheat crops is facing the challenge of climate change with crops predicted to encounter higher temperatures, and more frequent extreme drought and flooding potentially affecting global grain yields (Asseng et al., 2015). In fact, plateaus and decreases in grain yield progress in wheat and rice have been reported in some countries (Grassini et al., 2013). During the Green Revolution, when the semi-dwarf wheat cultivars of wheat were introduced (1960's and 1970's), an increase in grains per m² and harvest index was achieved due to a reduction in plant height favouring assimilate partitioning to the spike during the pre-anthesis stage (Youssefian et al., 1992; Miralles et al., 1998). However, harvest index has generally not shown consistent genetic progress since the early 1990's in spring wheat from values ca. 0.45 - 0.50 (Foulkes et al., 2011). For example, Sadras and Lawson (2011)

in Australia demonstrated under optimal conditions that genetic gains in grain yield in recent decades were associated with gains in biomass but not in HI in wheat. In addition, trade-offs between HI and biomass at physiological maturity have been found in spring wheat cultivars (Aisawi et al., 2015; Molero et al., 2019; Sierra-Gonzalez et al., 2021). It has been estimated that there is hypothetical limit of HI in wheat of ca. 0.64. (Austin et al., 1980; Foulkes et al., 2011). Although this threshold is now being gradually approached in some countries in winter wheat, average values of HI for CIMMYT spring winter wheat are still typically in the range 0.50 - 0.55 (Rivera-Amado et al., 2019). Therefore, for future gains in yield potential it will be important alongside future gains in biomass to increase HI in high biomass backgrounds.

Many studies have shown that grain growth of modern wheat cultivars under optimal conditions is sink limited (Acreche and Slafer, 2009; Aisawi et al., 2015). Moreover, genetic variation in grain yield was explained by grain number per unit area in modern wheat cultivars under yield potential conditions as determined by assimilates partitioned to the spike before anthesis (Fischer, 2008, 2011; García et al., 2014). Similarly, genetic gains in grain yield in spring wheat cultivars were achieved by favouring biomass partitioning to the juvenile spikes before anthesis in response to a reduction of plant height with the semi-dwarf *Rht* genes (Fischer and Stockman, 1986; Calderini and Slafer, 1999). Spike and stem growth overlap during the terminal spikelet to anthesis period (Brooking and Kirby, 1981) and competition between these plant organs influences the amount of assimilates that reaches the spike determining the final number of grains per spike (Kirby, 1988; Siddique et al., 1989a). Floret abortion in the spikelets occurs from booting to anthesis and fertile floret number per spike at anthesis is linked to the assimilate supply to the spike during this phase (Kirby, 1988). Therefore, it has been suggested to modify the duration of the stem elongation (when grain number is determined) to increase the spike dry matter during anthesis hence grain number (Slafer *et al.*, 2005; Foulkes *et al.*, 2011; González *et al.*, 2011). One strategy is by manipulating the photoperiod sensitivity and earliness *per se* genes to advance onset of stem extension whilst maintaining anthesis date (Slafer, 1996). An alternative strategy is to increase partitioning to the spike at anthesis by reducing competition during the stem-elongation period from other plant organs such as stems, leaves, roots and infertile tillers (Fischer, 1985; Foulkes et al., 2011). The optimum range for plant height has been estimated to be ca. 70 - 100 cm in wheat; taller genotypes have a decreased grain partitioning with lodging problems, whereas shorter plants (< 70 cm) would result in

lower crop growth due to lower radiation-use efficiency (RUE) associated with sub-optimal distribution of light among the leaf layers of the canopy (Miralles and Slafer, 1995). So ideally, any changes in partitioning would be achieved whilst maintaining plants within the optimum plant height range.

Dry-matter partitioning is defined as the end-result of the distribution of dry-matter to each organ in a plant (Marcelis, 1996). One avenue to improve spike partitioning without altering partitioning of leaf lamina, which may affect photosynthetic capacity, or plant height significantly might be reducing the length of specific internodes whilst broadly maintaining the plant height, e.g. stem-internode 2 and 3 lengths (stem internode 2 = internode below the peduncle) (Foulkes et al., 2011). Reducing leaf partitioning may have impacts on photosynthetic capacity and biomass. For example, the leaf-sheath is an important organ for nitrogen storage (Pask et al., 2012c) and contributes to photosynthesis (Rivera-Amado et al., 2020). Decreases in leaf-sheath partitioning might affect N remobilization during grain filling and hence accelerate canopy senescence rate (Gaju et al., 2011). In addition, plant breeders should take into consideration that any leaf lamina reduction may cause a reduction in light interception and RUE (Murchie and Reynolds, 2012).

With regard to stem-internode partitioning, a field study in spring wheat cultivars in Mexico showed ranges of spike partitioning index (spike dry matter / above-ground dry matter; SPI) at anthesis + 7 days from 0.20 to 0.26, stem partitioning index from 0.32 to 0.41 and leaf partitioning index from 0.18 to 0.23 (Rivera-Amado et al., 2019). Reducing the length of stem-internode 2 or stem-internode 3 led to an increase in SPI and spike dry-matter per m² at anthesis + 7 days and was suggested to be a better strategy to increase spike growth than reducing the peduncle length. Half the extension of the peduncle occurs after anthesis (Sierra-Gonzalez et al., 2021), and there may be stronger competition between internode 2 and 3 and the spike than the peduncle (Rivera-Amado et al., 2019).

Another trait that may complement SPI to increase grain number is the fruiting efficiency (FE) (Reynolds et al., 2012a; Bustos et al., 2013) which is defined as the number of grains set per unit spike dry weight at anthesis (Fischer, 2011; Ferrante et al., 2012; García et al., 2014; Slafer et al., 2015). Trade-offs between FE and SPI (Sierra-Gonzalez et al., 2021) and between FE and TGW (Ferrante et al., 2012; Sierra-Gonzalez et al., 2021) have been found in durum wheat and spring bread wheat cultivars (Slafer et al., 2015). There are two alternative strategies to increase fruiting efficiency (Slafer et al., 2015). The first is to

increase the amount of assimilates to the florets during spike growth in the period before anthesis by investing less in structural spike organs such as glumes, rachis, etc. The second is to reduce the threshold requirement for assimilate for fertile floret development which may allow more of the distal florets to form fertile florets at anthesis. Several studies in wheat reported genetic variation in grain number per m² related to FE rather than spike dry weight (Bustos et al., 2013; García et al., 2014; Slafer et al., 2015). However, FE has not been investigated under different planting systems.

In the Yaqui Valley in NW Mexico, a raised beds planting system was introduced in the last decades, which consists of 2 or 3 rows per bed with a furrow gap between the beds to supply the irrigation. This is different from the traditional flat basins planting system consisting of rows in flat basins and flood irrigation (Sayre and Moreno Ramos, 1997; Fahong et al., 2004). Some investigations have reported better performance in raised beds than flat basins: greater grain yield, greater grain lodging resistance, better nitrogen fertilizer efficiency, water savings and less weeds and diseases (Fahong et al., 2004; Limon-Ortega, 2011; Majeed et al., 2015). To date, there are no studies in wheat comparing the relation between grain partitioning traits and grain number, HI and grain yield for wheat cultivars in the two planting systems. The objectives of this study were: i) identify grain partitioning traits to increase grain number per m², harvest index and grain yield in twelve spring wheat cultivars in two planting systems, raised beds and flat basins and ii) investigate any trade-offs between grain sink traits and source traits affecting photosynthetic capacity and biomass production in the two planting systems.

4.3 Materials and methods

4.3.1 Experimental site, design and treatment

Field experiments were conducted at CIMMYT (Campo Experimental Norman E. Borlaug) in the Yaqui Valley in NW Mexico (27°39'5 N, 109°9'26 W, 38 masl) in 2017-18, 2018-19 and 2019-20 under high yield potential conditions. The soil type was a sandy clay, mixed montmorillonitic typic calciorthid, low in organic matter, and slightly alkaline (pH 7.7) (Sayre et al., 1997). There were two planting systems: raised beds and flat basins. The experimental design was a completely randomized block design with three replicates. Each planting system (PS) in an experiment was sown in a rectangular matrix of 36 plots with border plots. The two planting systems were sown in adjacent areas in the field, with a 5 m gap between the border plots of the two planting systems. Ten spring wheat genotypes were chosen from the HiBAP I (High Biomass Association Panel I) (Molero et al., 2019) and two from the ESWYT (Elite Selection Wheat Yield Trial series) in the CIMMYT wheat breeding program. The genotypes were selected based on contrasting radiation-use efficiency, biomass and canopy architecture from previous datasets (Molero et al., 2019). From the twelve cultivars, three were elite CIMMYT cultivars and the others were elite advanced lines; the genotype names are abbreviated in figures, tables and text as indicated in **Supplementary Table 4.1**. The plot sizes and sowing dates, seed rates and agronomic inputs to supply ample nutrition and maintain the plots free from weeds, diseases and pests and irrigation applications were as described in **Chapter 2.3.1** (see also **Appendix Table 1**).

4.3.2 Crop measurements

4.3.2.1 Phenology

The phenology was recorded in each year according to Zadoks et al. (1974) when 50% of the shoots in the plot reached the stage (Pask et al., 2012a). The phenological stages recorded were initiation of booting (GS41), anthesis (GS65) and physiological maturity (GS87).

4.3.2.2 Growth analysis at GS41 and GS65 + 7 days

Above-ground biomass samples were taken at three stages (emergence + 40 days, initiation of booting and anthesis + 7 days) by cutting at ground level at least 0.5 m from the end of the plot to avoid border effects in 2017-18, 2018-19 and 2019-20 and processed as described in **Chapter 2.3.2**.

In 2017-18 and 2018-19, detailed analysis of dry matter partitioning and internode traits was carried out at GS65 + 7 days. From the remaining sample after taking the subsample for biomass estimation, 12 randomly selected shoots were taken (fertile shoots, those with a spike) and separated into leaf lamina, stem-and leaf sheath and spike and the weight recorded separately after drying at 70 °C for 48 h. The DM partitioning index of each component was calculated as the ratio of plant component DM to the above-ground DM. Peduncle, stem-internode 2 and stem-internode 3 lengths of each shoot were measured with a ruler. The stem-and-leaf-sheath of the 12 shoots was further separated into true-stem (TS) and leaf sheath (LS) for each of the peduncle (Ped), internode 2 (Int2), internode 3 (Int3); and the internode 4 (Int4+) (internode 4 and below; true stem and leaf sheath not separated) and the weight recorded for each component after drying at 70 °C for 48 h. In 2018 - 19, the spikes of the same 12 shoots were dissected into awn, glume, lemma, palea, rachis and developing grain and each component was separately weighed after drying at 70 °C for 48 h. The spike component partitioning index was calculated as the ratio of spike component DM to the spike DM (excluding developing grain). Fruiting efficiency (FE) was calculated as the ratio of the grains per m² to the spike DM per m² (DM_{spkA7}) at GS65 + 7 days. The percentage water-soluble carbohydrate (WSC) of the stem (leaf-sheath was removed before milling) and spike were assessed using the anthrone method (Yemm and Willis, 1954). The concentration of WSC was expressed as total WSC concentration on a DM basis (%).

4.3.2.3 Radiation-use efficiency

Radiation-use efficiency (RUE) was measured in each plot as the increment in the above-ground dry matter divided by the increment in intercepted PAR for the phase (Monteith and Moss, 1977) during 2018-19. For this study RUE measured in one year was used (2018-19) as partitioning traits was only measured in the cycles 2017-18 and 2018-19 and RUE was measured during 2018 - 19 and 2019 - 20. RUE was measured from emergence + 40 days to anthesis + 7 days (RUE_{preGF}; pre grain-filling) as described in **Chapter 2.3.2.3**. The intercepted PAR for the phenophase was calculated from the sum of the incident PAR on the days for the phase and applying the average LI% from the start to the end of the phase as described in **Chapter 2.3.2.2**.

4.3.2.4 Canopy architecture

Canopy architecture was assessed for each plot at seven days after anthesis in 2017-18 and 2018-19. Canopy architecture measurements were taken on six fertile shoots per plot as described in the **Chapter 3.3.2.4**. In 2017-18 and 2018-19 plant height was measured

from the ground to the tip of the spike (awns were not considered) shortly before physiological maturity at six random locations within the plot.

4.3.2.5 Growth analysis at physiological maturity, grain yield and yield components

Measurements at physiological maturity were carried out in each of the three years. For biomass at physiological maturity, 50 fertile shoots (those with a spike) were sampled randomly by cutting at ground level to estimate harvest index (ratio of grain dry matter to above-ground dry matter), above-ground biomass and grain yield components as described in **Chapter 2.3.2**. Grain yield was measured in each plot by machine-harvesting an average plot area of 3.2 and 4.0 m² in raised beds and flat basins, respectively, adjusted to moisture percentage calculated in each plot. After harvesting, a subsample of *ca.* 20 g of machine-harvested grain was taken and dried at 70°C to calculate thousand-grain weight using the digital image system Seed Counter (SeedCountSC5000 Image Analyzer).

4.3.3 Statistical analysis

Adjusted means for grain yield, yield components and physiological traits were calculated using a general linear model (GLM) ANOVA procedure from META R 6.04 (Alvarado et al., 2020). Replications, years and planting systems were considered as random effects, and genotypes as fixed effects. A covariate for anthesis date was used as a fixed effect and was included when significant. Phenotypic correlations between traits were Pearson's correlation coefficient calculated using either the three-year genotype means or the two-year genotype means. Linear regression analysis was applied to the three-year or two-year genotype means for selected traits. Biplots were made using one year data (2018-19) using Rstudio (<https://www.rproject.org/>). Broad sense heritability (H²) was calculated using across the three or two years, using equation (4.1):

$$H^2 = \frac{\sigma_g^2}{\sigma_g^2 + \frac{\sigma_{gy}^2}{y} + \frac{\sigma_{gs}^2}{s} + \frac{(\sigma_{gy})^2(s)}{ys} + \frac{\sigma_e^2}{rys}} \quad (4.1)$$

Where σ^2 = error variance, σ_g^2 = genotypic variance, σ_{gy}^2 = G × Y variance, σ_{gs}^2 = PS variance, s = number of PS, y= number of years, σ_e^2 = residual variance, r = number of replicates.

4.4 Results

Harvest results for grain yield and yield components in the three years were reported previously in **Chapter 2.4**. The dry matter partitioning analysis at anthesis + 7 days and analysis of stem internode traits was only carried out in two years, 2017-18 and 2018-19. Unless stated otherwise the following results relate to the two seasons 2017-18 and 2018-19.

4.4.1 Genetic variation in grain yield, yield components and grain partitioning traits

Analysis of variance for yield and yield components showed a wide genetic variation evaluated across either two years (2017-18 and 2018-19) (**Fig. 4.1**) or three years (2017-18, 2018-19 and 2019-20; **Supplementary table 4.2**) ($P < 0.001$). Averaging over the two years, grain yield was 4.1% higher in raised beds (B) than flat basins (F) ($P < 0.05$) with a genetic range from 527 to 699 g m⁻² and 540 to 744 g m⁻², respectively. Harvest index (HI) was also greater in beds than flats ($P < 0.001$) with an overall mean of 0.47 and 0.44, respectively. In addition, grains per m² (GM2) was 3.8% higher in raised beds than flat basins ($P < 0.05$) with a genetic range from 10752 to 17356 and 10463 to 17550 m⁻², respectively ($P < 0.001$). Biomass at physiological maturity (BMPM) was 7.6 % higher in beds than flats averaging across the three years, but averaging over the two years did not differ significantly between the planting systems. Each of the yield and yield component traits evaluated in the two years (2017-18 and 2018-19) showed a PS \times G interaction ($P < 0.05 - 0.001$; **Fig. 4.1**) except for thousand-grain weight (TGW).

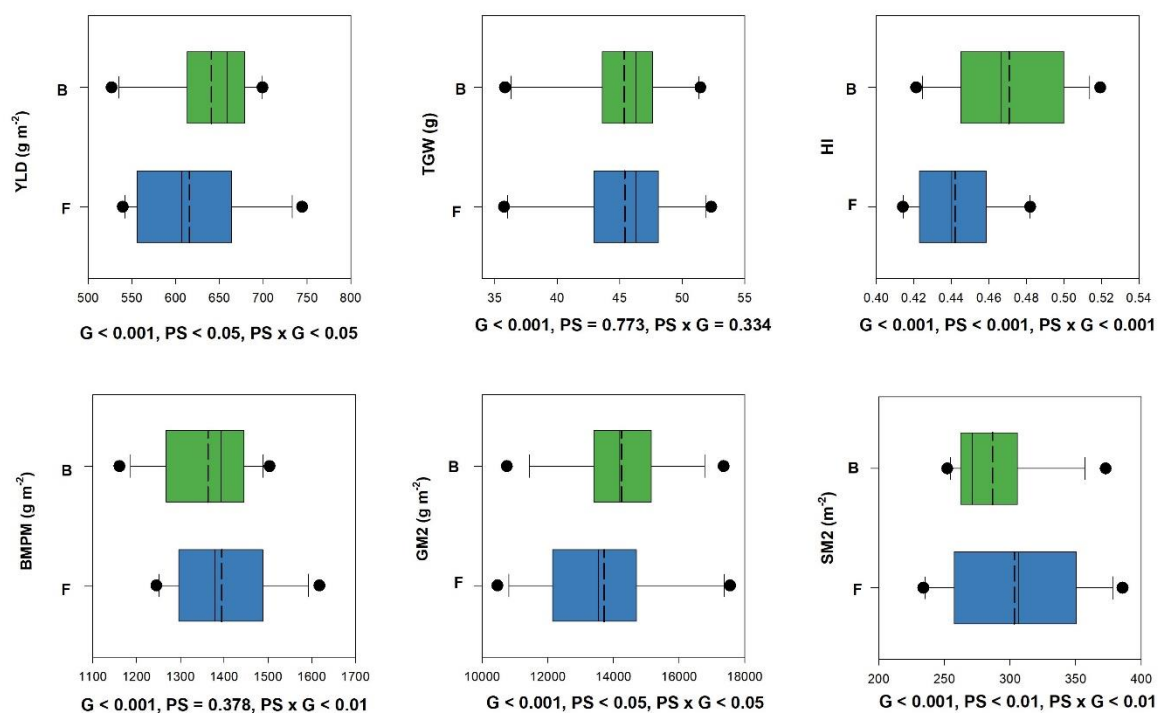


Fig. 4.1. Boxplots of genetic variation in **A** grain yield (YLD, 0 % DM), **B** thousand-grain weight (TGW), **C** harvest index (HI), **D** biomass at physiological maturity (BMPM), **E** grains per square meter (GM2) and **F** spikes per square meter (SM2) for 12 CIMMYT spring wheat genotypes evaluated across-years 2017-18 and 2018-19 in raised beds (B) and flat basins (F). The dotted line is the adjusted mean across lines. Statistical significances for genotype (G), planting systems (PS) and the interaction (PS × G) are presented below each boxplot.

Dry matter partitioning analysis was carried out across the two years 2017-18 and 2018-19. Differences among cultivars were found in all the partitioning traits at seven days after anthesis (GS65 + 7 days, A7), and for plant height (**Table 4.1**). In beds, StemPI had the highest DM partitioning with 0.566 followed by SPI with 0.246 and then LamPI with 0.188. Similar results were found in flats: StemPI (0.563) > SPI (0.244) > LamPI (0.194). Biomass at GS65 + 7 days ranged from 675 to 1058 g m⁻² in beds and 886 to 1213 g m⁻² in flats and was higher in F than B (P < 0.001).

No differences between planting systems were found for the spike, stem and lamina partitioning indices but the traits did show a PS × G interaction (P < 0.001, P < 0.01 and P < 0.001, respectively). The increase in SPI in beds compared to flats ranged from 0.06 (CHIPAK*2//) to -0.03 (C80.1/3*QT4118) and for StemPI from 0.06 (C80.1/3*QT4118) to -0.02 (KUTZ). Spike dry-matter per m² at GS65 + 7 days (DMspkA7) ranged from 187 to 318 g m⁻² in beds and 210 to 305 g m⁻² in flats and was higher in flats by 9.1% (P < 0.01).

Table 4.1. Spike partitioning index (SPI), stem partitioning index (StemPI), lamina partitioning index (LamPI), spike dry matter at seven days after anthesis (DMspkA7), fruiting efficiency (FE), plant height at physiological maturity and biomass at seven days after anthesis (BMA7) for 12 CIMMYT spring wheat genotypes. Values represent means across 2017-18 and 2018-19 in raised beds (B) and flat basins (F) planting systems. *P < 0.05, **P < 0.01, ***P < 0.001, *italics*: P < 0.10, ns: not significant.

Gen	SPI		StemPI		LamPI		DMspkA7 (g m ⁻²)		FE grains ⁻¹		HeightPM (cm)		BMA7 g m ⁻²	
	B	F	B	F	B	F	B	F	B	F	B	F	B	F
BACANORA T88	0.259	0.255	0.556	0.552	0.185	0.194	216	249	72.40	72.74	89.8	90.0	835	982
C80.1/3*QT4118	0.194	0.221	0.630	0.565	0.176	0.211	199	242	59.46	48.86	121.6	123.2	1031	1094
CHEWINK#1	0.230	0.235	0.583	0.576	0.187	0.189	218	260	54.98	43.94	110.4	114.2	953	1113
SOKOLL//PUB94	0.260	0.249	0.573	0.581	0.167	0.170	266	238	46.11	46.09	111.8	115.5	1024	956
NELOKI	0.279	0.297	0.508	0.517	0.213	0.186	187	263	69.27	47.14	94.0	97.4	675	886
W15.92/4/PASTOR	0.227	0.249	0.566	0.568	0.206	0.184	203	234	52.47	40.43	107.9	109.8	897	944
KUKRI	0.238	0.251	0.577	0.564	0.185	0.185	224	283	59.61	43.90	106.5	112.5	943	1133
KUTZ	0.212	0.195	0.585	0.597	0.204	0.208	223	210	61.87	56.45	111.7	115.9	1058	1078
SOKOLL	0.263	0.240	0.545	0.553	0.192	0.207	277	259	48.90	44.40	109.6	107.6	1058	1088
BORLAUG100	0.248	0.235	0.553	0.553	0.198	0.212	253	257	56.81	51.45	102.6	105.4	1033	1096
ITP40/AKURI	0.232	0.251	0.589	0.602	0.177	0.153	217	292	56.97	52.69	105.6	112.3	963	1174
CHIPAK*2//	0.310	0.253	0.525	0.529	0.162	0.225	318	305	44.78	50.54	101.6	101.9	1042	1213
Mean	0.246	0.244	0.566	0.563	0.188	0.194	234	258	56.97	49.88	106.1	108.8	959	1063
H ²	0.81		0.63		0.00		0.77		0.72		0.95		0.73	
LSD (G) (5%)	0.025		0.032		0.031		34.173		13.418		4.100		109.357	
CV%	6.35		3.45		9.97		8.83		15.29		2.34		6.77	
G (p value)	***		***		***		***		***		***		***	
PS (p value)	ns		ns		ns		***		***		*		***	
Y (p value)	***		***		ns		0.144		*		***		***	
PS×G (p value)	***		**		***		***		*		*		***	

Fruiting efficiency (FE) was higher in raised beds than flat basins by 14.2% ($P < 0.05$) with genetic ranges from 46.1 to 72.4 grains g^{-1} in raised beds and 40.4 to 72.7 grains g^{-1} in flat basins. In addition, plant height at physiological maturity (HeightPM) was 2.7 cm higher in flat basins than raised beds ($P < 0.05$). DMspkA7, FE and HeightPM showed a PS \times G interaction ($P < 0.001$, $P < 0.05$ and $P < 0.05$, respectively). NELOKI showed the greatest increase in FE in beds compared to flats (22.1 grains g^{-1}) and CHIPAK*2// the least (-5.8 grains g^{-1}).

4.4.2 Phenotypic correlations between grain partitioning traits, yield and yield components

Linear regression analyses between GM2 and each of FE, SPI and biomass at GS65 + 7 days (BMA7) were carried out (**Fig. 4.2**). A significant positive association was found between GM2 and FE in flats ($R^2 = 0.39$, $P < 0.05$) and a trend for a positive association in beds ($R^2 = 0.25$, $P = 0.097$). However, GM2 was not associated with SPI and BMA7 in either PS. Negative associations between SPI and Int2 length were found in flats ($R^2 = -0.58$, $P < 0.01$) and in beds ($R^2 = -0.30$, $P = 0.067$) (**Fig. 4.3**). SPI was also negatively associated with Int3 length in beds ($R^2 = -0.38$, $P < 0.05$) with a trend for a negative association in flats ($R^2 = -0.26$, $P = 0.094$). SPI and PedL were not associated in beds or flats.

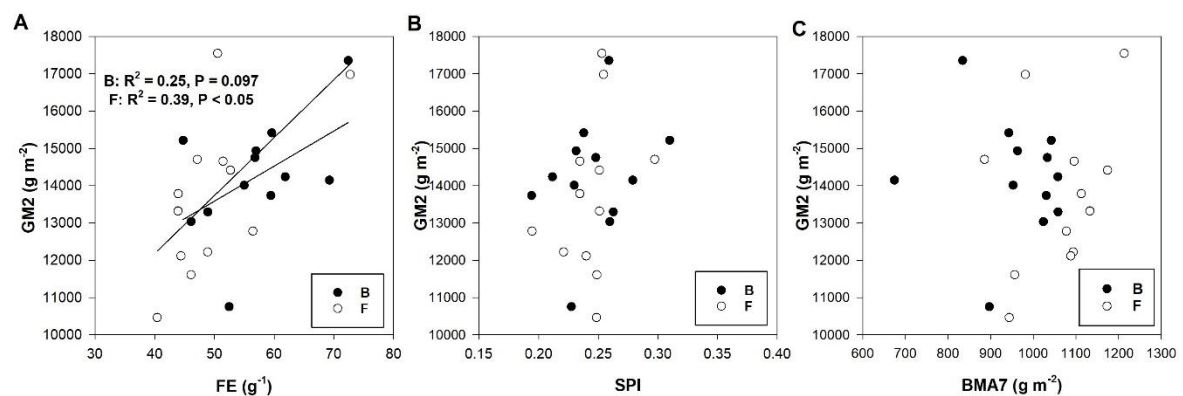


Fig. 4.2. Regression of grains per m^2 (GM2) on **A** fruiting efficiency (FE), **B** spike partitioning index (SPI) and **C** biomass at seven days after anthesis (BMA7) for 12 CIMMYT spring wheat cultivars across 2017-18 and 2018-19 in raised beds (B) and flat basins (F).

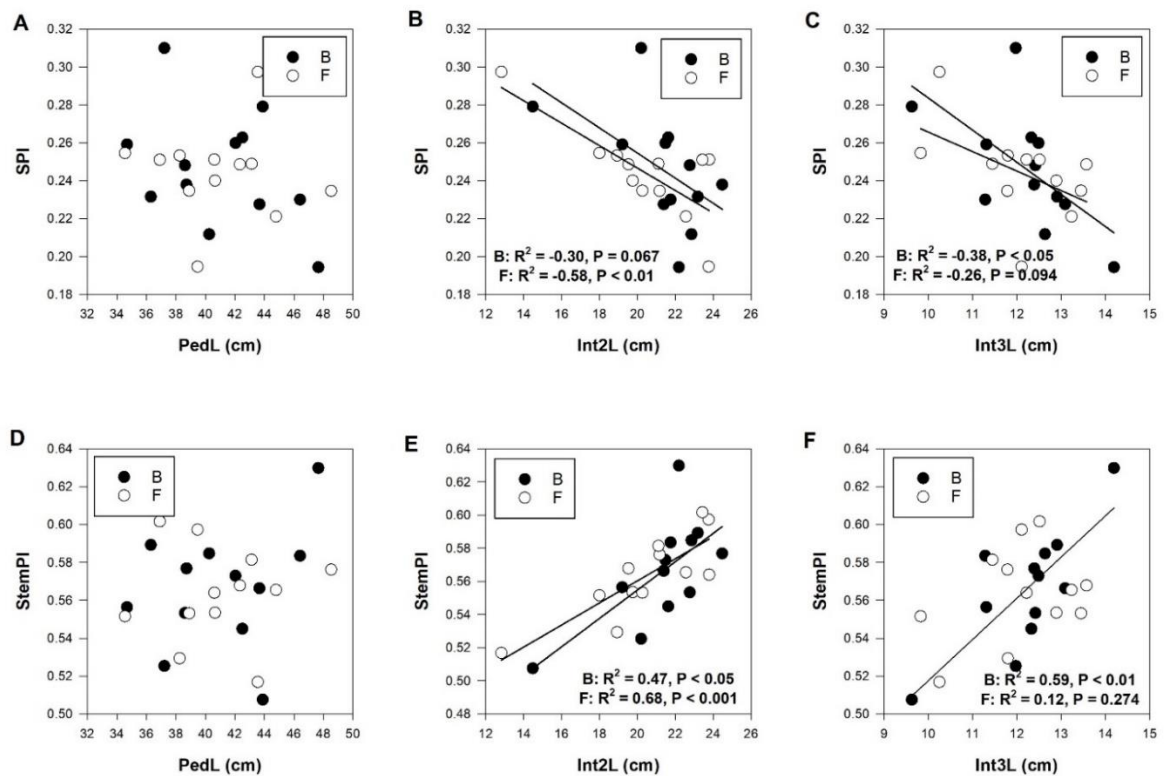


Figure 4.3. Linear regressions of each of spike partitioning index (SPI) and stem partitioning index (StemPI) on peduncle length at physiological maturity, stem-internode 2 length at seven days after anthesis and stem-internode 3 length at seven days after anthesis for 12 CIMMYT spring wheat cultivars across 2017-18 and 2018-19 in raised beds (B) and flat basins (F).

Negative correlations among cultivars were found between SPI and StemPI in raised beds ($r = -0.88$, $P < 0.001$) and flat basins ($r = -0.65$, $P < 0.05$) (Table 4.2). Plant height was also negatively associated with SPI in beds ($r = -0.65$, $P < 0.05$) and flats ($r = -0.61$, $P < 0.05$). There was a positive correlation between SPI and DMspkA7 in beds ($r = 0.63$, $P < 0.05$) and a trend in flats ($r = 0.51$, $P = 0.09$). However, no correlations were found between SPI and GM2 or HI for either planting system. Spike dry-matter at GS65 + 7 days was negatively related to FE only in raised beds ($r = -0.74$, $P < 0.01$). Grains per m² was negatively correlated with peduncle length in beds ($r = -0.67$, $P < 0.05$) and flats ($r = -0.53$, $P < 0.05$). Peduncle length was also negatively correlated with HI in beds ($r = -0.73$, $P < 0.01$) and flats ($r = -0.74$, $P < 0.01$). Negative correlations between GM2 and TGW were found in both planting systems (B: $r = -0.74$, $P < 0.01$; F: $r = -0.76$, $P < 0.01$). In addition, FE was negatively correlated with TGW in beds ($r = -0.69$, $P < 0.05$) and flats ($r = -0.58$, $P < 0.05$). A positive correlation between YLD and stem water-soluble carbohydrate (CHOS_s; g m⁻²) was found in beds ($r = 0.75$, $P < 0.01$).

Table 4.2. Phenotypic correlations among 12 CIMMYT spring wheat genotypes evaluated across 2017-18 and 2018-19 in raised beds and flat basins (*italics*) between grain partitioning traits and yield, yield components and biomass.

Trait	1	2	3	4	5	6	7	8	9	10	11	12	13	14
1.YLD	.	<i>-0.00</i>	<i>0.58*</i>	<i>0.86***</i>	<i>0.65*</i>	<i>0.22</i>	<i>0.73**</i>	<i>-0.14</i>	<i>0.02</i>	<i>0.24</i>	<i>0.57†</i>	<i>0.24</i>	<i>0.46</i>	<i>-0.10</i>
2.TGW	0.31	.	<i>-0.19</i>	<i>0.12</i>	<i>-0.76**</i>	<i>-0.82***</i>	<i>0.15</i>	<i>-0.54†</i>	<i>0.63*</i>	<i>-0.16</i>	<i>-0.32</i>	<i>-0.58*</i>	<i>0.23</i>	<i>-0.78**</i>
3.HI	0.55†	<i>-0.42</i>	.	<i>0.09</i>	<i>0.56†</i>	<i>0.28</i>	<i>0.25</i>	<i>-0.08</i>	<i>-0.09</i>	<i>0.24</i>	<i>0.18</i>	<i>0.58†</i>	<i>0.34</i>	<i>-0.51†</i>
4.BMPM	<i>0.64*</i>	<i>0.71**</i>	<i>-0.29</i>	.	<i>0.44</i>	<i>0.07</i>	<i>0.73**</i>	<i>-0.13</i>	<i>0.12</i>	<i>0.11</i>	<i>0.57†</i>	<i>-0.05</i>	<i>0.36</i>	<i>0.20</i>
5.GM2	0.41	<i>-0.74**</i>	<i>0.79**</i>	<i>-0.23</i>	.	<i>0.76**</i>	<i>0.32</i>	<i>0.32</i>	<i>-0.47</i>	<i>0.27</i>	<i>0.58*</i>	<i>0.63*</i>	<i>0.12</i>	<i>-0.69*</i>
6.SM2	<i>-0.54†</i>	<i>-0.79**</i>	<i>-0.01</i>	<i>-0.60*</i>	<i>0.34</i>	.	<i>-0.03</i>	<i>0.78**</i>	<i>-0.70*</i>	<i>-0.01</i>	<i>0.67*</i>	<i>0.28</i>	<i>-0.39</i>	<i>-0.85***</i>
7.BMA7	<i>0.72**</i>	<i>0.66*</i>	<i>0.02</i>	<i>0.80**</i>	<i>-0.13</i>	<i>-0.78**</i>	.	<i>-0.42</i>	<i>0.24</i>	<i>0.28</i>	<i>0.56†</i>	<i>-0.02</i>	<i>0.70*</i>	<i>0.30</i>
8.SPI	<i>-0.23</i>	<i>-0.47</i>	<i>0.29</i>	<i>-0.51†</i>	<i>-0.27</i>	<i>0.40</i>	<i>-0.23</i>	.	<i>-0.65*</i>	<i>-0.36</i>	<i>0.51†</i>	<i>-0.10</i>	<i>-0.71**</i>	<i>-0.61*</i>
9.StemPI	0.50	<i>0.52†</i>	<i>-0.12</i>	<i>0.67*</i>	<i>-0.12</i>	<i>-0.61*</i>	<i>0.45</i>	<i>-0.88***</i>	.	<i>-0.47</i>	<i>-0.35</i>	<i>0.00</i>	<i>0.64*</i>	<i>0.66*</i>
10.LamPI	<i>-0.58†</i>	<i>-0.13</i>	<i>-0.37</i>	<i>-0.34</i>	<i>-0.29</i>	<i>0.45</i>	<i>-0.48</i>	<i>-0.21</i>	<i>-0.28</i>	.	<i>-0.08</i>	<i>0.13</i>	<i>0.09</i>	<i>-0.11</i>
11.DMspkA7	0.37	<i>0.16</i>	<i>0.23</i>	<i>0.22</i>	<i>0.10</i>	<i>-0.31</i>	<i>0.61*</i>	<i>0.63*</i>	<i>-0.35</i>	<i>-0.56*</i>	.	<i>-0.11</i>	<i>0.02</i>	<i>-0.27</i>
12.FE	<i>-0.26</i>	<i>-0.69*</i>	<i>0.20</i>	<i>-0.46</i>	<i>0.50†</i>	<i>0.62*</i>	<i>-0.67*</i>	<i>-0.23</i>	<i>-0.01</i>	<i>0.50</i>	<i>-0.74**</i>	.	<i>0.35</i>	<i>-0.53†</i>
13.CHOS _{st}	<i>0.75**</i>	<i>0.40</i>	<i>0.26</i>	<i>0.60*</i>	<i>0.14</i>	<i>-0.48</i>	<i>0.57†</i>	<i>-0.66*</i>	<i>0.78**</i>	<i>-0.30</i>	<i>-0.10</i>	<i>-0.04</i>	.	<i>0.41</i>
14.HeightPM	0.34	<i>0.80**</i>	<i>-0.46</i>	<i>0.79**</i>	<i>-0.55†</i>	<i>-0.70*</i>	<i>0.67*</i>	<i>-0.65*</i>	<i>0.75**</i>	<i>-0.23</i>	<i>0.01</i>	<i>-0.49</i>	<i>0.55†</i>	.

YLD: grain yield (g m⁻²), TGW: thousand grain-weight (g), HI: harvest index, BMPM: biomass at physiological maturity (g m⁻²), GM2: grain number (m⁻²), SM2: spikes per square meter, BMA7: biomass at anthesis + 7 days (g m⁻²), SPI: spike partitioning index, StemPI: stem partitioning index, LamPI: lamina partitioning index, DMspkA7: dry-matter of spike at anthesis + 7 days (g m⁻²), FE: fruiting efficiency (grains⁻¹), CHOS_{st}: spike water- soluble carbohydrates, HeightPM: height at physiological maturity (cm). *P < 0.05, **P < 0.01, ***P < 0.001, †P < 0.10.

4.4.3 Radiation-use efficiency and canopy architecture traits

Genetic variation of RUE_preGF and canopy architecture traits was found in 2018-19 ($P < 0.001$) (**Supplementary Table 4.3**). A PS \times G interaction was found for each trait ($P < 0.05 - 0.001$). Flag-leaf curvature (FLcvA7) was higher in beds than flats ($P < 0.05$) whereas RUE_preGF was higher in flats ($P < 0.01$). For a full description of the results for these RUE and canopy architecture traits averaged over 2018-19 and 2019-20 see **Chapter 3.4**.

4.4.4 Stem-internode partitioning traits and correlations with source and sink traits

In beds, peduncle length accounted for the highest percentage of stem length with 55.0% followed by internode 2 with 25.6% and then internode 3 with 16.4%. Similar values were found in flats (PedL (55.8%) > Int2L (27.8%) > Int3L (16.5%)) (**Table 4.3**). Stem-internode 2 length was 4.4% higher in raised beds than flats ($P < 0.01$) ranging among cultivars from 14.5 to 24.5 cm in beds and from 12.8 to 23.8 cm in flat basins. Peduncle and stem internode 3 lengths did not differ between the planting systems. All the stem-internode lengths showed a PS \times G interaction except PedL ($P < 0.05 - 0.001$). The cultivar BORLAUG100 had the greatest increase in stem internode 2 length in beds compared to flats among the cultivars (2.5 cm) and KUTZ the least (-0.9 cm); and for internode 3 length BACANORA T88 (1.48 cm) and BORLAUG100 (-1.0 cm), respectively.

Genetic variation was found in all the stem-internode DM partitioning traits measured at GS65 + 7 days ($P < 0.05 - < 0.001$; **Fig. 4.4**). Int2TSPI was higher in beds than flats (8.2%) ranging from 0.069 to 0.125 in beds compared to 0.062 to 0.119 in flats. Int4+PI was higher in flats than beds by 5.7% ranging from 0.061 to 0.099 in flats and 0.038 to 0.079 in beds. A PS \times G interaction was found for Int2TSPI ($P < 0.001$) and PedLSPI ($P < 0.01$). The specific weight of stem internode 2 (Int2SW) was higher in flats than beds ($P < 0.01$) ranging among cultivars from 0.015 to 0.022 g cm⁻¹ in flats and 0.011 to 0.023 g cm⁻¹ in beds (**Supplementary Table 4.4**). Additionally, a PS \times G interaction was found for Int2SW ($P < 0.001$).

The correlations among genotypes between stem-internode partitioning traits and grain sink-related traits are shown in **Table 4.4**. PedTSPI was positively correlated with SPI in flats ($r = 0.58$, $P < 0.05$). In addition, SPI was negatively correlated with Int2TSPI in beds ($r = -0.58$, $P < 0.05$) and flats ($r = -0.73$, $P < 0.01$). However, Int3TSPI was only negatively correlated with SPI in beds ($r = -0.65$, $P < 0.05$). A negative correlation was found between PedLSPI and each of SPI and SM2 in raised beds ($r = -0.65$, $P < 0.05$ and $r = -0.68$, $P < 0.05$,

respectively). Int2SW was negatively related with HI in flats ($r = -0.78$, $P < 0.01$). Grain yield was negatively associated with Int2TSPI ($r = 0.72$, $P < 0.01$) and PedLSPI ($r = 0.78$, $P < 0.01$) in beds. BMA7 and Int2TSPI were positively correlated with Int2TSPI in beds ($r = 0.73$, $P < 0.01$) and flats ($r = 0.64$, $P < 0.05$).

Table 4.3. Peduncle (PedL), internode 2 (Int2L) and internode 3 (Int3L) length at GS65 + 7 days for 12 CIMMYT spring wheat genotypes. Values represent means across 2017-18 and 2018-19 in raised bed (B) and flat basin (F) planting systems. * $P < 0.05$, ** $P < 0.01$, *** $P < 0.001$, *italics: $P < 0.10$* , ns: not significant.

Gen	PedL (cm)		Int2L (cm)		Int3L (cm)	
	B	F	B	F	B	F
BACANORA T88	34.7	34.6	19.2	18.0	11.3	9.8
C80.1/3*QT4118	47.7	44.8	22.2	22.6	14.2	13.2
CHEWINK#1	46.4	48.5	21.8	21.2	11.3	11.8
SOKOLL//PUB94	42.0	43.1	21.5	21.1	12.5	11.4
NELOKI	43.9	43.6	14.5	12.8	9.6	10.3
W15.92/4/PASTOR	43.7	42.3	21.4	19.5	13.1	13.6
KUKRI	38.7	40.6	24.5	23.8	12.4	12.2
KUTZ	40.3	39.5	22.9	23.8	12.6	12.1
SOKOLL	42.5	40.7	21.6	19.8	12.3	12.9
BORLAUG100	38.6	38.9	22.8	20.3	12.4	13.4
ITP40/AKURI	36.3	36.9	23.2	23.4	12.9	12.5
CHIPAK*2//	37.2	38.3	20.2	18.9	12.0	11.8
Mean	41.0	41.0	21.3	20.4	12.2	12.1
H ²	0.94		0.98		0.90	
LSD (G) (5%)	3.501		1.773		1.401	
CV%	5.16		5.25		7.11	
G (p value)	***		***		***	
PS (p value)	ns		**		ns	
Y (p value)	0.077		***		**	
PS×G (p value)	0.176		*		*	

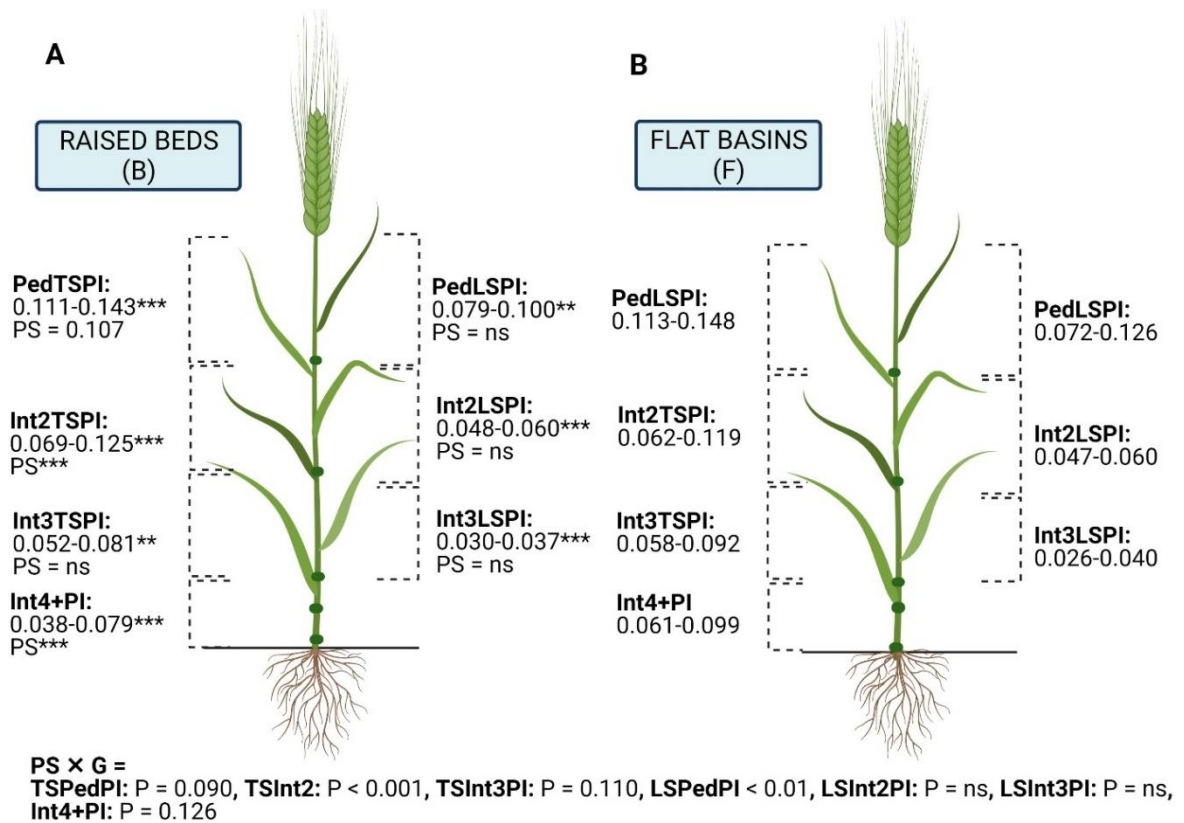


Fig. 4.4. Diagram showing the genetic variation in PedTSPI: peduncle true-stem partitioning index, Int2TSPI: internode 2 true-stem partitioning index, Int3TSPI: internode 3 true-stem partitioning index, PedLSPI: peduncle leaf-sheath partitioning index, Int2LSPI: internode 2 leaf-sheath partitioning index, Int3LSPI: internode 3 leaf-sheath partitioning index, Int4+PI: internode 4+ partitioning index (TS-LS), PedLSW: peduncle specific weight, Int2SW: internode 2 specific weight, Int 3SW: internode 3 specific weight for 12 CIMMYT spring wheat genotypes across 2017-18 and 2018-19 in **A** raised beds and **B** flat basins. Genotype and planting system significance are shown in **A** raised beds. Diagram created with BioRender.com.

Table 4.4. Phenotypic correlations among 12 CIMMYT spring wheat genotypes across 2017-18 and 2018- 19 in raised beds (B) and flat basins (F) between internode traits and sink strength traits.

RAISED BEDS (B)								
	YLD	HI	GM2	SM2	BMA7	SPI	DMspkA7	FE
PedL	-0.39	-0.73**	-0.68*	-0.19	-0.02	-0.41	-0.34	-0.15
Int2	0.77**	0.14	-0.08	-0.70*	0.76**	-0.55†	0.18	-0.38
Int3	0.49	-0.12	-0.32	-0.76**	0.72**	-0.62*	0.07	-0.40
PedTSPI	-0.23	-0.50†	-0.20	0.24	-0.19	-0.17	-0.33	0.18
Int2TSPI	0.72**	0.13	0.04	-0.77**	0.73**	-0.58*	0.12	-0.21
Int3TSPI	0.46	-0.19	-0.26	-0.71**	0.77**	-0.65*	0.09	-0.28
PedLSPI	0.22	-0.38	-0.40	-0.49	0.33	-0.83***	-0.41	-0.01
Int2LSPI	-0.53†	-0.24	-0.09	0.43	-0.50	-0.02	-0.40	0.53†
Int3LSPI	-0.44	-0.21	-0.26	0.23	-0.43	-0.42	-0.70*	0.43
Int4+PI	0.20	-0.23	-0.24	-0.38	0.47	-0.53†	-0.06	-0.04
Int2SW	0.45	-0.16	-0.14	-0.69*	0.57†	-0.60*	-0.04	-0.16
Int3SW	0.55†	-0.18	-0.19	-0.74**	0.75**	-0.64*	0.07	-0.30
FLAT BASINS (F)								
	YLD	HI	GM2	SM2	BMA7	SPI	DMspkA7	FE
PedL	-0.40	-0.74**	-0.53†	-0.39	-0.20	-0.03	-0.22	-0.70*
Int2	0.25	0.09	-0.34	-0.69*	0.61*	-0.76**	-0.10	-0.08
Int3	0.10	-0.06	-0.56†	-0.60*	0.39	-0.51†	-0.08	-0.54†
PedTSPI	-0.24	-0.40	0.24	0.45	-0.48	0.58*	0.07	-0.04
Int2TSPI	-0.24	0.12	-0.27	-0.57†	0.64*	-0.73**	-0.06	-0.03
Int3TSPI	0.20	-0.08	-0.22	-0.26	0.39	-0.21	0.17	-0.09
PedLSPI	0.11	-0.05	-0.15	-0.07	0.21	-0.04	0.18	-0.03
Int2LSPI	-0.54†	-0.12	-0.23	-0.19	-0.68*	-0.19	0.83***	0.29
Int3LSPI	-0.30	0.06	0.13	0.41	-0.46	0.34	-0.16	0.25
Int4+PI	0.26	0.35	-0.08	-0.60*	0.42	-0.81**	-0.33	0.41
Int2SW	-0.27	-0.78**	-0.33	-0.27	-0.32	0.11	-0.22	-0.34
Int3SW	0.20	-0.35	-0.28	-0.55†	0.35	-0.41	-0.05	-0.09

PedL: peduncle length (cm), Int2: stem internode 2 length (cm), Int3: stem internode 3 length (cm), PedTSPI: peduncle true-stem partitioning index, Int2TSPI: internode 2 true-stem partitioning index, Int3TSPI: internode 3 true-stem partitioning index, PedLSPI: peduncle leaf-sheath partitioning index, Int2LSPI: internode 2 leaf-sheath partitioning index, Int3LSPI: internode 3 leaf-sheath partitioning index, Int4+PI: internode 4+ partitioning index (TS-LS), Int2SW: internode 2 specific weight (g cm⁻¹), Int 3SW: internode 3 specific weight (g cm⁻¹), YLD: grain yield (g m⁻²), HI: harvest index, GM2: grains per square meter (g m⁻²), SM2: spikes per square meter (m⁻²), BMA7: biomass at seven days after anthesis (g m⁻²), SPI: spike partitioning index, DMspkA7: spike dry-matter at seven days after anthesis (g m⁻²), FE: fruiting efficiency (g⁻¹). *P < 0.05, **P < 0.01, ***P < 0.001, †P < 0.10. ‡One year data (2018 – 19).

The correlations among genotypes between stem-internode traits and source traits are shown in **Table 4.5**. True-stem soluble carbohydrate (g m^{-2}) was strongly correlated with internode 2 length in beds ($r = 0.80, P < 0.01$) and flats ($r = 0.83, P < 0.001$). Similarly, CHOS_{st} was positively associated with Int2PI in raised beds ($r = 0.65, P < 0.05$) and flats ($r = 0.85, P < 0.001$) and with Int4+ PI in beds ($r = 0.62, P < 0.05$) and flats ($r = 0.84, P < 0.001$). A positive correlation was found between RUE in the pre-grain filling phase and stem-internode 3 length ($r = 0.65, P < 0.05$) but only in beds. GAI at GS65 + 7 days was strongly positively correlated with internode 2 length ($r = 0.74, P < 0.01$) in beds with a trend for a positive correlation in flats ($r = 0.50, P = 0.10$). Flag-leaf angle at GS65 + 7 days was positively related with stem-internode 3 length in beds ($r = 0.63, P < 0.05$) and flats ($r = 0.64, P < 0.05$). Additionally, a positive correlation was found between flag-leaf length at anthesis + 7 days (LLA7) and PedL in beds ($r = 0.65, P < 0.05$) and flats ($r = 0.59, P < 0.05$). The fractional radiation interception at GS65 + 7 days was positively correlated with Int2L ($r = 0.81, P < 0.01$) and Int2TSPI ($r = 0.79, P < 0.01$) in beds but there was no correlation in flats.

The principal component analysis (PCA) in **Fig. 4.5** shows associations in year 2018-19 for stem-internode traits and source and sink traits. The first two principal components explained 64.5% of the phenotypic variation in beds (PC1: 37.6% and PC2: 26.9%) and 55.6% in flats (PC1: 30.07% and PC2: 25.5%). In beds, the traits Int3L and Int3TSPI were associated with the PC1 whereas PedL and PedTSPI were associated with PC2. In flats, the traits Int3TSPI and Int3L were associated with PC1, whereas PedL was associated with PC2.

Table 4.5. Phenotypic correlations among 12 CIMMYT spring wheat cultivars evaluated across the years 2017- 18 and 2018-19 in raised beds (B) and flat basins (F) between internode traits and source strength traits.

RAISED BEDS (B)								
	CHOS _{st}	RUE _{preGF} ‡	GAI	FIA7‡	FLAA7‡	FLCA7‡	LLA7‡	LWA7‡
PedL	-0.18	-0.09	0.18	-0.06	0.15	-0.11	0.65*	0.53‡
Int2L	0.80**	0.55‡	0.74**	0.81**	0.46	-0.36	0.26	0.40
Int3L	0.73**	0.65*	0.50‡	0.47	0.63*	-0.35	0.39	0.48
PedTSPI	-0.14	0.00	-0.42	-0.24	-0.35	-0.04	-0.16	-0.47
Int2TSPI	0.65*	0.75**	0.73**	0.79**	0.64*	-0.32	-0.62*	0.56‡
Int3TSPI	0.62*	0.53‡	0.52‡	0.47	0.33	-0.31	0.24	-0.01
PedLSPI	0.52‡	0.47	0.18	0.71**	0.42	-0.29	0.40	0.41
Int2LSPI	-0.37	-0.20	-0.61*	-0.26	-0.15	-0.22	-0.04	-0.01
Int3LSPI	0.21	-0.58*	-0.32	-0.48	-0.45	-0.16	-0.60*	-0.32
Int4+PI	0.62*	0.17	0.10	0.14	0.49	-0.45	0.11	0.31
Int2SW	0.45	0.37	0.59*	0.53‡	0.45	-0.11	0.76**	0.67*
Int3SW	0.59*	0.46	0.73**	0.56‡	0.40	-0.03	0.80**	0.67*
FLAT BASINS (F)								
	CHOS _{st}	RUE _{preGF} ‡	GAI	FIA7‡	FLAA7‡	FLCA7‡	LLA7‡	LWA7‡
PedL	-0.36	-0.29	0.13	-0.33	0.20	0.01	0.59*	0.54‡
Int2	0.83***	0.35	0.50‡	0.07	0.57‡	-0.45	0.32	0.20
Int3	0.29	0.23	0.45	-0.29	0.64*	-0.43	0.34	0.40
PedTSPI	-0.64*	-0.03	-0.28	0.08	-0.44	0.29	-0.18	-0.23
Int2TSPI	0.85***	0.35	0.51‡	0.22	0.42	-0.36	0.08	-0.06
Int3TSPI	0.45	0.11	0.11	0.10	-0.14	0.30	-0.11	-0.25
PedLSPI	0.26	0.30	0.09	0.23	0.01	-0.07	-0.00	-0.40
Int2LSPI	-0.35	-0.77**	-0.35	-0.33	-0.26	0.21	0.22	0.31
Int3LSPI	-0.31	-0.45	-0.46	0.04	-0.19	0.04	-0.40	-0.16
Int4+PI	0.84***	0.19	0.25	0.08	0.22	-0.22	-0.08	-0.11
Int2SW	-0.29	0.16	-0.19	0.03	0.23	0.01	0.34	0.03
Int3SW	0.52‡	-0.02	0.20	0.20	-0.24	0.43	0.23	-0.13

PedL: peduncle length (cm), Int2: internode 2 length (cm), Int3: internode 3 length (cm), PedTSPI: peduncle true-stem partitioning index, Int2TSPI: internode 2 true-stem partitioning index, Int3TSPI: internode 3 true-stem partitioning index, PedLSPI: peduncle leaf-sheath partitioning index, Int2LSPI: internode 2 leaf-sheath partitioning index, Int3LSPI: internode 3 leaf-sheath partitioning index, Int4+PI: internode 4+ partitioning index (TS-LS), Int2SW: internode 2 specific weight (g cm⁻¹), Int 3SW: internode 3 specific weight (g cm⁻¹), CHOS_{st}: stem water-soluble carbohydrate of the whole stem (g m⁻²). RUE_{preGF}: radiation-use efficiency pre-grain filling (g MJ⁻¹), GAI: green area index at seven days after anthesis, FIA7: fractional radiation interception at seven days after anthesis, FLAA7: flag-leaf angle at seven days after anthesis (°), FLCA7: flag-leaf curvature (point of inflexion to the tip of the flag-leaf; cm), LLA7: flag-leaf length at seven days after anthesis (cm), LWA7: flag-leaf width at seven days after anthesis (cm). *P < 0.05, **P < 0.01, ***P < 0.001, ‡P < 0.10.

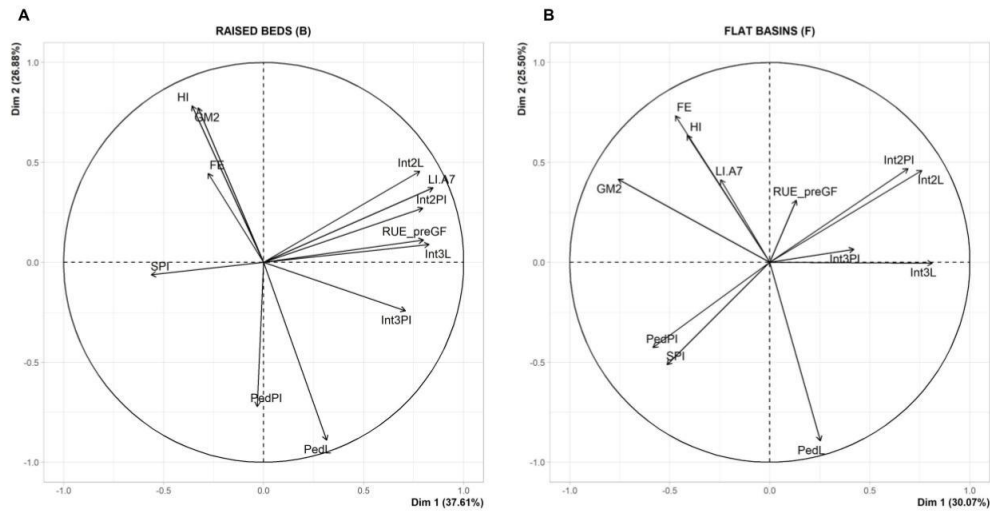


Fig. 4.5. Principal component analyses (PCA) for grain number (GM2), harvest index (HI), fruiting efficiency (FE), and traits measure at seven days after anthesis: spike partitioning index (SPI), peduncle, internode 2 and internode 3 length (PedL, Int2L, Int3L, respectively), internode 2 and 3 true-stem partitioning index, light interception (LI%A7) for 12 CIMMYT spring wheat cultivars during 2018-19 in **A** raised beds and **B** flat basins.

4.4.5 Spike morphological partitioning and correlations with fruiting efficiency and yield components

Genetic variation was found for AwPI ($P < 0.05$) and for GluPI ($P = 0.059$) in 2018 – 19 (**Table 4.6**). Only RaPI and RaSW differed between the planting systems ($P < 0.001$) both being higher in beds. LemPI, PalPI, RaPI and RaSW showed a $PS \times G$ interaction ($P < 0.05$, $P < 0.001$, $P < 0.001$, respectively). A positive association among cultivars was found between awPI and FE in beds ($r = 0.63$, $P < 0.05$) and flats ($r = 0.74$, $P < 0.01$). A negative association was observed between RaPI and GM2 ($P < 0.001$) and FE ($P < 0.10$) in raised beds. GluPI was positively correlated with SPI in raised beds ($r = 0.67$, $P < 0.05$) with a trend for this association also in flat basins ($r = -0.50$, $P = 0.10$). In addition, GluPI was negatively correlated with the amount of spike water-soluble carbohydrates in beds ($r = -0.74$, $P < 0.01$).

Table 4.6. Mean, minimum, maximum, and ANOVA for spike partitioning indices (PI) at seven days after anthesis for 12 CIMMYT spring wheat genotypes in raised beds (B) and flat basins (F) planting systems evaluated in 2018-19 and phenotypic correlations with yield, yield components and physiological traits measured at seven days after anthesis.

Gen	GluPI		AwPI		LemPI		PalPI		RaPI		RaSW	
	B	F	B	F	B	F	B	F	B	F	B	F
Mean	0.21	0.21	0.25	0.28	0.21	0.21	0.12	0.16	0.21	0.13	0.012	0.007
Min	0.18	0.18	0.15	0.21	0.14	0.17	0.10	0.08	0.14	0.10	0.008	0.006
Max	0.27	0.24	0.29	0.35	0.27	0.29	0.14	0.27	0.25	0.17	0.017	0.009
H ²	0.49		0.58		0.00		0.00		0.00		0.00	
G (p value)	<i>0.059</i>		*		ns		ns		ns		ns	
PS (p value)	ns		ns		ns		ns		***		***	
PSxG (p value)	ns		<i>0.071</i>		*		***		***		***	
Corr: (r)												
YLD (g m ⁻²)	-0.23	-0.21	-0.034	-0.39	0.55†	-0.40	0.06	0.55†	-0.52†	-0.05	0.05	0.30
TGW (g)	-0.52†	0.07	-0.19	-0.15	0.28	-0.15	-0.06	0.04	0.31	0.37	0.42	0.46
HI	0.46	0.05	-0.19	-0.00	0.18	-0.001	0.38	0.09	-0.51†	-0.25	-0.32	-0.27
GM2 (g m ⁻²)	0.32	-0.17	0.15	-0.11	0.21	-0.14	0.06	0.31	-0.75**	-0.33	-0.38	-0.18
SPI	0.67*	-0.50†	-0.54†	-0.44	0.14	0.28	0.11	0.31	0.02	-0.24	0.03	-0.13
DM _{spkA7} (g m ⁻²)	0.36	-0.51†	-0.60*	-0.70*	0.43	-0.31	0.23	0.80**	0.15	-0.15	0.05	0.26
FE (g ⁻¹)	-0.01	0.17	0.63*	0.74**	-0.16	-0.07	-0.24	-0.34	-0.51†	-0.24	-0.39	-0.35
CHOS _{spk} (g m ⁻²)	-0.74**	0.23	-0.15	0.70*	0.62*	-0.13	-0.45	0.54†	0.16	-0.18	0.51†	0.07

GluPI: glume partitioning index, AwPI: awn partitioning index, LemPI: lemma partitioning index, PalPI: palea partitioning index, RaPI: rachis partitioning index, RaSW: rachis specific weight (g cm⁻¹), YLD: grain yield, TGW: thousand-grain weight, HI: harvest index, GM2: grains per square meter, SPI: spike partitioning index, DM_{spkA7}: spike dry-matter at seven days after anthesis, FE: fruiting efficiency, CHOS_{spk}: spike water-soluble carbohydrate. *P < 0.05, **P < 0.01, ***P < 0.001, †P < 0.10, *italics*: P < 0.10, ns: not significant.

4.5 Discussion

4.5.1 Optimizing internode traits for spike growth

Higher grain yield, grains per m² and grains per spike were found in the raised beds compared to the conventional flat system, although spikes per m² were lower in beds than flats. Similar results were found by Wang et al. (2011) in wheat crops with a reduction in spikes per m² but an increase in grains per spike, thousand grain weight and grain yield in beds compared to flat basins. The present study did not find a PS × G interaction for HI for the three years (see **Chapter 4.4**), although there was an interaction when just analysing the results in 2017-18 and 2018-19. So the present results for grain partitioning traits averaged over the 2 years need to be interpreted cautiously. The interactions for grain partitioning traits did not in general explain the HI interaction over the 2 years. A positive correlation between GY and HI was found among cultivars in flats and a similar trend was shown in raised beds. A similar correlation was reported by Molero et al. (2019) and Sierra-Gonzalez et al. (2021) in spring wheat germplasm in raised beds at the same site as the present study. PS × G interactions in grain partitioning

traits (SPI, StemPI, LamPI, and DMspkA7) and internode 2 and 3 lengths were found in the present study. These interactions, however, did not associate with the interaction for HI. Furthermore, considering the results for three years, the responses to PS for the cultivars for the grain partitioning traits were likely not explaining the responses for grain yield as there was no PS \times G interaction for HI over the three years.

Several previous studies demonstrated that improving spike growth is an important target for plant breeding programs to increase harvest index under different environments (Fischer, 2011; Slafer et al., 2015). Genetic variation in spike partitioning has been shown to be associated with grain number, HI and grain yield in wheat cultivars in raised (Gaju et al., 2009; Rivera-Amado et al., 2019; Sierra-Gonzalez et al., 2021) or in conventional flat planting systems (Shearman et al., 2005). In the present study no difference in spike partitioning index was found between the raised beds and flat basins. A wide genetic range in spike dry weight was found in both planting systems, but a slightly greater range in flat basins. However, there was only a positive association between spike dry-weight at GS65 + 7 days and grains m⁻² in flat basins. Similar results in wheat genotypes were found by in the studies of Siddique et al. (1989a) and Shearman et al. (2005) reporting a positive association between spike dry weight and grains m⁻² in flat plant systems. No association between SPI and grains m⁻² was found in beds, as in the study on CIMMYT spring wheat cultivars reported by Rivera-Amado et al. (2019). Nevertheless, Sierra-Gonzalez et al. (2021) found a positive correlation between spike dry weight per unit area and GM2 in the CIMMYT spring wheat high biomass association panel (HIBAP I) in raised beds. In the present study, the lack of an association between SPI and spike DM per m² in raised beds was partly explained by a negative correlation between spike DM per m² and FE in raised beds, but no association in flat basins. As mentioned above, there were some differences in the results between the three year and two year analysis; both showed higher grain yield in beds and a PS \times G interaction for YLD. However, the three year analysis showed an interaction for biomass at maturity but not for HI; whereas the analysis across the two years showed an interaction for HI but not for biomass at maturity. Future studies therefore need to be carried out to confirm the present findings for grain partitioning traits.

In a study in CIMMYT spring wheat cultivars with plant heights from 100 to 110 cm, it was suggested that reductions in specific stem-internode lengths with overall small effects on plant height might be a way to increase spike partitioning index and harvest index (Aisawi et al., 2015). Genetic variation of partitioning indices measured at anthesis + 7 days was found in beds and flats with similar ranges to those reported in a field study in a spring wheat DH

population of 150 lines derived from a cross between the CIMMYT spring wheat advanced line LSP2 and UK winter wheat cultivar Rialto in field experiments in NW Mexico (Gaju et al., 2009). Present results showed in beds negative correlations between stem-internode 2 and 3 length and SPI as reported by Rivera et al., 2019 and Sierra-Gonzalez et al. (2021) in beds. Similarly, in flats, stem-internode 2 and 3 length showed negative correlations with SPI. However, no significant associations were found between peduncle length and SPI in either PS, as reported by Sierra-Gonzalez et al. (2021) in the HIBAP I panel in raised beds. In addition, similar genetic ranges in internode partitioning indices were found with the study by Sierra-Gonzalez et al. (2021) that reported values of Int2PI from 0.094 to 0.153 and Int3PI from 0.060 to 0.085. The peduncle stem growth overlaps less temporally with the floret mortality phase from booting to anthesis compared with stem growth of internodes 2 and 3 (Rivera-Amado et al., 2019). This is the first time that a field study evaluated stem partitioning traits in raised beds and flat basins planting systems. Present results showed peduncle and stem-internode 3 lengths and PIs did not differ between PS except for internode 2 length and PI with a small increase in raised beds compared to flat basins. Greater stem-internode 4+ PI was also found in flats compared to beds.

The basal stem internodes are important for lodging resistance (Piñera-Chavez et al., 2016), so present results for stem int4+ PI might indicate lodging risk was increased in beds compared to flats. However, there is reported to be less lodging in beds compared to the conventional flat basin system (Wang et al., 2011). In addition, lodging risk effects of PS may not be due only to the Int4PI effects. For example, the increased row spacing in beds likely results in wider root plate spread and increased root anchorage and lodging resistance (Piñera-Chavez et al., 2016). Another study on wheat cultivars in India reported that the basal internodes were thicker as well as having shorter internode length with an increase of dry matter produced in raised beds compared with flat basins, hence lodging resistance was increased in raised beds (Wang et al., 2005). However, present results for TSPI showed that only internode 2 increased in raised beds compared to flat basins. Int2L and Int3 although they were associated with SPI were not associated with spike dry-matter at anthesis + 7 days. This lack of association might be partly because above-ground biomass at anthesis + 7 days decreased with shorter plants counteracting an effect of decreasing internode lengths to increase SPI. Present results showed internode 2 and 3 length were not related to HI and GM2 among cultivars in beds and flats in contrast to the findings of Sierra-Gonzalez et al. (2021) who reported associations in beds. In beds, Int2L was, however, positively associated with grain yield. However, this

association depended strongly on one genotype KUKRI which had one of the longest internode 2 lengths and high grain yield; amongst the other 11 genotypes there was no significant association. Additionally, negative associations between peduncle length and HI were found in both PS whereas no associations between internode 2 and 3 length and HI were found. This could be partly explained by decreases in stem internode 2 and 3 length decreasing CHOS_{st} whereas decreases in peduncle length had no effect on CHOS_{st}.

4.5.2 FE and its correlation with GM2 and grain yield

Wide genetic variation in FE was found as in previous studies in wheat (Gaju et al., 2009; Gonzalez-Navarro et al., 2016; Rivera-Amado et al., 2019) and FE was higher in raised beds than flat basins by 14.2% ($P < 0.001$). The higher FE in beds might be partly associated with a trade-off between FE and spike DM (Gaju et al., 2009); and a lower spike dry matter at anthesis + 7 days in beds than flat basins. FE showed a PS \times G interaction ($P < 0.05$). In this study the interaction PS \times G for FE was not associated with the interaction for HI. It has been demonstrated that improving FE is a feasible and promising way to enhance grain number (González *et al.*, 2011) and grain yield (Slafer et al., 2015; Gerard et al., 2020), and to maximize genetic gains in grain number it is necessary to increase not only in spike dry-matter at anthesis but also FE (Acreche et al., 2008; Lo Valvo et al., 2018). Effects of PS on FE were discussed previously in **Chapter 2.4**. In the present study correlations between FE and GM2 were stronger than correlations between SPI and GM2 in both PS. Several previous studies reported genetic variation in grain number was more related to FE than dry-matter of spike at anthesis (García et al., 2014; Elía et al., 2016). However, a negative association among genotypes was found in the present study between DM_{spkA7} and FE in raised beds as in the study of Gaju et al. (2009). This trade-off might be associated with restrictions to assimilate supply due to the vascular architecture within the spikelet affecting translocation of assimilate to the distal floral primordia within a spikelet (Wolde and Schnurbusch, 2019). However, some investigations did not find this negative association between FE and spike dry weight (Fischer, 2007). Fischer suggested that FE and spike dry weight are independent traits in which improvements could be additive. In addition, present results showed a negative correlation between peduncle length and FE in flat basins. This trade-off might be due to less competition for grain growth and less grain abortion in the 7-10 days after anthesis with reduced peduncle length. In addition, it could be speculated that more soluble sugars might be available to increase the spike soluble carbohydrate DM when the peduncle length is shorter leading to higher floret survival and FE.

A negative trade-off between TGW and FE was also found in both planting systems. This agreed with several previous investigations in wheat (Gaju et al., 2009; Ferrante et al., 2012). However, González et al. (2014) did not find any significant relation between these two traits. Gaju et al. (2009) reported that wheat genotypes with a higher rachis length per spikelet had a reduced trade-off between FE and TGW possibly due to reduced physical restrictions in spikelets to potential grain weight and/or increased spike photosynthesis. Rivera-Amado et al. (2019) found that a reduced allocation of dry-matter to the rachis per unit length combined with an increased allocation of dry-matter within the spike structural components to the lemma increased FE in CIMMYT spring wheat cultivars in raised beds. In this study, a negative trend between FE and rachis PI was found but only in beds; no associations between FE and lemma PI were found. The negative association with rachis PI might be due to a reduction in rachis structural dry weight but not a reduction in the number and size of the vascular bundles and assimilate transport within the rachis.

It has been suggested that a decreased allocation of assimilate to the awns might be an alternative strategy to increase FE allowing more assimilates to be translocated to support floret growth (Sierra-Gonzalez et al., 2021). Present results did not support this as positive correlations between awns PI and FE were found in beds and flats. A field study in spring wheat genotypes in Australia under irrigated and rainfed conditions also reported that reducing awns led to a decreased grain number (Rebetzke et al., 2016a). López-Castañeda et al. (2014) reported that awned spikes intercepted between 18 and 45% incident radiation during grain filling and Sanchez-Bragado et al. (2014) and (Molero and Reynolds, 2020) demonstrated that spike photosynthesis plays an important role in the carbon assimilation. Another avenue to increase harvest index might be by a reduction of the chaff in relation to unit grain dry matter at physiological maturity (Foulkes et al., 2011). However, no differences in the ratio of chaff DM to grain DM were found between the 12 genotypes in this study. At the metabolic level, it has been reported that the spike cytokinin content has a positive effect on grain number in rice (Ashikari et al., 2005) and wheat (Li et al., 2018) crops, so genetic variation in spike cytokinin content may also be associated with floret fertility and FE. Cytokinins are known to promote mitotic cell division in the shoot (Schaller et al., 2014).

4.5.3 Associations between grain partitioning traits and source traits

When optimizing grain partitioning traits to enhance grain sink strength it is also important to assess the effects on source traits to identify any possible trade-offs on photosynthetic capacity. In the present study, a positive correlation between $CHOS_{st}$ was found

with stem internodes 2 and 3 PI but no association with the peduncle PI in both PS. These correlations were consistent with previous studies in spring wheat CIMMYT genotypes (Ehdaie et al., 2006; Rivera-Amado, 2015; Sierra-Gonzalez et al., 2021) in raised beds. The strongest positive correlation was found between CHOS_{st} and internode 2 true-stem PI in both planting systems. It can be speculated that a stronger correlation for CHOS_{st} with stem internode 2 PI than peduncle PI was due to a higher soluble dry matter allocation per unit length in internode 2. A previous study in spring wheat CIMMYT genotypes in the HIBAP I panel (Sierra-Gonzalez et al., 2021) in raised beds reported a positive association between CHOS_{st} and HI. However, no associations between CHOS_{st} and HI were found in beds and flats in the present study. Additionally, CHOS_{st} was positively related to the internode 4+PI in both PS in this study. Stored assimilates from the stem and leaf sheath can contribute around 20 - 40% of the final grain weight under yield potential conditions (Foulkes et al., 2002; Dreccer et al., 2009). Positive association among genotypes between grain yield and CHOS_{st} was found but only in beds. This might indicate that the irrigated, high radiation environment of the experiments tended to relate to sink limitation rather than source limitation of grain growth but that the grain growth was closer to source limitation in the beds than the flats.

RUE_{preGF} was positively correlated with internode 2 true-stem PI but only in raised beds. Genetic variation in RUE during the pre-anthesis period therefore could have caused differences in Int2TSPI; for example, if RUE differences occurred mainly during the time of stem internode 2 extension and growth. Alternatively, it could be speculated that greater Int2L provided an increased sink size for assimilates pre-anthesis which resulted in an increased RUE through alleviation of feedback effects and upregulation of photosynthesis. Since Int2L showed a small increase in beds compared to flats, this mechanism would be expected to be more evident in raised beds than flat basins. Several investigations in wheat have suggested that RUE improvements could be achieved due to an optimal source - sink balance (Richards, 1996; Calderini et al., 1997; Shearman et al., 2005; Reynolds et al., 2009). Increasing RUE before flowering is another way to improve grain sink strength since more assimilates are available to increase spike mass and grain number due to increased floret survival (Reynolds et al., 2009) (see **Chapter 2**) and more upright leaves were associated with increased RUE in the flat basins (see **Chapter 3**). Present results showed strong correlations between the flag-leaf angle at anthesis + 7 days and internode 3 length in both PS. Thus, the planophile canopies tended to have longer internode 3 compared to the erectophile ones. Additionally, genotypes with longer flag-leaves at anthesis + 7 days had increased peduncle length. Foulkes et al. (2011) suggested

that canopy leaf layers can be compacted due to severe decreases in plant height (< 60 cm) leading to sub-optimal vertical light distribution and reduced RUE. However, it is unlikely the differences in internode 2 length amongst the cultivars were large enough to lead to sub-optimal light interception in compacted canopies in the present study.

Overall, these correlations suggested there may be some trade-offs between source traits and partitioning traits to optimize spike growth and grain number in the 12 genotypes, particularly in raised beds. For example, a decrease in Int3L was associated with an increased SPI favouring sink but reduced RUE_preGF in raised beds. In addition, int2L and int3L were positively associated with stem soluble DM in both raised beds and flats. Encouragingly, reduced int3 length was associated with decreased flag-leaf angle suggesting these two traits could be jointly optimised in flats (but not in beds where less upright leaves may be required to maximize light capture during stem elongation). Therefore, in optimizing grain partitioning traits in wheat breeding programs the likely source-sink balance, according to the both germplasm and environment, should be taken into account in the respective planting systems.

4.6 Implications for plant breeders

In this study, results showed that internode 2 and 3 TS competed more for assimilates with the spike than the peduncle TS, according to the correlations between SPI and internode TSPIs, which agrees with previous studies as mentioned earlier. SPI did not, however, correlate with GM2 and HI likely partly due to the confounding effects of plant height on above-ground biomass among the 12 cultivars. Additionally, positive correlations were found between FE and GM2 as well as trade-off between FE and TGW in both PS although the compensation was not complete. Overall the results demonstrated that FE was the most important component determining genetic variation in GM2 and is a promising trait to increase grain sink strength and yield (Slafer et al., 2015) in plant breeding programs (see **Chapter 2.4**). HI was higher under raised beds than flat basins and genetic variation in grain number was associated with HI in beds. Internode lengths and true-stem partitioning indices showed high heritability in this study. Therefore, these traits could potentially be deployed by plant breeding programs for enhancing harvest index, grain number and hence grain yield.

The grain partitioning traits are relatively easy to measure, however, they are time-consuming measurements and it would be impractical to obtain phenotypic data in breeders' trials with 1000s of genotypes. Therefore, there is a need to develop molecular markers for these traits for marker-assisted selection. No main effect PS effects were found for stem-

internode traits apart from internode 2 length and true-stem internode PI; and these traits only showed a small difference. The PS × G interaction was not significant for PedTSPI and Int3TSPI but there was a significant interaction for Int2TSPI, but again the relative differences in responses among cultivars were small. Therefore, in a plant breeding program stem-internode traits could probably be measured in just one of the two planting systems and results applied to the other. Overall, according to the three-year analysis, grain yield responses to PS were mainly driven by responses of biomass and RUE traits rather than HI and grain partitioning traits. In wheat breeding programs any improvements made in source-strength would not result in improvements in yield if those improvements were not linked to adequate sink-strength. Encouragingly the present study did not show any major negative trade-off of grain sink traits with erect flag-leaves in the flat basins which is the planting system used by the majority of wheat growers worldwide. However, in the raised beds there was trade-off between decreased int2 length and decreased RUE_preGF and between decreased int2 length and more upright leaves in raised beds with less upright leaves being favoured in raised beds for radiation interception. Future studies are required to confirm these results on a wider range of germplasm to identify trait combinations to optimize jointly source and sink traits to raise yield potential in the two planting systems.

4.7 Author contribution

MMP, JF, MR and GM contributed to the conceptualization. MMP, JF, MR and GM contributed to the methodology. MMP contributed to the data analysis. MMP performed the experiments. MAMP, JF, GM and OG contributed to the investigation. MMP and JF contributed to the writing of the original manuscript. MMP, JF, GM, MR, OG and EM contributed to the writing, editing and revising the manuscript. JF and MR contributed to the funding acquisition and project administration. All the authors approved the final version of this manuscript.

4.8 Funding

This work was supported by The National Council of Science and Technology (CONACYT) (CVU 839945), the Sustainable Modernization of Traditional Agriculture (MasAgro) initiative from the Secretariat of Agriculture and Rural Development (SADER) and the International Wheat Yield Partnership Program (IWYP).

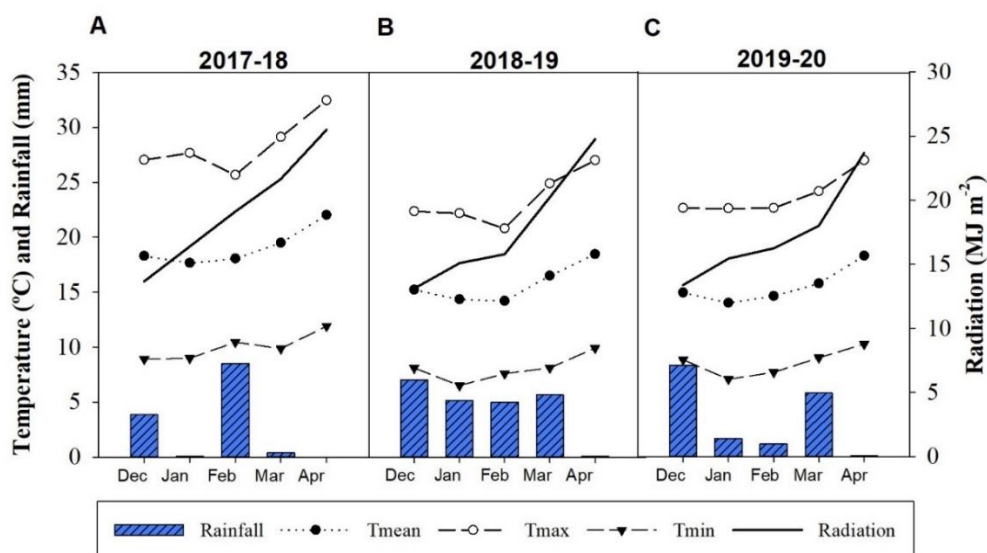
4.9 Acknowledgements

We thank to the physiology team at CIMMYT for their technical support. We also acknowledge Richard Richards for his invaluable support in the genotype selection and Angela Pacheco for her advice in the statistical analysis.

4.10 Supplementary information

Supplementary Table 4.1. List of twelve CIMMYT elite spring bread wheat cultivars and advanced lines in the experiments in 2017-2018, 2018-19 and 2019-20.

	Year of release	Genotype	Canopy architecture
1†	1988	BACANORA T88	erectophile
2†		C80.1/3*QT4118//KAUZ/RAYON/3/2*TRCH/7/CMH79A.955/4/AGA/3/4*SN64/CNO67//INIA66/5/NAC/6/RIALTO	planophile
3†	2008	CHEWINK #1	planophile
4†		SOKOLL//PUB94.15.1.12/WBLL1	planophile
5†		NELOKI	erectophile
6†		W15.92/4/PASTOR//HXL7573/2*BAU/3/WBLL1	planophile
7†		KUKRI	planophile
8†		KUTZ	planophile
9		SOKOLL	planophile
10	2014	BORLAUG100 F2014	planophile
11*		ITP40/AKURI//FRNCLN*2/TECUE #1	erectophile
12*		CHIPAK*2//SUP152/KENYA SUNBIRD	erectophile



Supplementary Fig. 4.1. Environmental conditions in the field experiments (average mean temperature (°C), average minimum temperature (Tmin, °C), average maximum temperature (Tmax, °C), average monthly rainfall (mm) and average monthly radiation (MJ m⁻²) in the field experiments during (A) 2017-18, (B) 2018-19 and (C) 2019-20.

Supplementary Table 4.2. Genetic variation for 12 CIMMYT spring wheat cultivars for yield, yield components and biomass at maturity from the three years combined analysis (2017-18, 2018-19 and 2019-20) in raised beds (B) and flat basins (F).

Gen	YLD		TGW		HI		BMPM		GM2		SM2	
	B	F	B	F	B	F	B	F	B	F	B	F
BACANORA T88	634	591	35.18	35.20	0.50	0.49	1281	1204	18067	16785	335	343
C80.1/3*QT4118	668	565	47.85	46.82	0.44	0.42	1494	1338	13958	12092	255	227
CHEWINK#1	683	610	46.61	45.70	0.47	0.44	1459	1396	14654	13377	277	280
SOKOLL//PUB94	680	592	51.21	50.44	0.44	0.43	1512	1373	13284	11730	263	261
NELOKI	539	525	36.64	37.32	0.45	0.44	1192	1210	14800	14109	379	353
W15.92/4/PASTOR	593	547	51.20	51.57	0.45	0.45	1324	1219	11584	10611	272	254
KUKRI	695	607	44.07	44.63	0.49	0.47	1407	1290	15792	13637	317	306
KUTZ	696	605	47.54	46.66	0.46	0.45	1508	1338	14654	12995	286	241
SOKOLL	638	561	44.91	44.30	0.43	0.44	1503	1277	14251	12662	318	311
BORLAUG100	730	682	47.78	47.71	0.50	0.50	1460	1381	15300	14301	285	283
ITP40/AKURI	741	646	46.16	45.63	0.49	0.48	1505	1371	16029	14158	303	297
CHIPAK*2//	693	693	42.89	41.99	0.50	0.48	1393	1444	16227	16511	299	311
Mean	666	602	45.17	44.83	0.47	0.46	1420	1320	14883	13581	299	289
LSD (G) (5%)	68.239		2.227		0.035		165.653		1659.615		41.868	
CV%	6.79		3.05		4.73		7.55		7.37		8.87	
G (p value)	***		***		***		***		***		***	
PS (p value)	***		<i>0.097</i>		*		***		***		**	
Y (p value)	*		***		***		**		*		***	
PS × G (p value)	*		ns		ns		*		0.184		<i>0.068</i>	

YLD: grain yield (g m⁻²), TGW: thousand grain weight (g), HI: harvest index, BMPM: biomass at physiological maturity (g m⁻²), GM2: grains per m⁻², SM2: spikes per m⁻². *P < 0.05, **P < 0.01, ***P < 0.001, *italics*: P < 0.10, ns: not significant.

Supplementary Table 4.3. Min, Max and average and ANOVA significance levels for RUE during pre grain-filling (RUE_preGF; g MJ⁻¹), flag leaf angle (FLAA7; °), flag-leaf curvature (FLCA7; cm), flag-leaf length (LLA7; cm) and flag-leaf width (LWA7; cm) for 12 CIMMYT spring wheat cultivars. Values represent one-year data (2018 – 19) in raised beds (B) and flat basins (F) planting systems. *P < 0.05, **P < 0.01, ***P < 0.001, *italics*: P < 0.10, ns: not significant.

	RUE_preGF		FLAA7		FLCA7		LLA7		LWA7	
	B	F	B	F	B	F	B	F	B	F
Min	1.51	2.20	35	30	9.35	5.43	21.82	21.49	1.7	1.6
Max	2.77	2.99	101	99	22.31	19.14	34.91	29.32	2.3	2.0
Mean	2.20	2.59	70	67	17.61	12.70	27.61	25.03	1.9	1.8
G (p value)	*		***		***		***		***	
PS (p value)	**		ns		**		0.104		0.071	
PS × G (p value)	*		***		***		*		*	

Supplementary Table 4.4. Min, Max and average and ANOVA significance levels for plants per m⁻², spikes per square meter, internode 2 and 3 specific weight (g cm⁻¹) for 12 CIMMYT spring wheat cultivars. Values represent means across 2018-19 and 2019-20 in raised beds (B) and flat basins (F) planting systems.

	Plants (m ⁻²) ‡		SM2		Int2SW		Int3SW	
	B	F	B	F	B	F	B	F
Min	145	154	252	234	0.011	0.015	0.013	0.014
Max	238	222	373	386	0.023	0.022	0.024	0.024
Mean	178	185	287	303	0.016	0.019	0.018	0.018
G (p value)	**		***		***		***	
PS (p value)	ns		**		***		ns	
Y (p value)	-		***		ns		***	
PS × G (p value)	*		**		***		0.200	

Plants (m⁻²): plants per square meter (m⁻²), SM2: spikes per square meter at physiological maturity (m⁻²), Int2SW: internode 2 specific weight (g cm⁻¹), Int3SW: internode 3 specific weight (g cm⁻¹). ‡Only one year data (2017-18) and 10 genotypes. *P < 0.05, **P < 0.01, ***P < 0.001, ns: not significant.

5 CHAPTER 5. GLASSHOUSE EXPERIMENTS: IDENTIFYING FLAG-LEAF PHOTOSYNTHETIC TRAITS TO ENHANCE RUE, BIOMASS, GRAIN YIELD AND N-USE EFFICIENCY IN SPRING WHEAT CULTIVARS

5.1 Introduction

Wheat is one of the three main staple crops which provides 20% of the global calorie consumption (Shiferaw et al., 2013). Wheat grain contains apart from carbohydrates other important nutrients including proteins, fibre and other minor components such as lipids, vitamins, minerals and phytochemicals (Shewry and Hey, 2015). Since harvest index may be approaching its theoretical maximum of ca. 0.65 in the last years in some regions (Austin et al., 1980) enhancing photosynthetic capacity and biomass is key to improving wheat yields (Song et al., 2016). For example, above-ground biomass has been associated with recent genetic gains in grain yield in CIMMYT spring wheat (Aisawi et al., 2015) (see **Chapter 1.1**). Nevertheless, genetic improvements in HI have still been observed in some regions, e.g. grain yield increases due to an increase of HI of 0.25% per year but without associations with biomass were reported in Argentina (Lo Valvo et al., 2018).

Leaf light-saturated photosynthesis rate (A_{\max}) is considered a key trait for increasing photosynthetic capacity and grain yield (Reynolds et al., 2012a; Man et al., 2015). Free-air CO₂ enrichment (FACE) studies found that there is scope for improvement in RUE due to flag-leaf photosynthesis (Ainsworth and Long, 2020) associated, in turn, with increases in grain yield (Parry et al., 2011). Post-anthesis leaf photosynthesis rate increases may also be due to a result of upregulation by grain sink strength (Richards, 2000). It has been demonstrated that enhancing spike partitioning at GS65 and grains per unit area has increased RUE during grain-filling by upregulation of photosynthesis due to increased sink strength (Reynolds et al., 2005). Qingfeng et al. (2016) concluded in their review that genetic improvements in photosynthesis should be linked to optimized leaf biochemical traits in crops such as leaf chlorophyll and rubisco content as well as parameters linked to stomatal behaviour.

Several studies have been carried out on genetic yield improvements via the maximum leaf CO₂ assimilation rate (Reynolds et al., 2000b). A_{\max} at the leaf level differs depending on the environmental conditions and metabolic processes during the crop cycle (Horton, 2000). Light saturation of the flag leaf occurs during some periods of the day where photoinhibition may take place (Murchie et al., 1999) related to excess solar energy causing damage to the photosystem II (PSII) (Demmig-Adams and Adams Iii, 2003). In addition, it has been

suggested that leaf A_{\max} improvements are observed with leaf N increases, so that there is a positive association between leaf photosynthesis rate and specific leaf N content (SLN; leaf N per unit area) (Peng et al., 1995). In a field study, fifteen wheat genotypes (five landraces, five synthetic-derivatives and five UK modern cultivars) showed a positive association between flag-leaf chlorophyll content and flag-leaf A_{\max} at anthesis (Gaju et al., 2016). The latter study also found a positive association between flag-leaf A_{\max} at anthesis and grain yield.

A decline in leaf A_{\max} , dark respiration and leaf N has been reported with increasing canopy depth in spring and winter wheat in the UK (Townsend et al., 2018). They concluded that a feasible strategy to improve A_{\max} in lower leaves might be through improved light harvesting (according to increasing chlorophyll a:b ratio) and a maintenance of a low leaf respiration and light compensation point. Chlorophyll a:b ratio indicated the dynamic of photoacclimation in that greatest changes occurred in the upper half of the canopy where the biggest proportional changes in light levels occurred (Townsend et al., 2018). An investigation on 18 winter wheat cultivars in China showed an increase in the leaf photosynthesis with year of release; also, grain yield showed a positive relationship with year of release from 1945 to 1995 and with flag leaf area (Jiang et al., 2003). Additionally, a field study of 10 cultivars of rice in the Philippines reported a strong positive association between year of release from 1966 to 1995 and flag-leaf A_{\max} , leaf Rubisco content and leaf stomatal conductance (Hubbart et al., 2007). Therefore, enhancing leaf photosynthesis traits is a feasible way to increase biomass in grain crops.

Canopy architecture traits such as leaf size, shape, angle, number of leaves and tiller density have also been highlighted as targets for raising RUE (Qingfeng et al., 2016); see **chapter 3.1**. For example, upper leaves should be more erect than those at the bottom of the canopy to optimize vertical light distribution. In addition, chlorophyll of lower leaves should be modified for more efficient light capture to maintain light interception (Ort et al., 2010), as mentioned above. A maximum efficiency of canopy photosynthesis is reached by an improved canopy architecture due to an optimized distribution of light among the canopy leaf layers (Long et al., 2006).

Up to 75% of the reduced N in grain crops is located in the chloroplast of mesophyll cells, mainly as Rubisco (Evans and Seemann, 1989). As defined by Moll et al. (1982) NUE is the grain dry matter yield per unit of N available (from the soil and/or fertilizer) and is divided into two components: N-uptake efficiency (above-ground N uptake/N available; NU_{PE}) and N-utilization efficiency (grain dry matter yield/above-ground N uptake; NU_{TE}). Improvements in NU_{TE} can be due to increasing the rate of photosynthesis for a given concentration of leaf N

(Foulkes et al., 2009). Nitrogen fertilizer represents a high cost for the farmer but may also have negative environmental impacts such as nitrate leaching and N_2O (a greenhouse gas) release from denitrification by soil bacteria (Foulkes and Murchie, 2011c). Therefore, it is important to increase RUE without commensurate increases in N fertilizer requirements by improving canopy photosynthesis per unit N. Two glasshouse experiments were carried out, one in each of two years (2018 and 2019) at University of Nottingham, UK investigating eight CIMMYT spring wheat genotypes. The objectives of this chapter are to quantify genetic variation in flag-leaf A_{max} and stomatal conductance in a set of eight spring wheat CIMMYT cultivars in glasshouse experiments and quantify relations with: i) flag-leaf chlorophyll content, biomass and grain yield in the same glasshouse experiments and ii) genetic variation in radiation-use efficiency, canopy architecture traits, N-use efficiency, biomass and grain yield and their components in the same set of cultivars in the field experiments at CENEB, Mexico.

The specific hypotheses examined are:

- There is a variation in flag-leaf photosynthetic traits among the eight spring wheat genotypes in the glasshouse experiments.
- Genetic variation in flag-leaf photosynthetic rate (A_{max}) is associated with biomass and yield per plant in the glasshouse experiments.
- Genetic variation in flag-leaf A_{max} measured in the glasshouse is associated with RUE measured in the field experiments.
- There is genetic variation for nitrogen-use efficiency (NUE) and its components (NUpE and NUtE) in the subset of eight spring wheat CIMMYT cultivars in the field experiments.
- Genetic variation for flag-leaf A_{max} in glasshouse experiments is correlated with NUpE and NUtE in the field experiments.

5.2 Materials and methods

Two glasshouse experiments were carried out, one in each of two years (2018 and 2019) at Sutton Bonington, University of Nottingham, UK campus. The seeds were sown in a modular tray containing John Innes No. 2 soil medium in a controlled-environment room at 20°C. The sowing dates were 12 July 2018 and 1 July 2019. Approximately 2 weeks after sowing the plants were transferred from the CE room to the glasshouse and transplanted into 2 L pots (one per pot). Each experiment used a completely randomised block design with three replicates testing eight spring wheat CIMMYT cultivars or advanced lines. The genotypes were selected based on contrasting RUE, biomass and canopy architecture genetic variation from the HiBAP I (High Biomass Association Panel I) from CIMMYT based on previous data sets (**Table 5.1**, (Molero et al., 2019)). The genotype names are abbreviated in graphs, tables and text but the full names are provided in **Table 5.1**. The eight genotypes are selected based on representative full range in canopy architecture traits from within the set of 12 genotypes grown in the field experiments reported on in **Chapters 2 - 4**. The soil medium was John Innes No. 2 compost. The experiments were kept well watered using a drip irrigation system supplied with complete nutrient solution.. Herbicides, fungicides and pesticides were applied as necessary in order to minimize the effects of weeds, diseases and pests (see **Appendix Table 2** for details). Average, minimum and maximum air temperature was measured using a Tin-tag temperature data logger (Tinytag Ultra 2 - TGU - 4500, Gemini data loggers) (**Fig. 5.1**). No supplementary lighting was used.

Table 5.1. List of eight CIMMYT elite spring bread wheat cultivars and advanced lines used in the glasshouse experiments.

	Year of release	Genotype	Architecture
1	1988	BACANORA T88	erectophile
2		C80.1/3*QT4118//KAUZ/RAYON/3/2*TRCH/7/CMH79A.955/4/ AGA/3/4*SN64/CNO67//INIA66/5/NAC/6/RIALTO	planophile
3	2008	CHEWINK #1	planophile
4		SOKOLL//PUB94.15.1.12/WBLL1	planophile
5		NELOKI	erectophile
6		W15.92/4/PASTOR//HXL7573/2*BAU/3/WBLL1	planophile
7		KUKRI	planophile
8		KUTZ	planophile

5.2.1 Plant measurements

5.2.1.1 Phenology and growth analysis

Dates of reaching initiation of booting (GS41), heading (GS55), anthesis (GS65) and physiological maturity (GS87) were recorded (Zadoks et al., 1974) according to the main shoot. In both glasshouse experiments, at physiological maturity, plants were sampled by cutting at ground level to estimate grain yield, above-ground biomass, harvest index and yield components including grain number per plant and grain weight. The number of fertile (those with a spike) and infertile shoots per plant was counted. The plant was separated into stem and leaf sheath, spike and leaf-lamina for each of the: i) main shoot and ii) other fertile shoots and dry-weights recorded separately for each component after drying for 48 h at 80°C. The total dry weight was recorded for the infertile shoots (those without a spike) after drying for 48 h at 80°C. Plant height was recorded at physiological maturity from the ground level to the tip of the spike for the main shoot using a ruler (without considering the awns).



Figure 5.1. Glasshouse experiment at Sutton Bonington Campus in 2018.

5.2.1.2 Flag-leaf photosynthesis and stomatal conductance

Gas-exchange photosynthesis was measured for each plant on the flag leaf of the main shoot using a LI-COR 6400 XT Portable Photosynthesis System (Li-Cor Biosciences, NE, USA) in the glasshouse in 2018 and 2019 (**Fig. 5.2**). Light-saturated photosynthetic rate (A_{max}) and stomatal conductance (g_s) were measured on the flag-leaf. One measurement per flag leaf in each of four replicates was taken at initiation of booting (GS41) and anthesis (GS65) between 10.00 and 14.00. The genotypes were measured on different calendar dates depending on the date of each plant reaching the stage at GSS41 and GS65. The settings for the cuvette used a

flow rate of $400 \mu\text{mol s}^{-1}$, block temperature of 25°C and light intensity of $1800 \mu\text{mol m}^{-2} \text{s}^{-1}$ photosynthetically active radiation (PAR). Relative humidity (RH %) was set between 50 and 70% (aiming for 55%).



Figure 5.2. Measurements with LI-COR 6400 XT Portable Photosynthesis System in glasshouse experiment.

5.2.1.3 Flag-leaf chlorophyll content

In the glasshouse experiments in 2018 and 2019, flag-leaf relative chlorophyll content of the main shoot was measured using a hand-held SPAD meter (SPAD 502 Minolta, Japan) at initiation of booting (GS41) and anthesis (GS65) taking three readings per leaf (middle part of the leaf). The genotypes were measured on different calendar dates depending on the date of each plant reaching the stage at GSS41 and GS65.

5.2.1.4 Radiation-use efficiency and canopy architecture traits

Radiation-use efficiency (RUE) in the field experiments was measured in each plot as the increment in the above-ground dry matter divided by the increment in intercepted photosynthetically active radiation (PAR) for the relevant phase (Monteith and Moss, 1977) in 2018-19 and 2019-20 as described in **Chapter 2.3.2.3**. Canopy architecture traits in the field experiments were measured as described in **Chapter 3.3.2.4**.

5.2.1.5 Nitrogen-use efficiency (NUE), NUE components, NHI and flag-leaf N content

In the field experiments at CIMMYT, CENEB, NW Mexico in 2017 – 18 and 2018 – 19, flag-leaf samples at anthesis + 7 days and grain and straw at physiological maturity were milled to analyse N content. The plant N% at 100% DM was determined using the Dumas method using a FP828: elemental analyser by combustion (LECO Corporation, USA). Soil N% analysis was carried out at Colegio de Postgraduados, Campus Montecillo, Estado de Mexico, Mexico for the NUE calculations, using the Kjeldahl method. Nitrogen-use efficiency and its components (N-uptake efficiency and N-utilization efficiency) (as described by Moll et al. (1982)) and nitrogen harvest index (NHI) were calculated according to Equation. 5.1-5.4 below:

$$\text{NUE} = \text{Grain Yield DM (Kg ha}^{-1}\text{)} / \text{Available N (Kg ha}^{-1}\text{)} \quad (5.1)$$

$$\text{NUE}_{\text{P}} (\text{nitrogen-uptake efficiency}) = \text{AGN}_{\text{H}} (\text{Kg ha}^{-1}\text{)} / \text{available N (Kg ha}^{-1}\text{)} \quad (5.2)$$

$$\text{NUE}_{\text{T}} (\text{nitrogen-utilization efficiency}) = \text{Grain Yield DM (Kg ha}^{-1}\text{)} / \text{AGN}_{\text{H}} (\text{Kg ha}^{-1}\text{)} \quad (5.3)$$

$$\text{NHI} = \text{grain N (Kg ha}^{-1}\text{)} / (\text{AGN}_{\text{H}} (\text{Kg ha}^{-1}\text{)}) \quad (5.4)$$

Where available N is the soil N plus the fertilizer N and AGN_{H} is the above-ground N at harvest.

5.2.2 Statistical analysis

In the glasshouse experiments, adjusted means for grain yield, yield components and physiological traits were calculated using a general linear model (GLM) ANOVA procedure from META R 6.04 (Alvarado et al., 2020). Replications and years were considered as random effects, and genotypes as fixed effects. A covariate for anthesis date was used as a fixed effect and was included when significant. Phenotypic correlations between traits were Pearson's correlation coefficient calculated using either the two-year genotype means. Linear regression analysis was applied to two-year genotype means for selected traits. Broad sense heritability (H^2) was calculated using across the two years, using equation (5.5):

$$H^2 = \frac{\sigma_g^2}{\sigma_g^2 + \frac{\sigma_{gy}^2}{y} + \frac{\sigma_{gs}^2}{s} + \frac{(\sigma_{gy})(s)}{ys} + \frac{\sigma_e^2}{rys}} \quad (5.5)$$

where σ^2 = error variance, σ_g^2 = genotypic variance, σ_{gy}^2 = G × Y variance, σ_{gs}^2 = PS variance, s = number of PS, y = number of years, σ_e^2 = residual variance, r = number of replicates. In the field experiment, the statistical analysis was as described in **Chapter 2.3.3**.

5.3 Results

5.3.1 Growing conditions in glasshouse experiments

In the glasshouse during 2018, the average daily mean temperature was 19.2°C whereas in 2019 it was 22.3°C (**Fig. 5.3**). The average daily mean temperature pre-anthesis in the two years was 15.9°C whereas during the post-anthesis period it was 14.7°C.

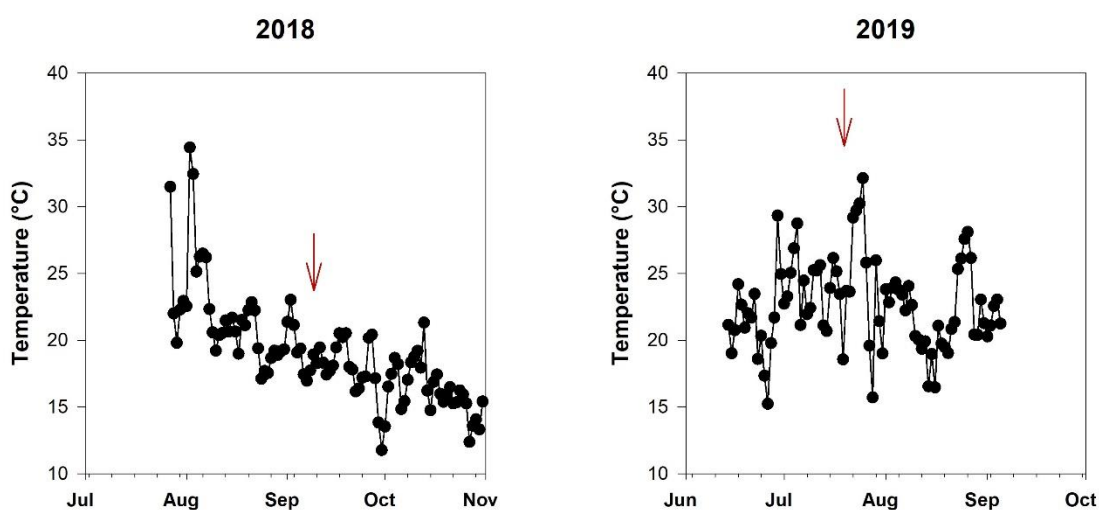


Fig. 5.3. Daily mean (average minimum and maximum) temperature (°C) in the glasshouse experiments in a) 2018 and b) 2019. Arrows indicate anthesis date.

5.3.2 Developmental stages and plant height

The eight spring CIMMYT cultivars showed genetic variation in the sequential development stages ($P < 0.05$ - $P < 0.001$) except for physiological maturity, and similarly according to thermal time after emergence ($P < 0.05$ - $P < 0.001$) (**Table 5.2**). Averaging across years, at GS65, days after emergence (DAE) varied among genotypes from 45 to 53 and at GS87 from 82 to 87. Plant height at physiological maturity ranged from 90 cm (BACANORA T88) to 115.9 cm (KUTZ) ($P < 0.001$).

Table 5.2. Ranges for phenology expressed in days after emergence (DAE) and thermal time after emergence (TT) (base temp. 0°C) and plant height for 8 CIMMYT spring wheat genotypes. Values represent means across 2018 and 2019.

Genotype	DTInB (DAE)	DTH (DAE)	DTA (DAE)	DAE.PM (DAE)	TTInB (°Cd)	TTH (°Cd)	TTA (°Cd)	TTPM (°Cd)	HeightPM (cm)
BACANORA T88	40	49	53	84	669	848	931	1551	90.0
C80.1/3*QT4118	40	47	53	85	660	807	925	1562	123.2
CHEWINK#1	36	43	49	87	588	743	871	1617	114.2
SOKOLL//PUB94	38	44	48	85	612	760	832	1559	115.5
NELOKI	33	42	45	84	520	704	774	1530	97.4
W15.92/4/PASTOR	34	42	46	84	547	710	792	1537	109.8
KUKRI	34	41	45	82	533	675	766	1506	112.5
KUTZ	39	47	51	84	645	798	880	1551	115.9
Mean	37	44	49	84	597	755	847	1552	109.81
H ²	0.74	0.77	0.63	0.00	0.80	0.81	0.65	0.00	0.97
LSD (5%)	4.859	4.775	6.575	7.464	88.613	86.740	130.428	142.405	5.86
CV (%)	3.50	3.11	2.80	1.42	4.58	4.58	4.03	1.27	2.97
p value:									
Gen	**	***	*	ns	***	***	*	ns	***
Year	***	***	***	***	***	***	***	**	**
Gen × Year	***	***	***	***	***	***	***	***	ns

DTInB (DAE): days to initiation of booting (GS41), DTH (DAE): days to heading (GS55), DTA (DAE): days to anthesis (GS65), DTPM (DAE): days to physiological maturity (GS87), TTInB: thermal time at initiation of booting, TTH: thermal time at heading, TTA: thermal time at anthesis (GS65), TT: thermal time, HeightPM: plant height at physiological maturity (cm). *P < 0.05, **P < 0.01, ***P < 0.001, *italics*: P < 0.10, ns: not significant.

5.3.3 Harvest measurements in glasshouse experiments

Grain yield per plant and HI did not show genetic variation. However, a Genotype × Year interaction was found in each case (P < 0.001) (**Table 5.3**). Above-ground biomass at physiological maturity ranged from 20.6 to 30.3 g plant⁻¹ among the eight cultivars (P < 0.001) and there was a Gen × Year interaction (P < 0.05). Grains ear⁻¹ for the main shoot varied from 42 to 51 (P < 0.01), but the G × Y interaction was not significant. Grains plant⁻¹ ranged from 258 to 332 (P < 0.001) with a Gen × Year interaction (P < 0.001). The grain weight for the main shoot ranged from 1.62 to 2.58 mg among cultivars (P < 0.001), but the Genotype × Year interaction was not significant. Thousand-grain weight ranged from 32.6 to 47.3 g (P < 0.05) with a Gen × Year interaction (P < 0.01).

Table 5.3. Grain yield, yield components and above-ground biomass at maturity from the combined analysis; values represent means across 2018 and 2019.

Genotype	YLD (g plant)	HI	BM (g plant)	GN.MS #	GN.T #	GW.MS (mg spike)	GW.T (mg plant)	TGW g	Spikes (per plant)‡
BACANORA T88	10.09	0.49	20.58	46	311	1.96	10.09	32.62	9
C80.1/3*QT4118	12.60	0.42	30.28	48	323	2.48	12.60	39.31	8
CHEWINK#1	10.13	0.43	23.64	42	258	1.61	10.13	40.51	8
SOKOLL//PUB94	11.94	0.50	23.88	47	313	2.58	11.94	38.81	8
NELOKI	11.57	0.48	24.28	46	312	2.28	11.57	37.42	7
W15.92/4/PASTOR	11.30	0.44	26.17	51	332	2.15	11.30	34.62	9
KUKRI	11.12	0.46	24.19	47	318	1.62	11.12	35.32	8
KUTZ	12.40	0.43	28.62	42	262	1.93	12.40	47.34	7
Mean	11.39	0.46	25.20	46	303	2.08	11.39	38.24	8
H ²	0.11	0.00	0.77	0.74	0.80	0.93	0.11	0.55	0.00
LSD	2.96	0.108	4.895	5.148	41.294	0.329	2.962	10.179	1.747
CV (%)	7.46	7.46	9.26	6.66	11.651	12.72	7.46	11.77	15.15
p value:									
Gen	ns	ns	***	**	***	***	ns	*	ns
Year	ns	ns	ns	0.112	ns	ns	ns	ns	-
Gen × Year	***	***	*	0.190	***	ns	***	**	-

YLD: grain yield, HI: harvest index, BM: above-ground biomass at physiological maturity, GN.MS: grain number per main shoot, GN.T: grain number per plant, GW.MS: grain weight per main shoot, GW.T: grain weight per plant, TGW: thousand-grain weight, Shoots: number of spikes per plant. *P < 0.05, **P < 0.01, ***P < 0.001, *italics*: P < 0.10, ns: not significant. ‡ One year data (2018). §Low heritability, calculation failed to optimize.

5.3.4 Flag-leaf photosynthesis rate and stomatal conductance

Readings for flag-leaf photosynthesis were carried out at initiation of booting (GS41) and anthesis (GS65) for the eight cultivars (**Table 5.4**). Flag-leaf light-saturated photosynthesis rate at GS41 showed a strong trend for genotype differences (P = 0.053) with a range from 29.4 to 33.7 $\mu\text{mol m}^{-2}\text{s}^{-1}$ and a Gen × Year interaction (P < 0.05). Flag-leaf stomatal conductance (g_s) at GS41 did not showed a significant genotype difference but it showed a Gen × Year interaction (P < 0.01). Flag-leaf A_{max} at GS65 varied from 29.5 to 34.0 $\mu\text{mol m}^{-2}\text{s}^{-1}$ (P < 0.01). Genotypes did not differ significantly in flag-leaf g_s at GS65. No Gen × Year interaction was found at GS65 for either A_{max} or g_s .

Table 5.4. Flag-leaf photosynthesis and stomatal conductance (g_s ; $\text{mol m}^{-2} \text{s}^{-1}$) for eight spring wheat CIMMYT cultivars. Values represent means across 2018 and 2019 across 2018 and 2019.

Genotype	GS41		GS65	
	A_{\max} $\mu\text{mol m}^{-2} \text{s}^{-1}$	g_s $\text{mol m}^{-2} \text{s}^{-1}$	A_{\max} $\mu\text{mol m}^{-2} \text{s}^{-1}$	g_s $\text{mol m}^{-2} \text{s}^{-1}$
BACANORA T88	29.7	0.415	31.2	0.522
C80.1/3*QT4118	34.2	0.513	33.8	0.549
CHEWINK#1	33.7	0.597	34.0	0.572
SOKOLL//PUB94	31.5	0.472	33.9	0.582
NELOKI	29.4	0.489	29.5	0.534
W15.92/4/PASTOR	31.5	0.598	32.0	0.525
KUKRI	32.5	0.564	32.4	0.592
KUTZ	32.3	0.497	32.9	0.577
Mean	31.9	0.518	34.0	0.557
H^2	0.55	0.12	0.73	0.23
LSD	3.83	0.20	2.79	0.08
CV (%)	4.60	14.33	4.94	7.76
p value:				
Gen	<i>0.053</i>	ns	**	ns
Year	0.155	ns	ns	ns
Gen \times Year	*	**	ns	ns

A_{\max} ; light-saturated net CO_2 assimilation rate ($\mu\text{mol m}^{-2} \text{s}^{-1}$) and stomatal conductance (g_s ; $\text{mol m}^{-2} \text{s}^{-1}$). * $P < 0.05$, ** $P < 0.01$, *** $P < 0.001$, italics: $P < 0.10$, ns: not significant.

5.3.5 Correlations between grain yield, yield components and physiological traits in glasshouse experiments

Phenotypic correlations among genotypes between grain yield, yield components, plant height and flag-leaf photosynthesis traits are shown in **Table 5.5**. A strong positive correlation between grain yield plant^{-1} and biomass plant^{-1} was found ($r = 0.84$, $P < 0.01$), but there was no correlation with HI. There was a trend for positive correlations between grain yield per plant and main-shoot grain weight ($r = 0.63$, $P = 0.09$) and plant height ($r = 0.65$, $P = 0.08$). There was a strong correlation between flag-leaf A_{\max} at GS41 and GS61. No correlations between flag-leaf photosynthesis traits and grain yield per plant or per main shoot were found. A negative correlation was found between biomass plant^{-1} and harvest index ($r = -0.76$, $P < 0.05$) and flag-leaf A_{\max} at GS41 ($r = -0.79$, $P < 0.05$). In addition, biomass plant^{-1} was positively correlated with individual grain weight per plant ($r = 0.84$, $P < 0.01$) and plant height ($r = 0.77$, $P < 0.05$). Flag-leaf SPAD at initiation of booting showed a weak positive association with grain yield plant^{-1} ($r = 0.64$, $P = 0.09$). No associations between spikes per plant with yield,

yield components and flag-leaf photosynthesis were found in 2018. TGW and spikes plant⁻¹ was negatively correlated ($r = 0.77$, $P < 0.05$).

5.3.6 RUE, NUE, NUE components and flag-leaf N% in field experiments

There was wide significant genetic variation for RUE calculated for the different phenophases in 2018-19 and 2019-20 in raised beds (B) and flat basins (F) ($P < 0.01 - 0.001$) (see **Chapter 2.3.3**). Only RUE_InBA7 and RUET showed a PS effect ($P < 0.05$). In addition, all the RUEs showed a PS \times G interaction except for RUE_InBA7 ($P < 0.05 - 0.01$). Nitrogen-related traits showed genetic variation for the main effect of genotype ($P < 0.001$) except for flag-leaf N concentration at anthesis + 7 days (N%FL) (**Table 5.6**). There was a PS effect on NUE with higher NUE in beds than flats ($P < 0.05$) as well for NU_TE ($P < 0.001$). However, NU_PE was higher in flats than beds ($P < 0.001$). A Gen \times Year interaction was found for the grain N percentage (N%Grain) ($P < 0.01$), NUE ($P = 0.056$), NU_TE ($P < 0.05$) and nitrogen harvest index ($P < 0.001$). NU_PE did not show genetic variation or a Gen \times Year interaction.

A positive correlation between NUE and RUE pre grain-filling (RUE_preGF) was found in beds ($r = 0.74$, $P < 0.05$) and flats ($r = 0.82$, $P < 0.05$) (**Table 5.7**). In addition, there was a strong positive association between NUE and RUE from initiation of booting to anthesis + 7 days ($r = 0.87$, $P < 0.01$). RUE_preGF was also strongly correlated with NU_TE ($r = 0.78$, $P < 0.08$) in beds but there was no correlation in flats. A positive correlation was found between NU_TE and RUE during grain-filling (RUE_GF) in flats ($r = 0.76$, $P < 0.05$) and NHI was strongly correlated with NU_PE in beds ($r = 0.84$, $P < 0.01$) and flats ($r = 0.76$, $P < 0.05$).

Table 5.5. Phenotypic correlations between grain yield, yield components and physiological traits for eight spring wheat CIMMYT cultivars in glasshouse experiments. Values based on means across 2018 and 2019.

	1	2	3	4	5	6	7	8	9	10	11	12	13	14	15
1.YLD	-														
2.HI	-0.30	-													
3.BM	0.84**	-0.76*	-												
4.GN.MS	0.16	0.03	0.13	-											
5. GN.T	0.17	0.30	-0.02	0.93***	-										
6.GW.MS	0.63†	0.24	0.32	0.48	0.52	-									
7.GW.T	1.00	-0.30	0.84**	0.16	0.17	0.63†	-								
8. TGW	0.55	-0.47	0.60	-0.66†	-0.73*	-0.01	0.55								
9.HeightPM	0.65†	-0.67†	0.77*	-0.08	-0.21	-0.00	0.65†	0.65†	-						
10. A _{max} GS41	0.26	-0.79*	0.61	-0.12	-0.31	-0.17	0.26	0.45	0.68†	-					
11.gs.GS41	-0.10	-0.66†	0.27	0.16	-0.11	-0.42	-0.10	0.07	0.61	0.57	-				
12.A _{max} GS65	0.21	-0.44	0.36	-0.15	-0.32	0.01	0.21	0.42	0.46	0.85**	0.31	-			
13.gs.GS65	0.22	-0.11	0.15	-0.48	-0.43	-0.28	0.22	0.52	0.60	0.53	0.24	0.61	-		
14.SPAD.InB	0.64†	-0.36	0.63†	0.51	0.38	0.22	0.64†	0.15	0.52	0.16	0.26	0.09	0.08	-	
15.Shoots‡	-0.16	0.46	-0.46	0.57	0.45	0.06	-0.16	-0.77*	-0.61	-0.26	0.13	0.16	-0.22	0.16	-

YLD: grain yield per plant (g), HI: harvest index, BM: above-ground biomass at physiological maturity (g), GN.MS: grain number per main shoot, GN.T: grain number per plant, GW.MS: grain weight per main shoot (g), GW.T: grain weight per plant (g), TGW: thousand-grain weight (g), HeightPM: plant height at physiological maturity (cm), A_{max}: light-saturated net CO₂ assimilation rate (μmol m⁻² s⁻¹) and stomatal conductance (gs; mol m⁻² s⁻¹), SPAD.InB: SPAD at initiation of booting, Shoots: number of spikes per plant. *P < 0.05, **P < 0.01, ***P < 0.001, †P < 0.10, ns: not significant.

Table 5.6. N-use efficiency (NUE), NUE components and flag-leaf and grain N% for eight spring wheat CIMMYT cultivars across 2017-18 and 2018-19 in beds (B) and flat basins (F) in the field experiments at CIMMYT, Sonora, Mexico.

Genotype	N%Grain		NUE		NU _p E		NU _T E		NHI		N%FL‡	
	B	F	B	F	B	F	B	F	B	F	B	F
BACANORA T88	2.25	2.22	22.22	22.73	0.88	0.76	23.59	29.43	0.60	0.64	3.50	4.57
C80.1/3*QT4118	2.36	2.22	21.13	23.94	0.85	0.82	23.13	28.67	0.62	0.64	4.04	4.15
CHEWINK#1	2.29	2.25	23.05	23.66	0.97	0.89	22.10	27.43	0.57	0.61	4.10	4.68
SOKOLL//PUB94	2.31	2.27	21.67	24.28	0.98	0.90	20.29	26.83	0.56	0.62	4.06	4.54
NELOKI	2.46	2.41	19.73	19.27	0.94	0.79	19.65	24.12	0.54	0.60	4.00	4.58
W15.92/4/PASTOR	2.32	2.34	20.04	20.23	0.92	0.82	20.72	24.17	0.54	0.55	4.48	4.65
KUKRI	2.32	2.20	22.38	24.87	0.89	0.80	23.53	30.64	0.61	0.66	4.00	4.20
KUTZ	2.42	2.20	22.16	24.70	0.91	0.92	22.59	26.41	0.62	0.62	4.18	4.44
Mean	2.27	2.34	22.96	21.55	0.84	0.92	27.21	21.95	0.62	0.58	4.05	4.48
H ²	0.66		0.94		0.19		0.29		0.38		0.14	
LSD	0.14		2.23		0.102		2.088		0.039		0.55	
CV (%)	3.78		6.14		7.14		5.19		3.98		6.73	
p value:												
Gen	***		***		***		***		***		ns	
Year	***		<i>0.062</i>		***		ns		**		-	
PS	***		*		***		***		***		*	
Gen × PS	*		*		<i>0.073</i>		**		*		ns	

N%Grain: percentage of nitrogen in the grain, NUE: nitrogen-use efficiency, NU_pE: nitrogen-uptake efficiency, NU_TE: nitrogen-utilization efficiency, NHI: nitrogen harvest index, N%FL: percentage of nitrogen in the flag-leaf at anthesis + 7 days (GS65 + 7 days). *P < 0.05, **P < 0.01, ***P < 0.001, *italics*: < 0.10, ns: not significant. ‡One year data (2018-19).

5.3.7 Correlations between flag-leaf A_{max} and g_s in the glasshouse experiments and grain yield, yield components, NUE and NUE components and canopy architecture traits in the field experiments

A positive association was found between genetic variation in flag-leaf A_{max} at GS65 in the glasshouse experiments and biomass at physiological maturity in the field experiments in beds (r = 0.93, P < 0.001) and flats (r = 0.76, P < 0.01) (**Table 5.8**). NUE was positively related to flag-leaf A_{max} at anthesis (r = 0.76, P > 0.05) and to flag-leaf g_s at GS65 (r = 0.78, P < 0.05). In addition, flag-leaf A_{max} at anthesis showed a correlation with RUE_{GF} (r = 0.75, P < 0.05) and RUET (r = 0.91, P < 0.01) in the beds. Grain yield in raised beds was positively associated with flag-leaf A_{max} (r = 0.76, P < 0.05) and g_s (r = 0.78, P < 0.05) at anthesis + 7 days. With regard to canopy architecture traits measured in the field experiments, flag-leaf A_{max} at GS65 was negatively correlated with flag-leaf curvature at GS65 + 7 days (FLCA7) in flat basins (r = -0.79, P < 0.05).

Table 5.7. Phenotypic correlations among eight spring wheat cultivars between nitrogen-related traits and radiation-use efficiencies measured in raised beds (B) and flat basins (F) (*italics*) the field experiment in 2018-19.

	<i>1</i>	<i>2</i>	<i>3</i>	<i>4</i>	<i>5</i>	<i>6</i>	<i>7</i>	<i>8</i>	<i>9</i>	<i>10</i>
1.N%FL	-	<i>-0.18</i>	<i>0.02</i>	<i>0.60</i>	<i>-0.60</i>	<i>-0.76*</i>	<i>-0.29</i>	<i>0.74*</i>	<i>-0.43</i>	<i>0.28</i>
2.N%Grain	0.17	-	<i>-0.87**</i>	<i>-0.31</i>	<i>-0.47</i>	<i>0.16</i>	<i>-0.72*</i>	<i>-0.35</i>	<i>-0.70†</i>	<i>-0.78*</i>
3.NUE	<i>-0.19</i>	<i>-0.53</i>	-	<i>0.40</i>	<i>0.48</i>	<i>-0.07</i>	<i>0.87**</i>	<i>0.15</i>	<i>0.82*</i>	<i>0.55</i>
4.NU _T E	0.33	<i>-0.58</i>	0.60	-	<i>-0.61</i>	<i>-0.89**</i>	<i>0.32</i>	<i>0.76*</i>	<i>-0.04</i>	<i>0.60</i>
5.NU _P E	<i>-0.58</i>	<i>-0.11</i>	0.66†	<i>-0.20</i>	-	<i>0.79*</i>	<i>0.46</i>	<i>-0.59</i>	<i>0.76*</i>	<i>-0.07</i>
6. NHI	<i>-0.52</i>	<i>-0.34</i>	0.68†	<i>-0.02</i>	<i>0.84**</i>	-	<i>0.03</i>	<i>-0.90**</i>	<i>0.37</i>	<i>-0.60</i>
7.RUE_InBA7	<i>-0.22</i>	0.02	<i>-0.02</i>	<i>-0.08</i>	0.05	<i>-0.28</i>	-	<i>-0.06</i>	<i>0.90**</i>	<i>0.57</i>
8.RUE_GF	<i>-0.17</i>	0.13	0.35	0.09	0.35	<i>-0.05</i>	<i>0.80*</i>	-	<i>-0.35</i>	<i>0.68*</i>
9.RUE_preGF	0.37	<i>-0.53</i>	<i>0.74*</i>	<i>0.78*</i>	0.18	0.17	0.20	0.37	-	0.35
10. RUET	0.19	<i>-0.15</i>	0.60	0.60	0.34	0.16	0.42	<i>0.75*</i>	<i>0.84**</i>	-

N%Grain: percentage of nitrogen in the grain, N%FL: percentage of nitrogen in the flag-leaf at anthesis + 7 days (GS65 + 7 days), NUE: nitrogen-use efficiency, NU_TE: nitrogen-utilization efficiency, NU_PE: nitrogen-uptake efficiency, NHI: nitrogen harvest index, RUE_InBA7: radiation-use efficiency calculated from initiation of booting to GS65 + 7 days (g MJ⁻¹), RUE_GF: radiation-use efficiency calculated during grain filling, from GS65 + 7 days to physiological maturity (g MJ⁻¹), RUE_preGF: radiation-use efficiency calculated from emergence + 40 days to GS65 + 7 days (g MJ⁻¹), RUET: radiation-use efficiency total, from emergence + 40 days to physiological maturity (g MJ⁻¹). *P < 0.05, **P < 0.01, ***P < 0.001, †P < 0.10.

Table 5.8. Phenotypic correlations among 8 spring wheat cultivars between flag-leaf photosynthesis rate (A_{\max}) and stomatal conductance (g_s) in glasshouse experiments (mean 2018 and 2019) and nitrogen-related traits (mean 2017 – 18 and 2018- 19), radiation-use efficiencies and flag-leaf relative chlorophyll content (mean 2018-19 and 2019- 20), grain yield and yield components (mean 2017-18 and 2018-19) in the field experiments in raised beds and flat basins.

RAISED BEDS (B)				
	A_{\max} GS41	g_s .GS41	A_{\max} GS65	g_s .GS65
N% grain	-0.54	0.12	-0.61	-0.52
NUE	0.62†	-0.05	0.76*	0.78*
NU _p E	0.49	0.21	0.21	0.62
NU _t E	0.34	-0.17	-0.17	0.39
NHI	0.24	-0.41	0.24	0.49
RUE_InBA7	-0.23	-0.29	0.23	-0.16
RUE_GF	0.48	0.53	0.60	0.37
RUE_preGF	0.50	-0.07	0.75*	0.61
RUET	0.65†	0.26	0.91**	0.63†
SPAD.GS41	0.16	0.26	0.09	0.08
SPAD.GS65	0.39	0.46	0.43	0.19
Height.PM	0.68†	0.61	0.46	0.60
GY	0.62†	-0.05	0.76*	0.78*
BM	0.73*	0.10	0.93***	0.73*
N%FL‡	0.41	0.75*	0.28	0.16
FLAA7	0.24	0.38	0.11	0.50
FLCA7	0.23	0.05	0.24	-0.47
FLAT BASINS (F)				
	A_{\max} GS41	g_s .GS41	A_{\max} GS65	g_s .GS65
N% grain	-0.13	-0.06	-0.39	-0.00
NUE	0.44	0.01	-0.58	0.61
NU _p E	-0.15	0.21	0.09	0.28
NU _t E	0.41	-0.09	0.29	0.19
NHI	0.47	-0.22	0.37	0.38
RUE_InBA7‡	0.19	0.14	0.19	0.59
RUE_GF‡	-0.33	-0.38	0.09	-0.36
RUE_preGF‡	0.04	-0.13	0.23	0.56
RUET‡	0.17	-0.00	0.59	0.42
SPAD.GS41	0.16	0.26	0.09	0.08
SPAD.GS65	0.39	0.46	0.43	0.19
Height.PM	0.68†	0.61	0.46	0.60
GY	0.44	0.01	0.58	0.61
BM	0.70†	0.24	0.76*	0.66
N%FL‡	-0.61	0.19	-0.94	0.13
FLAA7	0.59	0.14	0.46	0.04
FLCA7	-0.80*	0.01	-0.79*	-0.02

Glasshouse: A_{\max} GS41: flag-leaf photosynthesis at initiation of booting ($\mu\text{mol m}^{-2} \text{s}^{-1}$), g_s .GS41: stomatal conductance at initiation of booting ($\text{mol m}^{-2} \text{s}^{-1}$), A_{\max} GS65: flag-leaf photosynthesis at anthesis ($\mu\text{mol m}^{-2} \text{s}^{-1}$), g_s .GS65: stomatal conductance at anthesis ($\text{mol m}^{-2} \text{s}^{-1}$), SPAD.GS41: SPAD at initiation of booting, SPAD.GS65: SPAD at anthesis, Height.PM: plant height at physiological maturity. Fields: N% Grain: percentage of nitrogen in the grain, NUE: nitrogen-use efficiency, NU_pE: nitrogen-uptake efficiency, NU_tE: nitrogen-utilization efficiency, NHI: nitrogen harvest index, N%FL: percentage of nitrogen in the flag-leaf at anthesis + 7 days (GS65 + 7 days), RUE_InBA7: radiation-use efficiency from initiation of booting to anthesis + 7 days (g MJ^{-1}), RUE_GF: radiation-use efficiency during grain-filling period (g MJ^{-1}), RUE_preGF: radiation-use efficiency during pre grain-filling period (g MJ^{-1}), RUET: radiation-use efficiency total from emergence + 40 days to physiological maturity (g MJ^{-1}), GY: grain yield (g m^{-2}), BM: biomass at physiological maturity (g m^{-2}), N%FL: nitrogen concentration on the flag-leaf at anthesis + 7 days, FLAA7: flag-leaf angle at anthesis + 7 days, FLCA7: flag-leaf curvature at anthesis + 7 days. * $P < 0.05$, ** $P < 0.01$, *** $P < 0.001$, ns: not significant. †: one-year data (2018-19).

5.4 Discussion

5.4.1 Flag-leaf photosynthesis traits

The study of physiological traits related to photosynthesis provides a way to improve biomass in wheat and other crops (McAusland et al., 2020). Present results showed a strong positive correlation between genetic variation in flag-leaf A_{\max} at anthesis in the glasshouse experiments and biomass per unit area at physiological maturity in the field experiments in both the raised beds and flat basins planting systems. Flag-leaf A_{\max} at GS41 was also correlated with biomass at physiological maturity in beds and a trend was found in flats. Some previous studies in wheat have found correlations between genetic variation in flag-leaf photosynthesis pre- and post-anthesis and grain yield in field experiments under rain-fed conditions in the UK (Gaju et al., 2016; Carmo-Silva et al., 2017). However, Driever et al. (2014) did not find a relation between leaf photosynthesis rate measured pre-anthesis and grain yield in 64 wheat cultivars in the UK. Gaju et al. (2016) suggested that higher post-anthesis A_{\max} might be due to a source-sink interaction with the upregulation of A_{\max} by increased grain sink size. In the present study the association between A_{\max} at GS65 and biomass was observed in both planting systems; and since the measurement of A_{\max} was at the very start of the grain filling phase the genetic variation was unlikely to be related to upregulation by grain sink strength. Indeed, no significant association between grain number per main shoot and A_{\max} was found. From the present results, it can be speculated that the genetic variation pre-anthesis flag-leaf A_{\max} measured in the glasshouse was representative of A_{\max} expression in the field experiments. Similar heritabilities of flag-leaf A_{\max} and stomatal conductance measured at anthesis were found in the glasshouse experiment ($H^2 = 0.23 - 0.73$) compared to other studies in a range of 0.31 to 0.76 (Carmo-Silva et al., 2017; Silva-Pérez et al., 2019).

Plant height at physiological maturity had a weak positive correlation with genetic variation in flag-leaf A_{\max} at GS41 in the glasshouse experiment across the two years. Additionally, flag-leaf chlorophyll content at initiation of booting was weakly correlated with grain yield, above-ground biomass and grain weight. No associations between anthesis flag-leaf A_{\max} and chlorophyll content were found in the present study. However, other studies in wheat reported a positive correlation (Austin et al., 1982; Gaju et al., 2016). Leaf photosynthetic rate is an important trait to enhance biomass through improving radiation-use efficiency in cereal crops (Parry et al., 2011). In this study, positive associations between flag-leaf A_{\max} at anthesis (measured in the glasshouse) and

RUE_{GF} and RUE_T (measured in the field) were found but only in beds. It is speculated that this might be because the glasshouse conditions are more similar to beds than flats since plants in beds can intercept more light among the leaf layers due to the larger row spacings and the gaps between the beds. Wheat genotypes with erectophile leaves allow a more optimal light distribution among the canopy leaf layers increasing the canopy photosynthetic CO₂ uptake rate (Long et al., 2006). A strong negative association was found between flag-leaf A_{max} at anthesis and flag-leaf curvature at anthesis + 7 days in the field experiments. The cultivars with flag-leaves with a shorter distance from the point of inflexion to the tip of the leaf (more floppy leaves) had higher A_{max}. A possible mechanism for higher A_{max} in floppy leaves might be that these leaves had higher SPAD or higher SLN. However, this study did not find any correlation between flag-leaf SPAD measured in the glasshouse and flag-leaf curvature measured in the field.

In the present study, no trade-offs between flag-leaf size at initiation of booting or anthesis and A_{max} were found. Previously a study on diploid and hexaploid wheat found that leaf morphology traits such as leaf width and area showed a negative association with photosynthetic rate per unit area (Austin et al., 1982). A study in rice showed that genetic variation of leaf Rubisco content in leaves was positively associated with flag-leaf A_{max} (Hubbart et al., 2007). However, Rubisco traits were not measured in the present study. The present results showed genetic variation in flag-leaf A_{max} was independent of leaf angle and that there is therefore scope to jointly optimize these two traits to enhance RUE and grain yield in wheat crops. Additionally, plant breeders should aim to combine these traits with increased grain sink strength to maximize the radiation conversion efficiency and increase grain yield.

5.4.2 Nitrogen traits and correlation with flag-leaf photosynthetic traits and RUE

Leaf nitrogen is an important trait affecting photosynthetic capacity since around half of the nitrogen in leaves in C3 crops is associated with photosynthesis and 20% with Rubisco (Evans and Clarke, 2019). It has been suggested that one strategy to increase NU_TE is to decrease specific leaf nitrogen (SLN) while maintaining leaf A_{max} (Foulkes et al., 2009). Alternatively, Reynolds et al. (2000b) demonstrated that increasing SLN above values of 2.3 g m⁻² seems to be beneficial for NU_TE since the leaves have a better performance under low light saturation in the canopy. This may depend on the level of SLN; the breakpoint at which SLN reaches the plateau for RUE

is about 2 g N m⁻² (Pask et al., 2012c). Therefore, decreasing SLN from 3 to 2 g N m⁻² could increase NU_TE, but decreasing from 2 to 1 g N m⁻² would likely decrease NU_TE (Pask et al., 2012c). Reynolds et al. (2000b) concluded that generally selection for higher leaf photosynthesis at saturating light intensities (A_{\max}) had not resulted in improved RUE, and this could be because leaves at the bottom of the canopy are not light saturated. In this study, nitrogen concentration on the flag-leaf at anthesis + 7 days was not associated with A_{\max} or NU_TE in beds and flats.

In the field experiments, genetic variation in NUE was weakly correlated with NU_PE in raised beds but there was no association in flats. No correlations were found between NUE and NU_TE either in beds and flats; or between NU_TE and NHI or N% grain. NUE was slightly higher in beds than flats and this was due to higher NU_TE in beds than flats; NU_PE was lower in beds compared to flats. Some studies in wheat showed that thinner roots improve N capture since root systems with thinner roots (i.e. greater specific root length; length per unit dry weight) have a larger surface area (Carvalho and Foulkes, 2012). It could be speculated that plants in flats have thicker roots compared to beds. Other root traits affecting N supply that may potentially be associated with variation in NU_PE are rooting depth and root longevity (Foulkes et al., 2009). Differences in NU_PE, however, could be also caused by differences in above-ground biomass demand for N rather than N supply (below ground) effects, which may be more likely than effects of root traits under high N availability conditions. Previous studies in Mexico and Finland found genetic variation in NUE was explained approximately equally by NU_TE and NU_PE under high N conditions (Ortiz-Monasterio et al., 1997; Muurinen et al., 2006). Gaju et al. (2016) reported a strong negative correlation in wheat genotypes between NU_TE and N% grain under low and high N conditions whereas no significant associations were found in this study. However, genetic variation in grain N% (2.25 - 2.46% in beds and 2.20 - 2.41% in flats) in the present study was less than in previous study of (Gaju et al., 2016).

In this study, genetic variation in NUE was strongly positively associated with RUE_{InBA7} and RUE_{preGF} but only in flats. In addition, NU_TE was strongly positively correlated with RUE_{preGF} in both PS. RUE is an important trait for NUE improvements in grain crops, particularly in the context of improvements in canopy photosynthesis per unit N. However, there have been few previous investigations showing association between genetic variation in leaf or canopy N traits and RUE. In

this study, RUE_{preGF} was strongly positively correlated with NUE in both PS and was also positively correlated with NU_TE. Flag leaf N% was positively related with RUE during the grain filling period but only in flats. This correlation might indicate that N remobilization to grains was greater in flats than beds leading to poorer maintenance of RUE during the latter stages of grain filling for genotypes with low flag-leaf N% at GS65. However, future work is required to test this.

Flag-leaf traits measured in the glasshouse experiments were linked to important yield-related traits measured in the field experiments including biomass. However, biomass per plant in the glasshouse and biomass per unit area in the field were not correlated among cultivars in the present study. One reason for this lack of correlation might be that genetic variation in tillering was expressed very differently in the field compared to the glasshouse as well as other effects of the different shoot population densities. Flag-leaf traits are useful for line selection since they may be evaluated relatively easily and there is evidence they scale to whole crop effects at harvest. For example, Blake et al. (2007) found that lines with prolonged flag-leaf greenness after spike emergence led to an improvement in grain yield, grain number and grain weight in spring wheat varieties. High-throughput phenotyping of flag-leaf A_{max} is not yet feasible for large numbers of breeding plots; therefore, there is a need for the development of high-throughput measurements, e.g. through hyperspectral reflectance measurements (Robles-Zazueta et al., 2021), for deployment in breeding programs.

5.5 Conclusion

This study showed a wide genetic variation in above-ground biomass per plant at physiological maturity and yield components in the glasshouse experiments. Among the eight spring wheat CIMMYT cultivars, variation in the flag-leaf photosynthetic traits was found. A strong association was found between biomass at physiological maturity in raised beds in the field experiments and flag-leaf A_{\max} at anthesis + 7 days measured in the glasshouse. In addition, grain yield in raised beds showed a positive association with A_{\max} measured in the glasshouse. Furthermore, strong and positive correlations were found between NUE and NU_{TE} and RUE measured at different phenophases in both PS. Flag-leaf A_{\max} was not associated with NU_{TE} , so these results suggested that A_{\max} was not increasing canopy photosynthesis per unit N. Therefore, further work on Rubisco traits might be needed to increase canopy photosynthesis per unit N and NU_{TE} . Higher RUE_{preGF} increased NU_{TE} among genotypes in both PS, so further investigations are required to identify which leaf and traits in addition to canopy architecture traits were increasing RUE_{preGF} and hence NU_{TE} in the CIMMYT spring wheat cultivars.

Encouragingly there were no trade-offs between flag-leaf A_{\max} and favourable canopy architecture traits for increasing RUE. It is concluded that to raise RUE in addition to optimized canopy architecture traits wheat breeders should consider selection for enhanced flag-leaf photosynthetic rate. However, this will be require high-throughput methods for phenotyping genotypes for A_{\max} in the plant breeding programs. One possible strategy might be remote sensing through hyperspectral reflectance data combined with modelling in order to predict leaf gas-exchange traits (Robles-Zazueta et al., 2021). Bread-making wheat cultivars require high protein content and an appropriate levels of N are needed to achieve this (Foulkes et al., 2009). In some cultivars NU_{TE} may be associated with higher RUE but low grain nitrogen concentration. Therefore, plant breeders also need to consider the end-use classification when selecting physiological leaf and canopy photosynthesis traits for increasing NU_{TE} .

6 GENERAL DISCUSSION

6.1 Review of hypotheses

The discussion examines the effects of canopy architecture traits on RUE and grain yield in twelve spring wheat CIMMYT cultivars in raised beds and flat basins planting systems in NW Mexico. In this thesis a novel methodology to quantify canopy architecture traits in wheat was applied since previous research focused more on a visual score to identify cultivar differences in canopy architecture relating to erect and floppy leaves. Presently more detailed quantitative measurements were taken in the twelve spring wheat CIMMYT cultivars considering separately the angle and curvature of the flag leaf in addition to other traits, e.g. leaf length and leaf width.

Hypothesis 1 as in **Chapter 1** stated “*There are differences in grain yield, yield components and biomass through the season between planting systems*”. Grain yield averaged across the 3 years was higher in raised beds than flat basins by 10.6%. Differences in yield components between the two planting systems were also found in the present study: harvest index, grain number, grains per spike, being higher in beds than flats. However, TGW did not show significant difference between the two PS. Biomass was higher in flats at emergence + 40 days and initiation of booting; but then flat basins had a greater biomass at physiological maturity. Therefore hypothesis 1 was supported except for the trait TGW. Results in previous investigations are also consistent with the present results (Ram et al., 2005; Tripathi et al., 2005; Zhang et al., 2007; Zaman et al., 2017a).

Hypothesis 2 stated that “*There are differences in RUE calculated at different phenophases between beds and flats and a PS × G interaction.*” RUE for different phenophases differed between beds and flats and showed a PS × G interaction. RUE showed PS differences from initiation of booting to anthesis + 7 days with higher values in beds, whereas RUE during the grain filling period did not show a PS effect. PS × G interactions were found for all of the phenophases except for RUE_InBA7. Therefore, hypothesis 2 was supported.

The results in **Chapter 3** confirmed the hypothesis 3 which stated: “*Genotypes with more prostrate flag-leaves increase light interception pre-anthesis (by capturing light in the gaps between the beds) in the raised beds but not in the flat basins*”. Genetic variation of flag-leaf angle and curvature was found in the present study as well as PS × G interaction. Genotypes with more erect flag-leaves increased RUE more in the flat basins. Conversely

genotypes with more prostrate flag leaves at GS41 showed better light capture in beds from booting to anthesis + 7 days (likely better light capture in the gaps between the beds). Genotypes with more erect canopies performed relatively better in flat basins in terms of grain yield. These results supported hypothesis 3. These effects of canopy architecture traits may be the reason why most of the spring wheat cultivars from CIMMYT which are selected in the raised-bed planting system still have floppy leaves compared to other wheat breeding programs. In addition, plant height was associated with PS \times G for grain yield and biomass at physiological maturity, with taller lines having relatively higher biomass at physiological maturity and grain yield under raised beds than flat basins associated with better light capture

The hypothesis 4 “*Genotypes with more erect flag-leaves allow a better vertical distribution of light among the canopy leaf layers and increase RUE in both planting systems, but relatively more in the flat basins than raised beds*” was partially confirmed in the results presented in chapter 3. The genotypes with more erect flag leaves showed a negative association with RUE during grain filling in the flat basins but not in the raised beds. Therefore this hypothesis was partially supported.

A new methodology was implemented in this study to measure flag-leaf curvature by measuring the flag-leaf using a ruler from the point of inflexion to the tip of the leaf. Genetic variation was shown in both PS at anthesis. In chapter 4, the results supported hypothesis 5 “*Flag-leaf curvature affects the genetic variation of RUE and LI% in raised beds and flat basins*”. Flag-leaf curvature at anthesis + 7 days affected the genetic variation of RUE calculated during the grain-filling period in flat basins but not in raised beds. In addition, an association between flag-leaf curvature at GS41 and IPARacc from GS41 to GS65 + 7 days was found in raised beds. Therefore the hypothesis was supported.

Partitioning traits were analysed in both planting systems in 2017-18 and 2018-19. The hypothesis 6 “*Raised beds have higher spike partitioning index than flat basins associated with reduced above-ground biomass accumulation during early stem extension but similar biomass accumulation during later stem extension than flat basins with relatively more assimilates to be partitioned into the spike*” was confirmed in the results presented in chapter 5. PS did not show a significant effect on spike partitioning index, leaf-lamina and stem partitioning index. The hypothesis was not supported by the results in **Chapter 4**.

The hypothesis 7 stated “*Spike partitioning index is negatively related to the stem-internode lengths 2 and 3 but there is no association with the peduncle in both PS*”. Results

in chapter 5 showed a negative association between SPI and stem-internode 2 and 3 length with no significant associations with peduncle length. This can be explained since the extension of the peduncle occurs before and after anthesis which overlaps less with the rapid spike growth period pre-anthesis than for internode 2 and 3. The hypothesis 7 was therefore confirmed. The findings of a study in spring wheat cultivars in NW of Mexico were consistent with the present results (Rivera-Amado et al., 2019).

These results in **Chapter 4** did not support the hypothesis 8 that “*A reduction in stem-internode 2 and 3 lengths allows a greater spike dry-matter per unit area at GS65 + 7 days in both PS*”. Results in chapter 5 did not show a significant correlation between internode lengths and spike dry-matter at GS65 + 7 days in beds or flats. Hypothesis 8 was not supported in this study.

Hypothesis 9 stated “*Genetic variation in flag-leaf A_{max} measured in the glasshouse is associated with RUE measured in the field*”. Eight spring wheat cultivars were tested in the glasshouse experiments which showed genetic variation in flag-leaf A_{max} at initiation of booting and anthesis. Genetic variation at anthesis was positively associated with RUE_preGF measured in the field experiment. Therefore the results in **Chapter 5** supported hypothesis 9.

6.2 Ideal crop ideotype in raised bed and flat basin planting systems

This section discusses the ideal crop ideotype for optimized canopy architecture for light interception and radiation-use efficiency, combined with optimized dry matter partitioning among the plant organs to raise HI and grain yield in wheat plants in raised beds and flat basins. A previous investigation proposed an ideal canopy structure - a “smart canopy”- related to more prostrate leaves from the top to the bottom of the canopy (Ort et al., 2015). More upright leaves in the upper canopy allow an improved canopy photosynthetic efficiency (Long et al., 2006; Zhu et al., 2010; Ort et al., 2015).

The genetic variation in flag-leaf angle and curvature although statistically significant was relatively small in some cases in the two PS. However, these trait ranges were large enough to have a meaningful impact on RUE. To prove this, some calculations were made to quantify the yield improvement in g m^{-2} (data not shown) from the least to most favourable trait expression with the range. For example, assuming canopies with contrasting flag-leaf angles from 90° to 30° at A7, the linear regression of FLA on RUE_GF in flat basins showed

an increase in RUE_GF from 0.96 to 1.68 g MJ⁻¹. Then applying the average value of PAR interception in flats for A7-PM of 293 MJ m⁻² in both cases; the corresponding grain yields (from current photosynthesis) would be 283.8 g m⁻² at 90° and 496.2 g m⁻² at 30°. So the yield benefit of the most upright versus the least upright leaf angle within the range is 212 g m⁻². Therefore, the benefits of using erect canopies in flats can be seen. Similarly, for canopies with most contrasting leaf curvature at anthesis + 7 days in flat basis (6 vs 17 cm), RUE showed an increase from 1.45 to 0.45 g MJ⁻¹. Then applying the average value of PAR interception in flats for A7-PM of 293 MJ m⁻² in both cases; the corresponding grain yields (from current photosynthesis) would be of 293.63 g m⁻² was found. In addition, canopies with flag-leaf angles from 3 to 8° at initiation of booting did not showed a yield benefit (from current photosynthesis). Therefore, it is suggested that plant breeders should consider the measurements taken at anthesis +7 days rather than initiation of booting for future studies.

The crop ideotype maximizing grain yield differed in the two planting systems. In raised beds, cultivars with higher SPAD value in leaf 3 increased RUE_preGF. In addition, greater flag-leaf angle at initiation of booting (less upright leaves) showed a positive association with radiation interception pre-anthesis, explaining the fact that cultivars with floppy leaves tended to yield relatively better in raised beds than flats. Less upright leaves were associated with greater radiation interception pre-anthesis. RUE_InBA7 seemed to favour HI. Additionally, RUE_preGF, RUET, CGR_preGF and biomass at GS65 + 7 days were positively correlated with grain yield. Furthermore, cultivars with higher FE in beds showed increases in GM2. Plant height partly explained the PS × G interaction for grain yield. In flat basins, cultivars with more erect leaves increased RUE_GF. In addition, greater flag-leaf curvature (a higher distance between the point of inflexion and the tip of the leaf) increased RUE_InBA7 and RUE_GF. These results confirm the importance of canopy architecture traits on light-use optimization among the cultivars. However, these associations were found only in flats which might indicate that the canopy in this system is more compacted than raised beds due to narrower row-gaps and therefore leaves arrangements become a crucial factor for light capture. These results for flag-leaf traits should be confirmed in other genotypes and environments for increased confidence. As in raised beds, SPAD value in leaf 3 showed a positive correlation with RUE_preGF. In addition, cultivars with higher values of RUE_InBA7 and RUE_preGF showed higher biomass and GY in flats. Additionally, HI and GM2 showed positive associations with grain yield. As in beds, BMA7

and BMPM showed a positive association with grain yield and FE was positively associated with GM2 in flats.

In the study of López-Castañeda et al. (2014), RUEs in raised beds and flat basins were measured for similar stages as the present study in one season. In that study, RUE_InBA7 (from initiation of booting to anthesis + 7 days) and RUET (from emergence + 40 days to physiological maturity) were higher in flat basins than raised beds which differed with present results. However, RUE_GF (grain-filling period; from anthesis + 7 days to physiological maturity) did not show a significant difference between PS as in the present study. Grain yield, grain number, biomass at physiological maturity were higher in flats basins than raised beds in the study of López-Castañeda et al. (2014). Notwithstanding, this present findings for higher grain yield, yield components and final biomass in raised beds than flat basins agree with many other studies evaluated in other locations. The study of López-Castañeda et al. (2014) did not, however, report canopy-architecture traits.

With regard to partitioning traits, SPI at GS65 + 7 days showed genetic variation and, in both PS, a negative association with StemPI confirming previous findings in spring wheat (Rivera-Amado et al., 2019). A study in winter wheat on a flat PS demonstrated that spike growth might be affected by competition from infertile tillers (Berry et al., 2003). However, dry matter partitioning in infertile tillers was not quantified in the present study. To increase SPI whilst broadly maintaining plant height present results showed one alternative might be decreasing stem-internode 2 and 3 but not peduncle length. However, these modifications should be made cautiously since reductions in plant height might affect the light interception, RUE and above-ground biomass. The study of Sierra-Gonzalez et al. (2021) showed similar results to the present study. In both studies, it was demonstrated that decreasing stem-internode 2 and 3 length increased SPI. In addition, positive associations between FE and grains per m² in both PS were found. However, the present study is the first study which reported RUE and canopy architecture traits in both PS and their relation to grain partitioning traits.

Other differences between previous studies and the present study were found. For example, a study in spring wheat in Australia in flat basins demonstrated that less upright leaves have lower RUE (Richards et al., 2019). However, even though the present study found evidence of the benefits of erect leaves on RUE in flats, the results showed, associations in raised beds between higher flag-leaf angle at initiation of booting and higher

RUET and a trend with higher RUE_preGF. The latter investigation (Richards et al., 2019) used the same visual score to estimate canopy architecture as in the present study and a similar protocol to evaluate grain yield and yield components. However, these positive associations were found in a large trial of ~1000 lines with very contrasting canopy architecture. The present study is the first to use a quantitative protocol to measure the genetic variation in leaf angle and curvature separately in wheat.

Table 6.1. Traits that contribute to the ideal crop ideotype in raised beds (B) in the twelve spring CIMMYT wheat cultivars.

Trait	Genetic variation	Reasons	Trade-off	References
FLAInB (°)	3-9	Increased fractional light interception at GS41	-	Richards et al. (2019)
RUE_preGF (g MJ ⁻¹)	1.81-2.81	Increased biomass at GS65 + 7 days	-	(Molero et al., 2019; Robles-Zazueta et al., 2021)
RUE_GF (g MJ ⁻¹)	1.10-1.93	Increased biomass at physiological maturity	-	(Molero et al., 2019; Robles-Zazueta et al., 2021)
FE (grains g ⁻¹)	44.78-72.40	Positive correlation with grain number per m ²	TGW, spike DM at GS65+7days	(Gaju et al., 2009; Ferrante et al., 2012; Slafer et al., 2015; Elía et al., 2016; Terrile et al., 2017)
HeightPM (cm)	90.1-121.3	Taller plants increase interception and RUE more in beds compared to flats	-	-
Int2L, Int3L (cm)	15.06-24.02/9.55-15.27	Negative correlation with SPI; more assimilates to the spike	BMPM	(Rivera-Amado et al., 2019; Sierra-Gonzalez et al., 2021)

FLAA7: flag-leaf angle, FLCA7 flag-leaf curvature, RUE_preGF: radiation-use efficiency during pre-grain filling, RUE_GF: radiation-use efficiency during grain-filling, FE: fruiting efficiency, HeightPM: plant height at physiological maturity, Int2L, Int3L: internode 2 and 3 length.

Table 6.2. Traits that contribute to the ideal crop ideotype in flat basins (F) in the twelve spring CIMMYT wheat cultivars.

Trait	Genetic range	Reasons	Trade-off	References
FLAA7 (°)	28 -98	More erect leaves allow a greater light distribution to lower leaves and reduces light saturation of the flag-leaf increasing RUE	RUE_GF	Richards et al. (2019)
FLCA7 (cm)	5.82-18.52	Greater distance between the point of inflexion of the leaf and the tip allows a greater penetration of light and increased RUE	RUE_InBA7, RUE_GF	(Song et al., 2013); similar protocol used to measure leaf-curvature in rice
HI	0.42- 0.50	GY increased through HI	-	(Sierra-Gonzalez et al., 2021)
RUE_preGF (g MJ ⁻¹)	2.12- 2.80	Increases of biomass at anthesis + 7 days in raised beds and flats	-	(Molero et al., 2019; Robles-Zazueta et al., 2021)
RUE_GF (g MJ ⁻¹)	0.67-1.95	Increases of biomass at physiological maturity in beds and flats	-	(Molero et al., 2019; Robles-Zazueta et al., 2021)
FE (grains g ⁻¹)	40.43-72.74	Higher FE associated with increased GM2	TGW	(Gaju et al., 2009; Ferrante et al., 2012; Slafer et al., 2015; Elía et al., 2016; Terrile et al., 2017)
Int2L, Int3L (cm)	13.55-23.26 / 10.00-13.48	Negative correlation with SPI; more assimilates to the spike	BMPM	(Rivera-Amado et al., 2019; Sierra-Gonzalez et al., 2021)

FLAA7: flag-leaf angle, FLCA7 flag-leaf curvature, HI: harvest index, RUE_preGF: radiation-use efficiency during pre-grain filling, RUE_GF: radiation-use efficiency during grain-filling, FE: fruiting efficiency, Int2L, Int3L: internode 2 and 3 length.

6.3 Implications for plant breeders

Grain yield is the most important phenotypic trait for plant breeders (Reynolds et al., 2020). To be deployed by plant breeders selection traits for yield require: i) genetic variation and high heritability, ii) high correlation with grain yield and iii) availability of high-throughput screens (Gaju, 2007). Most of the canopy architecture traits, RUE and grain partitioning traits in this study showed genetic variation. High heritability (H^2) was found for grain yield (0.90), yield components (0.73 - 0.97), flag-leaf angle (0.47 - 0.97), flag-leaf curvature (0.53 - 0.80) and RUE calculated at different phenophases (0.42 - 0.82). However, some H^2 values for RUE were inconsistent such as RUE_GF (0.09). RUE showed strong and positive associations with grain yield, biomass and other yield components.

It was necessary to use destructive and/or time-consuming methods to measure RUE, canopy architecture traits such as flag-leaf angle, curvature, leaf size in the field experiments. It required ~ 40 person-hours to measure flag-leaf angle, flag-leaf curvature, flag-leaf length and width at one developmental stage in 100 plots. In addition, to measure stem-internode lengths in ~100 plots required ~30 person-hours. To measure true-stem and leaf-sheath partitioning indices was also very time-consuming taking ~ 90 person-hours for 100 plots. Therefore, when 1,000s of breeding lines are tested, it is necessary to use other more feasible, alternatives by deploying new high-throughput tools and technology. Flag-leaf angle and flag-leaf curvature cannot be scored visually reliably and other methods are required to evaluate these traits. High-throughput phenotyping (HTP) allows breeding programs to investigate potentially thousands of genotypes in different environments deploying non-destructive methodologies (Araus and Cairns, 2014). For canopy architecture traits, analyzing 2D visible light image sequence using a graph base approach is a method that could potentially allow measurement of flag-leaf angle for a large number of plants in a short time with or without manual intervention (Das Choudhury et al., 2018). To measure RUE in a certain phenophase requires collecting biomass samples and measuring light interception at least two stages of the plant cycle which is time consuming and requires larger plot areas. In addition, in plant breeding programs there are not enough seeds for larger plots in early generations. The use of HTP such as imaging systems and unmanned aerial vehicles (UAVs) using powerful cameras will potentially reduce labour requirements in the field and laboratory for plant breeding programs (Araus and Cairns, 2014; Araus et al., 2018; Reynolds et al., 2020). For example, a recent study in the NW of Mexico, measured RUE in

spring wheat cultivars using a combination of remote sensing techniques using hyperspectral reflectance to calculate vegetation indices (VIs) and partial least squares regression (PLSR) to develop statistical models (Robles-Zazueta et al., 2021). The use of UAVs with sensors combined with ground-truth data from hand-held sensors can be used to establish calibrations to measure certain traits for line selection, e.g. infrared thermometers for measuring canopy temperature indicative of canopy photosynthesis (Reynolds et al., 2020). Additionally, in plant breeding programs, the use of marker-assisted selection (MAS) may allow a more efficient selection by tagging novel alleles and genes for physiological traits (Collard et al., 2005; Xu and Crouch, 2008; Molero et al., 2019). In a recent study in spring wheat in Mexico, SNP markers for grain yield, biomass at physiological maturity and RUE were identified on chromosomes 5A and 7A and for HI on chromosomes 2B and 6A (Molero et al., 2019).

The present study found significant PS effects for RUE, biomass and grain yield, and PS x genotype interactions as well. Therefore, plant breeders should make selections for specific PS, i.e. select positive traits for raised beds, but perhaps different traits that provide increased RUE and biomass on flats basins. At the physiology department at CIMMYT, Mexico, to identify good advanced lines in raised beds Prof Matthew Reynolds (Head of Wheat Physiology) has used a trait-based breeding strategy in the last decades. In this trait-based breeding, lines with improved RUE and high biomass have been identified. However, the measurements are time consuming and are not feasible to do in more than one planting system in the trait-based breeding. Therefore, Matthew Reynolds gives the best lines to Prof Ravi Singh (Head of Global Wheat Improvement) who includes these lines in full breeding trials at CIMMYT Mexico in both planting systems. At this stage, Ravi Singh does not measure RUE and light interception as it is too time consuming. However, the canopy architecture traits identified in the present study would be feasible to measure in selected trials in the breeding programme if they can be validated as reliable indicators of light interception and RUE. So further work is needed to validate the present correlation between canopy architecture traits and light interception and RUE across a wider range of CIMMYT germplasm and more environments with a view to potentially deploying these traits as selection criteria in the CIMMYT wheat breeding program.

Many of the results published on sets of cultivars contrasting for canopy architecture traits including the present results could be confounded by genetic variation in other traits e.g., plant height. Therefore, a set of near-isogenic lines that differed only for a gene(s)

determining leaf angle and/or curvature would be useful to validate more precisely the canopy architecture traits presented in this thesis. To date, there are few studies reporting effects for near-isogenic lines in wheat contrasting for leaf angle, e.g., Innes, P., & Blackwell, R., 1983, a study in wheat but not in modern germplasm, which found that canopies with erect lines produced more biomass than canopies with lax leaves. In addition, there was a study in Australia that use NILs to explore relationships between tillering, canopy architecture and resource capture (Moeller et al., 2014). The latter study demonstrated that tin genes in wheat modifies the canopy architecture by increases in tiller economy and changing the distribution of organ sizes. Future work is required to identify genes regulating leaf angle and to develop near-isogenic lines providing a more precise and uniform background to validate the canopy architecture traits examined in this study.

6.4 Translating from glasshouse to field experiments

In this study, three field experiments were carried out in NW Mexico and two glasshouse experiments at Sutton Bonington, UK using eight common spring wheat CIMMYT cultivars. In field experiments there is generally greater environmental variation compared to the glasshouse and therefore the genotype \times environment variation is greater. This was confirmed in the present results in chapter 6. Therefore, one of the advantages of performing a glasshouse experiment is a more precise estimation of genetic variation with a more uniform environmental background. However, it is necessary to consider if the trait expression at the individual plant scale is representative of trait expression at the crop scale in a field plot. Some studies focus more with traits measured at the individual shoot scale, e.g. flag-leaf photosynthesis rate; therefore, a glasshouse experiment may be better suited better for these purposes. In this study, no associations among the eight common genotypes in the field and glasshouse experiments were found between grain yield per main shoot or per plant measured in the glasshouse and in grain yield per m² in the field. In addition, no significant associations were found between grains per main shoot or per plant in the glasshouse and grains per m² in the field, or for harvest index in the glasshouse and field experiments. This was the case for both the raised beds and flat basins for which the correlations between the field and glasshouse results were similar. However, a strong correlation among cultivars was found between flag-leaf A_{max} measured at anthesis in the glasshouse and RUE_preGF, RUET and biomass per m² at physiological maturity in the

field experiments in raised beds. This correlation is encouraging implying future studies could be carried out on flag-leaf photosynthesis in both field and glasshouse environments but in which more detailed measurements could be taken in the glasshouse: for example, on flag-leaf light and CO₂ response curves, measuring quantum yield of PSII, maximal carboxylation rate ($V_{C_{Max}}$) and maximal light-driven electron flux (J_{Max}).

7 CONCLUSIONS

The present results showed a wide genetic variation in grain yield and yield components in the twelve spring wheat CIMMYT cultivars under two planting systems: raised beds and flat basins. PS \times G interaction was found for grain yield, which was higher by 10.6% in beds than flat basins. PS \times G interaction was also shown in grains per m², biomass at physiological maturity and plant height at maturity. BMPM was higher also in beds by 7.6% as well as RUE_InBA7 (9.7%). The results showed that grain yield responses of cultivar to PS were mainly explained through effects on final biomass. Biomass responses to planting systems were, in turn, partly associated with responses of RUE to planting system in the pre-anthesis period. There was a wide genetic variation in canopy architecture traits in both PS and RUE at different phenophases. Results showed that canopies with erect flag-leaves had higher RUE during grain-filling in flats. No significant associations between flag-leaf angle and RUE were found for the pre-anthesis period. Flag-leaf curvature at GS41 was positively associated with RUE_InBA7 in flats and with IPARaccInA7 in beds. Additionally, flag-leaf curvature at GS65 + 7 days was positively associated with RUE_GF. Positive correlations between fractional PAR interception and plant height were found but only in beds. More studies using a wider range of germplasm but with a reduced variation of plant height are required to confirm the results in the present study. Since there were relatively few trade-offs between grain partitioning traits and RUE, results indicated it is feasible to combine high RUE and high expression of grain partitioning traits for spring wheat cultivars.

In conclusion, a wide number of publications have investigated genetic variation in grain yield, biomass and RUE and associations with canopy architecture in wheat and other crop species such as maize, barley and rice. Breeders at CIMMYT today continue to produce high yielding spring wheat lines that do not exhibit erect flag leaves. Why? How can lines with large, lax leaves, which defy the ideotype for reduced light saturation of flag leaves,

out-yield lines that exhibit the ‘superior’ canopy-architecture ideotype in the same environment? Plant breeders at CIMMYT continue to produce high yielding lines with planophile leaves in the raised-bed planting system. In summary, present results showed in raised beds this is mainly due to greater light interception by the canopy particularly in the pre-anthesis phase for planophile canopies. However, the present results in flat basins actually showed that CIMMYT lines with erect flag leaves are higher yielding than planophile lines mainly related to higher RUE during grain filling agreeing with the canopy-architecture ideotype. In future studies it will be important to confirm these results in a wider range of spring wheat germplasm and environments and to examine the basis of the planting system x genotype interactions further in relation to the associations between canopy architecture, light distribution, and photosynthesis in the different canopy leaf layers.

8 FUTURE WORK

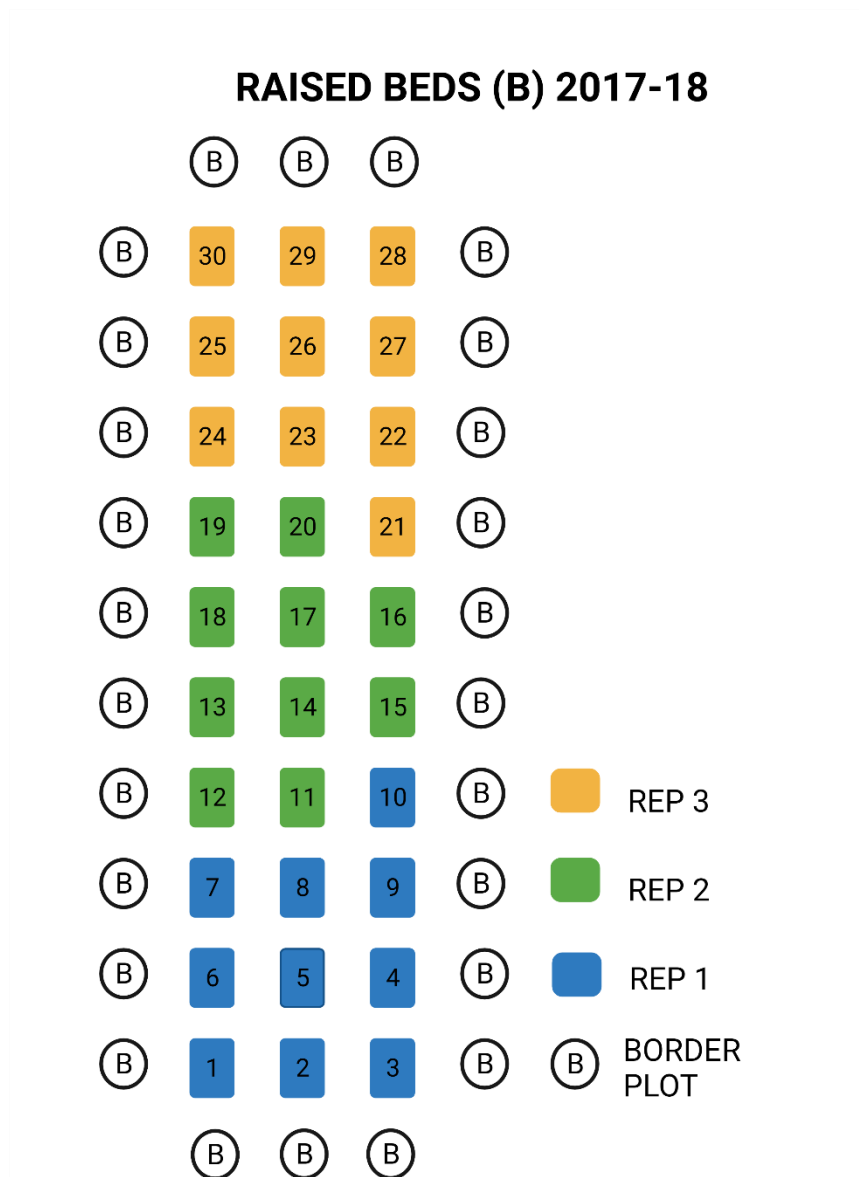
In the present research, genetic diversity was identified in spring wheat CIMMYT cultivars for canopy architecture traits and RUE. The effects of these canopy architecture traits was evaluated and associations were found with light interception, RUE and hence grain yield. However, it is necessary in future work to validate the present findings but using a greater number of genotypes with a reduced range of plant height. In addition, it is important to corroborate the present results at different locations comparing the two planting systems. Most bread-wheat cultivars at CIMMYT have planophile characteristics in contrast with most elite winter wheat cultivars in Europe which are erectophile (Shearman et al., 2005). So it is important to confirm these findings in winter wheat with detailed canopy architecture measurements as in the present experiments. Results showed a $PS \times G$ interaction in canopy architecture traits, RUE, grain yield and yield components. Effects of grain yield and yield components evaluated in barley and rice under two planting systems were also reported previously (Kukal et al., 2010; Kendal, 2019). Present results showed the importance to test new germplasm using the two planting systems at different locations for selection in order to avoid eliminating a good line since farmers might use a different planting system than the one the plant breeder used for the selection. Additionally, it might be useful to evaluate canopy architecture traits under drought and heat stress at different locations for a more reliable information on $G \times E$ effects.

Future studies on the genetic regulation of leaf angle and leaf curvature are required focused on understanding the underlying mechanisms, e.g. effects of brassinosteroids (BRs) which play an important role in regulating the leaf erectness in cereals by altering the cytological structure of the lamina joint (Wang et al., 2020). In the present study, canopy architecture traits were measured manually and also using a visual score which was possible since the two experiments performed each year consisted of only twelve cultivars with three replicates. However, plant breeders will require new tools and technology to evaluate canopy architecture traits on 1,000s of lines. Despite the advances in high-throughput phenotyping (HTP), variation of flag-leaf angle and also leaf angle among the canopy layers has been poorly evaluated (Mantilla-Perez et al., 2020). Therefore, further investigation is also required on effects of leaf position on canopy architecture traits. It is sometimes complex to analyse these type of traits under field conditions due to challenges imposed by wind and overlapping plants (Mantilla-Perez et al., 2020). Additionally, most of the studies on effect of canopy architecture traits using canopy reconstruction have been made in the glasshouse (Burgess et al., 2017) but there is a need to study the same traits under field conditions. For a more optimized standard method for canopy architecture phenotyping in the fields not only in wheat but also in maize, rice, barley and sorghum it might be possible to use high-resolution cameras through different times during the day combined with the protocol used in **Chapter 3**. Additionally, the development and use of molecular markers could contribute to selection for canopy architecture traits in plant breeding programs. For example, future genetic studies could be carried out in the HIBAP panel (**see Chapter 2**) using GWAS to detect candidate genes and then these candidate genes validated using tilling mutant populations.

This study showed that reducing the length of the stem internodes 2 and 3 might increase the dry-matter of the spike. However, further investigation is required to test if there is a trade-off with light distribution and RUE in the canopies and hence on above-ground biomass. Additionally, the present findings could be used in future crop simulation modelling studies to predict joint optimization of canopy architecture traits to increase light interception and RUE and joint optimization of source and sink traits.

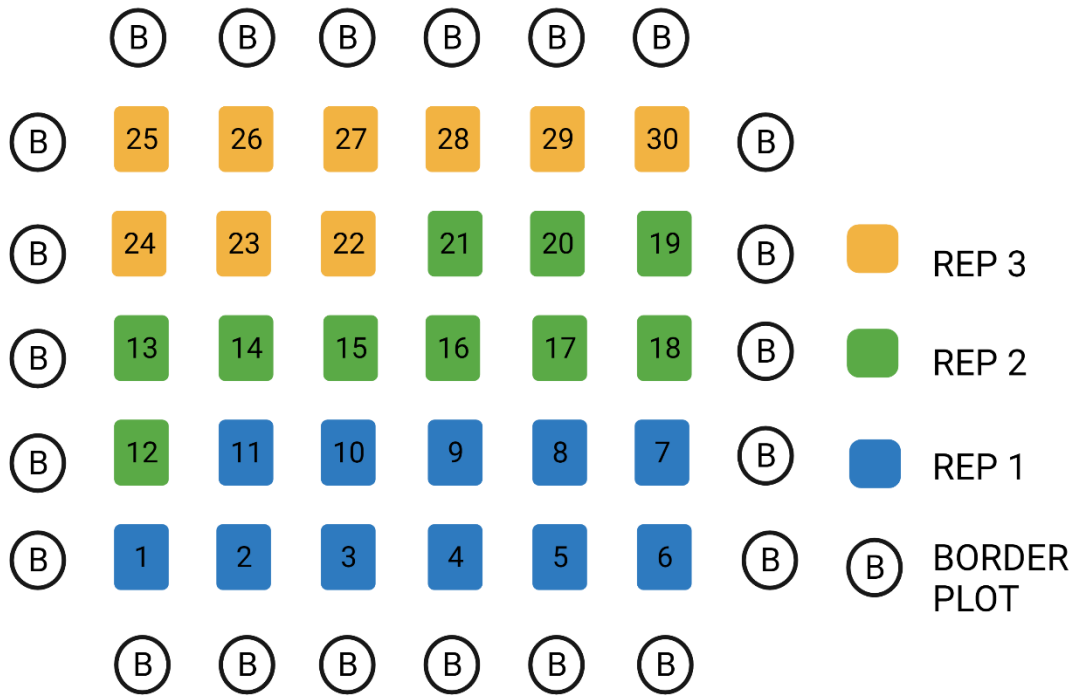
Results in **Chapter 5** were encouraging, showing positive correlations between genetic variation in flag-leaf A_{max} in the glasshouse and biomass at maturity in the fields. Therefore, in further work it might be feasible to evaluate high expression of leaf level photosynthesis rate in the glasshouse which translates to high expression of canopy level

under field conditions for the cultivars in the HIBAP. The effect of the canopy architecture traits on RUE, biomass and grain yield in other cereals which have yet to be quantified should also be studied, and the new methods for quantifying flag-leaf and curvature tested in these cereals in the future.



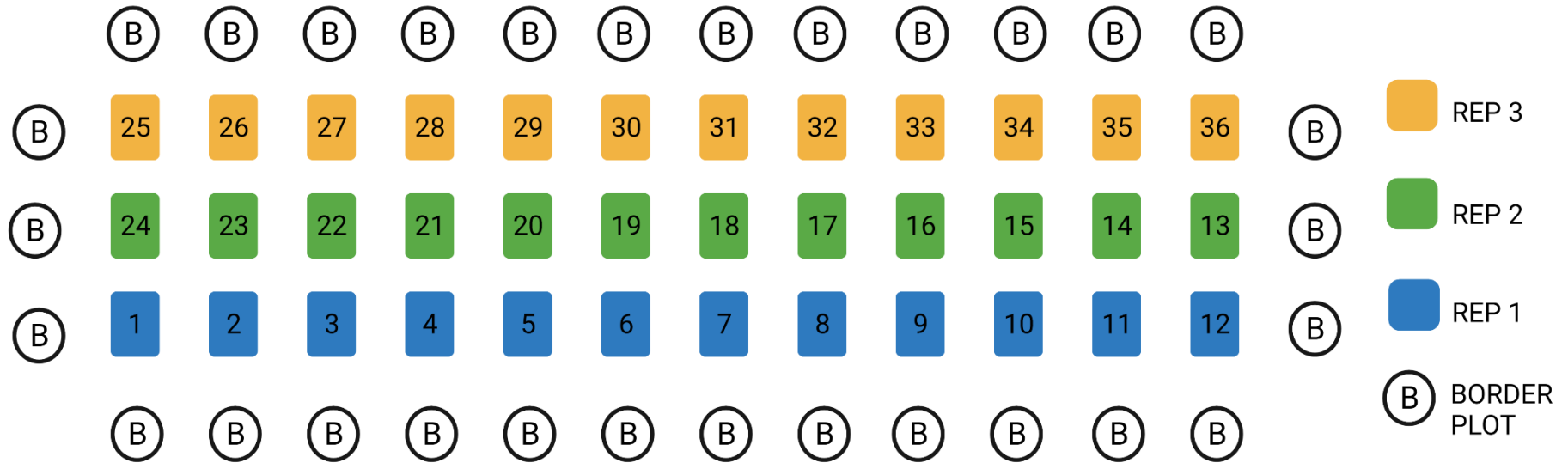
Appendix Fig. 1. Field arrangement in raised beds (B) in 2017-18.
Created with BioRender.com.

FLAT BASINS (F) 2017-18



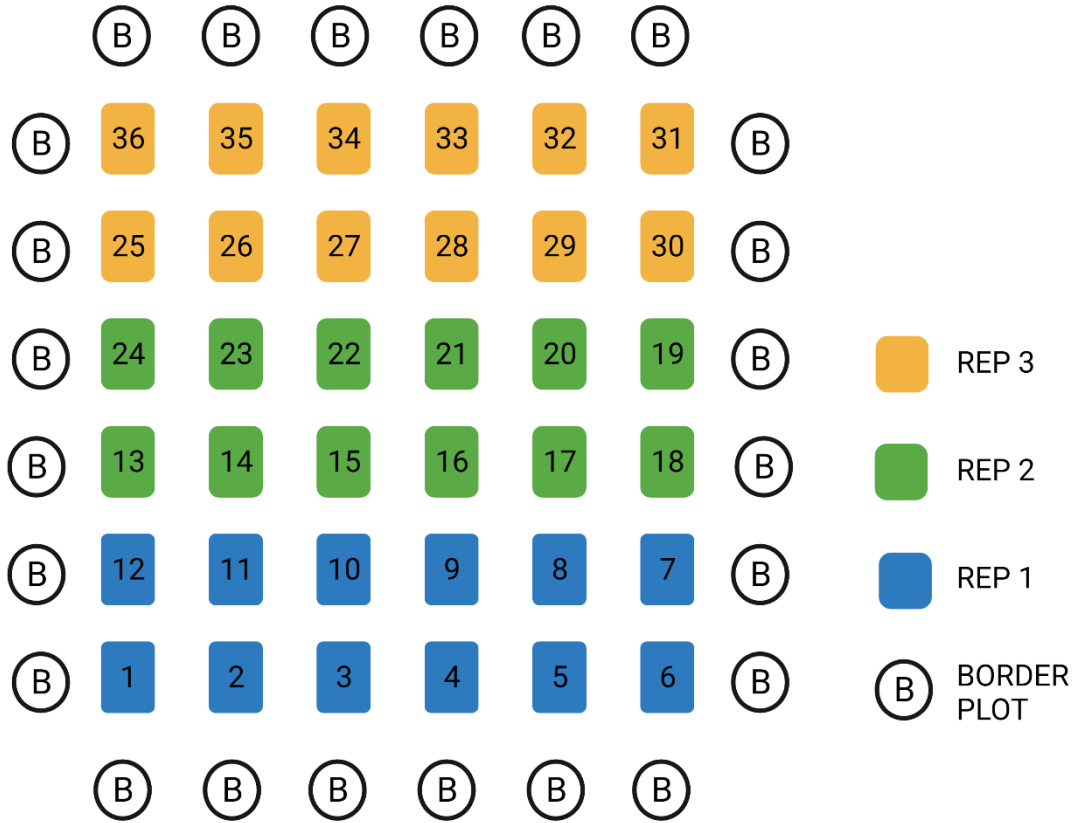
Appendix Fig. 2. Field arrangement in flat basins (F) in 2017-18. Created with BioRender.com.

RAISED BEDS (B) 2018-19



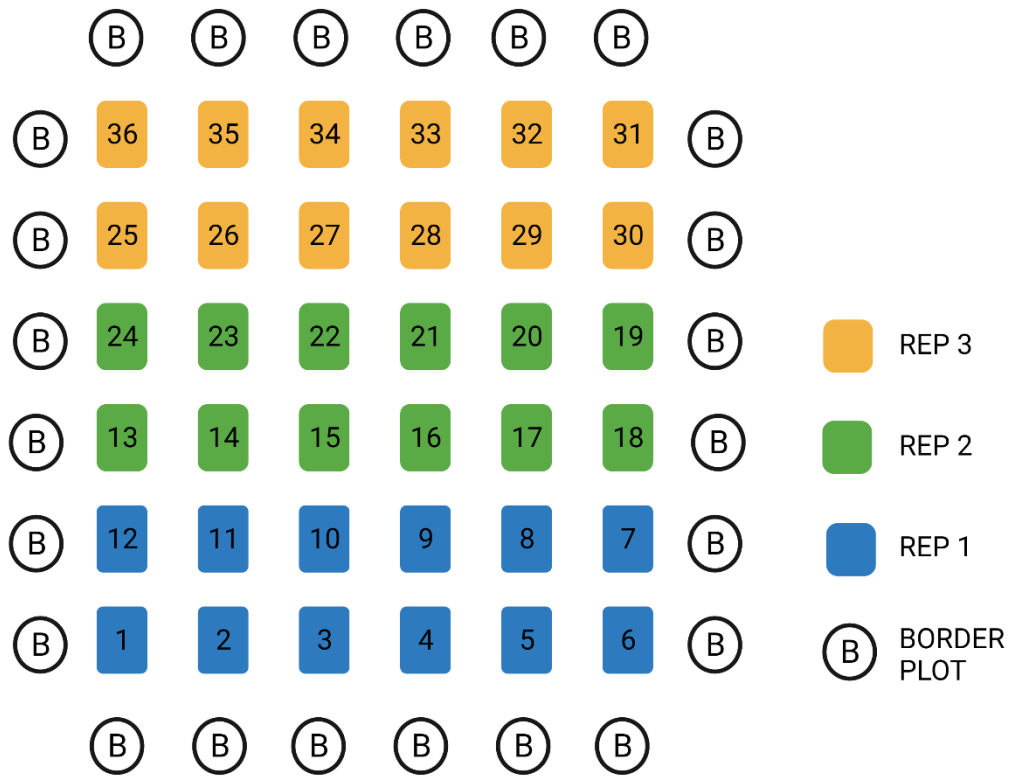
Appendix Fig. 3. Field arrangement in raised beds (B) in 2018-19. Created with BioRender.com.

FLAT BASINS (F) 2018-19



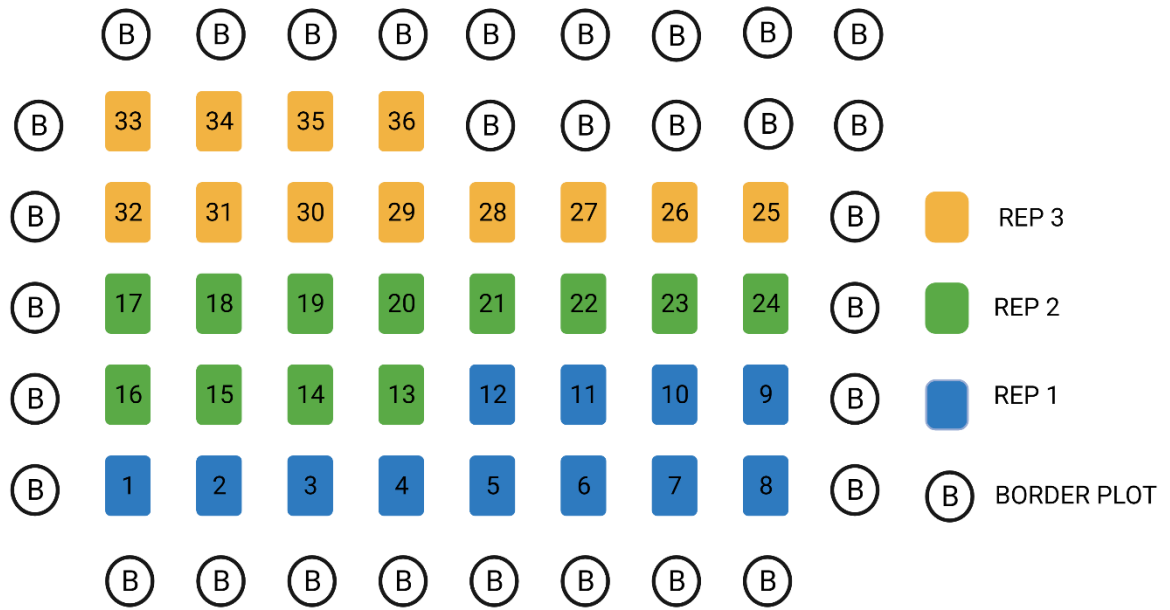
Appendix Fig. 4. Field arrangement in flat basins (F) in 2018-19. Created with BioRender.com.

RAISED BEDS (B) 2019-20



Appendix Fig. 5. Field arrangement in raised beds (B) in 2019-20. Created with BioRender.com.

FLAT BASINS (F) 2019-20



Appendix Fig. 6. Field arrangement in flat basins (F) in 2019-20. Created with BioRender.com.

Appendix Table 1. Growing conditions for three years (2017-18, 2018-19 and 2019-20) field experiments in the planting systems (PS) raised beds (B) and flat basins (F). ‡Drip irrigation in flat basins in 2019-20.

Cycle	Sowing date	Emergence date	Herbicide	Date	Fungicide	Date	Insecticide	Date	Irrigation	Fertilizer (N-P) (Kg ha ⁻¹)
2017-18										
B	01/12/2017	07/12/2017	350 ml/ha (Buctril+starane)	02/01/2018	Folicur (1L/ha)	30/01/2018	Muralla (1L/ha)	07/02/2018	At sowing	300-50
					Folicur (1L/ha)	01/03/2018			15/12/2017	
									09/02/2018	
									08/03/2018	
F	30/11/2017	07/12/2017	350 ml/ha (Buctril+starane)	05/01/2018	Folicur (1L/ha)	01/03/2018	Muralla (1L/ha)	07/02/2018	At sowing	300-50
					Folicur (1L/ha)	08/03/2018			15/12/2017	
									11/01/2018	
									01/02/2018	
									02/03/2018	
2018-19										
B	30/11/2018	07/12/2018	-	-	Folicur (1L/ha)	29/01/2019	Admire (1L/ha)	10/01/2019	At Pre-sowing	250-50
					Folicur (1L/ha)	13/02/2019	Lorsban (1L/ha)	01/02/2019	02/12/2018	
					Folicur (1L/ha)	21/03/2019	Muralla (1L/ha)	22/03/2019	17/01/2019	
									15/02/2019	
									07/03/2019	
									28/03/2019	

F	01/12/2018	07/12/2018	28/160 ml/ha (Starane/broclean)	20/12/2018	Folicur (1L/ha)	29/01/2019	Admire (1L/ha)	10/01/2019	At Pre- sowing	250-50
					Folicur (1L/ha)	21/03/2019	Lorsban (1L/ha)	31/01/2019	21/12/2018	
							Muralla (1L/ha)	29/03/2019	17/01/2019	
									15/02/2019	
									07/03/2019	
									28/03/2019	
2019- 20										
B	21/12/2019	23/12/2019	-	-	Folicur (1/2L/ha)	19/03/2020	Muralla/Lorsban (250/ha/1L/ha)	31/01/2020	At sowing	250-50
					Folicur (1/2L/ha)	24/03/2020	Muralla/Lorsban (250/ha/1L/ha)	19/03/2020	16/01/2020	
									11/02/2020	
									29/02/2020	
									26/03/2020	
									13/04/2020	
F‡	17/12/2019	26/12/2019	-	-	Folicur (1/2L/ha)	09/03/2020	Muralla/Lorsban (250/ha/1L/ha)	30/01/2020	At sowing	250-50
					Folicur (1/2L/ha)	13/03/2020	Muralla/Lorsban (250/ha/1L/ha)	13/03/2020	10/01/2020	
									24/01/2020	
									13/02/2020	
									28/02/2020	
									13/03/2020	
									27/03/2020	
									30/03/2020	
									08/04/2020	

Appendix Table 2. Fungicide and insecticide applications for glasshouse experiments in 2018 and 2019.

Experiment	Sowing date	Emergence date	Fungicide	date	Insecticide	date
2018	12/07/2018	16/07/2018	Taliux	15/08/2018	Aphox	15/08/2018
			Amistar opti	24/08/2018	Chess WG	06/09/2018
					Aphox	14/09/2018
					Aphox	15/10/2018
2019	01/07/2019	5/07/2019	Talius	08/07/2019	Apres	30/07/2019
					Chess WG	07/08/2019

10 REFERENCES

Abbate, P.E., Andrade, F.H., Culot, J.P., Bindraban, P.S., 1997. Grain yield in wheat: Effects of radiation during spike growth period. *Field Crops Research* 54, 245-257. doi:[https://doi.org/10.1016/S0378-4290\(97\)00059-2](https://doi.org/10.1016/S0378-4290(97)00059-2).

Abberton, M., Batley, J., Bentley, A., Bryant, J., Cai, H., Cockram, J., Costa de Oliveira, A., Cseke, L.J., Dempewolf, H., De Pace, C., 2016. Global agricultural intensification during climate change: a role for genomics. *Plant biotechnology journal* 14, 1095-1098. doi:<https://doi.org/10.1111/pbi.12467>.

Acreche, M.M., Briceño-Félix, G., Martín Sánchez, J.A., Slafer, G.A., 2009. Radiation interception and use efficiency as affected by breeding in Mediterranean wheat. *Field Crops Research* 110, 91-97. doi:<https://doi.org/10.1016/j.fcr.2008.07.005>.

Acreche, M.M., Briceño-Félix, G., Sánchez, J.A.M., Slafer, G.A., 2008. Physiological bases of genetic gains in Mediterranean bread wheat yield in Spain. *European Journal of Agronomy* 28, 162-170. doi:<https://doi.org/10.1016/j.eja.2007.07.001>.

Acreche, M.M., Slafer, G.A., 2006. Grain weight response to increases in number of grains in wheat in a Mediterranean area. *Field Crops Research* 98, 52-59. doi:<https://doi.org/10.1016/j.fcr.2005.12.005>.

Acreche, M.M., Slafer, G.A., 2009. Grain weight, radiation interception and use efficiency as affected by sink-strength in Mediterranean wheats released from 1940 to 2005. *Field Crops Research* 110, 98-105. doi:<https://doi.org/10.1016/j.fcr.2008.07.006>.

Ahmad, M., Ghafoor, A., Asif, M., Farid, H.U., 2010. Effect of irrigation techniques on wheat production and water saving in soils. *Soil & Environment* 29, 69-72.

Ahmad, S., Ali, H., Ismail, M., Shahzad, M.I., Nadeem, M., Anjum, M.A., 2012. Radiation and Nitrogen Use Efficiency of C3 winter cereals to nitrogen split application. *Pakistan Journal of Botany* 44, 139-149. doi:<https://doi.org/10.1093/jxb/err389>.

Ahmadi, A., Joudi, M., Janmohammadi, M., 2009. Late defoliation and wheat yield: Little evidence of post-anthesis source limitation. *Field Crops Research* 113, 90-93. doi:<https://doi.org/10.1016/j.fcr.2009.04.010>.

Ainsworth, E.A., Long, S.P., 2020. 30 years of free-air carbon dioxide enrichment (FACE): What have we learned about future crop productivity and its potential for adaptation? *Global change biology* 27, 27-49. doi:<https://doi.org/10.1111/gcb.15375>.

Aisawi, K.A.B., Reynolds, M.P., Singh, R.P., Foulkes, M.J., 2015. The Physiological Basis of the Genetic Progress in Yield Potential of CIMMYT Spring Wheat Cultivars from 1966 to 2009. *Crop Science* 55, 1749-1764. doi:<https://doi.org/10.2135/cropsci2014.09.0601>.

Albajes, R., Cantero-Martínez, C., Capell, T., Christou, P., Farre, A., Galceran, J., López-Gatius, F., Marin, S., Martín-Belloso, O., Motilva, M.J., Nogareda, C., Peman, J., Puy, J., Recasens, J., Romagosa, I., Romero, M.P., Sanchis, V., Savin, R., Slafer, G.A., Soliva-Fortuny, R., Viñas, I., Voltas, J., 2013. Building bridges: an integrated strategy for sustainable food production throughout the value chain. *Molecular Breeding* 32, 743-770. doi:<https://doi.org/10.1007/s11032-013-9915-z>.

Alvarado, G., Rodríguez, F.M., Pacheco, A., Burgueño, J., Crossa, J., Vargas, M., Pérez-Rodríguez, P., Lopez-Cruz, M.A., 2020. META-R: A software to analyze data from multi-environment plant breeding trials. *The Crop Journal* 8, 745-756. doi:<https://doi.org/10.1016/j.cj.2020.03.010>.

Araus, J.L., Brown, H.R., Febrero, A., Bort, J., Serret, M.D., 1993a. Ear photosynthesis, carbon isotope discrimination and the contribution of respiratory CO₂ to

differences in grain mass in durum wheat. *Plant, Cell & Environment* 16, 383-392. doi:<https://doi.org/10.1111/j.1365-3040.1993.tb00884.x>.

Araus, J.L., Cairns, J.E., 2014. Field high-throughput phenotyping: the new crop breeding frontier. *Trends in Plant Science* 19, 52-61. doi:<https://doi.org/10.1016/j.tplants.2013.09.008>.

Araus, J.L., Kefauver, S.C., Zaman-Allah, M., Olsen, M.S., Cairns, J.E., 2018. Translating High-Throughput Phenotyping into Genetic Gain. *Trends in Plant Science* 23, 451-466. doi:<https://doi.org/10.1016/j.tplants.2018.02.001>.

Araus, J.L., Reynolds, M.P., Acevedo, E., 1993b. Leaf Posture, Grain Yield, Growth, Leaf Structure, and Carbon Isotope Discrimination in Wheat. *Crop Science* 33, 1273-1279. doi:<https://doi.org/10.2135/cropsci1993.0011183X003300060032x>.

Ashikari, M., Sakakibara, H., Lin, S., Yamamoto, T., Takashi, T., Nishimura, A., Angeles, E.R., Qian, Q., Kitano, H., Matsuoka, M., 2005. Cytokinin oxidase regulates rice grain production. *Science* 309, 741-745. doi:<https://doi.org/10.1126/science.1113373>.

Asseng, S., Ewert, F., Martre, P., Rötter, R.P., Lobell, D., Cammarano, D., Kimball, B., Ottman, M., Wall, G., White, J., Reynolds, M., Alderman, P., Prasad, P.V.V., Aggarwal, P.K., Anothai, J., Basso, B., Biernath, C., Challinor, A., De Sanctis, G., Zhu, Y., 2015. Rising temperatures reduce global wheat production. *Nature Climate Change* 5, 143-147. doi:<https://doi.org/10.1038/nclimate2470>.

Asseng, S., Kassie, B., Labra, M., Amador, C., Calderini, D., 2016. Simulating the impact of source-sink manipulations in wheat. *Field Crops Research* 202. doi:<https://doi.org/10.1016/j.fcr.2016.04.031>.

Austin, R.B., 1980. Physiological limitations to cereal yields and ways of reducing them by breeding. In: Hurd, R.G., Biscoe, P. V, Dennis, C. (Ed.), *Opportunities for increasing crop yields*, London: Association of Applied Biology/Pitman, 3-19.

Austin, R.B., Bingham, J., Blackwell, R.D., Evans, L.T., Ford, M.A., Morgan, C.L., Taylor, M., 1980. Genetic improvements in winter wheat yields since 1900 and associated physiological changes. *Journal of agricultural science*. 94, 675-689. doi:<https://doi.org/10.1017/s0021859600028665>.

Austin, R.B., Ford, M.A., Edrich, J.A., Hooper, B.E., 1976. Some effects of leaf posture on photosynthesis and yield in wheat. *Annals of Applied Biology* 83, 425-446. doi:<https://doi.org/10.1111/j.1744-7348.1976.tb01714.x>.

Austin, R.B., Ford, M.A., Morgan, C.L., 1989. Genetic improvement in the yield of winter wheat: a further evaluation. *The Journal of Agricultural Science* 112, 295-301. doi:<https://doi.org/10.1017/S0021859600085749>.

Austin, R.B., Morgan, C.L., Ford, M.A., Bhagwat, S.G., 1982. Flag Leaf Photosynthesis of *Triticum aestivum* and Related Diploid and Tetraploid Species. *Annals of Botany* 49, 177-189. doi:<https://doi.org/10.1093/oxfordjournals.aob.a086238>.

Bakker, D., Hamilton, G., Houlbrooke, D., Spann, C., Burgel, A., 2007. Productivity of crops grown on raised beds on duplex soils prone to waterlogging in Western Australia. *Australian Journal of Experimental Agriculture - AUST J EXP AGR* 47, 1368-1376. doi:10.1071/EA06273.

Bar-Even, A., Noor, E., Savir, Y., Liebermeister, W., Davidi, D., Tawfik, D.S., Milo, R., 2011. The Moderately Efficient Enzyme: Evolutionary and Physicochemical Trends Shaping Enzyme Parameters. *Biochemistry* 50, 4402-4410. doi:<https://doi.org/10.1021/bi2002289>.

Barthélémy, D., Caraglio, Y., 2007. Plant Architecture: A Dynamic, Multilevel and Comprehensive Approach to Plant Form, Structure and Ontogeny. *Annals of Botany* 99, 375-407. doi:10.1093/aob/mcl260.

Beche, E., Benin, G., da Silva, C.L., Munaro, L.B., Marchese, J.A., 2014. Genetic gain in yield and changes associated with physiological traits in Brazilian wheat during the 20th century. *European Journal of Agronomy* 61, 49-59. doi:<https://doi.org/10.1016/j.eja.2014.08.005>.

Beed, F.D., Paveley, N., Sylvester-Bradley, R., 2007. Predictability of wheat growth and yield in light-limited conditions. *The Journal of Agricultural Science* 145, 63-79.

Berry, P.M., Spink, J.H., Foulkes, M.J., Wade, A., 2003. Quantifying the contributions and losses of dry matter from non-surviving shoots in four cultivars of winter wheat. *Field Crops Research* 80, 111-121. doi:[https://doi.org/10.1016/S0378-4290\(02\)00174-0](https://doi.org/10.1016/S0378-4290(02)00174-0).

Bhuyan, M.H.M., Ferdousi, M.R., Iqbal, M.T., 2012. Yield and Growth Response to Transplanted Aman Rice under Raised Bed over Conventional Cultivation Method. *ISRN Agronomy* 2012, 646859. doi:<https://10.5402/2012/646859>.

Biswal, A.K., Kohli, A., 2013. Cereal flag leaf adaptations for grain yield under drought: knowledge status and gaps. *Molecular Breeding* 31, 749-766. doi:<https://doi.org/10.1007/s11032-013-9847-7>.

Blake, N.K., Lanning, S.P., Martin, J.M., Sherman, J.D., Talbert, L.E., 2007. Relationship of Flag Leaf Characteristics to Economically Important Traits in Two Spring Wheat Crosses. *Crop Science* 47, 491-494. doi:<https://doi.org/10.2135/cropsci2006.05.0286>.

Bogard, M., Jourdan, M., Allard, V., Martre, P., Perretant, M.R., Ravel, C., Heumez, E., Orford, S., Snape, J., Griffiths, S., Gaju, O., Foulkes, J., Le Gouis, J., 2011. Anthesis date mainly explained correlations between post-anthesis leaf senescence, grain yield, and grain protein concentration in a winter wheat population segregating for flowering time QTLs. *Journal of Experimental Botany* 62, 3621-3636. doi:<https://doi.org/10.1093/jxb/err061>.

Bonan, G., 2002. *Ecological climatology: concepts and applications*. Cambridge University Press, Cambridge.

Borrás, L., Slafer, G.A., Otegui, M.a.E., 2004. Seed dry weight response to source-sink manipulations in wheat, maize and soybean: a quantitative reappraisal. *Field Crops Research* 86, 131-146. doi:<https://doi.org/10.1016/j.fcr.2003.08.002>.

Braun, H.-J., Atlin, G., Payne, T., 2010. Multi-location testing as a tool to identify plant response to global climate change. In: Reynolds, M.P. (Ed.), *Climate change and crop production*, CABI. 115-138. doi:<https://10.1079/9781845936334.0115>.

Brisson, N., Gate, P., Gouache, D., Charmet, G., Oury, F.-X., Huard, F., 2010. Why are wheat yields stagnating in Europe? A comprehensive data analysis for France. *Field Crops Research* 119, 201-212. doi:<https://doi.org/10.1016/j.fcr.2010.07.012>.

Brooking, I.R., Kirby, E.J.M., 1981. Interrelationships between stem and ear development in winter wheat: the effects of a Norin 10 dwarfing gene, Gai/Rht2. *The Journal of Agricultural Science* 97, 373-381. doi:<https://doi.org/10.1017/S0021859600040806>.

Burgess, A.J., 2017. *The variable light environment within complex 3D canopies*. University of Nottingham.

Burgess, A.J., Retkute, R., Herman, T., Murchie, E.H., 2017. Exploring Relationships between Canopy Architecture, Light Distribution, and Photosynthesis in Contrasting Rice Genotypes Using 3D Canopy Reconstruction. *Frontiers in Plant Science* 8. doi:<https://doi.org/10.3389/fpls.2017.00734>.

Bush, M.G., Evans, L.T., 1988. Growth and development in tall and dwarf isogenic lines of spring wheat. *Field Crops Research* 18, 243-270. doi:[https://doi.org/10.1016/0378-4290\(88\)90018-4](https://doi.org/10.1016/0378-4290(88)90018-4).

Bustos, D.V., Hasan, A.K., Reynolds, M.P., Calderini, D.F., 2013. Combining high grain number and weight through a DH-population to improve grain yield potential of wheat

in high-yielding environments. *Field Crops Research* 145, 106-115. doi:<https://doi.org/10.1016/j.fcr.2013.01.015>.

Cabrera-Bosquet, L., Fournier, C., Bricchet, N., Welcker, C., Suard, B., Tardieu, F., 2016. High-throughput estimation of incident light, light interception and radiation-use efficiency of thousands of plants in a phenotyping platform. *The New phytologist* 212, 269-281. doi:<https://doi.org/10.1111/nph.14027>.

Calderini, D.F., Dreccer, M.F., Slafer, G.A., 1997. Consequences of breeding on biomass, radiation interception and radiation-use efficiency in wheat. *Field Crops Research* 52, 271-281. doi:[https://doi.org/10.1016/S0378-4290\(96\)03465-X](https://doi.org/10.1016/S0378-4290(96)03465-X).

Calderini, D.F., Savin, R., Abeledo, L.G., Reynolds, M.P., Slafer, G.A., 2001. The importance of the period immediately preceding anthesis for grain weight determination in wheat. *Euphytica* 119, 199-204. doi:<https://doi.org/10.1023/a:1017597923568>.

Calderini, D.F., Slafer, G.A., 1998. Changes in yield and yield stability in wheat during the 20th century. *Field Crops Research* 57, 335-347. doi:[https://doi.org/10.1016/S0378-4290\(98\)00080-X](https://doi.org/10.1016/S0378-4290(98)00080-X).

Calderini, D.F., Slafer, G.A., 1999. Has yield stability changed with genetic improvement of wheat yield? *Euphytica* 107, 51-59. doi:<https://doi.org/10.1023/A:1003579715714>.

Carmo-Silva, E., Andralojc, P.J., Scales, J.C., Driever, S.M., Mead, A., Lawson, T., Raines, C.A., Parry, M.A.J., 2017. Phenotyping of field-grown wheat in the UK highlights contribution of light response of photosynthesis and flag leaf longevity to grain yield. *Journal of Experimental Botany* 68, 3473-3486. doi:<https://doi.org/10.1093/jxb/erx169>.

Carvalho, P., Foulkes, M., 2012. Roots root and Uptake of Water and Nutrients roots uptake of water and nutrients. In *Encyclopedia of Sustainability Science and Technology*, 1390-1404. doi:https://doi.org/10.1007/978-1-4614-5797-8_195.

Cavanagh, A.P., Kubien, D.S., 2014. Can phenotypic plasticity in Rubisco performance contribute to photosynthetic acclimation? *Photosynth Res* 119, 203-214. doi:10.1007/s11120-013-9816-3.

Chang, T.G., Zhu, X.G., Raines, C., 2017. Source-sink interaction: a century old concept under the light of modern molecular systems biology. *J Exp Bot* 68, 4417-4431. doi:10.1093/jxb/erx002.

Charret, G., 2011. Wheat domestication: Lessons for the future. *Comptes Rendus Biologies* 334, 212-220. doi:<https://doi.org/10.1016/j.crv.2010.12.013>.

Chaudhary, J.L., Patel, s.R., Verma, P., Narayanan, M., Khavse, R., 2016. Thermal and radiation effect studies of different wheat varieties in Chhattisgarh plains zone under rice-wheat cropping system. *Mausam* 67, 677-682.

Chen, J.M., Black, T.A., 1992. Defining leaf area index for non-flat leaves. *Plant, Cell & Environment* 15, 421-429. doi:<https://doi.org/10.1111/j.1365-3040.1992.tb00992.x>.

Chen, W., Deng, X.-P., Eneji, A., Wang, L., Xu, Y., Cheng, Y., 2014. Dry-Matter Partitioning across Parts of the Wheat Internode during the Grain Filling Period as Influenced by Fertilizer and Tillage Treatments. *Communications in Soil Science and Plant Analysis* 13, 1779-1812. doi:<https://doi.org/10.1080/00103624.2014.907918>.

Chibane, N., Caicedo, M., Martinez, S., Marcet, P., Revilla, P., Ordás, B., 2021. Relationship between Delayed Leaf Senescence (Stay-Green) and Agronomic and Physiological Characters in Maize (*Zea mays* L.). *Agronomy* 11, 276. doi:<https://doi.org/10.3390/agronomy11020276>.

Choudhury, B., 2000. A sensitivity analysis of the radiation use efficiency for gross photosynthesis and net carbon accumulation by wheat. *Agricultural and Forest Meteorology* 101, 217-234. doi:[https://doi.org/10.1016/S0168-1923\(99\)00156-2](https://doi.org/10.1016/S0168-1923(99)00156-2).

Chow, W.S., 1994. Photoprotection and Photoinhibitory Damage. In: Bittar, E.E., Barber, J. (Eds.), *Advances in Molecular and Cell Biology*, Elsevier, 151-196. doi:[https://doi.org/10.1016/S1569-2558\(08\)60397-5](https://doi.org/10.1016/S1569-2558(08)60397-5).

Collard, B.C.Y., Jahufer, M.Z.Z., Brouwer, J.B., Pang, E.C.K., 2005. An introduction to markers, quantitative trait loci (QTL) mapping and marker-assisted selection for crop improvement: The basic concepts. *Euphytica* 142, 169-196. doi:10.1007/s10681-005-1681-5.

Crespo-Herrera, L.A., Crossa, J., Huerta-Espino, J., Autrique, E., Mondal, S., Velu, G., Vargas, M., Braun, H.J., Singh, R.P., 2017. Genetic Yield Gains In CIMMYT's International Elite Spring Wheat Yield Trials By Modeling The Genotype × Environment Interaction. *Crop Sci* 57, 789-801. doi:<https://doi.org/10.2135/cropsci2016.06.0553>.

Das Choudhury, S., Bashyam, S., Qiu, Y., Samal, A., Awada, T., 2018. Holistic and component plant phenotyping using temporal image sequence. *Plant Methods* 14, 35. doi:10.1186/s13007-018-0303-x.

Demmig-Adams, B., Adams Iii, W.W., 2003. PHOTOSYNTHESIS AND PARTITIONING | Photoinhibition A2 - Thomas, Brian. *Encyclopedia of Applied Plant Sciences*, Elsevier, Oxford, 707-714. doi:<https://doi.org/10.1016/B0-12-227050-9/00091-0>.

Distelfeld, A., Avni, R., Fischer, A.M., 2014. Senescence, nutrient remobilization, and yield in wheat and barley. *Journal of Experimental Botany* 65, 3783-3798. doi:<https://doi.org/10.1093/jxb/ert477>.

, C., Gruszka, D., Braumann, I., Druka, A., Druka, I., Franckowiak, J., Gough, S.P., Janeczko, A., Kurowska, M., Lundqvist, J., Lundqvist, U., Marzec, M., Matyszczyk, I., Müller, A.H., Oklestkova, J., Schulz, B., Zakhrebekova, S., Hansson, M., 2014. Induced Variations in Brassinosteroid Genes Define Barley Height and Sturdiness, and Expand the Green Revolution Genetic Toolkit. *Plant Physiology* 166, 1912-1927. doi:<https://doi.org/10.1104/pp.114.250738>.

Donmez, E., Sears, R., Shroyer, J., Paulsen, G., 2001. Genetic Gain in Yield Attributes of Winter Wheat in the Great Plains. *Crop Science* 41, 1412-1419. doi:<https://doi.org/10.2135/cropsci2001.4151412x>.

Dreccer, M., Van Oijen, M., Schapendonk, A., Pot, C., Rabbinge, R., 2000. Dynamics of vertical leaf nitrogen distribution in a vegetative wheat canopy. Impact on canopy photosynthesis. *Annals of Botany* 86, 821-831. doi:<https://doi.org/10.1006/anbo.2000.1244>.

Dreccer, M.F., Fainges, J., Whish, J., Ogbonnaya, F.C., Sadras, V.O., 2018. Comparison of sensitive stages of wheat, barley, canola, chickpea and field pea to temperature and water stress across Australia. *Agricultural and Forest Meteorology* 248, 275-294. doi:<https://doi.org/10.1016/j.agrformet.2017.10.006>.

Dreccer, M.F., van Herwaarden, A.F., Chapman, S.C., 2009. Grain number and grain weight in wheat lines contrasting for stem water soluble carbohydrate concentration. *Field Crops Research* 112, 43-54. doi:<https://doi.org/10.1016/j.fcr.2009.02.006>.

Driever, S.M., Lawson, T., Andralojc, P.J., Raines, C.A., Parry, M.A.J., 2014. Natural variation in photosynthetic capacity, growth, and yield in 64 field-grown wheat genotypes. *Journal of Experimental Botany* 65, 4959-4973. doi:<https://doi.org/10.1093/jxb/eru253>.

Dubcovsky, J., Dvorak, J., 2007. Genome Plasticity a Key Factor in the Success of Polyploid Wheat Under Domestication. *Science* 316, 1862-1866. doi:10.1126/science.1143986.

Duncan, W.G., 1971. Leaf Angles, Leaf Area, and Canopy Photosynthesis1. *Crop Science* 11, crops1971.0011183X001100040006x. doi:<https://doi.org/10.2135/cropsci1971.0011183X001100040006x>.

Ehdaie, B., Alloush, G.A., Madore, M.A., Waines, J.G., 2006. Genotypic Variation for Stem Reserves and Mobilization in Wheat: I. Postanthesis Changes in Internode Water-Soluble Carbohydrates. *Crop Science* 46, 735-746. doi:<https://doi.org/10.2135/cropsci2006.01.0013>.

Elía, M., Savin, R., Slafer, G.A., 2016. Fruiting efficiency in wheat: physiological aspects and genetic variation among modern cultivars. *Field Crops Research* 191, 83-90. doi:<https://doi.org/10.1016/j.fcr.2016.02.019>.

Evans, J.R., Clarke, V.C., 2019. The nitrogen cost of photosynthesis. *Journal of Experimental Botany* 70, 7-15. doi:<https://doi.org/10.1093/jxb/ery366>.

Evans, J.R., Seemann, J.R., 1989. The allocation of protein nitrogen in the photosynthetic apparatus: costs, consequences, and control. *Photosynthesis*, 183-205.

Evans, L.T., 1993. Crop evolution, adaptation and yield. Cambridge University Press. 1: 1-500. doi:<https://doi.org/10.1017/S0889189300005361>.

Fahong, W., Xuqing, W., Sayre, K., 2004. Comparison of conventional, flood irrigated, flat planting with furrow irrigated, raised bed planting for winter wheat in China. *Field Crops Research* 87, 35-42. doi:<https://doi.org/10.1016/j.fcr.2003.09.003>.

FAOSTAT, 2018. FAOSTAT Crops production database. Food and Agriculture Organization, Rome. <http://www.fao.org/faostat/en/#data/QC>.

FAOSTAT, 2019. FAOSTATcrops production database. Food and Agriculture Organization, Rome. <https://www.fao.org/faostat/en/#data/QC>.

Feekes, W., 1941. De tarwe en haar milieu [Wheat and its environment]. (in Dutch and English).

Ferrante, A., Savin, R., Slafer, G.A., 2012. Differences in yield physiology between modern, well adapted durum wheat cultivars grown under contrasting conditions. *Field Crops Research* 136, 52-64. doi:<https://doi.org/10.1016/j.fcr.2012.07.015>.

Field, C., 1983. Allocating leaf nitrogen for the maximization of carbon gain: Leaf age as a control on the allocation program. *Oecologia* 56, 341-347. doi:<https://doi.org/10.1007/bf00379710>.

Fischer, R., 2007. Understanding the physiological basis of yield potential in wheat. *The Journal of Agricultural Science* 145, 99. doi:<https://doi.org/doi:10.1017/S0021859607006843>.

Fischer, R., Rees, D., Sayre, K., Lu, Z.M., Condon, A., Saavedra, A.L., 1998. Wheat yield progress associated with higher stomatal conductance and photosynthetic rate, and cooler canopies. *Crop science* 38, 1467-1475. doi:<https://doi.org/10.2135/cropsci1998.0011183X003800060011x>.

Fischer, R., Stockman, Y., 1986. Increased Kernel Number in Norin 10-Derived Dwarf Wheat: Evaluation of the Cause. *Functional Plant Biology* 13, 767-784. doi:<https://doi.org/10.1071/PP9860767>.

Fischer, R.A., 1985. Number of kernels in wheat crops and the influence of solar radiation and temperature. *The Journal of Agricultural Science* 105, 447-461. doi:<https://doi.org/10.1017/S0021859600056495>.

Fischer, R.A., 2008. The importance of grain or kernel number in wheat: A reply to Sinclair and Jamieson. *Field Crops Research* 105, 15-21. doi:<https://doi.org/10.1016/j.fcr.2007.04.002>.

Fischer, R.A., 2011. Wheat physiology: a review of recent developments. *Crop and Pasture Science* 62, 95-114. doi:<https://doi.org/10.1071/CP10344>.

Fischer, R.A., Moreno Ramos, O.H., Ortiz Monasterio, I., Sayre, K.D., 2019. Yield response to plant density, row spacing and raised beds in low latitude spring wheat with ample soil resources: An update. *Field Crops Research* 232, 95-105. doi:<https://doi.org/10.1016/j.fcr.2018.12.011>.

Fischer, R.A., Sayre, K., Ortiz-Monasterio, I., 2005. The effect of raised beds planting on irrigated wheat yield as influenced by variety and row spacing. In: Roth, C.H., Fischer, R.A., Meisner, C.A., (Ed.), Evaluation and Performance of Permanent Raised Bed Cropping Systems in Asia, Australia and Mexico. ACIAR Proceeding Vol. 121, 1-11. doi:<https://aciar.gov.au/publication/technical-publications/evaluation-and-performance-permanent-raised-bed-cropping-systems-asia-australia-and>.

Flintham, J.E., BÖRner, A., Worland, A.J., Gale, M.D., 1997. Optimizing wheat grain yield: effects of Rht (gibberellin-insensitive) dwarfing genes. *The Journal of Agricultural Science* 128, 11-25. doi:<https://doi.org/10.1017/S0021859696003942>.

Foulkes, J., Murchie, E., 2011a. Optimizing canopy physiology traits to improve the nutrient-utilization efficiency of crops. In: Malcolm J. Hawkesford, P.B. (Ed.), *The molecular and physiological basis of nutrient use efficiency in crops*, John Wiley & Sons.

Foulkes, J., Murchie, E.H., 2011b. Optimizing canopy physiology traits to improve the nutrient-utilization efficiency of crops. In: Malcolm J. Hawkesford, P.B. (Ed.), *The molecular and physiological basis of nutrient use efficiency in crops*, John Wiley & Sons, Inc. 65-82. doi:<https://doi.org/10.1002/9780470960707.ch4>.

Foulkes, M., Hawkesford, M., Barraclough, P., Holdsworth, M., Kerr, S., Kightley, S., Shewry, P., 2009. Identifying traits to improve the nitrogen economy of wheat: recent advances and future prospects. *Field Crops Research* 114, 329-342. doi:<https://doi.org/10.1016/j.fcr.2009.09.005>.

Foulkes, M.J., Murchie, E.H., 2011c. Optimizing canopy physiology traits to improve the nutrient utilization efficiency of crops.

Foulkes, M.J., Scott, R.K., Sylvester-Bradley, R., 2002. The ability of wheat cultivars to withstand drought in UK conditions: formation of grain yield. *The Journal of Agricultural Science* 138, 153-169. doi:<https://doi.org/10.1017/S0021859601001836>.

Foulkes, M.J., Slafer, G.A., Davies, W.J., Berry, P.M., Sylvester-Bradley, R., Martre, P., Calderini, D.F., Griffiths, S., Reynolds, M.P., 2011. Raising yield potential of wheat. III. Optimizing partitioning to grain while maintaining lodging resistance. *Journal of experimental botany* 62, 469-486. doi:<https://doi.org/10.1093/jxb/erq300>.

Foyer, C.H., Paul, M.J., 2001. Source-sink relationships. e LS.

Freeman, K.W., Girma, K., Teal, R.K., Arnall, D.B., Klatt, A., Raun, W.R., 2007. Winter Wheat Grain Yield and Grain Nitrogen as Influenced by Bed and Conventional Planting Systems. *Journal of Plant Nutrition* 30, 611-622. doi:10.1080/01904160701209378.

Furbank, R.T., Jimenez-Berni, J.A., George-Jaeggli, B., Potgieter, A.B., Deery, D.M., 2019. Field crop phenomics: enabling breeding for radiation use efficiency and biomass in cereal crops. *New Phytologist* 223, 1714-1727. doi:<http://10.1111/nph.15817>.

Gaju, O., 2007. Identifying physiological processes limiting genetic improvement of ear fertility in wheat. University of Nottingham.

Gaju, O., Allard, V., Martre, P., Snape, J.W., Heumez, E., LeGouis, J., Moreau, D., Bogard, M., Griffiths, S., Orford, S., Hubbart, S., Foulkes, M.J., 2011. Identification of traits to improve the nitrogen-use efficiency of wheat genotypes. *Field Crops Research* 123, 139-152. doi:<https://doi.org/10.1016/j.fcr.2011.05.010>.

Gaju, O., DeSilva, J., Carvalho, P., Hawkesford, M.J., Griffiths, S., Greenland, A., Foulkes, M.J., 2016. Leaf photosynthesis and associations with grain yield, biomass and nitrogen-use efficiency in landraces, synthetic-derived lines and cultivars in wheat. *Field Crops Research* 193, 1-15. doi:<https://doi.org/10.1016/j.fcr.2016.04.018>.

Gaju, O., Reynolds, M.P., Sparkes, D.L., Foulkes, M.J., 2009. Relationships between Large-Spike Phenotype, Grain Number, and Yield Potential in Spring Wheat. *Crop Science* 49, 961-973. doi:<https://doi.org/10.2135/cropsci2008.05.0285>.

Gale, M.D., Youssefian., S., 1985. Dwarfing genes in wheat Progress in Plant Breeding.

García-Rodríguez, A., García-Rodríguez, S., Díez-Mediavilla, M., Alonso-Tristán, C., 2020. Photosynthetic Active Radiation, Solar Irradiance and the CIE Standard Sky Classification. Applied Sciences 10, 8007.

García, G., Hasan, A., Puhl, L., Reynolds, M., Calderini, D., Miralles, D., 2013. Grain Yield Potential Strategies in an Elite Wheat Double-Haploid Population Grown in Contrasting Environments. Crop Science 53, 2577-2587. doi:<https://doi.org/10.2135/cropsci2012.11.0669>.

García, G.A., Serrago, R.A., González, F.G., Slafer, G.A., Reynolds, M.P., Miralles, D.J., 2014. Wheat grain number: Identification of favourable physiological traits in an elite doubled-haploid population. Field Crops Research 168, 126-134. doi:<https://doi.org/10.1016/j.fcr.2014.07.018>.

Geiger, D.R., 1994. General Lighting Requirements for Photosynthesis. International Lighting in Controlled Environments Workshop, pp. 3-18.

Gerard, G.S., Crespo-Herrera, L.A., Crossa, J., Mondal, S., Velu, G., Juliana, P., Huerta-Espino, J., Vargas, M., Rhandawa, M.S., Bhavani, S., Braun, H., Singh, R.P., 2020. Grain yield genetic gains and changes in physiological related traits for CIMMYT's High Rainfall Wheat Screening Nursery tested across international environments. Field Crops Research 249, 107742. doi:<https://doi.org/10.1016/j.fcr.2020.107742>.

Ghiglione, H.O., Gonzalez, F.G., Serrago, R., Maldonado, S.B., Chilcott, C., Curá, J.A., Miralles, D.J., Zhu, T., Casal, J.J., 2008. Autophagy regulated by day length determines the number of fertile florets in wheat. The Plant Journal 55, 1010-1024. doi:10.1111/j.1365-313X.2008.03570.x.

Gifford, R.M., Thorne, J.H., Hitz, W.D., Giaquinta, R.T., 1984. Crop Productivity and Photoassimilate Partitioning. Science 225, 801-808. doi:<https://doi.org/10.1126/science.225.4664.801>.

Godfray, H.C.J., Beddington, J.R., Crute, I.R., Haddad, L., Lawrence, D., Muir, J.F., Pretty, J., Robinson, S., Thomas, S.M., Toulmin, C., 2010. Food Security: The Challenge of Feeding 9 Billion People. Science 327, 812-818. doi:10.1126/science.1185383.

Gonzalez-Navarro, O.E., Griffiths, S., Molero, G., Reynolds, M.P., Slafer, G.A., 2016. Variation in developmental patterns among elite wheat lines and relationships with yield, yield components and spike fertility. Field Crops Research 196, 294-304. doi:<https://doi.org/10.1016/j.fcr.2016.07.019>.

González, F.G., Aldabe, M.L., Terrile, I.I., Rondanini, D.P., 2014. Grain Weight Response to Different Postflowering Source:Sink Ratios in Modern High-Yielding Argentinean Wheats Differing in Spike Fruiting Efficiency. Crop Science 54, 297-309. doi:<https://doi.org/10.2135/cropsci2013.03.0157>.

González, F.G., Slafer, G.A., Miralles, D.J., 2002. Vernalization and photoperiod responses in wheat pre-flowering reproductive phases. Field Crops Research 74, 183-195. doi:[https://doi.org/10.1016/S0378-4290\(01\)00210-6](https://doi.org/10.1016/S0378-4290(01)00210-6).

González, F.G., Terrile, I.I., Falcón, M.O., 2011. Spike Fertility and Duration of Stem Elongation as Promising Traits to Improve Potential Grain Number (and Yield): Variation in Modern Argentinean Wheats. Crop Science 51, 1693-1702. doi:<https://doi.org/10.2135/cropsci2010.08.0447>.

Goyne, P., Milroy, S., Lilley, J., Hare, J., 1993. Radiation interception, radiation use efficiency and growth of barley cultivars. Australian Journal of Agricultural Research 44, 1351-1366. doi:<https://doi.org/10.1071/AR9931351>.

Grassini, P., Eskridge, K.M., Cassman, K.G., 2013. Distinguishing between yield advances and yield plateaus in historical crop production trends. *Nature Communications* 4, 2918. doi:<https://doi.org/10.1038/ncomms3918>.

Green, C.F., 1987. Nitrogen nutrition and wheat growth in relation to absorbed solar radiation. *Agricultural and Forest Meteorology* 41, 207-248. doi:[https://doi.org/10.1016/0168-1923\(87\)90080-3](https://doi.org/10.1016/0168-1923(87)90080-3).

Gutiérrez-Rodríguez, M., Reynolds, M.P., Larqué-Saavedra, A., 2000. Photosynthesis of wheat in a warm, irrigated environment: II. Traits associated with genetic gains in yield. *Field Crops Research* 66, 51-62. doi:[https://doi.org/10.1016/S0378-4290\(99\)00078-7](https://doi.org/10.1016/S0378-4290(99)00078-7).

Hagemann, M., Weber, A.P.M., Eisenhut, M., 2016. Photorespiration: origins and metabolic integration in interacting compartments. *Journal of Experimental Botany* 67, 2915-2918. doi:<https://doi.org/10.1093/jxb/erw178>.

Hassan, I., Hussain, Z., Akbar, G., 2005. Effect of permanent raised beds on water productivity for irrigated maize-wheat cropping system. In: Roth, C.H., Fischer, R.A., Meisner, C.A. (Eds.), *Evaluation and Performance of Permanent Raised Bed Cropping Systems in Asia, Australia and Mexico*. ACIAR Proceeding Vol. 121, 59-65. doi:<https://aciarc.gov.au/publication/technical-publications/evaluation-and-performance-permanent-raised-bed-cropping-systems-asia-australia-and>.

Haun, J.R., 1973. Visual Quantification of Wheat Development1. *Agronomy Journal* 65, 116-119. doi:<https://doi.org/10.2134/agronj1973.00021962006500010035x>.

Hedden, P., 2003. The genes of the Green Revolution. *Trends in Genetics* 19, 5-9. doi:[https://doi.org/10.1016/S0168-9525\(02\)00009-4](https://doi.org/10.1016/S0168-9525(02)00009-4).

Hikosaka, K., 2005. Leaf canopy as a dynamic system: ecophysiology and optimality in leaf turnover. *Ann Bot* 95, 521-533. doi:10.1093/aob/mci050.

Hikosaka, K., 2014. Optimal nitrogen distribution within a leaf canopy under direct and diffuse light. *Plant, Cell & Environment* 37, 2077-2085. doi:<https://doi.org/10.1111/pce.12291>.

Hirose, T., 2004. Development of the Monsi–Saeki Theory on Canopy Structure and Function. *Annals of Botany* 95, 483-494. doi:<https://doi.org/10.1093/aob/mci047>.

Hirose, T., Werger, M.J.A., 1987. Maximizing Daily Canopy Photosynthesis with Respect to the Leaf Nitrogen Allocation Pattern in the Canopy. *Oecologia* 72, 520-526.

Hoogendoorn, J., Rickson, J.M., Gale, M.D., 1990. Differences in Leaf and Stem Anatomy Related to Plant Height of Tall and Dwarf Wheat (*Triticum aestivum* L.). *Journal of Plant Physiology* 136, 72-77. doi:[https://doi.org/10.1016/S0176-1617\(11\)81618-4](https://doi.org/10.1016/S0176-1617(11)81618-4).

Horton, P., 2000. Prospects for crop improvement through the genetic manipulation of photosynthesis: morphological and biochemical aspects of light capture. *Journal of Experimental Botany* 51, 475-485. doi:https://doi.org/doi:10.1093/jexbot/51.suppl_1.475.

Huang, X., Börner, A., Röder, M., Ganai, M., 2002. Assessing genetic diversity of wheat (*Triticum aestivum* L.) germplasm using microsatellite markers. *Theoretical and Applied Genetics* 105, 699-707. doi:10.1007/s00122-002-0959-4.

Hubbart, S., Peng, S., Horton, P., Chen, Y., Murchie, E.H., 2007. Trends in leaf photosynthesis in historical rice varieties developed in the Philippines since 1966. *Journal of Experimental Botany* 58, 3429-3438. doi:<https://doi.org/10.1093/jxb/erm192>.

Hyles, J., Bloomfield, M.T., Hunt, J.R., Trethowan, R.M., Trevaskis, B., 2020. Phenology and related traits for wheat adaptation. *Heredity* 125, 417-430. doi:10.1038/s41437-020-0320-1.

Innes, P., Blackwell, R.D., 2009. Some effects of leaf posture on the yield and water economy of winter wheat. *The Journal of Agricultural Science* 101, 367-376. doi:<https://doi.org/10.1017/S0021859600037680>.

- IPCC, 2014. Climate change 2014. IPCC.
- Iqbal, M.M., Khan, I., Sanauallah, M., Farooq, M., 2021. Influence of seed size on the growth, productivity, and water use efficiency of bread wheat planted by different methods. *Archives of Agronomy and Soil Science* 67, 354-370. doi:[10.1080/03650340.2020.1729979](https://doi.org/10.1080/03650340.2020.1729979).
- Isidro, J., Knox, R., Singh, A., Clarke, F., Krishna, P., DePauw, R., Clarke, J., Somers, D., 2012. Brassinosteroid leaf unrolling QTL mapping in durum wheat. *Planta* 236, 273-281. doi:<https://doi.org/10.1007/s00425-012-1603-4>.
- Jamieson, P.D., Martin, R.J., Francis, G.S., Wilson, D.R., 1995. Drought effects on biomass production and radiation-use efficiency in barley. *Field Crops Research* 43, 77-86. doi:[https://doi.org/10.1016/0378-4290\(95\)00042-0](https://doi.org/10.1016/0378-4290(95)00042-0).
- Jat, M.L., Gupta, R., Saharawat, Y.S., Khosla, R., 2011. Layering Precision Land Leveling and Furrow Irrigated Raised Bed Planting: Productivity and Input Use Efficiency of Irrigated Bread Wheat in Indo-Gangetic Plains. *American Journal of Plant Sciences* 2, 578-588. doi:<https://10.4236/ajps.2011.24069>.
- Jiang, G.M., Sun, J.Z., Liu, H.Q., Qu, C.M., Wang, K.J., Guo, R.J., Bai, K.Z., Gao, L.M., Kuang, T.Y., 2003. Changes in the rate of photosynthesis accompanying the yield increase in wheat cultivars released in the past 50 years. *Journal of Plant Research* 116, 347-354. doi:<https://doi.org/10.1007/s10265-003-0115-5>.
- Jobson, E.M., Johnston, R.E., Oiestad, A.J., Martin, J.M., Giroux, M.J., 2019. The Impact of the Wheat Rht-B1b Semi-Dwarfing Allele on Photosynthesis and Seed Development Under Field Conditions. *Frontiers in Plant Science* 10, 200-207. doi:<https://doi.org/10.3389/fpls.2019.00051>.
- Joshi, A.K., Kumari, M., Singh, V.P., Reddy, C.M., Kumar, S., Rane, J., Chand, R., 2007. Stay green trait: variation, inheritance and its association with spot blotch resistance in spring wheat (*Triticumaestivum* L.). *Euphytica* 153, 59-71. doi:<https://doi.org/10.1007/s10681-006-9235-z>.
- Kakar, K., Amanullah, J., Saleem, M., Iqbal, A., 2015. Effect of irrigation levels and planting methods on phenology, growth, biomass and harvest index of spring Wheat under semiarid condition. *Pure and Applied Biology* 4, 375-383. doi:<http://dx.doi.org/10.19045/bspab.2015.43013>.
- Kendal, E., 2019. Compare to Planting on Bed and Flad Surface Systems in Wheat and Barley. *Global Journal of Agricultural Innovation, Research & Development* 6, 1-10. doi:[10.15377/2409-9813.2019.06.1](https://doi.org/10.15377/2409-9813.2019.06.1).
- Kiliç, H., 2010. The effect of planting methods on yield and yield components of irrigated spring durum wheat varieties. *Scientific Research and Essays* 5, 3063-3069. doi:<https://doi.org/10.5897/SRE.9000899>.
- King, J., Grewal, S., Yang, C.-Y., Hubbart Edwards, S., Scholefield, D., Ashling, S., Harper, J.A., Allen, A.M., Edwards, K.J., Burridge, A.J., King, I.P., 2018. Introgression of *Aegilops speltoides* segments in *Triticum aestivum* and the effect of the gametocidal genes. *Annals of botany* 121, 229-240. doi:[10.1093/aob/mcx149](https://doi.org/10.1093/aob/mcx149).
- Kirby, E.J.M., 1988. Analysis of leaf, stem and ear growth in wheat from terminal spikelet stage to anthesis. *Field Crops Research* 18, 127-140. doi:[https://doi.org/10.1016/0378-4290\(88\)90004-4](https://doi.org/10.1016/0378-4290(88)90004-4).
- Kong, L.a., Wang, F., Feng, B., Li, S., Si, J., Zhang, B., 2010. A Root-Zone Soil Regime of Wheat: Physiological and Growth Responses to Furrow Irrigation in Raised Bed Planting in Northern China. *Agronomy Journal* 102, 154-162. doi:<https://doi.org/10.2134/agronj2009.0288>.
- Ku, L., Zhao, W., Zhang, J., Wu, L., Wang, C., Wang, P., Zhang, W., Chen, Y., 2010. Quantitative trait loci mapping of leaf angle and leaf orientation value in maize (*Zea mays*

- L.). *Theoretical and Applied Genetics* 121, 951-959. doi:<https://doi.org/DOI10.1007/s00122-010-1364-z>.
- Kukal, S., Humphreys, E., Saharawat, Y., Timsina, J., Sekhon, K., 2005. Performance of raised beds in rice-wheat systems of northwestern India. *ACIAR Proceedings No. 121*. In: Roth, C.H., Fischer, R.A., Meisner, C.A. (Eds.), 26-40.
- Kukal, S.S., Sudhir, Y., Humphreys, E., Amanpreet, K., Yadvinder, S., Thaman, S., Singh, B., Timsina, J., 2010. Factors affecting irrigation water savings in raised beds in rice and wheat. *Field Crops Research* 118, 43-50. doi:<https://doi.org/10.1016/j.fcr.2010.04.003>.
- Kumakov, V.A., Evdokimova, O.A., Buyanova, M.A., 2001. Dry Matter Partitioning between Plant Organs in Wheat Cultivars Differing in Productivity and Drought Resistance. *Russian Journal of Plant Physiology* 48, 359-363. doi:10.1023/A:1016670501685.
- Kumar, A., Sharma, K.D., Yadav, A., 2010. Enhancing yield and water productivity of wheat (*Triticum aestivum*) through furrow irrigated raised bed system in the Indo-Gangetic Plains of India. *Indian Journal of Agricultural Sciences* 80, 198-202.
- Ledent, J.F., 1978. Mechanisms Determining Leaf Movement and Leaf Angle in Wheat (*Triticum aestivum*L.). *Annals of Botany* 42, 345-351. doi:<https://doi.org/10.1093/oxfordjournals.aob.a085466>.
- Li, Q., Chen, Y., Liu, M., Zhou, X., Yu, S., Dong, B., 2008. Effects of irrigation and planting patterns on radiation use efficiency and yield of winter wheat in North China. *Agricultural Water Management* 95, 469-476. doi:<https://doi.org/10.1016/j.agwat.2007.11.010>.
- Li, Y., Song, G., Gao, J., Zhang, S., Zhang, R., Li, W., Chen, M., Liu, M., Xia, X., Risacher, T., Li, G., 2018. Enhancement of grain number per spike by RNA interference of cytokinin oxidase 2 gene in bread wheat. *Hereditas* 155, 33. doi:<https://doi.org/10.1186/s41065-018-0071-7>.
- Lichthardt, C., Chen, T.-W., Stahl, A., Stützel, H., 2020. Co-Evolution of Sink and Source in the Recent Breeding History of Winter Wheat in Germany. *Frontiers in Plant Science* 10. doi:<https://doi.org/10.3389/fpls.2019.01771>.
- Lim, P.O., Woo, H.R., Nam, H.G., 2003. Molecular genetics of leaf senescence in *Arabidopsis*. *Trends in Plant Science* 8, 272-278. doi:[https://doi.org/10.1016/S1360-1385\(03\)00103-1](https://doi.org/10.1016/S1360-1385(03)00103-1).
- Limon-Ortega, A., 2011. Planting System on Permanent Beds; A Conservation Agriculture Alternative for Crop Production in the Mexican Plateau. doi:<https://doi.org/10.13140/2.1.3612.0005>.
- Limon-Ortega, A., Sayre, K.D., Francis, C.A., 2000. Wheat Nitrogen Use Efficiency in a Bed Planting System in Northwest Mexico. *Agronomy Journal* 92, 303-308. doi:<https://doi.org/10.2134/agronj2000.922303x>.
- Lin, M.T., Occhialini, A., Andralojc, P.J., Parry, M.A.J., Hanson, M.R., 2014. A faster Rubisco with potential to increase photosynthesis in crops. *Nature* 513, 547-550. doi:10.1038/nature13776.
- Liu, K., Xu, H., Liu, G., Guan, P., Zhou, X., Peng, H., Yao, Y., Ni, Z., Sun, Q., Du, J., 2018. QTL mapping of flag leaf-related traits in wheat (*Triticum aestivum* L.). *Theoretical and Applied Genetics* 131, 839-849. doi:<https://doi.org/10.1007/s00122-017-3040-z>.
- Liu, Y., Li, M., Li, J., Li, X., Yang, X., Tong, Y., Zhang, A., Li, B., Lin, J., Kuang, T., Li, Z., 2009. Dynamic changes in flag leaf angle contribute to high photosynthetic capacity. *Chinese Science Bulletin* 54, 3045-3052. doi:<https://doi.org/10.1007/s11434-009-0470-2>.
- Lo Valvo, P.J., Miralles, D.J., Serrago, R.A., 2018. Genetic progress in Argentine bread wheat varieties released between 1918 and 2011: Changes in physiological and

numerical yield components. *Field Crops Research* 221, 314-321. doi:<https://doi.org/10.1016/j.fcr.2017.08.014>.

Long, S.P., ZHU, X.G., Naidu, S.L., Ort, D.R., 2006. Can improvement in photosynthesis increase crop yields? *Plant, Cell & Environment* 29, 315-330. doi:<https://doi.org/10.1111/j.1365-3040.2005.01493.x>.

Lopes, M.S., Reynolds, M.P., 2012. Stay-green in spring wheat can be determined by spectral reflectance measurements (normalized difference vegetation index) independently from phenology. *Journal of Experimental Botany* 63, 3789-3798. doi:<https://doi.org/10.1093/jxb/ers071>.

López-Castañeda, C., Molero, G., Reynolds, M., 2014. Genotypic variation in light interception and radiation use efficiency: A comparison of two different planting systems. In: Reynolds, M.P., Molero, G., Quilligan, E., Listman, M., Braun, H.J. (Eds.), *Proceedings of the 4th International Workshop of the Wheat Yield Consortium*, 187-195.

Luche, H.d.S., Silva, J.G.d., Nornberg, R., Zimmer, C.M., Arenhardt, E.G., Caetano, V.d.R., Maia, L.C.d., Oliveira, A.C.d., 2015. Stay-green effects on adaptability and stability in wheat. *African Journal of Agricultural Research* 10, 1142-1149. doi:<https://doi.org/10.5897/AJAR2013.9308>.

Majeed, A., Muhmood, A., Niaz, A., Javid, S., Ahmad, Z.A., Shah, S.S.H., Shah, A.H., 2015. Bed planting of wheat (*Triticum aestivum* L.) improves nitrogen use efficiency and grain yield compared to flat planting. *The Crop Journal* 3, 118-124. doi:<https://doi.org/10.1016/j.cj.2015.01.003>.

Maliba, B.G., Inbaraj, P.M., Berner, J.M., 2019. Photosynthetic Responses of Canola and Wheat to Elevated Levels of CO₂, O₃ and Water Deficit in Open-Top Chambers. *Plants (Basel)* 8, 171. doi:10.3390/plants8060171.

Man, J., Shi, Y., Yu, Z., Zhang, Y., 2015. Dry Matter Production, Photosynthesis of Flag Leaves and Water Use in Winter Wheat Are Affected by Supplemental Irrigation in the Huang-Huai-Hai Plain of China. *PloS one* 10, e0137274. doi:<https://doi.org/10.1371/journal.pone.0137274>.

Mann, C.C., 1999. Crop Scientists Seek a New Revolution. *Science* 283, 310-314. doi:10.1126/science.283.5400.310.

Mantilla-Perez, M.B., Bao, Y., Tang, L., Schnable, P.S., Salas-Fernandez, M.G., 2020. Toward “Smart Canopy” Sorghum: Discovery of the Genetic Control of Leaf Angle Across Layers. *Plant Physiology* 184, 1927-1940. doi:10.1104/pp.20.00632.

Mantilla-Perez, M.B., Salas Fernandez, M.G., 2017. Differential manipulation of leaf angle throughout the canopy: current status and prospects. *Journal of Experimental Botany* 68, 5699-5717. doi:<https://doi.org/10.1093/jxb/erx378>.

Marcelis, L.F., 1996. Sink strength as a determinant of dry matter partitioning in the whole plant. *J Exp Bot* 47 Spec No, 1281-1291. doi:https://doi.org/10.1093/jxb/47.Special_Issue.1281.

Mathan, J., Bhattacharya, J., Ranjan, A., 2016. Enhancing crop yield by optimizing plant developmental features. *Development* 143, 3283-3294. doi:10.1242/dev.134072.

Maydup, M.L., Antonietta, M., Guiamet, J.J., Graciano, C., López, J.R., Tambussi, E.A., 2010. The contribution of ear photosynthesis to grain filling in bread wheat (*Triticum aestivum* L.). *Field Crops Research* 119, 48-58. doi:<https://doi.org/10.1016/j.fcr.2010.06.014>.

McAusland, L., Violet-Chabrand, S., Jauregui, I., Burridge, A., Hubbart-Edwards, S., Fryer, M.J., King, I.P., King, J., Pyke, K., Edwards, K.J., Carmo-Silva, E., Lawson, T., Murchie, E.H., 2020. Variation in key leaf photosynthetic traits across wheat wild relatives is accession dependent not species dependent. *New Phytologist* 228, 1767-1780. doi:<https://doi.org/10.1111/nph.16832>.

Meleha, A.M.I., Hassan, A.F., El-Bialy, M.A., El-Mansoury, M.A.M., 2020. Effect of Planting Dates and Planting Methods on Water Relations of Wheat. *International Journal of Agronomy* 2020, 8864143. doi:10.1155/2020/8864143.

Merah, O., Monneveux, P., 2015. Contribution of Different Organs to Grain Filling in Durum Wheat under Mediterranean Conditions I. Contribution of Post-Anthesis Photosynthesis and Remobilization. *Journal of Agronomy and Crop Science* 201, 344-352. doi:<https://doi.org/10.1111/jac.12109>.

Merry, A., Acuna, T., Riffkin, P., Richards, R., 2017. Can leaf architecture improve crop biomass and yield in wheat? 18th Australian Agronomy Conference 2017, 1-4.

Miralles, D., Slafer, G., 2007. Sink limitations to yield in wheat : how could it be reduced? *J. Agric. Sci.* 145. doi:<https://doi.org/10.1017/S0021859607006752>

Miralles, D.J., Katz, S.D., Colloca, A., Slafer, G.A., 1998. Floret development in near isogenic wheat lines differing in plant height. *Field Crops Research* 59, 21-30. doi:[https://doi.org/10.1016/S0378-4290\(98\)00103-8](https://doi.org/10.1016/S0378-4290(98)00103-8).

Miralles, D.J., Slafer, G.A., 1995. Yield, biomass and yield components in dwarf, semi-dwarf and tall isogenic lines of spring wheat under recommended and late sowing dates. *Plant Breeding* 114, 392-396. doi:<https://doi.org/10.1111/j.1439-0523.1995.tb00818.x>.

Moeller, C., Evers, J.B., Rebetzke, G., 2014. Canopy architectural and physiological characterization of near-isogenic wheat lines differing in the tiller inhibition gene tin. *Frontiers in Plant Science* 5. doi:10.3389/fpls.2014.00617.

Molero, G., Joynson, R., Pinera-Chavez, F.J., Gardiner, L.-J., Rivera-Amado, C., Hall, A., Reynolds, M.P., 2019. Elucidating the genetic basis of biomass accumulation and radiation use efficiency in spring wheat and its role in yield potential. *Plant Biotechnology Journal* 17, 1276-1288. doi:<https://doi.org/10.1111/pbi.13052>.

Molero, G., Reynolds, M.P., 2020. Spike photosynthesis measured at high throughput indicates genetic variation independent of flag leaf photosynthesis. *Field Crops Research* 255, 107866. doi:<https://doi.org/10.1016/j.fcr.2020.107866>.

Moll, R., Kamprath, E., Jackson, W., 1982. Analysis and interpretation of factors which contribute to efficiency of nitrogen utilization. *Agronomy Journal* 74, 562-564. doi:<https://doi.org/10.2134/agronj1982.00021962007400030037x>.

Mollah, M., Bhuiya, M., Kabir, M.H., 2009. Bed Planting—A New Crop Establishment Method for Wheat in Rice-Wheat Cropping System. doi:<https://doi.org/10.3329/jard.v7i1.4418>.

Monsi, M., 1953. *Über den Lichtfaktor in den Pflanzengesellschaften und seine Bedeutung für die Stoffproduktion.*

Monteith, J.L., 1969. Light interception and radiative exchange in crop stands. *Physiological aspects of crop yield*, 89-111. doi:<https://doi.org/10.2135/1969.physiologicalaspects.c9>.

Monteith, J.L., 1977. Climate and the efficiency of crop production in Britain. *Philosophical Transactions of the Royal Society of London. B, Biological Sciences* 281, 277-294. doi:<https://doi.org/10.1098/rstb.1977.0140>.

Monteith, J.L., Moss, C., 1977. Climate and the efficiency of crop production in Britain. *Philosophical Transactions of the Royal Society of London B: Biological Sciences* 281, 277-294. doi:<https://doi.org/10.1098/rstb.1977.0140>.

Moreau, D., Allard, V., Gaju, O., Le Gouis, J., Foulkes, M.J., Martre, P., 2012. Acclimation of Leaf Nitrogen to Vertical Light Gradient at Anthesis in Wheat Is a Whole-Plant Process That Scales with the Size of the Canopy. *Plant Physiology* 160, 1479-1490. doi:10.1104/pp.112.199935.

Morgan, J.A., LeCain, D.R., Wells, R., 1990. Semidwarfing Genes Concentrate Photosynthetic Machinery and Affect Leaf Gas Exchange of Wheat. *Crop Science* 30, crops1990.0011183X003000030027x.

doi:<https://doi.org/10.2135/cropsci1990.0011183X003000030027xa>.

Murchie, Reynolds, 2012. Crop Radiation Capture and Use Efficiency. In: Christou P., Savin R., Costa-Pierce B.A., Misztal I., Whitelaw C.B.A. (eds) *Sustainable Food Production*. Springer, New York, NY. doi:https://doi.org/10.1007/978-1-4614-5797-8_171.

Murchie, E., Pinto, M., Horton, P., 2009. Agriculture and the new challenges for photosynthesis research. *New Phytologist* 181, 532-552. doi:<https://doi.org/10.1111/j.1469-8137.2008.02705.x>.

Murchie E., Reynolds M., 2012. Crop radiation capture and use efficiency. RA Meyers, *Encyclopedia of Sustainability Science and Technology*. Springer, New York, 2615-2638. doi:https://doi.org/10.1007/978-1-4614-5797-8_171.

Murchie, E.H., Chen, Y.-z., Hubbart, S., Peng, S., Horton, P., 1999. Interactions between Senescence and Leaf Orientation Determine in Situ Patterns of Photosynthesis and Photoinhibition in Field-Grown Rice. *Plant Physiology* 119, 553-564. doi:<https://doi.org/10.1104/pp.119.2.553>

Murchie, E.H., Niyogi, K.K., 2010. Manipulation of Photoprotection to Improve Plant Photosynthesis. *Plant Physiology* 155, 86-92. doi:<https://doi.org/10.1104/pp.110.168831>.

Muurinen, S., Peltonen-Sainio, P., 2006. Radiation-use efficiency of modern and old spring cereal cultivars and its response to nitrogen in northern growing conditions. *Field Crops Research* 96, 363-373. doi:<https://doi.org/10.1016/j.fcr.2005.08.009>.

Muurinen, S., Slafer, G.A., Peltonen-Sainio, P., 2006. Breeding Effects on Nitrogen Use Efficiency of Spring Cereals under Northern Conditions. *Crop Science* 46, 561-568. doi:<https://doi.org/10.2135/cropsci2005-05-0046>.

Nations, U., 2011. World population to reach 10 billion by 2100 it fertility in all countries converges to replacement level., pp. 635-635.

Nelson, G.C., Rosegrant, M.W., Koo, J., Robertson, R., Sulser, T., Zhu, T., Ringler, C., Msangi, S., Palazzo, A., Batka, M., 2009. Climate change: Impact on agriculture and costs of adaptation. *Intl Food Policy Res Inst*.

Niinemets, Ü., 2007. Photosynthesis and resource distribution through plant canopies. *Plant, Cell & Environment* 30, 1052-1071. doi:<https://doi.org/10.1111/j.1365-3040.2007.01683.x>.

Nobel, P., Forseth, I., Long, S., 1993. Canopy structure and light interception. *Photosynthesis and production in a changing environment*, Springer, 79-90.

Noorka, I., Tabasum, S., 2013. Performance of Raised Beds and Conventional Planting Method for Wheat (*Triticum Aestivum* L.) Cultivation in Punjab, Pakistan. *Sustainable Food Security in the Era of Local and Global Environmental Change*, 321-335. doi:https://doi.org/10.1007/978-94-007-6719-5_20.

O'Connell, M.G., O'Leary, G.J., Whitfield, D.M., Connor, D.J., 2004. Interception of photosynthetically active radiation and radiation-use efficiency of wheat, field pea and mustard in a semi-arid environment. *Field Crops Research* 85, 111-124. doi:[https://doi.org/10.1016/S0378-4290\(03\)00156-4](https://doi.org/10.1016/S0378-4290(03)00156-4).

Ochagavía, H., Prieto, P., Savin, R., Griffiths, S., Slafer, G., 2018. Dynamics of leaf and spikelet primordia initiation in wheat as affected by Ppd-1a alleles under field conditions. *Journal of Experimental Botany* 69, 2621-2631. doi:10.1093/jxb/ery104.

Ort, D.R., Merchant, S.S., Alric, J., Barkan, A., Blankenship, R.E., Bock, R., Croce, R., Hanson, M.R., Hibberd, J.M., Long, S.P., Moore, T.A., Moroney, J., Niyogi, K.K., Parry, M.A.J., Peralta-Yahya, P.P., Prince, R.C., Redding, K.E., Spalding, M.H., van Wijk, K.J.,

Vermaas, W.F.J., von Caemmerer, S., Weber, A.P.M., Yeates, T.O., Yuan, J.S., Zhu, X.G., 2015. Redesigning photosynthesis to sustainably meet global food and bioenergy demand. *Proceedings of the National Academy of Sciences* 112, 8529-8536. doi:<https://doi.org/10.1073/pnas.1424031112>.

Ort, D.R., Zhu, X., Melis, A., 2010. Optimizing Antenna Size to Maximize Photosynthetic Efficiency. *Plant Physiology* 155, 79-85. doi:10.1104/pp.110.165886.

Ortiz-Monasterio, R., Sayre, K., Rajaram, S., McMahon, M., 1997. Genetic progress in wheat yield and nitrogen use efficiency under four nitrogen rates. *Crop Science* 37, 898-904.

Parkhurst D.F., OL., L., 1972. OPTIMAL LEAF SIZE IN RELATION TO ENVIRONMENT *Journal of Ecology* 60, 505-537.

Parry, M., Madgwick, P., Carvalho, J., Andralojc, P., 2007. Prospects for increasing photosynthesis by overcoming the limitations of Rubisco. *The Journal of Agricultural Science* 145, 31.

Parry, M.A., Andralojc, P.J., Scales, J.C., Salvucci, M.E., Carmo-Silva, A.E., Alonso, H., Whitney, S.M., 2013. Rubisco activity and regulation as targets for crop improvement. *J Exp Bot* 64, 717-730. doi:<https://doi.org/10.1093/jxb/ers336>.

Parry, M.A.J., Reynolds, M., Salvucci, M.E., Raines, C., Andralojc, P.J., Zhu, X.-G., Price, G.D., Condon, A.G., Furbank, R.T., 2011. Raising yield potential of wheat. II. Increasing photosynthetic capacity and efficiency. *Journal of Experimental Botany* 62, 453-467. doi:<https://doi.org/10.1093/jxb/erq304>.

Pask, A., Pietragalla, J., Mullan, D.M., Reynolds, M., 2012a. Physiological breeding II. a field guide to wheat phenotyping CIMMYT, Mexico, DF (Mexico). doi:<https://doi.org/10.1017/CB09781107415324.004>.

Pask, A., Pietragalla, J., Mullan, D.M., Reynolds, M., 2012b. Physiological breeding II: a field guide to wheat phenotyping. CIMMYT, Mexico, DF (Mexico). doi:<https://doi.org/10.1017/CBO9781107415324.004>.

Pask, A.J.D., Sylvester-Bradley, R., Jamieson, P.D., Foulkes, M.J., 2012c. Quantifying how winter wheat crops accumulate and use nitrogen reserves during growth. *Field Crops Research* 126, 104-118. doi:<https://doi.org/10.1016/j.fcr.2011.09.021>.

Patra, S., Sahoo, S., Mishra, P., Mahapatra, S.C., 2018. Impacts of urbanization on land use /cover changes and its probable implications on local climate and groundwater level. *Journal of Urban Management* 7, 70-84. doi:<https://doi.org/10.1016/j.jum.2018.04.006>.

Pearcy, R.W., 1990. Sunflecks and photosynthesis in plant canopies. *Annual review of plant biology* 41, 421-453. doi:<https://doi.org/10.1146/annurev.pp.41.060190.002225>.

Pendleton, J.W., Smith, G.E., Winter, S.R., Johnston, T.J., 1968. Field Investigations of the Relationships of Leaf Angle in Corn (*Zea mays* L.) to Grain Yield and Apparent Photosynthesis I. *Agronomy Journal* 60, 422-424. doi:<https://doi.org/10.2134/agronj1968.00021962006000040027x>.

Peng, S., Cassman, K.G., Kropff, M.J., 1995. Relationship between leaf photosynthesis and nitrogen content of field-grown rice in tropics. *Crop science* 35, 1627-1630. doi:<https://doi.org/10.2135/cropsci1995.0011183X003500060018x>.

Peng, S., Khush, G.S., Virk, P., Tang, Q., Zou, Y., 2008. Progress in ideotype breeding to increase rice yield potential. *Field Crops Research* 108, 32-38. doi:<https://doi.org/10.1016/j.fcr.2008.04.001>.

Perdomo, J.A., Buchner, P., Carmo-Silva, E., 2021. The relative abundance of wheat Rubisco activase isoforms is post-transcriptionally regulated. *Photosynthesis Research* 148, 47-56. doi:10.1007/s11120-021-00830-6.

Piñera-Chavez, F.J., Berry, P.M., Foulkes, M.J., Molero, G., Reynolds, M.P., 2016. Avoiding lodging in irrigated spring wheat. II. Genetic variation of stem and root structural properties. *Field Crops Research* 196, 64-74. doi:<https://doi.org/10.1016/j.fcr.2016.06.007>.

Preece, C., Livarda, A., Christin, P.-A., Wallace, M., Martin, G., Charles, M., Jones, G., Rees, M., Osborne, C.P., 2017. How did the domestication of Fertile Crescent grain crops increase their yields? *Functional ecology* 31, 387-397. doi:[10.1111/1365-2435.12760](https://doi.org/10.1111/1365-2435.12760).

Price, G.D., Pengelly, J.J.L., Forster, B., Du, J., Whitney, S.M., von Caemmerer, S., Badger, M.R., Howitt, S.M., Evans, J.R., 2012. The cyanobacterial CCM as a source of genes for improving photosynthetic CO₂ fixation in crop species. *Journal of Experimental Botany* 64, 753-768. doi:[https://10.1093/jxb/ers257](https://doi.org/10.1093/jxb/ers257).

Qingfeng, S., Chengcai, C., J., P.M.A., Xin-Guang, Z., 2016. Genetics-based dynamic systems model of canopy photosynthesis: the key to improve light and resource use efficiencies for crops. *Food and Energy Security* 5, 18-25. doi:<https://doi.org/doi:10.1002/fes3.74>.

Quanqi, L., Xunbo, Z., Yuhai, C., Songlie, Y., 2012. Water consumption characteristics of winter wheat grown using different planting patterns and deficit irrigation regime. *Agricultural Water Management* 105, 8-12. doi:<https://doi.org/10.1016/j.agwat.2011.12.015>.

Quintero, A., Molero, G., Reynolds, M.P., Calderini, D.F., 2018. Trade-off between grain weight and grain number in wheat depends on GxE interaction: A case study of an elite CIMMYT panel (CIMCOG). *European Journal of Agronomy* 92, 17-29. doi:<https://doi.org/10.1016/j.eja.2017.09.007>.

Ram, H., Singh, Y.-S., Timsina, J., Humphreys, E., Dhillon, S.S., Kumar, K., 2005. Performance of upland crops on beds in North-west India. In: Roth, C.H., Fischer, R.A., Meisner, C.A. (Eds.), *Evaluation and Performance of Permanent Raised Bed Cropping Systems in Asia, Australia and Mexico*. ACIAR Proceeding Vol. 121, 41-58. doi:<https://aciarc.gov.au/publication/technical-publications/evaluation-and-performance-permanent-raised-bed-cropping-systems-asia-australia-and>.

Ray, D.K., Mueller, N.D., West, P.C., Foley, J.A., 2013. Yield Trends Are Insufficient to Double Global Crop Production by 2050. *PLoS one* 8, e66428. doi:<https://doi.org/10.1371/journal.pone.0066428>.

Ray, D.K., Ramankutty, N., Mueller, N.D., West, P.C., Foley, J.A., 2012. Recent patterns of crop yield growth and stagnation. *Nature Communications* 3, 1293. doi:<https://doi.org/10.1038/ncomms2296>.

Rebetzke, G.J., Bonnett, D.G., Reynolds, M.P., 2016a. Awns reduce grain number to increase grain size and harvestable yield in irrigated and rainfed spring wheat. *Journal of Experimental Botany* 67, 2573-2586. doi:<https://doi.org/10.1093/jxb/erw081>.

Rebetzke, G.J., Jimenez-Berni, J.A., Bovill, W.D., Deery, D.M., James, R.A., 2016b. High-throughput phenotyping technologies allow accurate selection of stay-green. *Journal of Experimental Botany* 67, 4919-4924. doi:<https://doi.org/10.1093/jxb/erw301>.

Reynolds, M., 1996. Increasing yield potential in wheat: breaking the barriers: proceedings of a workshop held in Ciudad Obregón, Sonora, Mexico. CIMMYT.

Reynolds, M., Chapman, S., Crespo-Herrera, L., Molero, G., Mondal, S., Pequeno, D.N.L., Pinto, F., Pinera-Chavez, F.J., Poland, J., Rivera-Amado, C., Saint Pierre, C., Sukumaran, S., 2020. Breeder friendly phenotyping. *Plant Science* 295, 110396. doi:<https://doi.org/10.1016/j.plantsci.2019.110396>.

Reynolds, M., Foulkes, J., Furbank, R., Griffiths, S., King, J., Murchie, E., Parry, M., Slafer, G., 2012a. Achieving yield gains in wheat. *Plant, Cell & Environment* 35, 1799-1823. doi:<https://doi.org/10.1111/j.1365-3040.2012.02588.x>.

Reynolds, M., Foulkes, M.J., Slafer, G.A., Berry, P., Parry, M.A., Snape, J.W., Angus, W.J., 2009. Raising yield potential in wheat. *Journal of Experimental Botany* 60, 1899-1918. doi:<https://doi.org/10.1093/jxb/erp016>.

Reynolds, M., Pask, A., Mullan, D., 2012b. Physiological Breeding I: Interdisciplinary Approaches to Improve Crop Production.

Reynolds, M., Pfeiffer, W., 2000. Applying physiological strategies to improve yield potential. Durum wheat improvement in the Mediterranean region: New challenges. *Options Méditerranéennes* 40, 95-103. doi: <https://om.ciheam.org/om/pdf/a40/00600010.pdf>.

Reynolds, M.P., Calderini, D.F., Condon, A.G., Rajaram, S., 2001. Physiological basis of yield gains in wheat associated with the LR19 translocation from *Agropyron elongatum*. *Euphytica* 119, 139-144. doi:10.1023/A:1017521800795.

Reynolds, M.P., Gutiérrez-Rodríguez, M., Larqué-Saavedra, A.F., 2000a. Photosynthesis of wheat in a warm, irrigated environment: I: Genetic diversity and crop productivity. *Field Crops Research* 66, 37-50. doi:[https://doi.org/10.1016/S0378-4290\(99\)00077-5](https://doi.org/10.1016/S0378-4290(99)00077-5).

Reynolds, M.P., Pask, A.J.D., Hoppitt, W.J.E., Sonder, K., Sukumaran, S., Molero, G., Pierre, C.S., Payne, T., Singh, R.P., Braun, H.J., Gonzalez, F.G., Terrile, I.I., Barma, N.C.D., Hakim, A., He, Z., Fan, Z., Novoselovic, D., Maghraby, M., Gad, K.I.M., Galal, E.G., Hagra, A., Mohamed, M.M., Morad, A.F.A., Kumar, U., Singh, G.P., Naik, R., Kalappanavar, I.K., Biradar, S., Sai Prasad, S.V., Chatrath, R., Sharma, I., Panchabhai, K., Sohu, V.S., Mavi, G.S., Mishra, V.K., Balasubramaniam, A., Jalal-Kamali, M.R., Khodarahmi, M., Dastfal, M., Tabib-Ghaffari, S.M., Jafarby, J., Nikzad, A.R., Moghaddam, H.A., Ghogh, H., Mehraban, A., Solís-Moya, E., Camacho-Casas, M.A., Figueroa-López, P., Ireta-Moreno, J., Alvarado-Padilla, J.I., Borbón-Gracia, A., Torres, A., Quiche, Y.N., Upadhyay, S.R., Pandey, D., Imtiaz, M., Rehman, M.U., Hussain, M., Hussain, M., Ud-Din, R., Qamar, M., Sohail, M., Mujahid, M.Y., Ahmad, G., Khan, A.J., Sial, M.A., Mustatea, P., von Well, E., Ncala, M., de Groot, S., Hussein, A.H.A., Tahir, I.S.A., Idris, A.A.M., Elamein, H.M.M., Manes, Y., Joshi, A.K., 2017. Strategic crossing of biomass and harvest index—source and sink—achieves genetic gains in wheat. *Euphytica* 213, 257. doi:<https://doi.org/10.1007/s10681-017-2040-z>.

Reynolds, M.P., Pellegrineschi, A., Skovmand, B., 2005. Sink-limitation to yield and biomass: a summary of some investigations in spring wheat. *Annals of Applied Biology* 146, 39-49. doi:<https://doi.org/10.1111/j.1744-7348.2005.03100.x>.

Reynolds, M.P., Rajaram, S., Sayre, K.D., 1999. Physiological and Genetic Changes of Irrigated Wheat in the Post-Green Revolution Period and Approaches for Meeting Projected Global Demand. *Crop Science* 39, 1611-1621. doi:<https://doi.org/10.2135/cropsci1999.3961611x>.

Reynolds, M.P., van Ginkel, M., Ribaut, J.M., 2000b. Avenues for genetic modification of radiation use efficiency in wheat. *Journal of Experimental Botany* 51, 459-473. doi:https://doi.org/10.1093/jexbot/51.suppl_1.459.

Richards, R., 1996. Increasing the yield potential of wheat: manipulating sources and sinks. *Increasing yield potential in wheat: breaking the barriers*, 134-149.

Richards, R., Lukacs, Z., 2002. Seedling vigour in wheat—sources of variation for genetic and agronomic improvement. *Australian Journal of Agricultural Research* 53, 41-50. doi:<https://doi.org/10.1071/AR00147>.

Richards, R.A., 2000. Selectable traits to increase crop photosynthesis and yield of grain crops. *Journal of Experimental Botany* 51, 447-458. doi:https://doi.org/10.1093/jexbot/51.suppl_1.447.

Richards, R.A., Cavanagh, C.R., Riffkin, P., 2019. Selection for erect canopy architecture can increase yield and biomass of spring wheat. *Field Crops Research* 244, 107649. doi:<https://doi.org/10.1016/j.fcr.2019.107649>.

Rivera-Amado, A.C., 2015. Identifying physiological traits to optimize assimilate partitioning and spike fertility for yield potential in wheat (*Triticum aestivum* L.) genotypes.,

PhD thesis. University of Nottingham School of Biosciences, Bonnington Campus, Leicestershire, UK, .

Rivera-Amado, C., Molero, G., Trujillo-Negrellos, E., Reynolds, M., Foulkes, J., 2020. Estimating Organ Contribution to Grain Filling and Potential for Source Upregulation in Wheat Cultivars with a Contrasting Source–Sink Balance. *Agronomy* 10, 1527. doi:<https://doi.org/10.3390/agronomy10101527>.

Rivera-Amado, C., Trujillo-Negrellos, E., Molero, G., Reynolds, M.P., Sylvester-Bradley, R., Foulkes, M.J., 2019. Optimizing dry-matter partitioning for increased spike growth, grain number and harvest index in spring wheat. *Field Crops Research* 240, 154-167. doi:<https://doi.org/10.1016/j.fcr.2019.04.016>.

Robles-Zazueta, C.A., Molero, G., Pinto, F., Foulkes, M.J., Reynolds, M.P., Murchie, E.H., 2021. Field-based remote sensing models predict radiation use efficiency in wheat. *Journal of Experimental Botany* 72, 3756-3773. doi:<https://10.1093/jxb/erab115>.

Sadras, V., Lawson, C., Montoro, A., 2012. Photosynthetic traits of Australian wheat varieties released between 1958 and 2007. *Field Crops Research* 62, <http://dx.doi.org/10.1016/j.fcr.2012.1004.1012>. doi:<https://doi.org/10.1016/j.fcr.2012.04.012>.

Sadras, V.O., Lawson, C., 2011. Genetic gain in yield and associated changes in phenotype, trait plasticity and competitive ability of South Australian wheat varieties released between 1958 and 2007. *Crop and Pasture Science* 62, 533-549. doi:<https://doi.org/10.1071/CP11060>.

Saeki, T., 1960. Interrelationships between Leaf Amount, Light Distribution and Total Photosynthesis in a Plant Community. *Shokubutsugaku Zasshi* 73, 55-63. doi:<https://doi.org/10.15281/jplantres1887.73.55>.

Saisho, D., Tanno, K.-i., Chono, M., Honda, I., Kitano, H., Takeda, K., 2004. Spontaneous brassinolide-insensitive barley mutants 'uzu' adapted to East Asia. *Breeding Science* 54, 409-416. doi:<https://doi.org/10.1270/JSBBS.54.409>.

Sakamoto, T., Morinaka, Y., Ohnishi, T., Sunohara, H., Fujioka, S., Ueguchi-Tanaka, M., Mizutani, M., Sakata, K., Takatsuto, S., Yoshida, S., Tanaka, H., Kitano, H., Matsuoka, M., 2006. Erect leaves caused by brassinosteroid deficiency increase biomass production and grain yield in rice. *Nature Biotechnology* 24, 105-109. doi:<https://doi.org/10.1038/nbt1173>.

Salamini, F., Özkan, H., Brandolini, A., Schäfer-Pregl, R., Martin, W., 2002. Genetics and geography of wild cereal domestication in the near east. *Nature Reviews Genetics* 3, 429-441. doi:10.1038/nrg817.

Sanchez-Bragado, R., Molero, G., Reynolds, M.P., Araus, J.L., 2014. Relative contribution of shoot and ear photosynthesis to grain filling in wheat under good agronomical conditions assessed by differential organ $\delta^{13}C$. *J Exp Bot* 65, 5401-5413. doi:<https://doi.org/10.1093/jxb/eru298>.

Sanchez-Bragado, R., Molero, G., Reynolds, M.P., Araus, J.L., 2016. Photosynthetic contribution of the ear to grain filling in wheat: a comparison of different methodologies for evaluation. *Journal of Experimental Botany* 67, 2787-2798. doi:<https://10.1093/jxb/erw116>.

Savin, R., Slafer, G.A., 1991. Shading effects on the yield of an Argentinian wheat cultivar. *The Journal of Agricultural Science* 116, 1-7. doi:<https://doi.org/10.1017/S0021859600076085>.

Sayre, K., Limon-Ortega, A., Gupta, R., 2008. Raised Bed Planting Technologies for Improved Efficiency, Sustainability and Profitability In: Reynolds, M.P., Pietragalla, J., Braun, H.J. (Eds.), *International Symposium on Wheat Yield Potential: Challenges to International Wheat Breeding*. Mexico, DF.: CIMMYT, 148-160. doi:<https://repository.cimmyt.org/handle/10883/1259>.

Sayre, K., Limon, A., Govaerts, B., 2005. Experiences with permanent bed planting systems CIMMYT, Mexico. In: Roth, C.H., Fischer, R.A., Meisner, C.A. (Eds.), Evaluation and Performance of Permanent Raised Bed Cropping Systems in Asia, Australia and Mexico. ACIAR Proceeding Vol. 121, 12-25. doi:<https://aciarcg.org/publication/technical-publications/evaluation-and-performance-permanent-raised-bed-cropping-systems-asia-australia-and>.

Sayre, K., Rajaram, S., Fischer, R., 1997. Yield potential progress in short bread wheats in northwest Mexico. *Crop science* 37, 36-42. doi:<https://doi.org/10.2135/cropsci1997.0011183X003700010006x>.

Sayre, K.D., Moreno Ramos, O.H., 1997. Applications of raised-bed planting systems to wheat. Mexico, Mexico.

Schaller, G.E., Street, I.H., Kieber, J.J., 2014. Cytokinin and the cell cycle. *Current Opinion in Plant Biology* 21, 7-15. doi:<https://doi.org/10.1016/j.pbi.2014.05.015>.

Schuler, M.L., Mantegazza, O., Weber, A.P.M., 2016. Engineering C4 photosynthesis into C3 chassis in the synthetic biology age. *The Plant Journal* 87, 51-65. doi:<https://doi.org/10.1111/tpj.13155>.

Shah, L., Yahya, M., Shah, S.M.A., Nadeem, M., Ali, A., Ali, A., Wang, J., Riaz, M.W., Rehman, S., Wu, W., Khan, R.M., Abbas, A., Riaz, A., Anis, G.B., Si, H., Jiang, H., Ma, C., 2019. Improving Lodging Resistance: Using Wheat and Rice as Classical Examples. *Int J Mol Sci* 20, 4211. doi:10.3390/ijms20174211.

Sharwood, R.E., Ghannoum, O., Whitney, S.M., 2016. Prospects for improving CO₂ fixation in C₃-crops through understanding C₄-Rubisco biogenesis and catalytic diversity. *Current Opinion in Plant Biology* 31, 135-142. doi:<https://doi.org/10.1016/j.pbi.2016.04.002>.

Shearman, V., Sylvester-Bradley, R., Scott, R., Foulkes, M., 2005. Physiological processes associated with wheat yield progress in the UK. *Crop Science* 45, 175-185. doi:<https://doi.org/10.2135/cropsci2005.0175a>.

Shearman, V.J., 2001. Changes in the yield limiting processes associated with the yield improvement of wheat. University of Nottingham, UK.

Shewry, P.R., 2009. Wheat. *Journal of Experimental Botany* 60, 1537-1553. doi:<https://doi.org/10.1093/jxb/erp058>.

Shewry, P.R., Hey, S.J., 2015. The contribution of wheat to human diet and health. *Food and energy security* 4, 178-202. doi:10.1002/fes3.64.

Shiferaw, B., Smale, M., Braun, H.-J., Duveiller, E., Reynolds, M., Muricho, G., 2013. Crops that feed the world 10. Past successes and future challenges to the role played by wheat in global food security. *Food Security* 5, 291-317. doi:<https://doi.org/10.1007/s12571-013-0263-y>.

Shrestha, R., Matteis, L., Skofic, M., Portugal, A., McLaren, G., Hyman, G., Arnaud, E., 2012. Bridging the phenotypic and genetic data useful for integrated breeding through a data annotation using the Crop Ontology developed by the crop communities of practice. *Frontiers in physiology* 3, 326-326. doi:10.3389/fphys.2012.00326.

Siddique, K., Belford, R., Perry, M., Tennant, D., 1989a. Growth, development and light interception of old and modern wheat cultivars in a Mediterranean-type environment. *Australian Journal of Agricultural Research* 40, 473-487. doi:<https://doi.org/10.1071/AR9890473>.

Siddique, K.H.M., Kirby, E.J.M., Perry, M.W., 1989b. Ear: Stem ratio in old and modern wheat varieties; relationship with improvement in number of grains per ear and yield. *Field Crops Research* 21, 59-78. doi:[https://doi.org/10.1016/0378-4290\(89\)90041-5](https://doi.org/10.1016/0378-4290(89)90041-5).

Sierra-Gonzalez, A., Molero, G., Rivera-Amado, C., Babar, M.A., Reynolds, M.P., Foulkes, M.J., 2021. Exploring genetic diversity for grain partitioning traits to enhance yield

in a high biomass spring wheat panel. *Field Crops Research* 260, 107979. doi:<https://doi.org/10.1016/j.fcr.2020.107979>.

Silva-Pérez, V., De Faveri, J., Molero, G., Deery, D.M., Condon, A.G., Reynolds, M.P., Evans, J.R., Furbank, R.T., 2019. Genetic variation for photosynthetic capacity and efficiency in spring wheat. *Journal of Experimental Botany* 71, 2299-2311. doi:<https://doi.org/10.1093/jxb/erz439>.

Simmons, S.R., Oelke, E.A., Anderson, P.M., 1985. *Growth and Development Guide for Spring Wheat*. St. Paul, MN: University of Minnesota Agricultural Extension Service.

Sinclair, T.R., Muchow, R.C., 1999. Radiation Use Efficiency. *Advances in Agronomy* 65, 215-265. doi:[https://doi.org/10.1016/S0065-2113\(08\)60914-1](https://doi.org/10.1016/S0065-2113(08)60914-1).

Sinclair, T.R., Sheehy, J.E., 1999. Erect Leaves and Photosynthesis in Rice. *Science* 283, 1455-1455. doi:<https://doi.org/10.1126/science.283.5407.1455c>.

Slafer, G., And, A., Araus, J., 2007. Physiological Traits for Improving Wheat Yield Under a Wide Range of Conditions. *Scale and Complexity in Plant Systems Research: Gene-Plant-Crop Relations* 21, 147-156. doi:https://10.1007/1-4020-5906-X_12.

Slafer, G., Rawson, H., 1994. Sensitivity of Wheat Phasic Development to Major Environmental Factors: a Re-Examination of Some Assumptions Made by Physiologists and Modellers. *Functional Plant Biology* 21, 393-426. doi:<https://doi.org/10.1071/PP9940393>.

Slafer, G.A., 1996. Differences in phasic development rate amongst wheat cultivars independent of responses to photoperiod and vernalization. A viewpoint of the intrinsic earliness hypothesis. *The Journal of Agricultural Science* 126, 403-419. doi:<https://doi.org/10.1017/S0021859600075493>.

Slafer, G.A., 2009. Differences in phasic development rate amongst wheat cultivars independent of responses to photoperiod and vernalization. A viewpoint of the intrinsic earliness hypothesis. *The Journal of Agricultural Science* 126, 403-419. doi:<https://10.1017/S0021859600075493>.

Slafer, G.A., Andrade, F.H., Satorre, E.H., 1990. Genetic-improvement effects on pre-anthesis physiological attributes related to wheat grain-yield. *Field Crops Research* 23, 255-263. doi:[https://doi.org/10.1016/0378-4290\(90\)90058-J](https://doi.org/10.1016/0378-4290(90)90058-J).

Slafer, G.A., Araus, J.L., Royo, C., Del Moral, L.F.G., 2005. Promising eco-physiological traits for genetic improvement of cereal yields in Mediterranean environments. *Annals of Applied Biology* 146, 61-70. doi:<https://doi.org/10.1111/j.1744-7348.2005.04048.x>.

Slafer, G.A., Elia, M., Savin, R., García, G.A., Terrile, I.I., Ferrante, A., Miralles, D.J., González, F.G., 2015. Fruiting efficiency: an alternative trait to further rise wheat yield. *Food and Energy Security* 4, 92-109. doi: <https://doi.org/10.1002/fes3.59>.

Slafer, G.A., Savin, R., 1994. Source—sink relationships and grain mass at different positions within the spike in wheat. *Field Crops Research* 37, 39-49. doi:[https://doi.org/10.1016/0378-4290\(94\)90080-9](https://doi.org/10.1016/0378-4290(94)90080-9).

Slattery, R.A., VanLooke, A., Bernacchi, C.J., Zhu, X.-G., Ort, D.R., 2017. Photosynthesis, Light Use Efficiency, and Yield of Reduced-Chlorophyll Soybean Mutants in Field Conditions. *Frontiers in Plant Science* 8. doi:<https://doi.org/10.3389/fpls.2017.00549>.

Soleymani, A., 2016. Light extinction of wheat as affected by N fertilisation and plant parameters. *Crop and Pasture Science* 67, 1075-1086, 1012.

Song, Q., Chu, C., Parry, M.A.J., Zhu, X.-G., 2016. Genetics-based dynamic systems model of canopy photosynthesis: the key to improve light and resource use efficiencies for crops. *Food and energy security* 5, 18-25. doi:<http://doi.org/10.1002/fes3.74>.

Song, Q., Zhang, G., Zhu, X.-G., 2013. Optimal Crop Canopy Architecture to Maximise Canopy Photosynthetic CO₂ Uptake Under Elevated CO₂ - a Theoretical Study

Using a Mechanistic Model of Canopy Photosynthesis. doi:<https://doi.org/10.1071/FP12056>.

Spano, G., Di Fonzo, N., Perrotta, C., Platani, C., Ronga, G., Lawlor, D.W., Napier, J.A., Shewry, P.R., 2003. Physiological characterization of 'stay green' mutants in durum wheat. *J Exp Bot* 54, 1415-1420. doi:<https://doi.org/10.1093/jxb/erg150>.

Sreenivasulu, N., Schnurbusch, T., 2012. A genetic playground for enhancing grain number in cereals. *Trends in Plant Science* 17, 91-101. doi:<https://doi.org/10.1016/j.tplants.2011.11.003>.

Sultana, N., Islam, S., Juhasz, A., Ma, W., 2021. Wheat leaf senescence and its regulatory gene network. *The Crop Journal* 9, 703-717. doi:<https://doi.org/10.1016/j.cj.2021.01.004>.

SylvesterBradley, R., Berry, P., Blake, J., Kindred, D., John Spink, Bingham, I., McVittie, J., Foulkes, J., 2008. *The wheat growth guide*.

. Home Grown Cereals Authority. Agriculture and Horticulture Development Board, Stoneleigh Park, Warwickshire, UK.

Tambussi, E.A., Nogués, S., Araus, J.L., 2005. Ear of durum wheat under water stress: water relations and photosynthetic metabolism. *Planta* 221, 446-458. doi:<https://doi.org/10.1007/s00425-004-1455-7>.

Tan, C.-W., Zhang, P.-P., Zhou, X.-X., Wang, Z.-X., Xu, Z.-Q., Mao, W., Li, W.-X., Huo, Z.-Y., Guo, W.-S., Yun, F., 2020. Quantitative monitoring of leaf area index in wheat of different plant types by integrating NDVI and Beer-Lambert law. *Scientific reports* 10, 929. doi:<https://10.1038/s41598-020-57750-z>.

Tan, C., Wang, D., Zhou, J., Du, Y., Luo, M., Zhang, Y., Guo, W., 2018. Remotely Assessing Fraction of Photosynthetically Active Radiation (FPAR) for Wheat Canopies Based on Hyperspectral Vegetation Indexes. *Frontiers in Plant Science* 9. doi:<https://10.3389/fpls.2018.00776>.

Taniguchi, Y., Ohkawa, H., Masumoto, C., Fukuda, T., Tamai, T., Lee, K., Sudoh, S., Tsuchida, H., Sasaki, H., Fukayama, H., Miyao, M., 2008. Overproduction of C4 photosynthetic enzymes in transgenic rice plants: an approach to introduce the C4-like photosynthetic pathway into rice. *J Exp Bot* 59, 1799-1809. doi:<https://10.1093/jxb/ern016>.

Tanveer, S., Hussain, I., M, S., N.S, K., S.G, A., 2003. Effects of Different Planting Methods on Yield and Yield Components of Wheat. *Asian Journal of Plant Sciences* 2, 811-813. doi:<https://doi.org/10.3923/ajps.2003.811.813>.

Tao, Z.-q., Wang, D.-m., Ma, S.-k., Yang, Y.-s., Zhao, G.-c., Chang, X.-h., 2018. Light interception and radiation use efficiency response to tridimensional uniform sowing in winter wheat. *Journal of Integrative Agriculture* 17, 566-578. doi:[https://doi.org/10.1016/S2095-3119\(17\)61715-5](https://doi.org/10.1016/S2095-3119(17)61715-5).

Terrile, I.I., Miralles, D.J., González, F.G., 2017. Fruiting efficiency in wheat (*Triticum aestivum* L): Trait response to different growing conditions and its relation to spike dry weight at anthesis and grain weight at harvest. *Field Crops Research* 201, 86-96. doi:<https://doi.org/10.1016/j.fcr.2016.09.026>.

Thind, H.S., Buttar, G.S., Aujla, M.S., 2010. Yield and water use efficiency of wheat and cotton under alternate furrow and check-basin irrigation with canal and tube well water in Punjab, India. *Irrigation Science* 28, 489-496. doi:<https://10.1007/s00271-010-0208-6>.

Thomas, H., Smart, C.M., 1993. Crops that stay green I. *Annals of Applied Biology* 123, 193-219. doi:<https://10.1111/j.1744-7348.1993.tb04086.x>.

Townsend, A.J., Retkute, R., Chinnathambi, K., Randall, J.W.P., Foulkes, J., Carmo-Silva, E., Murchie, E.H., 2018. Suboptimal Acclimation of Photosynthesis to Light in Wheat Canopies. *Plant Physiology* 176, 1233-1246. doi:<https://doi.org/10.1104/pp.17.01213>.

Tripathi, S.C., Sayre, K.D., Kaul, J.N., 2005. Planting Systems on Lodging Behavior, Yield Components, and Yield of Irrigated Spring Bread Wheat. *Crop Science* 45, 1448-1455. doi:<https://doi.org/10.2135/cropsci2003-714>.

Tshikunde, N.M., Mashilo, J., Shimelis, H., Odindo, A., 2019. Agronomic and Physiological Traits, and Associated Quantitative Trait Loci (QTL) Affecting Yield Response in Wheat (*Triticum aestivum* L.): A Review. *Frontiers in Plant Science* 10. doi:<https://10.3389/fpls.2019.01428>.

Tullberg, J., 2001. Controlled traffic for sustainable cropping. *Proceedings of the 10th Australian agronomy conference*. Citeseer, pp. 28.01-01.02.

Tullberg, J.N., Ziebarth, P.J., Li, Y., 2001. Tillage and traffic effects on runoff. *Soil Research* 39, 249-257. doi:<https://doi.org/10.1071/SR00019>.

Valladares, F., Niinemets, Ü., 2007. The Architecture of Plant Crowns. doi:<https://10.1201/9781420007626.ch4>.

Verma, V., Foulkes, M.J., Worland, A.J., Sylvester-Bradley, R., Caligari, P., Snape, J.W., 2004. Mapping quantitative trait loci for flag leaf senescence as a yield determinant in winter wheat under optimal and drought-stressed environments. *Euphytica* 135, 255-263.

Waddington, S.R., Ransom, J., Osmanzai, M., Saunders, D.A., 1986. Improvement in the yield potential of bread wheat adapted to northwest Mexico. *Crop Science* 26, 698-703. doi:<https://10.2135/cropsci1986.0011183X002600040012x>.

Wang, F., He, Z., Sayre, K., Li, S., Si, J., Feng, B., Kong, L., 2009. Wheat cropping systems and technologies in China. *Field Crops Research* 111, 181-188. doi:<https://doi.org/10.1016/j.fcr.2008.12.004>.

Wang, F., Kong, L., Sayre, K., Li, S., Si, J., Feng, B., Zhang, B., 2011. Morphological and yield responses of winter wheat (*Triticum aestivum* L.) to raised bed planting in Northern China. *African Journal of Agricultural Research* 6, 2991-2997. doi:<https://doi.org/10.5897/AJAR11.125>.

Wang, F., Wang, X., Feng, B., Si, J., Li, S., Ma, Z., 2005. Performance of upland crops on beds in North-west India. In: Roth, C.H., Fischer, R.A., Meisner, C.A. (Eds.), *Evaluation and Performance of Permanent Raised Bed Cropping Systems in Asia, Australia and Mexico*. ACIAR Proceeding Vol. 121, 112-119. doi:<https://aciarc.gov.au/publication/technical-publications/evaluation-and-performance-permanent-raised-bed-cropping-systems-asia-australia-and>.

Wang, R., Liu, C., Li, Q., Chen, Z., Sun, S., Wang, X., 2020. Spatiotemporal Resolved Leaf Angle Establishment Improves Rice Grain Yield via Controlling Population Density. *iScience* 23, 101489. doi:<https://doi.org/10.1016/j.isci.2020.101489>.

Whitney, S.M., Houtz, R.L., Alonso, H., 2010. Advancing Our Understanding and Capacity to Engineer Nature's CO₂-Sequestering Enzyme, Rubisco. *Plant Physiology* 155, 27-35. doi:<https://10.1104/pp.110.164814>.

Wightman, B., Peries, R., Bluett, C., Johnston, T., 2005. Permanent raised bed cropping in southern Australia: practical guidelines for implementation. *ACIAR Proceedings* 121.

Wit, C.T.d., 1965. *Photosynthesis of leaf canopies*. Pudoc, Wageningen.

Wolde, G.M., Schnurbusch, T., 2019. Inferring vascular architecture of the wheat spikelet based on resource allocation in the branched head (*bht-A1*) near isogenic lines. *Functional Plant Biology* 46, 1023-1035. doi:<https://doi.org/10.1071/FP19041>.

Xiao, Y.G., Qian, Z.G., Wu, K., Liu, J.J., Xia, X.C., Ji, W.Q., He, Z.H., 2012. Genetic Gains in Grain Yield and Physiological Traits of Winter Wheat in Shandong Province, China, from 1969 to 2006. *Crop Science* 52, 44-56. doi:10.2135/cropsci2011.05.0246.

Xie, Q., Mayes, S., Sparkes, D.L., 2016a. Early anthesis and delayed but fast leaf senescence contribute to individual grain dry matter and water accumulation in wheat. *Field Crops Research* 187, 24-34. doi:<https://doi.org/10.1016/j.fcr.2015.12.009>.

Xie, Q., Mayes, S., Sparkes, D.L., 2016b. Optimizing tiller production and survival for grain yield improvement in a bread wheat × spelt mapping population. *Ann Bot* 117, 51-66. doi:<https://doi.org/10.1093/aob/mcv147>.

Xu, Y., Crouch, J.H., 2008. Marker-Assisted Selection in Plant Breeding: From Publications to Practice. *Crop Science* 48, 391-407. doi:<https://doi.org/10.2135/cropsci2007.04.0191>.

Yang, C.-B., Yu, Z.-W., Zhang, Y.-L., Shi, Y., 2017. Effect of Soil Depth with Supplemental Irrigation on Canopy Photosynthetically Active Radiation Interception and Chlorophyll Fluorescence Parameters in Jimai 22. *Acta Agronomica Sinica* 43, 253-262. doi:<https://doi.org/10.3724/SP.J.1006.2017.00253>.

Yang, D., Liu, Y., Cheng, H., Chang, L., Chen, J., Chai, S., Li, M., 2016. Genetic dissection of flag leaf morphology in wheat (*Triticum aestivum* L.) under diverse water regimes. *BMC Genetics* 17, 94. doi:<https://doi.org/10.1186/s12863-016-0399-9>.

Ye, H., Huang, W., Huang, S., Wu, B., Dong, Y., Cui, B., 2018. Remote Estimation of Nitrogen Vertical Distribution by Consideration of Maize Geometry Characteristics. *Remote Sensing* 10, 1995.

Yemm, E.W., Willis, A.J., 1954. The estimation of carbohydrates in plant extracts by anthrone. *Biochem J* 57, 508-514. doi:<https://doi.org/10.1042/bj0570508>.

Youssefian, S., Kirby, E.J.M., Gale, M.D., 1992. Pleiotropic effects of the GA-insensitive Rht dwarfing genes in wheat. 2. Effects on leaf, stem, ear and floret growth. *Field Crops Research* 28, 191-210. doi:[https://doi.org/10.1016/0378-4290\(92\)90040-G](https://doi.org/10.1016/0378-4290(92)90040-G).

Yunusa, I.A.M., Siddique, K.H.M., Belford, R.K., Karimi, M.M., 1993. Effect of canopy structure on efficiency of radiation interception and use in spring wheat cultivars during the pre-anthesis period in a mediterranean-type environment. *Field Crops Research* 35, 113-122. doi:[https://doi.org/10.1016/0378-4290\(93\)90144-C](https://doi.org/10.1016/0378-4290(93)90144-C).

Zacharias, M., Kumar, S.N., Singh, S., Rani, D.S., Aggarwal, P., 2014. Assessment of impacts of climate change on rice and wheat in the Indo-Gangetic plains. *Journal of Agrometeorology* 16, 9.

Zadoks, J.C., Chang, T.T., Konzak, C.F., 1974. A decimal code for the growth stages of cereals. *Weed Research* 14, 415-421. doi:<https://doi.org/10.1111/j.1365-3180.1974.tb01084.x>.

Zaman, R., Akanda, A.R., Biswas, S.K., Islam, M.R., 2017a. Effect of Deficit Irrigation on Raised Bed Wheat Cultivation. *Cercetari Agronomice in Moldova* 50, 17 - 28.

Zaman, R., Akanda, A., Biswas, S., Islam, M., 2017b. Effect of Deficit Irrigation on Raised Bed Wheat Cultivation. doi:<https://10.1515/cerce-2017-0032>.

Zarzycki, J., Axen, S.D., Kinney, J.N., Kerfeld, C.A., 2013. Cyanobacterial-based approaches to improving photosynthesis in plants. *J Exp Bot* 64, 787-798. doi:<https://10.1093/jxb/ers294>.

Zhang, H., Richards, R., Riffkin, P., Berger, J., Christy, B., O'Leary, G., Acuña, T.B., Merry, A., 2019. Wheat grain number and yield: The relative importance of physiological traits and source-sink balance in southern Australia. *European Journal of Agronomy* 110, 125935. doi:<https://doi.org/10.1016/j.eja.2019.125935>.

Zhang, H., Turner, N., Poole, M., 2010. Source-sink balance and manipulating sink-source relations of wheat indicate that the yield potential of wheat is sink-limited in high-rainfall zones. *Crop and Pasture Science* 61, 852-861. doi:<https://doi.org/10.1071/CP10161>.

Zhang, H., Turner, N.C., Poole, M.L., 2012. Increasing the harvest index of wheat in the high rainfall zones of southern Australia. *Field Crops Research* 129, 111-123. doi:<https://doi.org/10.1016/j.fcr.2012.02.002>.

Zhang, H., Zhou, C., 2013. Signal transduction in leaf senescence. *Plant molecular biology* 82, 539-545. doi:<https://doi.org/10.1007/s11103-012-9980-4>.

Zhang, J., Sun, J., Duan, A., Wang, J., Shen, X., Liu, X., 2007. Effects of different planting patterns on water use and yield performance of winter wheat in the Huang-Huai-Hai plain of China. *Agricultural Water Management* 92, 41-47. doi:<https://doi.org/10.1016/j.agwat.2007.04.007>.

Zhang, L., Hu, Z., Fan, J., Zhou, D., Tang, F., 2014. A meta-analysis of the canopy light extinction coefficient in terrestrial ecosystems. *Frontiers of Earth Science* 8, 599-609. doi:<https://doi.org/10.1007/s11707-014-0446-7>.

Zhang, Z., Zhou, X.B., Chen, Y.H., 2016. Effects of Irrigation and Precision Planting Patterns on Photosynthetic Product of Wheat. *Agronomy Journal* 108, 2322-2328. doi:<https://10.2134/agronj2016.01.0051>.

Zhu, G., Peng, S., Huang, J., Cui, K., Nie, L., Wang, F., 2016. Genetic Improvements in Rice Yield and Concomitant Increases in Radiation- and Nitrogen-Use Efficiency in Middle Reaches of Yangtze River. *Scientific reports* 6, 21049. doi:10.1038/srep21049.

Zhu, X.-G., Long, S.P., Ort, D.R., 2010. Improving photosynthetic efficiency for greater yield. *Annual review of plant biology* 61, 235-261. doi:<https://doi.org/10.1146/annurev-arplant-042809-112206>.